STRUCTURAL CONTROLS AND CHEMICAL CHARACTERIZATION OF BRECCIATION AND URANIUM VANADIUM MINERALIZATION IN THE NORTHERN BIGHORN BASIN

by

Anita Louise Moore-Nall

A dissertation submitted in partial fulfillment
of the requirements for the degree

of

Doctor of Philosophy

in

Earth Sciences

MONTANA STATE UNIVERSITY
Bozeman, Montana

December, 2016

©COPYRIGHT

by

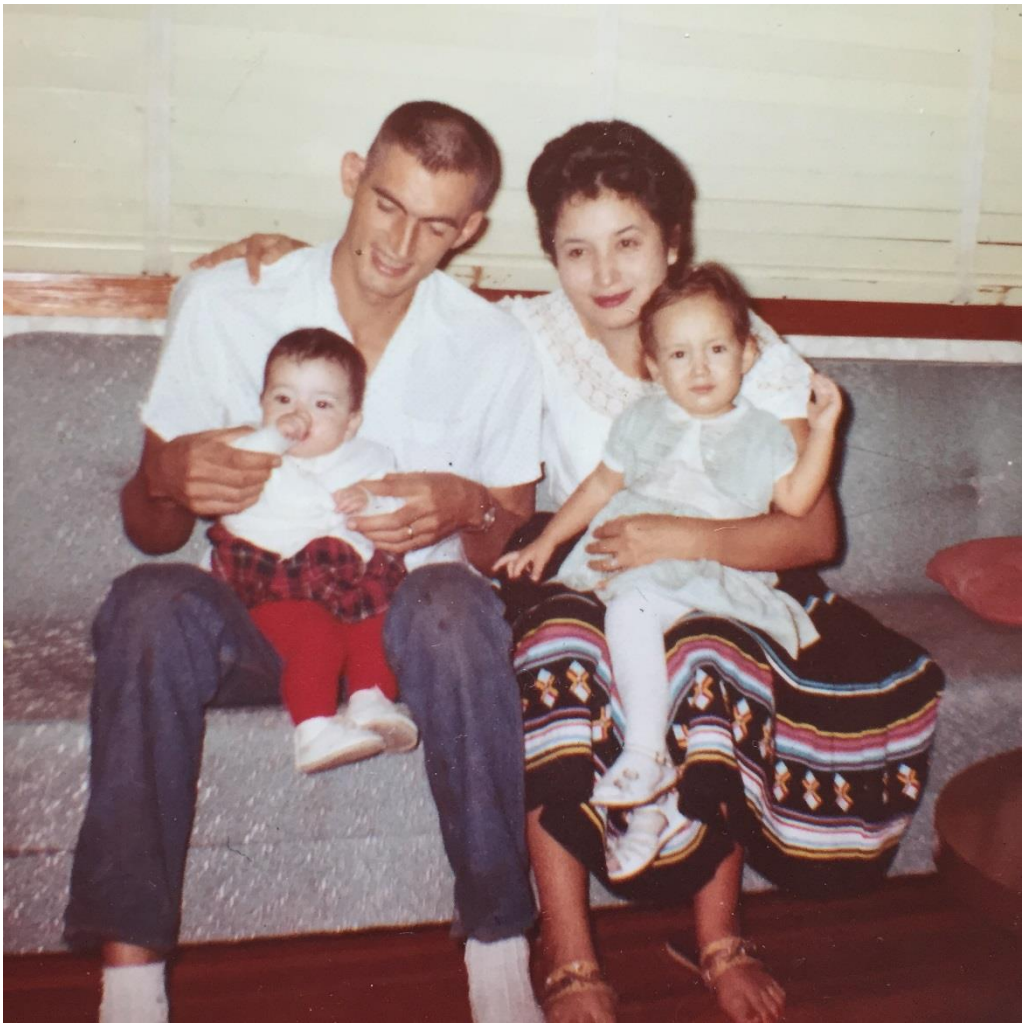
Anita Louise Moore-Nall

2016

All Rights Reserved

DEDICATION

I would like to dedicate this work to my extended family and my friends for all that they have given over the years so that I may have the time to focus so intently on so many different aspects of this project.



In memory and dedication to my parents and sister. Photo of my father Paul H. Moore holding my sister June F. Moore and Rosa M. (Dillon) Moore holding me. Taken in their home on the Seminole Indian Reservation in Florida, 1961.

ACKNOWLEDGMENTS

I would like to extend my gratitude and appreciation to my advisor and committee chair, Dr. David R. Lageson for his advice, assistance and support throughout various stages of this project. I would also like to thank Dr. David Mogk, Dr. David Bowen, and Dr. Colin Shaw for their thoughts, input and expertise in their fields and for serving as members on my committee.

Financial support was provided by the Tobacco Root Geological Society (TRGS), MSU Department of Earth Sciences, MSU Energy Research Institute, Zero Emissions Research Technology (ZERT), Dennis and Phyllis Washington Foundation Native American Graduate Fellowship, Alfred P. Sloan Graduate Scholarship Programs – Minority PhD Component/Sloan Indigenous Graduate Partnership, and the HOPA Mountain Native Science Fellowship program.

I would also like to extend special thanks to Mrs. Lauren (Kay) Sakai, Mrs. Janet Barkow and my son Thomas Nall for assistance with fieldwork. I would also thank Dr. Margaret J. Eggers for your friendship, encouragement and intellectual perspective on many aspects of my project; Dr. Chris Gammons, for use of instrumentation in his lab at Montana Tech, and input of expertise in his field; Dr. Ken W. Sims, Erin H.W. Phillips and Sean Scott, University of Wyoming, for guidance and use of their High Precision Isotope lab and Claire Lukens for hosting me during my stay while I worked in the lab; Nancy Equall and Laura Kellerman, Montana State University, for expertise and assistance with instrumentation at the Imaging and Chemical Analysis Laboratory and to my family and friends who gave me encouragement and support over the course of this project.

VITA

Anita Louise Moore-Nall is an enrolled member of the Apsaálooke (Crow) Nation, a member of the Greasy Mouth Clan. Anita grew up on three American Indian Reservations. She was born May 17th, 1960 in Okeechobee, Florida to Paul H. and Rosa M. (Dillon) Moore while Paul was working on the Seminole Reservation for the Bureau of Indian Affairs as an engineer. She lived on the Flathead Reservation, home to the Bitterroot Salish, Kootenai, and Pend d'Oreille Tribes - also known as the Confederated Salish and Kootenai Tribes of the Flathead Nation, from age 2 until the completion of first grade. The family relocated to the Blackfeet Reservation where Anita graduated from Browning High School. Anita attended Montana State University where she earned her first bachelor's degrees from the Department of Earth Sciences and the Department of Film and Television in 1984. Anita married Randall (Randy) Glenn Nall in 1983. Upon graduation from MSU she worked for the USGS in the branch of Geochemistry out of the Federal Center in Denver, Colorado, later for the Mineral Hill gold mine in Jardine, Montana and then for the USFS out of the Supervisor's Office in Bozeman, Montana until the birth of her son Tom, in 1993. Anita and Randy built their log home and raised a family in Bozeman, Montana. Their daughter Stella was born in 1997. Anita stayed home with her children until they were in school. She then worked as a consulting geologist for Eurasian Minerals and World Industrial Minerals until she decided to pursue an advanced degree in Earth Sciences studying something that would be related to her home reservation. After learning that the Lower Bighorn River was listed as a 303d impaired water body due to elevated lead and mercury downstream of the Crow Reservation she decided to examine the abandoned uranium and vanadium mining districts which are southwest of the reservation and whose watersheds contribute to the greater Bighorn hydrologic basin to see if these areas might give a clue to the source of contaminants in the river.

TABLE OF CONTENTS

1. SCOPE OF DISSERTATION 1

Description of Study Area 8
Dissertation Organization 14
References Cited 17

2. THE LEGACY OF URANIUM DEVELOPMENT ON OR NEAR INDIAN RESERVATIONS AND HEALTH IMPLICATIONS REKINDLING PUBLIC AWARENESS 22

Contribution of Authors and Co-Authors 22
Manuscript Information Page 23
Abstract 24
Introduction 25
The Quest for Uranium 26
Uranium Production on Native American Lands 27
Nuclear Weapons Development 33
Milling and Abandoned Mills 36
Indian Health Service, Census Data and Health Disparities 37
Census Data and Disparities 37
Toxic Waste Storage 37
Radiation Exposure Compensation Act 39
Discussion and Conclusions 42
Acknowledgements 45
References Cited 46

3. POTENTIAL HEALTH RISKS FROM URANIUM IN HOME WELL WATER: AN INVESTIGATION BY THE APSAÁLOOKE (CROW) TRIBAL RESEARCH GROUP 52

Contribution of Authors and Co-Authors 52
Manuscript Information Page 54
Abstract 56
Introduction 57
Crow Reservation 58
Study Area 61
Uranium 66
Methods 70
Community-Based Participatory Research 71
Volunteer Recruitment and Participation 71
Sample Collection and Analysis 72

TABLE OF CONTENTS - CONTINUED

Sample Collection and Analysis 72
Data Entry and Analysis 74
Risk Communication 76
Results 77
Discussion and Conclusions 84
Potential Sources of Uranium in Local Groundwater 84
Sources of Uncertainty 86
Uranium Contamination of Home Well
Water is a Priority Public Health Issue 88
Future Research, Community Education and Risk Mitigation 91
Conclusions 92
Acknowledgements 93
References Cited 97

4. STRUCTURAL CONTROLS AND GEOCHEMICAL CHARACTERIZATION OF BRECCIAS IN PALEOKARST IN THE NORTHERN BIGHORN BASIN 106

Abstract 106
Introduction 107
Pryor Mountain Study Area 110
Breccias in the Districts 115
Collapse Paleokarst Breccia 115
Lithified Collapse Breccia 116
Silica Cemented Tectonic Breccia 117
Lag Deposits 119
Tectonic Breccia, LMD 121
Methods 121
Computer Aided Lineament Analysis 122
Fieldwork 123
Geochemical Characterization 124
Results and Discussion 125
Stable C and O Isotopes 125
Radiogenic Sr Isotopes 128
Computer Aided Lineament Analysis 133
Movement along Fractures 136
Mineralization Orientations 138
Expected Laramide Stress Field 141
Discussion 143
Origin of Tectonic Breccia 145
Fluid Flow Model 148

TABLE OF CONTENTS - CONTINUED

Conclusions....151
References Cited....153

5. REE DATA SUPPORT OIL WITH A PERMIAN PHOSPHORIA FORMATION SOURCE AS A SOURCE OF METALS FOR U AND V MINERALIZATION IN THE NORTHERN BIGHORN BASIN....160

Contribution of Authors and Co-Authors....160
Manuscript Information Page....161
Abstract....162
Introduction....163
Theories for Origin of Deposits....165
Study Areas....167
Physiography....167
Stratigraphy....168
Structural Setting....170
Mineralization and Alteration....171
Tectonic Hydrothermal Breccia, PMD....173
Methods....175
Field Work....175
Mineralogical and Geochemical Characterization....175
Results, Mineralogy and Geochemistry....177
Mineralogy: Ore and Gangue Minerals....177
Cathodoluminescence....184
Fluid Inclusions....186
REE and Geochemical Assay Data....186
Discussion....195
Phosphoria Oil migration and Oilfields in the Bighorn Basin....196
Origin of Bitumen and Heavy Oil....196
Style of Breaching of Oil Traps in the Study Areas....198
Paragenesis of U Minerals in the Two Districts....199
Future Directions....208
Selective Solid Phase Extraction of U from Contaminated Water....209
Conclusions....212
Elements of Environmental Concern....213
Acknowledgements....215
References Cited....216

TABLE OF CONTENTS - CONTINUED

6. SUMMARY.....228

CUMMULATIVE REFERENCES 232

APPENDICES 262

APPENDIX A: Supporting Information for Chapter 1.....263
APPENDIX B: Supporting Information for Chapter 4.....272
APPENDIX C: Supporting Information for Chapter 5.....345

LIST OF TABLES

Table Page

1.1 Water data collected in re-sample study 5

3.1 Relationship of well water quality to consumption 82

4.1 Average $^{87}Sr/^{86}Sr$ compositions of some geologic materials.....128

5.1 Ore and gangue minerals 178

5.2 Elevated concentrations of metals in U-V breccia samples.....195

5.3 Geologic events or processes affecting the Madison Limestone in the Bighorn Basin and the mining districts.....207

B.1 C and O stable isotope results 274

B.2 Radiogenic Sr isotope results 279

B.3 GEP fracture analyses data.....282

B.4 Silica cemented breccia locations 313

B.5 Fracture analyses data silica cemented breccia.....317

C.1 PGM and Au Results AAS laboratory 346

C.2 Trace elements ALS laboratory results 348

C.3 REE plus Y ALS laboratory results 352

LIST OF FIGURES

Figure		Page
1.1	Study area and geologic map northern Bighorn Basin	7
1.2	Local structure of the two mining districts	10
1.3	Generalized stratigraphic column Billings-Pryor Mountain Area	13
2.1	Uranium locations from EPA agency database shown with Federal Land locations	28
2.2	Sign erected by the Navajo and U.S. EPA that is typical for many of the water sources on the reservation.	30
2.3	Hanford Nuclear Reservation and bordering Indian Reservations	33
3.1	Hydrologic basins in Study Area	61
3.2	Northern Bighorn Mountains and Bighorn River	63
3.3	Geologic map of the Reservation showing old uranium mines	65
3.4	Simplified Uranium-238 decay series figure	67
3.5	Crow Reservation map showing traditional districts of the Reservation.	75
3.6	Map showing U data used in study plotted in hydrologic drainage basins	78
3.7	Histograms of U concentrations in well water by river valley	80
4.1	Location of the U-V mining districts in Montana and Wyoming.	108
4.2	Model for Tectonic Hydrothermal Breccia Pipe Formation.	109
4.3	Block diagram of the Pryor Mountains.	110
4.4	Cross-Section of the showing location of PMD in Montana	113
4.5	Typical paleokarst collapse breccia	116

LIST OF FIGURES - CONTINUED

Figure Page

4.6 Typical lithified paleokarst collapse breccia....117

4.7 Typical silica cemented tectonic breccia 118

4.8 Silica cemented tectonic breccia following fracture sets....119

4.9 Lag Deposits 120

4.10 Tectonic Breccia, LMD 121

4.11 Stable C and O Isotope Cross-plot....126

4.12 Radiogenic Sr Isotope sample compositions by sample type 129

4.13 Radiogenic Sr Isotope sample compositions by location 130

4.14 Radiogenic Sr and stable O Isotope Cross-plot 132

4.15 Google Earth Pro Lineament Analysis 134

4.16 Google Earth Pro and silica cemented breccia locations 136

4.17 Mineralized and unmineralized breccias on DEMs 137

4.18 Unmineralized breccia fracture stations with slickenlines....139

4.19 Mineralized breccia fracture stations with slickenlines 140

4.20 DEM with expected Laramide Stress field 142

4.21 View west from Crooked Creek Road....146

4.22 Schematic figure showing fluid flow in the PMD 148

5.1 Map showing the location of the Pryor Mountain and the Little Mountain areas....164

5.2 Generalized stratigraphic column of the Pryor Mountain area 169

LIST OF FIGURES - CONTINUED

Figure		Page
5.3	Map showing the tectonic features of the Bighorn Basin	171
5.4	Outcrop photos of U-V mineral occurrences and boxwork	172
5.5	Hematite- and limonite-stained hydrothermal tectonic breccia and liesegang banding	174
5.6	Morphologies of some of the metal-uranyl vanadates	180
5.7	Images of bitumen and vugs in samples from this study	182
5.8	CL images of samples from the Pryor Mountain district	184
5.9	Spidergram plots of REE plus Y Chondrite-normalized samples	188
5.10	Index map showing location of dominant facies of rocks of Permian age	190
5.11	Permian Phosphoria Formation rock sample REE and Y data plotted with data from this study that have similar patterns	192
5.12	Map showing the oilfields in the Bighorn Basin	197
5.13	Barite and quartz in the PMD	202
5.14	Ligands modified SPCs and their applications to date.	211
A.1	Total sediment samples analyzed during the NURE Program in the Bighorn River hydrologic basin	266
A.2	Sediment samples with 0.02ppm or greater Hg	267
A.3	Sediment samples analyzed for Pb	268
A.4	Stream sediment samples analyzed for U	269
A.5	Pb concentrations in water samples	270
A.6	U concentrations in water samples	271

LIST OF FIGURES - CONTINUED

Figure Page

C.1 EDS spectrum of Au mineral from Lisbon mine sample 347

C.2 EDS spectrum of Carnotite, a K-uranyl vanadate 355

C.3 EDS spectrum for Old Glory mine fluorite sample with small grains of a K U-V mineral.....356

C.4 EDS spectrum for Tl-bearing uranyl vanadate.....357

C.5 EDS spectrum for Tl-bearing uranyl vanadate, Dandy mine 358

C.6 EDS spectrum Fe-V oxides from the Old Glory mine 359

C.7 EDS spectrum for FeV oxides from the Old Glory mine, with Tl or Pb 360

C.8 EDS spectrum from silica cemented breccia with Fe, V, and As 361

C.9 EDS spectrum from U V mineralized limestone breccia, Leo Incline area, LMD 362

C.10 EDS spectrum from East Pryor mine, PMD sample with Cu, Ni, and Zn 363

ABSTRACT

The goals of this research were to determine if the mode of mineralization and the geology of two abandoned uranium and vanadium mining districts that border the Crow Reservation might be a source for contaminants in the Bighorn River and a source of elevated uranium in home water wells on the Reservation. Surface and spring waters of the Crow Reservation have always been greatly respected by the Crow people, valued as a source of life and health and relied upon for drinking water. Upon learning that the Bighorn River has an EPA 303d impaired water listing due to elevated lead and mercury and that mercury has been detected in the fish from rivers of the Crow Reservation this study was implemented. Watersheds from both mining districts contribute to the Bighorn River that flows through the Crow Reservation.

Initial research used the National Uranium Resource Evaluation database to analyze available geochemistry for the study areas using GIS. The data showed elevated concentrations of lead in drainages related to the mining areas. The data also showed elevated uranium in many of the surface waters and wells that were tested as a part of the study on the Crow Reservation. The author attended meetings and presented results of the National Uranium Resource Evaluation data analyses to the Crow Environmental Health Steering Committee. Thus, both uranium and lead were added to the list of elements that were being tested in home water wells as part of a community based participatory research project addressing many issues of water quality on the Crow Reservation. Results from home wells tested on the reservation did show elevated uranium.

Rock samples were collected in the study areas and geochemically analyzed. The results of the analyses support a Permian Phosphoria Formation oil source of metals in the two mining districts. Structural data support fracturing accompanied by tectonic hydrothermal brecciation as a process that introduced oil and brines from the Bighorn Basin into the deposits where the uranium vanadium deposits later formed.

CHAPTER 1

SCOPE OF DISSERTATION

This dissertation was approached from both a medical and a traditional geology aspect. The research in this dissertation investigates the geology of the portions of the Pryor Mountains, Montana and northern Bighorn Mountains, Wyoming that host the Pryor Mountain and Little Mountain abandoned uranium and vanadium mining districts. The original impetus for study of these areas was to investigate the mode of the mineralization of the deposits to see if these areas may provide a geological source for the contaminants lead (Pb) and mercury (Hg) in the Bighorn River.

Once the river passes through the Crow Reservation it has a 303d impaired water listing due to elevated Pb and Hg (EPA, 2015). Under the U.S. Environmental Protection Agency Clean Water Act, 303d listings are waters which states and tribes are required to report to the U.S. EPA, for which technology-based regulations and other required controls are not stringent enough to meet the water quality standards set by those states (EPA). The 303d designation of the Bighorn River was based on data from a U.S. Geological Survey regional water resources investigation of the Yellowstone River drainage basin (Peterson and Boughton, 1998) and data on organic elements and trace elements concentrations in bed sediments and fish tissue (Peterson and Zelt, 1999). The fish of the Bighorn River had the highest Pb and Hg concentrations of all the EPA sites studied across the nation at that time. Drainages from the Little Mountain Mining District (LMD), Wyoming and Pryor Mountain Mining District (PMD), Montana both contribute

to the greater Bighorn River watershed. The river remains on the latest (July 2016, draft) final water quality integrated report submission to the US EPA for the State of Montana and the source of contamination is unknown (Montana CWA, 2016).

The author learned of this contamination issue while attending a presentation held in Bozeman, Montana at Montana State University (MSU) in the spring of 2009. Water quality and data collected on the Crow Reservation was being discussed. The data presented was generated after several years of community involvement and collaboration with educational partners at the Little Big Horn College on the Crow Reservation and MSU. The Tribal community came together to address water quality issues that affect the members living on the reservation. The community effort began in 2004 when the Apsaálooke [Crow] Water and Wastewater Authority for the Crow Reservation, a staff member of the Crow/Northern Cheyenne Indian Health Service Hospital and a science faculty member at Little Big Horn College on the Reservation conducted a community-wide environmental health assessment with volunteers from the Indian Country Environmental Hazard Assessment Program of the EPA and about ten Tribal members with various areas of expertise (DuFault, 2005; Eggers, 2014). Water contamination was identified as the environmental health issue with the most serious and widespread impacts on community health. The Crow Environmental Health Steering Committee was formed after the health assessment (Eggers, 2014). A formal Memorandum of Agreement among the Crow Tribe, Little Big Horn College and MSU was developed by the Crow Environmental Health Steering Committee to collaborate on addressing water quality issues on the Reservation (Eggers, 2014). The work of the Crow Environmental Health

Steering Committee evolved to a community based participatory research project addressing many issues of water quality including the effects of climate change. A Ph.D. dissertation and many studies were generated and continue to be generated from this work (Eggers, et al., 2008; Cummins, et al.; 2009, 2010a, 2010b; Doyle, et al., 2012a, 2012b; 2013, Eggers; 2014, Hamner, et al., 2014; Eggers, et al., 2015; McOliver, et al., 2015). A fish tissue study was one of the studies that involved students from the Little Big Horn College, on the Crow Reservation. Data from the study showed elevated Pb and Hg in fish from the rivers on the Crow Reservation (Cummins et al., 2009).

After learning of the contamination of the Bighorn River the author, an enrolled member of the Crow Tribe, started graduate school and pursued study related to this issue. In the early phases of this study the National Uranium Resource Evaluation (NURE) and Hydrogeochemical and Stream Sediment Reconnaissance (HSSR) database administered by the U.S. Geological Survey (Smith, et al., 1997) and Montana Ground Water Information Center (GWIC) data was reviewed to see what geochemistry was available for the Crow Reservation and areas near the Reservation. Both stream sediment and water data was reviewed in the NURE database (Appendix A, Figures A1-A6). The data was analyzed and plotted using GIS methods. The data showed elevated concentrations of Pb and Hg in sediments in drainages related to the mining areas and elevated Pb and U in surface and well water samples (Appendix A, Figures A2-A6). The NURE data was also examined in areas outside of the hydrologic basins associated with this study to see if the high Pb concentrations were localized in the study area. The data

showed extremely high levels of Pb (up to 23,890 ppb) for well water tested in the NURE study in other areas of the Billings Quadrangle (Smith, et al., 1997).

After several rounds of communication between the author, Montana Bureau of Mines and Geology staff, and U.S. Geological Survey staff via e-mail, it was concluded that the instrumentation, Plasma-Source Emission Spectrography (ICP-AES), used for analyses done by Los Alamos National Laboratory (LANL) of water samples 1978-1979 Los Alamos NURE lead concentrations for Ca, Co, Cr, Cu, Fe, Mg, Mn, Mo, Ni, Pb, Ti, and Zn, was not properly measuring the concentration of Pb. This was likely due to interference by other elements that the Pb spectral lines overlap. The instrumentation that LANL used during that time may have had problems with element discrimination; in some of the early instruments (1981) there were some problems (S. Smith, pers. comm.). The data from the other labs used in the program do not appear to have had this problem (S. Smith, pers. comm.).

The author used the locations for the anomalously high Pb readings in the NURE database and resampled wells and surface water in the Billings Quadrangle that could be located, as was suggested by Smith, to determine if the Pb values in the NURE database were valid. Water samples were tested by Inductively Coupled Plasma-Mass Spectrometry (ICP-MS) at Energy Labs in Billings, Montana, an accredited EPA laboratory (Energy Labs, 2011). The results for the analyses (n=24) did not detect anomalous Pb concentrations in any of the samples (Table 1.1).

Sample ID	Sample Source	GWIC ID	NURE FID	UTM Easting NAD 27	UTM Northing NAD 27	Nure Pb value ppb	Temp. °C	pH	Energy Lab Pb value ppb
FID9529S	Stream	none	9524	NR	NR	3857	12	8	<10 ppb
FID9529W	Well	261237	9523	NR	NR	4030	10	8	<10 ppb
ST001	Stream	none	9164	642801E	5051955N	916	10	8	<10 ppb
ST002	Stream	none	9162	643744E	5051639N	1538	13	8	<10 ppb
FID 8974	Stream	none	9158	657330E	5059686N	2972	13	8	<10 ppb
ST003	Stream	none	*8697	662084E	5080015N	677	15	8	<10 ppb
ST004	Stream	none	9866	681029E	5088135N	8393	10	8	<10 ppb
ST005	Stream	none	9831	696523E	5088135N	8875	9	8.5	<10 ppb
ST006	Stream	none		696485E	5088973N		8.5	8	<10 ppb
FID9830	Well	none	*9830	696254E	5090669N	1302	10	9	<10 ppb
ST007	Stream	none		695662E	5090651N		11	7.5	<10 ppb
ST008	Stream	none		693685E	5090586N		11	8	<10 ppb
ST009	Stream	none		690493E	5090472N		11	8	<10 ppb
ST010	Stream	none		683313E	5090278N		11	8	<10 ppb
ST011	Stream	none		694968E	5058594N		9	8	<10 ppb
ST012	Stream	none		696631E	5060793N		9	8	<10 ppb
ST013	Stream	none		702361E	5055644N		11	7	<10 ppb
FID10108	Stream	none	10108	709469E	5065492N	5852	9	8	<10 ppb
ST014	Stream	none	*10041	709190E	5065638N	1377	9	7.5	<10 ppb
ST015	Stream	none	*9863	688788E	5079452N	4105	4	7	<10 ppb
ST016	Well	10423	*9862	688645E	5078940N	6752	11	7	<10 ppb
ST017	Stream	none	9856	691389E	5077478N	8420	5	8	<10 ppb
ST018	Well	154253	none	702600E	5090251N	No data	12	8	<10 ppb
ST019	Well	none	9826	702675E	5090307N	23890	11	9	<10 ppb
*NURE designates NURE point nearest to sample collection site									

Table 1.1 Energy Labs data for re-sampling of NURE water data samples that had anomalous high concentrations of Pb. GWIC and NURE samples ID that corresponded to or were near the re-sample collection site are listed. The GWIC data that was near the sample sites or corresponded to the sample site had no Pb data recorded.

The erroneous Pb concentrations from water samples reported in the NURE database were likely not detected because elements other than U were rarely analyzed during the NURE program, only three quadrangles in Montana (Billings, Butte, and Dillon) analyzed elements other than U (NURE database, 2011). So unless the concentration of these metals in water were of interest in the few areas that covered the area the database may not have been queried. Uranium was the main element of concern

for the NURE program and the analysis and methods used for U in water by the NURE program included: delayed neutron counting; fluorescence spectroscopy; and mass spectrometry depending on the lab. The NURE database is publically available and the erroneous water data is only for the elements listed above and only in the Rocky Mountain States and Alaska, the regions using the Los Alamos Scientific Laboratory during the years of the program (approximately 1976 - 1984). The issue is still being addressed through the publications group of the USGS to update the website to provide a notice for the public on the use of this database (Smith, pers. comm.).

The author attended meetings with the Crow Environmental Health Steering Committee and presented findings of elevated U in the NURE data set. After presenting the findings, U and Pb were both included in the water study. Wells tested in the study did show elevated U but not elevated Pb (Chapter 3, this study). Work continues as the group collaborates with other researchers, which both brings in needed areas of expertise and provides opportunities for MSU faculty to work with the Crow Reservation community (Eggers, 2014).

The mining districts and some samples from the Kane Cave system located in the Little Sheep Mountain anticline (Figure 1.1) are the focus of the geochemistry and geologic field work for this study. Samples from these areas were analyzed for elements of concern (Pb, Hg and U). These elements have also been detected in coals in the area (USGS, 1999) and the highest Pb readings from aquifers near the Crow Reservation were from USGS monitoring wells in the Decker area (GWIC, 2011). Coal burning facilities likely contributed Hg to the environment before better scrubbers were implemented.

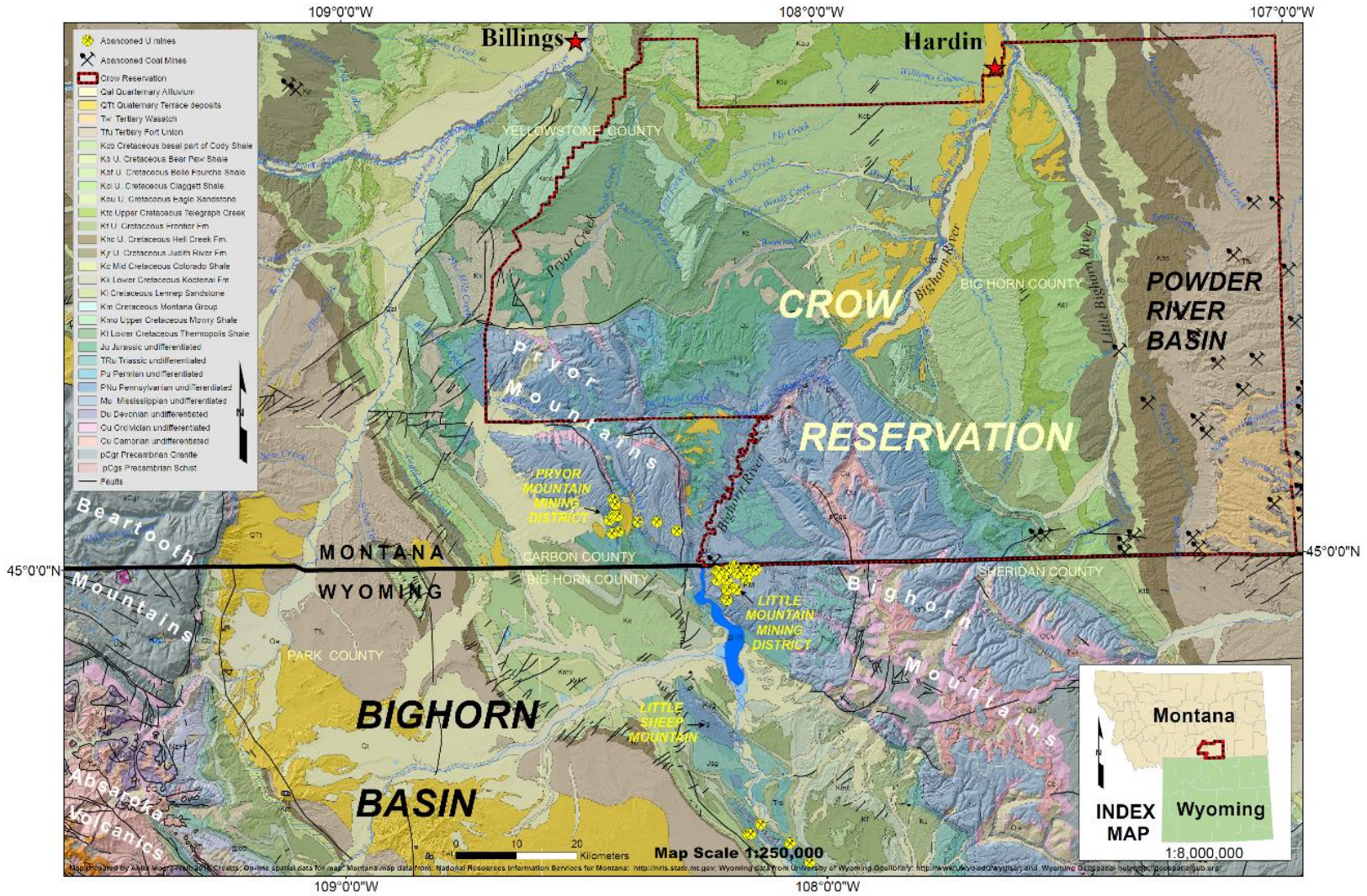


Figure 1.1. Study areas include the Crow Reservation, outlined in red and black, the Pryor Mountain and Little Mountain Mining Districts shown in the central part of the map, and Little Sheep Mountain anticline of north central Wyoming

Description of Study Areas

The study areas for this dissertation include the Crow Reservation, the PMD and LMD and the Little Sheep Mountain anticline. The Crow Reservation is located in the north western flank of the Powder River Basin and is separated from the Bighorn Basin by the Pryor Mountains. The PMD in the southern Pryor Mountains, Montana, the LMD in the northwestern flank of the Bighorn Mountains, and Little Sheep Mountain, of north central Wyoming are located in the northern rim of the Bighorn Basin (Figure 1.1).

The Bighorn Basin has been a major oil and gas producing basin for Wyoming for over a century (Wyoming State Geologic Survey, 2016). The basin extends from Montana southeastward toward the Bridger-Owl Creek Mountains in central Wyoming (Blackstone, 1986). The western margin is concealed beneath the Absaroka volcanic field; the north is constricted between the east face of the Beartooth Mountains and the west flank of the Pryor Mountains (Blackstone, 1986). To the east the basin is bounded by the Bighorn Mountains. Within the outcrop of Upper Cretaceous sedimentary rocks, the basin is approximately 322 kilometers long and 80 kilometers wide.

Regional Structural Setting

The Bighorn Basin of Wyoming and Montana and the arches that surround it have had a complex tectonic history. During the Laramide orogeny (80-35 Ma), the central Rocky Mountain region experienced a general NE-SW (40°- 55°) transpressional strain regime as a result of the low-angle subduction of the Farallon plate at its western continental margin (Blackstone, 1940; Bird, 2002; Neely and Erslev, 2009). Beginning in

the late Cretaceous, Laramide shortening was accommodated by uplift of broad basement arches that eventually isolated the Bighorn Basin (Blackstone, 1980; Dickenson, 1988; Brown, 1993, Erslev, 1993). Smaller scale folds in the form of anticlines and synclines formed along the basin margins and served to accommodate regional shortening (Thom, 1947, Fanshawe, 1971, Blackstone, 1980, Brown, 1993). The surface anticlines, which form a peripheral rim around the basin, are characterized by short steeply dipping forelimbs and long, gently dipping back limbs (Banerjee, 2008). Today, these folds host most of the oil and gas fields of the Bighorn Basin (Broadhead and Robertson, 1966; Blackmore, 1986; Dickinson et al., 1988). Both mining districts occur in folds created during the Laramide Orogeny and were likely hosts for oil before they were breached after which the U-V deposits formed.

Local Structural Setting Structurally the Pryor Mountains are located in an inferred sinistral transpressional accommodation zone along the northern perimeter of the Bighorn Basin (Wilson, 1936; Lopez, 1995). The range consists of four major uplifted crustal blocks tilted up in the northeast corners (Blackstone, 1940). The exposed boundaries of the blocks are bound by deep-seated basement faults, asymmetric folds displaced by faults or asymmetric folds likely underlain by faults (Blackstone, 1940). The moderate to steeply dipping reverse faults along the east front of the mountains bring Archean basement rock into fault contact with deformed and locally overturned Paleozoic and Mesozoic rock (Blackstone, 1940). The Pryor Mountains are divided into northern and southern segments by the Sage Creek fault zone (Figure 1.2), the eastern extension of

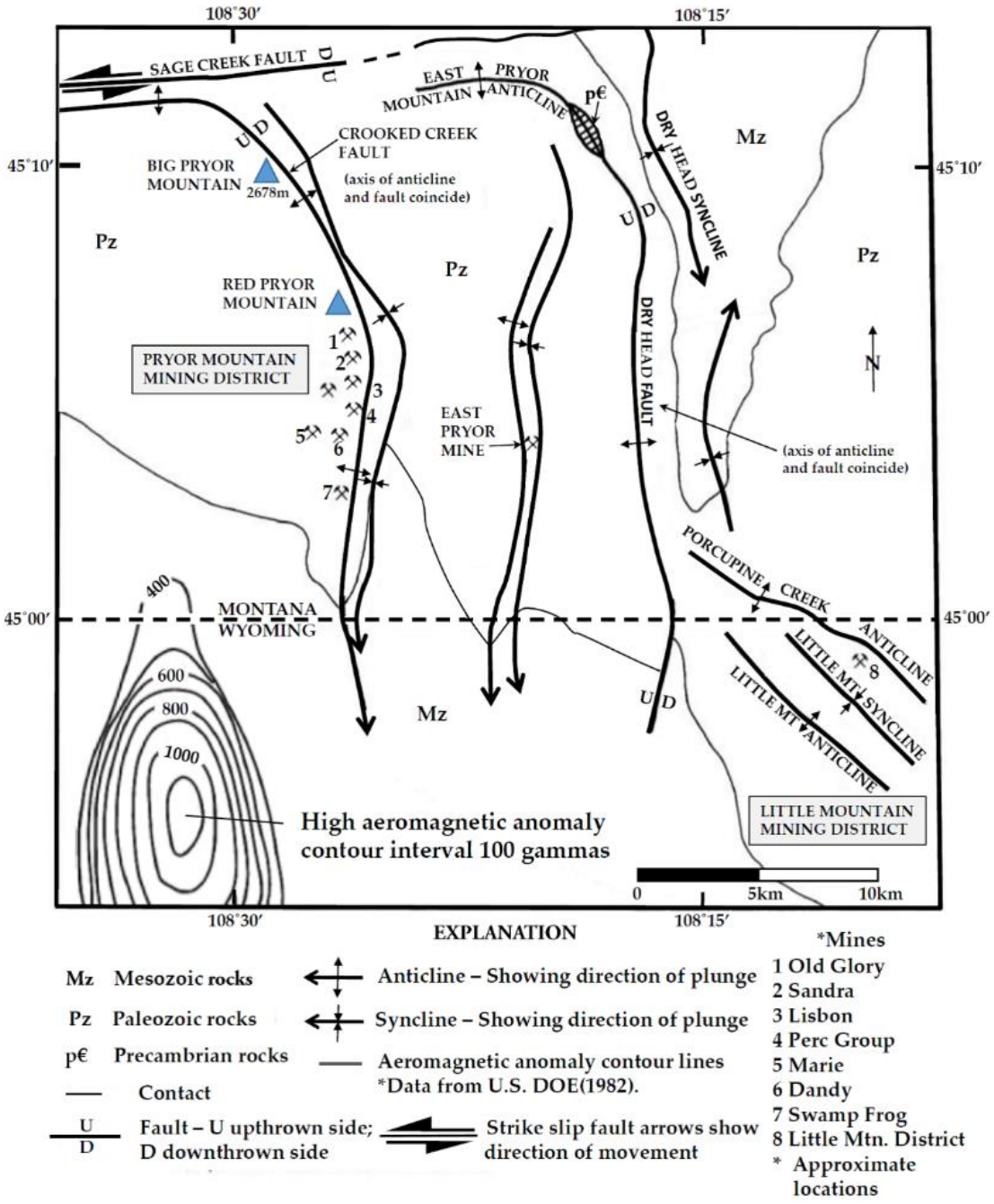


Figure 1.2. Map showing the structural features of the two mining districts. Approximate location of some of the mines referred to in the text are shown. A high aeromagnetic anomaly was identified in 1982 by the Department of Energy. This is discussed in Chapter 5, an intrusion at depth could be a potential source of the magnetic anomaly. Map modified from Patterson, et al., 1988.

the Nye-Bowler lineament (Blackstone, 1940; Lopez, 1995). The Nye-Bowler lineament, with an average trend of approximately N 70° W, is characterized by a core of NW-SE trending faults, folds and volcanic domes that is overprinted by a set of smaller N-NE trending normal faults extending for a distance of at least 150 km from the Pryor Mountains to Livingston, MT to the NW (Wilson, 1936; Foose, 1961). The lineament is interpreted to be the expression of a left-lateral wrench fault at depth (Wilson, 1936; Foose, 1961).

The U-V deposits of the PMD occur on the hanging wall of the Crooked Creek fault (Lopez, 2000). They are concentrated in an approximately 6.4 km zone along the crest of the axis of the south-plunging, fault- propagated Gypsum Creek anticline that forms Red Pryor Mountain (Van Gosen et al., 1996; Lopez, 2000). The deposits show a structural relationship to fractures that trend N 65° W and intersect the crest of the anticline on a trend that includes the East Pryor and LMD group of mines (Lopez, 2000; McEldowney et al., 1977). The East Pryor Mountain group of mines and the LMD are hosted in thrust fault cored structures where the faults have not propagated fully through the structures. The deposits occur near the axes of these structures.

The LMD is located on the gentle W flank portion of the northern Bighorn mountains immediately NW of Little Mountain, just south of the Montana Wyoming state line (McEldowney et al., 1977; Hurley, 1996). The U-V deposits of the LMD are concentrated along three major, broad open folds that trend NW-SE between East Pryor Mountain and the Bighorn Mountains (McEldowney et al., 1977; Hurley, 1996). The fold axes trend approximately N 55-60° W and tectonic maps of the area (McEldowney et al.,

1977) indicate that these structures plunge toward the NW and terminate in the north-trending Dryhead and Syke's fault zones, 3-5 km W of Bighorn Canyon. (McEldowney et al., 1977).

General Stratigraphy of the Area

Rocks in the region range from Archean to Quaternary in age (Figure 1.2). Approximately 760-915 m of Paleozoic rock overlie Archean gneiss and schist in the study areas (Stewart, 1958). The main formations of exposure relevant to the U-V deposits in the mining districts include limestones and dolomites of the Mississippian-age Madison Group (Madison Formation in WY) and the Mississippian- to Pennsylvanian-age Amsden Formation that unconformably overlies the Madison Group which host the U-V deposits (Patterson et. al, 1988; Sando and Dutro, 1975; Van Gosen et al., 1998). The uranium-vanadium deposits occur in the upper 58–73 m of the top paleokarst horizon in the Madison Limestone Group. The U-V deposits occur in shallow chaotic breccia bodies that fill solution caverns in the paleokarst. The breccias formed by the collapse of cavern roof and wall rocks accompanied by inflow of overlying Amsden Formation sediments (Van Gosen et al., 1988).

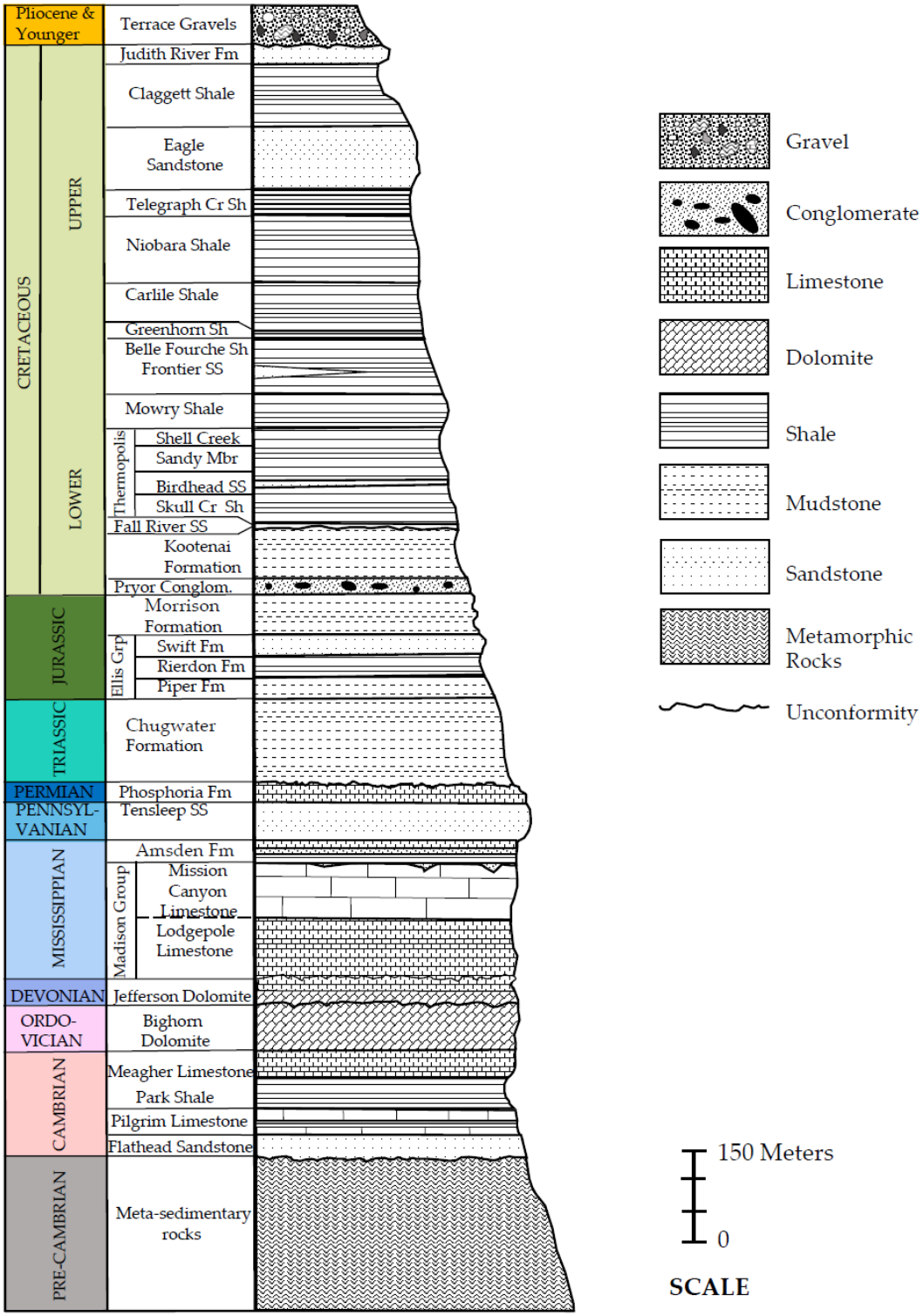


Figure 1.3 Generalized stratigraphic column of the Billings-Pryor Mountain area, Montana, modified from Lopez, 1995.

Dissertation Organization

This dissertation is organized into four chapters. Chapter 2, "The legacy of uranium development on or near Indian Reservations and health implications: rekindling public awareness " is a short review that aims to rekindle the public awareness of the plight of Native American communities living with the legacy of uranium procurement or living in areas that have naturally occurring uranium. The uranium and vanadium that was mined in the study areas of this dissertation was processed in a mill near Riverton, Wyoming. The mill is near the Wind River Reservation, home to Eastern Shoshone and Northern Arapaho Indians. Once milling of uranium ceased after the U.S. Atomic Energy Commission ended its uranium-buying program, the people of the area were left with a legacy of contaminated groundwater and tailings. Increased incidences of cancers among the people living near the site are attributed to the old Susquehanna-Western uranium mill tailings (Schilmoeller, 2012).

Chapter 3, “Potential health risks from uranium in home well water: an investigation by the Apsaálooke (Crow) Tribal Research Group” examines the health risks from uranium contaminated drinking water. After learning that the National Uranium Resource Evaluation (NURE) and Hydrogeochemical and Stream Sediment Reconnaissance (HSSR) database showed elevated uranium concentrations in surface water and well water samples on the Crow Reservation uranium was added as an analyte to test for in an ongoing study. The study is a community based participatory research project (Eggers, 2014). The paper goes through the process of community-based participatory research and looks at health risks associated with uranium in drinking water.

Chapter 4, “Structural controls and geochemical characterization of breccias in paleokarst in the northern Bighorn Basin” examines the geochemical characteristics of breccia cements and minerals to establish the origin of fluids that migrated into the deposits. Stable C, O, and radiogenic Sr isotope data are presented that support the episodic hydrothermal nature of tectonic brecciation. Fracture analysis data suggests that the structural control of the mineralization in the Pryor Mountain District is due to the proximity of the ruptured zone of the Crooked Creek fault on the Big Pryor Mountain Block. Structural data from siliceous tectonic breccias suggests that variations of mineralized versus unmineralized breccias are related to the greater frequency of fractures in four of six dominant orientations in the mineralized breccias.

Chapter 5, “REE data support Permian Phosphoria Formation sourced hydrocarbons as a source of metals for U-V mineralization in Mississippian Madison limestone and paleokarst, northern Bighorn basin, Montana and Wyoming” extends the previous chapter by examining the mineralization of the uranium and vanadium deposits to determine the origin of the mineralizing fluids and to define the association of the mineralization to the tectonic hydrothermal breccias to the mineralization. The chapter discusses the geochemical similarities of Permian Phosphoria rock samples and samples from the study areas using rare earth element and trace element analyses. Anomalous concentrations of metals that are often of environmental concern including As, Hg, Mo, Pb, Tl, U, and Zn, are present in both the samples from this study and in samples from many studies conducted by the U.S. Geological Survey over several decades. The mineralogy, including some previously unidentified metal-uranyl vanadate minerals in

the district are discussed. The chapter concludes with a section on the development of silica polyamine composites (SPC's) to aid in removal of U and other toxic metals from contaminated drinking water to tie in with Chapter 3 of U in home well water. The research is also a collaborative effort between tribal participants and academic partners.

Chapter 6 summarizes the main findings of each chapter of this dissertation and discusses their implications. Each chapter demonstrates a different lens through which to view the mobilization of uranium and the effects that uranium mobilization in the environment has had and will continue to have.

REFERENCES

1. Bird, P. Stress direction history of the western United States and Mexico since 85 Ma. *Tectonics* **2002**, 21, 1-12.

2. Blackstone, D. L., Jr. Structure of the Pryor Mountains, Montana. *J Geol* **1940**, 48, 6, 590-618.

3. Blackstone, D. L., Jr. Foreland deformation: compression as a cause. *Rocky Mountain Geology* **1980**, 18, 2, 83-100.

4. Blackstone, D.L., Jr. Foreland compressional tectonics: southern Bighorn Basin and adjacent areas, Wyoming: Geological Survey of Wyoming Report of Investigations, 1986, 34, 27.

5. Blackstone, D.L., Jr.; Huntoon, P.W. Tectonic structures responsible for anisotropic transmissivities in the Paleozoic aquifers of the southern Bighorn Basin: Wyoming: U.S. Geological Survey Research Project Technical Completion Report G-879, 1984, 2, 1-74.

6. Broadhead, R.F.; Robertson, J.M. Introduction to the atlas, *in* Robertson, J.M., and Broadhead, R.F., eds., Atlas of major Rocky Mountain gas reservoirs: New Mexico Bureau of Mines and Mineral Resources, 1993, 206 p.

7. Brown, W.G. Structural style of Laramide basement-cored uplifts and associated folds, *in* Snoke, A., Steidtmann, J., and Roberts, S., eds. Geology of Wyoming: Geological Survey of Wyoming Memoir 1993, 5, 312-371.

8. Cummins, C.; Eggers, M.; Hamner, S.; Camper, A.; Ford, T.E. Mercury levels detected in fish from rivers of the Crow Reservation, Montana. Poster presented at: 2009 SCREES National Water Conference; February 8-11, 2009; St. Louis, MO.

9. Cummins, C.; Doyle, J.; Kindness, L.; Young, S.; Ford, T.; Eggers, M. Community Based Risk Assessment of Exposure to Contaminants via Water Sources on the Crow Reservation in Montana. In Proceedings of the EPA National Tribal Science Forum, Traverse City, MI, USA, 6–10 June 2010.

10. Cummins, C.; Doyle, J.; Kindness, L.; Lefthand, M.J.; Bear Don't Walk, U.J.; Bends, A.L.; Broadaway, S.C.; Camper, A.K.; Fitch, R.; Ford, T.E.; *et al*. Community-based participatory research in Indian country: Improving health through water quality research and awareness. *Fam Community Health* **2010**, 33, 166–174.

11. Dickinson, W. R.; Klute, M. A.; Hayes, M. J.; Janecke, S. U.; Lundin, E. R.; McKittrick, M. A.; Olivares, M. D. Paleogeographic and paleotectonic setting of Laramide sedimentary basins in the central Rocky Mountain region. *Geol. Soc. Am. Bull.* **1988**, 100, 1023-1039.

12. Doyle, J.T., Kindness, L., Bear Don't Walk, U.J., Realbird, J., Eggers, M.J., Bends, A.L., Crow Environmental Health Steering Committee and Camper, A.K., 2012, For as Long as the Grass Shall Grow and the Rivers Shall Flow: Making Clean Water a Sovereign Responsibility. Plenary Talk. Proceedings of the National Congress of American Indians Tribal Leader/Scholar Forum, Lincoln, NE, USA.

13. Energy Laboratories, Billings, MT Branch. Certificate and laboratory results, October, 2011. Certifications/quality control. Available online: http://www.energylab.com/why-us/certifications-quality-control/ (accessed October 2011).

14. EPA, U.S. Environmental Protection Agency, Summary of the Clean Water Act. Available online: http://www.epa.gov/laws-regulations/summary-clean-water-act (accessed November 14, 2015).

15. Erslev, E.A. Thrusts, back-thrusts, and detachment of Rocky Mountain foreland arches, In *Laramide basement deformation in the Rocky Mountain foreland of the western United States*; Schmidt, C.J., Chase, R.B., Erslev, E.A., Eds.; *Geol. Soc. Am.* Special Paper 280, **1993**, 339-358.

16. Ford, T.E., Eggers, M.J., Old Coyote, T.J., Good Luck, B. and Felicia, D.L. Additional contributors: Doyle JT, Kindness L, Leider A, Moore-Nall A, Dietrich E, Camper AK. Comprehensive community-based risk assessment of exposure to water-borne contaminants on the Crow Reservation. EPA Tribal Environmental Health Research Program Webinar presented October 17, 2012.

17. Hamner, S., Broadaway, S.C., Berg, E., Stettner, S., Pyle, B.H., Big Man, N., Old Elk, J., Eggers, M.J., Doyle, J., Kindness, L.; et al. Detection and source tracking of *Escherichia coli*, harboring intimin and Shiga toxin genes, isolated from the Little Bighorn River, Montana. *Int J Environ Health Res* **2014**, 24, 341–362.

18. Hurley, G. Geology and Mineralogy of the Devil Canyon/Little Mountain Area, Northern Big Horn Mountains, Wyoming. In *Resources of the Bighorn Basin*; 47th Annual Field Conference Guidebook; Wyoming Geological Association: Casper, WY, USA, 1996, pp. 281-295.

19. Lopez, D.A. Field guide to the northern Pryor Bighorn structural block, south central Montana. Open-File Report 330. Montana Bureau of Mines and Geology, Butte, Montana, USA, 1995, 26 p.

20. McEldowney, R.C.; Abshier, J.F.; Lootens, D.J. Geology of uranium deposits in the Madison Limestone, Little Mountain area, Big Horn County, Wyoming. In *Exploration frontiers of the Central and Southern Rockies*; Veal, H.K., Ed.; Rocky Mountain Association of Geologists. 1977, pp. 321-336.

21. McOliver, C.A.; Camper, A.K.; Doyle, J.T.; Eggers, M.J.; Ford, T.E.; Lila, M.A.; Berner, J.; Campbell, L.; Donatuto, J. Community-Based Research as a Mechanism to Reduce Environmental Health Disparities in American Indian and Alaska Native Communities. *Int J Environ Health Res.* **2015**, 12, 4, 4076-4100.

22. Montana Bureau of Mines and Geology Ground Water Information Center. Available online: http://mbmggwic.mtech.edu/ (accessed February, 2011).

23. Montana Department of Environmental Quality Montana's Clean Water Act Information Center (MCWAIC). Available online: http://deq.mt.gov/wqinfo/cwaic/reports.mcpx (accessed July, 2016).

24. Montana Natural Resources Information System. Available online: http://nris.mt.gov (accessed February 2011).

25. National Uranium Resource Evaluation (NURE) Hydrogeochemical and Stream Sediment Reconnaissance (HSSR) Program's database for Montana and Wyoming. Available online: http://tin.er.usgs.gov/nure/water/ (accessed February 2011).

26. Natural Resource Conservation Service's Data Gateway. Available online: http://datagateway.nrcs.usda.gov/ (accessed February 2011).

27. Neely, T.G.; Erslev, E.A. The interplay of fold mechanisms and basement weaknesses at the transition between Laramide basement-involved arches, north-central Wyoming, USA. *J Struct Geol* **2009**, 31, 1012-1027.

28. Patterson, C.G.; Toth, M.I.; Kulik, D.M.; Esparza, L.E.; Schmauch, S.W.; Benham, J.R. *Mineral Resources of the Pryor Mountain, Burnt Timber Canyon, and Big Horn Tack-On Wilderness Study Areas, Carbon County, Montana and Big Horn County, Wyoming*; U.S. Geological Survey Bulletin 1723; U.S. Geological Survey: Denver, CO, USA. 1988, pp. 1–15.

29. Peterson, D.A.; Boughton, G.K. Organic compounds and trace elements in fish tissue and bed sediment from streams in the Yellowstone River Basin, Montana and Wyoming, U.S. Geologic Survey Water-Resources Investigations Report 00-4190, 1998, 46 p.

30. Peterson, D.A.; Zelt, R.B. Element concentrations in bed sediment of the Yellowstone River Basin, Montana, North Dakota, and Wyoming - A retrospective analysis, U.S. Geologic Survey Water-Resources Investigations Report 99-4185, 1999, 30 p.

31. Sando, W.J.; Gordon Jr., M.; Dutro Jr., J.T. Stratigraphy and geologic history of the Amsden Formation (Mississippian and Pennsylvanian) of Wyoming: U.S. Geological Survey Professional Paper 858-A, 1975, 78 p.

32. Schilmoeller, J. Decades of Environmental Injustice: Wyoming Indian Reservation Faces High Cancer Rates. Mint Press News, 2012. Available online: http://www.mintpress.net/decades-of-environmental-injustice-wyoming-indian-reservation-faces-deteramental-rates-of-cancer/ (accessed on 13 December 2012).

33. Smith, S. M. National Geochemical Database: Reformatted Data from the National Uranium Resource Evaluation (NURE) Hydrogeochemical and Stream Sediment Reconnaissance (HSSR) Program: U.S. Geological Survey Open-File Report 97-492, 1997.

34. Stewart, J.C. Geology of the Dryhead-Garvin Basin, Bighorn and Carbon Counties, Montana: Map G-2; Montana Bureau of Mines and Geology Special Publication 17; Montana Bureau of Mines and Geology: Montana Tech of the University of Montana, Butte, MT, USA, 1958.

35. Stricker, G.D.; Ellis, M.S. Coal Quality and Geochemistry, Powder River Basin, Wyoming and Montana. In *1999 Resource assessment of selected Tertiary coal beds and zones in the northern Rocky Mountains and Great Plains region*, U.S. Geological Survey Professional Paper 1625-A, 1999.

36. University of Wyoming's Water Resources Data System. Available online: http://www.wrds.uwyo.edu/ (accessed on 4 February 2013).

37. USGS Water Quality Data for Wyoming. Available online: http://waterdata.usgs.gov/wy/nwis/qw (accessed on 4 February 2013).

38. U.S. Department of Energy, Billings quadrangle-Residual intensity magnetic anomaly contour map: US Department of Energy, 1982, GJM-096, pl.4.

39. Van Gosen, B.S.; Wilson, A.B.; Hammarstrom, J.M. Mineral Resource Assessment of the Custer National Forest in the Pryor Mountains, Carbon County, South-Central Montana, U.S. Geological Survey Open-File Report 96-256; U.S. Geological Survey: Denver, CO, USA, 1996, 76 p. Available online: https://pubs.er.usgs.gov/publication/ofr96256

40. Wyoming Geographic Information Center. Available online: http://wygl.wygisc.org/wygeolib (accessed on 4 February 2013).

41. National Uranium Resource Evaluation (NURE) Hydrogeochemical and Stream Sediment Reconnaissance (HSSR) Program's data base for Montana and Wyoming. Available online: http://tin.er.usgs.gov/nure/water/ (accessed on 18 February 2013).

42. Wyoming State Geological Survey website. Oil and Gas map. Available online: http://www.wsgs.wyo.gov/products/wsgs-2016-ms-103.pdf (Accessed: 8 October, 2016).

CHAPTER 2

THE LEGACY OF URANIUM DEVELOPMENT ON OR NEAR INDIAN RESERVATIONS AND HEALTH IMPLICATIONS REKINDLING PUBLIC AWARENESS

Contribution of Authors and Co-Authors

Manuscript in Chapter 2

Author: Anita L. Moore-Nall

Contributions: Conceived the study, reviewed the literature, and wrote the manuscript.

Manuscript Information Page

Anita L. Moore-Nall
Journal name: GeoSciences
Status of Manuscript:
____ Prepared for submission to a peer-reviewed journal
____ Officially submitted to a peer-review journal
____ Accepted by a peer-reviewed journal
__X_ Published in a peer-reviewed journal

Published by MDPI AG, Basel, Switzerland
February 2015, Volume 5, Issue 1, Special Issue Medical Geology: Impacts of the Natural Environment on Public Health

COPYRIGHT

The following chapter has been published in the journal Geosciences. This is an open access article distributed under the Creative Commons Attribution License which permits unrestricted use, distribution, and reproduction in any medium, provided the original work is properly cited and is published here: doi:10.3390/geosciences5010015 in agreement with the journal's copyright policy. No written permission is needed. The full citation of the published article is:

Moore-Nall, A. The Legacy of Uranium Development on or Near Indian Reservations and Health Implications Rekindling Public Awareness. *Geosciences* **2015**, *5*, 15-29.

CHAPTER 2

THE LEGACY OF URANIUM DEVELOPMENT ON OR NEAR INDIAN RESERVATIONS AND HEALTH IMPLICATIONS REKINDLING PUBLIC AWARENESS

Anita Moore-Nall

Department of Earth Sciences, Montana State University, P.O. Box 173480, Bozeman, MT 59717, USA

Abstract: Uranium occurrence and development has left a legacy of long-lived health effects for many Native Americans and Alaska Natives in the United States. Some Native American communities have been impacted by processing and development while others are living with naturally occurring sources of uranium. The uranium production peak spanned from approximately 1948 to the 1980s. Thousands of mines, mainly on the Colorado Plateau, were developed in the western U.S. during the uranium boom. Many of these mines were abandoned and have not been reclaimed. Native Americans in the Colorado Plateau area including the Navajo, Southern Ute, Ute Mountain, Hopi, Zuni, Laguna, Acoma, and several other Pueblo nations, with their intimate knowledge of the land, often led miners to uranium resources during this exploration boom. As a result of the mining activity many Indian Nations residing near areas of mining or milling have had and continue to have their health compromised. This short review aims to rekindle the public awareness of the plight of Native American communities living with the legacy of uranium procurement, including mining, milling, down winders, nuclear weapon development and long term nuclear waste storage.

Keywords: uranium; Native Americans; community based participatory research; abandoned mines; reservations

1. Introduction

Native American communities on American Indian reservations located with natural resources on or near their lands may be at a greater risk for environmentally induced ailments [1]. The impact of natural resource development has not always been fully recognized with respect to the cultural and health effects of the people and animals of these lands. Sometimes the effects are not realized until after the fact when problems associated with resource extraction or cleanup may already be impacting the health of the population [2–8]. On some reservations a lack of education and knowledge about the effects of geologic materials such as uranium and coal led to long term health problems when resources were developed [7]. In this short review the effects of uranium procurement will be addressed, though many other factors may also be contributing to poor health of the Native American populations with natural resources on or near their lands.

Technologically-enhanced, naturally-occurring radioactive material (TENORM) is produced when activities such as uranium mining or milling concentrate or expose radioactive materials that occur naturally in ores, soils, water, or other natural materials [9]. Radioactive materials can be classified under two broad headings: man-made and naturally occurring radioactive materials (NORM). Both of these materials affect many Americans but especially the Native American populations in the United States and Canada, whose designated lands host uranium deposits. Mining of uranium by

underground and surface methods produces bulk waste material, including tailings and overburden. During mining the waste rock and soil have little or no practical use, they are generally stored on land near the mine site [10,11]. These materials contain NORM which may become dispersed in the environment through airborne dust and contaminated water. Continued exposure to these materials can cause severe health problems [10,12]. Abandoned conventional uranium mines often contain other hazardous contaminants, such as metals. For example, the carcinogen arsenic may be a problem at some uranium mines, contributing to increased health risks [11].

1.1. The Quest for Uranium

The origin of the Department of Energy is traced to World War II and the Manhattan Project effort to build the first atomic bomb [13]. The "Manhattan Project" was conducted mainly at the Los Alamos National Scientific Laboratory, a huge fortified compound created in 1943 [14] on the Pajarito Plateau, northwest of Santa Fe, New Mexico, on land supposedly reserved for the exclusive use and occupancy of the San Ildefonso Pueblo [15]. Uranium, the key material used in the lab's experiments and eventual fabrication of prototype nuclear weapons, was mined and milled in four centers of the nearby Navajo Reservation [6,9,16] including reservation land near Shiprock, New Mexico; Monument Valley, Utah; Church Rock, New Mexico; and Kayenta, Arizona. Hanford, a uranium enrichment/plutonium manufacturing facility, was added in 1943, near the town of Richland, on Yakima land in eastern Washington [16,17]. The Hanford area bordering the Columbia River was home to several tribes of Native Americans for centuries. Remnants, artifacts, and burial sites associated with historical Native American

activity are found throughout the Site and are protected by law [16]. On 16 July 1945, the world's first atomic bomb was detonated 200 miles south of Los Alamos at Trinity Site on the Alamogordo bombing range [13,14], now the White Sands Test Range, adjoining the Mescalero Apache Reservation. It is this quest for uranium and these different aspects of the procurement plus the disposal and storage of waste that continues to contribute to poor health among many Native American populations. Many cancer clusters and other ailments are attributed to this quest.

1.2. Uranium Production on Native American Lands

The uranium production peak spanned from approximately 1948 to the early 1980s primarily to produce uranium for weapons and later for nuclear fuel [9,10]. Thousands of mines, mainly on the Colorado Plateau, were developed in the western U.S. during the uranium boom. Native Americans in the area including the Navajo, Southern Ute, Ute Mountain, Hopi, Zuni, Laguna, Acoma, and several other Pueblo nations, with their intimate knowledge of the land often led miners to uranium resources during this exploration boom [5,8]. There are about 4000 uranium mines with documented production [10]. With information provided by other federal, state, and tribal agencies, the Environmental Protection Agency (EPA) has identified 15,000 abandoned uranium mine locations with uranium occurrence in 14 western states with about 75% of those on federal and tribal lands [10]. The majority of these sites were conventional (open pit and underground) mines [10]. Between 1950 and 1989 surface and underground mines in the U.S. produced more than 225 million tons of uranium ore [8]. Figure 2.1 shows the abandoned uranium mines in the western United States.

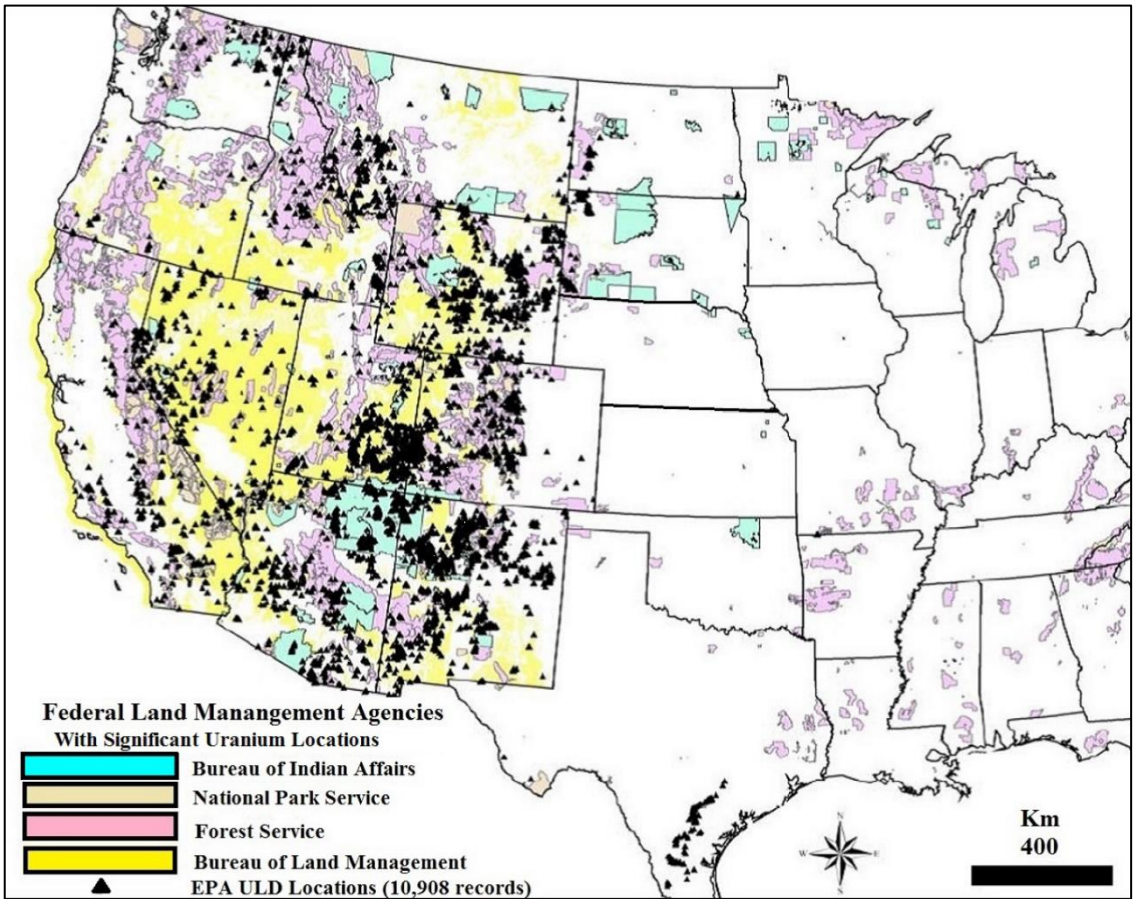


Figure 2.1. Uranium locations from Environmental Protection Agency (EPA) database and Federal Lands. The green federal lands are Native American reservations. About three-fourths of the uranium locations in the EPA Uranium Location Database are on Federal Lands. Figure is modified from Geographic Analysis on the Location of Uranium Mines [9].

1.2.1. The Navajo Nation

The Navajo Nation was one of the Indian nations heavily affected by this activity with more than a thousand mines and four uranium mills on the reservation lands [5,6,8]. When mining came to the reservation the Navajo men were ready to gain employment and the close work seemed ideal. What they didn't realize was that they were being exposed to radiation when they worked and brought it home with them in their clothing

to their families [6]. Energy material may contain harmful chemical substances that, if mobilized into air, water, or soil, can adversely impact human health and environmental quality [18]. As a result of the mining activity much of the population of the Navajo Nation residing near the areas of mining or milling has had their health compromised. Many of the miners developed cancers; some were lung cancer from inhalation of radioactive particles, *i.e.*, exposure to radon [6]. Of the 150 Navajo uranium miners who worked at the uranium mine in Shiprock, New Mexico until 1970, 133 died of lung cancer or various forms of fibrosis by 1980 [19]. Other potential health effects include bone cancer and impaired kidney function from exposure to radionuclides in drinking water [12]. The government and the mining companies failed to inform the people of the Navajo Nation that working with uranium might be hazardous to one's health [2–8]. The Public Health Service even conducted a study to document the development of illnesses as the mining progressed without consent or presenting the data to the miners involved [5,8]. Most of the 1000 unsealed tunnels, unsealed pits and radioactive waste piles still remain on the Navajo reservation today, with Navajo families living within a hundred feet of the mine sites [9,20]. Some of the homes were built with tailings material and much of the water is contaminated on the reservation [20]. Figure 2.2 shows a sign erected by the Navajo and U.S. EPA which is typical for many of the water sources on the reservation.



Figure 2.2. Sign erected by the Navajo and U.S. EPA which is typical for many of the water sources on the reservation. Figure from EPA Pacific Southwest Region 9 Addressing Uranium Contamination on the Navajo Nation [21].

1.2.2. Laguna Pueblo Tribe

The Village of Paguate (Laguna Pueblo), 40 miles west of Albuquerque, New Mexico was host to the largest open-pit uranium mine in the United States, the Jackpile Mine [22,23]. The mine was the largest producer of uranium ore in the Grants District [24]. Though the site was officially reclaimed in 1995 it is being considered for a National Priorities Listing (NPL) with the EPA after a Record of Decision (ROD) Compliance Assessment for Jackpile-Paguate Uranium Mine was performed to determine if the post-reclamation had met the requirements of the Environmental Impact Statement and ROD. This report concluded that reclamation of the mine was still not complete. The Laguna Pueblo, representing a population of about 8000, rejected mining company offers to operate a uranium mill on tribal land. The mill was built just down the road at Bluewater, now another Superfund site [25].

1.2.3. The Eastern Shoshone and Northern Arapaho Nations

Uranium mining and processing has also left a legacy of contaminated groundwater and tailings on the Wind River Reservation, Wyoming, home to Eastern Shoshone and Northern Arapaho Indians. Increased incidences of cancers among its peoples are attributed to the old Susquehanna-Western uranium mill tailings site [26]. The site is a few miles southwest of Riverton, the ninth most-populated city in Wyoming. In some areas of the Wind River Indian Reservation groundwater contamination is so bad that the Department of Energy (DOE) estimates drinking water from contaminated aquifers could make residents up to 10 times more likely to develop cancer than the general population [26]. Uranium was not mined on the Wind River Reservation but uranium mined in the Pryor Mountains, Montana and Northern Bighorn Mountains, Wyoming was some of the ore processed there.

1.2.4. The Sioux Nations

Uranium mining in South Dakota, Wyoming, Montana, and North Dakota began in the middle of the 1950s [1]. More than 1000 open-pit uranium mines and prospects can be found in the four state region according to U.S. Forest Service maps. There were numerous uranium mines throughout the southern Black Hills National Forest as well as in Custer National Forest near the Lakota-Sioux lands in the Black Hills of South Dakota, which also had mines [1]. Most of these have not been reclaimed.

1.2.5. The Spokane Nation

The only uranium mining in Washington State was on the Spokane Indian Reservation. The mines were the Sherwood Uranium Mine and the Midnite Uranium

Mine, which opened in the 1950s to produce uranium for the U.S.-Soviet nuclear arms race [27]. Just as on the Navajo reservation the mines brought needed employment to the reservation at that time and the miners were not informed of the dangers uranium mining [28]. About 33 million tons of radioactive waste rock and ore remain at the 350-acre site above the Spokane River [27]. The mines have been closed since the 1980s. The Midnite Mine site, the larger of the two uranium mines on the reservation is a superfund site [27]. Newmont Mining Co. (Greenwood Village, Colorado, USA) and its subsidiary, Dawn Mining Co. (Ford, Washington, USA) expects to begin cleanup of the Midnite Mine in 2015 [27]. "The plan is to fill in open pits left from the mine excavations with the waste rock and ore. The pits would be capped to keep radon gas from escaping. Groundwater in the pits will be collected and treated and then piped 7 miles to the Spokane River" stated a consultant from Newmont [27]. "Newmont already collects and treats water at the old mine site, but that water is currently discharged into Blue Creek, a tributary of the Spokane River. Discharging the treated wastewater directly into the Spokane River will reduce the impacts to Blue Creek, where the tribe is working to re-establish a native Redband Trout run" stated the Superfund director for the Spokane Tribe [27]. "The water discharged into the Spokane River must meet the tribe's water quality standards for radionuclides, heavy metals and other pollutants, which are stricter than state and federal standards. The cleanup work is also subject to permits from the U.S. Environmental Protection Agency" [27] Members of the Spokane Tribe who worked at the mine or who live on the reservation are questioning the high rates of cancer on the reservation [28].

The Spokane Tribe teamed up with the Washington Department of Health and the Northwest Indian Health Board to track cancer rates among the tribe's 2700 members living with the legacy of the mining from the Sherwood and Midnite uranium mines [28]. Study results are pending [28].

1.3. Nuclear Weapons Development

Pacific Northwest tribal groups on nine reservations in Washington, Idaho and Oregon were impacted by Hanford Nuclear reservation activities [29]. The Hanford Nuclear site is located on 1518 square km of shrub-steppe desert in southeastern Washington State [17] surrounded by these nine reservations (Figure 2.3).

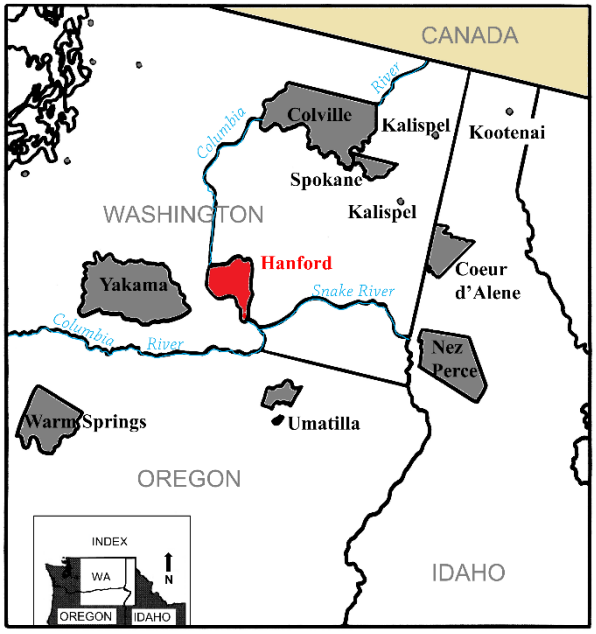


Figure 2.3 Hanford Nuclear Reservation, shown in red, was located in the state of Washington. Nine Native American reservations surround it. Figure modified from Edward Liebow in Hanford, Tribal Risks, and Public Health [29].

The people of these reservations traditionally used [17] and continue to use the lands and resources from the Columbia River Plateau region including land that was ceded to the government for which they retained hunting and gathering privileges [29]. Thus, they may have been exposed to more radiation and contaminants than the general public in practicing traditional lifestyles while fishing, hunting game, food gathering (berries, root plants, *etc.*) harvesting medicinal plants and traditional practices (*e.g.*, sweats), as well as social and spiritual interaction networks [29]. This region was contaminated by Hanford activities through primarily two distinct forms: airborne and river-borne releases, both normal operations and some accidental releases [29]. During the period from 1944 to 1972 Hanford released 25 million curies of radioactive contamination into the environment. As a comparison, the Chernobyl plant released between 35 and 49 million curies of iodine-131 (I-131) [29]. Five of the reservations, the Colville Confederated Tribes, Spokane, Kalispel, Kootenai, and Coeur D'Alene are primarily downwind of Hanford Nuclear site's 1450 square kilometer area (Figure 3.3) and would have been exposed to the airborne release of radioactive contamination for the most part normal by-product of chemical reactions used to separate weapons-grade plutonium from enriched uranium reactor rods, *i.e.*, I-131 with less of a contribution of the river borne releases [29]. The other four reservations, the Nez Perce, Confederated Tribes of the Umatilla, Confederated Tribes and Bands of the Warm Springs and the Yakama Nation are known to consume large quantities of fish and likely received higher doses of river borne releases which resulted from both accidental releases and normal operations that used Columbia River water to cool weapon-production reactor cores [29]. Additionally, liquid

waste that had been poured onto the ground or held in ponds or trenches at the Hanford reservation evaporated or soaked into the soil on the site [30]. The waste contaminated some of the soil and is thought to have also created underground “plumes” of contaminants [30] which could also affect the tribes who consumed native food sources in the area. These nine reservations were all part of the Intertribal Council on Hanford Health Projects established in 1994 when all tribal governing bodies involved agreed on bylaws and operations plans for the council [29]. The group sought to give the tribal perspective of the information needed for estimating radiation doses from distinctive traditional lifestyles of the represented tribes and protect their sovereignty in public health research while also ensuring the scientific integrity of the research involving their people and land [29]. The final report of the federal government’s Hanford Thyroid Disease Study (HTDS), a dose-based analysis epidemiological study conducted under contract by researchers at the Fred Hutchinson Cancer Research Center in Seattle from 1989 to 2002 [30], showed northwest U.S. residents with childhood radiation exposures from Washington State’s Hanford nuclear site had similar risk levels for thyroid cancer and other thyroid disease regardless of their radiation dose [31]. Many people were dissatisfied with the results of the report and have lawsuits pending [30]. The study was not specific to Native American communities though “the authorizing language which provided funding for the study specifically required that thyroid disease among Native Americans be studied. However, no study focusing on thyroid disease among Native Americans was ever completed.” ([29], p. 152). According to the HTDS summary report: “based on information from Native American Tribes and Nations, a study such as the

HTDS in Native American populations alone was not feasible because it would have too little chance of detecting any health effects from Hanford's iodine-131" [32]. Native Americans were included in the HTDS if they were identified in the group that made up the study cohort [32]. The study used computer programs from Hanford Environmental Dose Reconstruction Project (1987–1994) and interviews with participants to estimate I-131 doses for 3440 people born between 1940 and 1946 to mothers living in seven Washington counties. It took nearly 13 years to complete and cost $18 million dollars [31]. The site is an environmental cleanup project that approximately 11,000 Hanford employees are involved with today [30].

1.4. Milling and Abandoned Mills

Over ninety percent of all milling done in the U.S. occurred on or just outside the boundaries of American Indian reservations [33]. Mills logically would be located near the production or mine sites for infrastructure, thus many mills were on or near the reservations where uranium mining was operating. A disaster of huge consequence for the Navajo Nation occurred at the Church Rock uranium mill spill on 16 July 1979, in New Mexico when United Nuclear Corporation's Church Rock uranium mill tailings disposal pond breached its dam [34]. Over 1000 tons of solid radioactive mill waste and 93 million gallons of acidic, radioactive tailings solution flowed into the Puerco River, and contaminants traveled 130 km downstream onto the Navajo Nation [35]. The mill was located on privately owned land approximately 27 km north of Gallup, New Mexico, and bordered to the north and southwest by Navajo Nation Tribal Trust lands [35]. Local residents, who were mostly Navajos, used the Puerco River for irrigation and livestock

and were not immediately aware of the toxic danger [34]. The Navajo Nation asked the governor of New Mexico to request disaster assistance from the U.S. government and have the site declared a disaster area, but he refused, limiting disaster relief assistance to the Navajo Nation [34]. In terms of the amount of radiation released, the accident was larger in magnitude than the Three Mile Island accident of the same year [34] but received little public attention. This was likely due to the remoteness and sparsely populated area of the Navajo Nation which was impacted by the spill. The area was inhabited by mainly Navajo people, many who only spoke their native tongue [34]. This is in contrast to the highly populated area of Middletown, Pennsylvania located three miles from the Three Mile Island Nuclear Generating Station where the TMI accident occurred. Possibly the greater significance of a nuclear power plant *versus* a tailings dam may also have influenced media coverage.

2. Indian Health Service, Census Data and Health Disparities

2.1. Indian Health Service

To evaluate health issues of Native American populations one must be aware of the unique relationship that American Indians and Alaska Natives (AI/AN) have with the federal government. The provision of health services to members of federally recognized tribes grew out of the government-to-government relationship, established in 1787, between the federal government and Indian tribes in exchange for tribal lands. This relationship is based on Article I, Section 8 of the Constitution, and has been given form and substance by numerous treaties, laws, Supreme Court decisions, and Executive Orders [36,37]. The Indian Health Service (IHS), an agency within the Department of

Health and Human Services, is responsible for providing federal health services to AI/AN. Approximately 2 million of the 3.4 million AI/AN, members of 566 federally recognized tribes across the U.S., are served by the IHS [36,37]. The organization has fulfilled the federal government's responsibility since 1955. The AI/AN health system has evolved greatly since then and now consists of IHS hospitals and health centers managed by the federal government, tribally managed services, and urban Indian health programs [38]. There are 12 Area offices, which are further divided down into 168 Service Units that provide care at the local level; most of these are rural primary care systems and are staffed by 70% native employees [36].

Tribal involvement and collaboration is an important aspect of the IHS in meeting the health needs of its service population [37]. Tribal delegation meetings are a form of tribal consultation where elected tribal officials meet with the IHS Director or senior staff to discuss health policy and program management issues related to the provision of health services to the Indian population. The IHS has an official Tribal Consultation Policy [37]. There are also programs with committees, task forces, boards and workgroups set up within the IHS system to address different aspects of policy and communication between the tribes and the federal government.

One of these programs is the Environmental Health Services (EHS) program. It includes the specialty areas of injury prevention and institutional environmental health. The IHS EHS program identifies environmental hazards and risk factors in tribal communities and proposes control measures to prevent adverse health effects. These measures include monitoring and investigating disease and injury in tribal communities;

identifying environmental hazards in community facilities such as food service establishments, Head Start Centers, community water supply systems, and health care facilities; and providing training, technical assistance, and project funding to develop the capacity of tribal communities to address their environmental health issues [38]. The current IHS director is Yvette Roubideaux, M.D., M.P.H., a member of the Rosebud Sioux Tribe, South Dakota; she has served since May of 2009.

2.2. Census Data and Disparities

In the 2010 U.S. Census, 5.2 million people (about 1.7% of the U.S. population) identified themselves as AI/AN, solely or in combination with one or more racial/ethnic groups [39]. This population is concentrated in the west and south and proximate to AI/AN areas (reservations/trust lands) for most of the population [39]. AI/AN people consistently experience lower health status when compared with other Americans. The health status of AI/AN is affected by a number of environmental hazards, such as living in remote and isolated locations that expose residents to severe climatic conditions, hazardous geography, and disease-carrying insects and rodents, limited availability of housing and extensive use of sub-standard housing, unsanitary methods of sewage and waste disposal, and unsafe water supplies [40]. Lower life expectancy and the disproportionate disease burden exist possibly due to inadequate education, disproportionate poverty, discrimination in the delivery of health services, cultural differences and geographic location [40]. This population is concentrated in the west and south and proximate to AI/AN areas (reservations/trust lands) for most of the population [39]. AI/AN have the highest national poverty at 27.0%; nine states had poverty rates of

about 30% or more for AI/AN: Arizona, Maine, Minnesota, Montana, Nebraska, New Mexico, North Dakota, South Dakota, and Utah [39]. There are many interwoven quality of life issues associated with life in native settings. These are broad issues deeply rooted in economic adversity, poor social conditions and a struggle to maintain a cultural identity while assimilating with U.S. society. A major cause of poverty in Native American communities is the persistent lack of opportunity; even most of the communities with natural resources on their lands are faced with high poverty. The Economic Research Service reports that Native American communities have fewer full-time employed individuals than any other high-poverty community. Mortality rates in AN populations are 60% higher than those of the U.S. white population [41, 42], and mortality in AI populations are about twice that of the general U.S. population [43]. In addition, AI/AN have the lowest cancer survival rates among any racial group in the United States [44]. Native Americans in the Northern Plains region have a cancer mortality rate approximately 40% higher than that of the overall population [45].

There is sufficient evidence of disparities in health care financing, access to care, and quality of care to conclude that American Indians and Alaska Natives are disadvantaged in the health care system [33, 34]. Comparing per capita personal health care expenditures on user population the IHS expenditure is $2741 while the total U.S. population expenditure is $7239 [37]. Due to the remoteness of many of the IHS facilities and funding available not all IHS facilities have the capabilities to address all the needs of the population. Contract health services (CHS) are purchased based on a priority system. The IHS is the Payor of Last Resort which requires patients to exhaust all health care

resources available to them from private insurance, state health programs, and other federal programs before IHS can pay through the CHS program [40].

2.2.1. Toxic Waste Storage

When conditions exist of such extreme poverty for many Native American communities they have been approached by companies wanting to store toxic wastes on their lands. This creates hard situations for some tribes who would like the added "income" but desire to have a safe environment to live in. The Mescalero Apache, Prairie Island Mdewakanton, Minnesota Sioux, Skull valley Goshutes, Lower Brule, two Alaskan native communities, Chickasaw, Sac and Fox, Eastern Shawnee, Quassarie, and Ponca Tribes have all applied to be sites for Monitored Retrievable Storage (MRS), a temporary solution to the problem of storing vast amounts of high-level nuclear waste [46]. The safety of these sites is still under question.

2.2.2. Radiation Exposure Compensation Act

The Radiation Exposure Compensation Act passed in 1990 and amended in 2000 [46], was set up to make partial restitution to the people who contracted cancer and a number of other specified diseases as a direct result of mining, mill working or their exposure to atmospheric nuclear testing undertaken by the United States during the Cold War [6]. For miners the requirements such as whether the miner was a smoker, how long they had worked, whether the mine(s) they were employed in had radon exposure monitoring, medical proof of lung cancer or a nonmalignant respiratory disease, *etc.* made it very difficult for the people to be accepted in the program. Many miners were designated as smokers even though they may have only smoked the equivalent of a pack of cigarettes

over a year, in ceremonial practices which increased the WLM (working level months—a measure of radon exposure based on Social Security work records and exposure to radon) required to 500 unless they contracted lung cancer under age 45 then it was 300 WLM [6]. The stringent, often impossible requirements made attaining this compensation hard for most of the victims involved. Many of the people are still trying to be compensated.

3. Discussion and Conclusions

The legacy of uranium procurement has left a legacy of long-lived health effects for many Native Americans and Alaska Natives in the United States. There have been a number of studies that are starting to address the health impacts of this legacy. The largest population and some of the most impacted people are the tribes living in the southwestern USA, especially the Navajo. A consortium of federal and tribal agencies reported that a five-year, $110 million project to clean up uranium contamination in the Navajo Nation had addressed the most urgent risks there [47]. But the report also said that in the last five years the agencies have learned much more "about the scope of the problem and it is clear that additional work will be needed" [47]. The consortium included the U.S. Environmental Protection Agency, the Bureau of Indian Affairs, Nuclear Regulatory Commission, Department of Energy and Indian Health Service. The project started in 2007 to tackle the widespread uranium contamination on Navajo lands left over from the nation's atomic weapon production programs. Among their accomplishments, the agencies reported that they have cleaned up nine abandoned uranium mines, rebuilt 34 homes and replaced contaminated soil at 18 sites, many near homes. The agencies also assessed the status of 520 mines, 240 water sources and 800

homes and public structures, exceeding goals set in the five-year plan, the report said [48,49]. It added that officials shut down three contaminated wells and hauled clean water to affected areas of the Navajo Nation or started projects to pipe in water.

Another study in the Eastern Agency of the Navajo Nation in New Mexico [50], studied environmental uranium contamination in a former mining and milling area. Despite decades of inactivity in the mines and mills, environmental contamination was widespread, often in proximity to homes, areas grazed by livestock, and locations frequented by children and families. The uranium contamination in this area was predominantly in the highly soluble chemical forms that could be spread when disturbed or by the bursts of precipitation that occur in this semiarid region at certain times of the year [50].

The Navajo Birth Cohort Study will use Community Based Participatory Research (CBPR) methods [51] and is a collaborative effort to better understand the relationship between uranium exposures and early developmental delays on the Navajo Nation [52]. The five-year Study is funded by Congress at the request of the Navajo Nation and in response to concerns expressed by women about health impacts of living near abandoned uranium mines [53]. Partners in the Study include the Centers for Disease Control and Prevention/Agency for Toxic Substances and Disease Registry, Navajo Area Indian Health Service, Navajo Nation Division of Health, University of New Mexico Community Environmental Health Program, UNM Pediatrics Department Center for Development and Disability, and Southwest Research and Information Center [53]. Eligible women are between the ages of 14 and 45 who have lived on the Navajo Nation

for five years, are pregnant, and will deliver at the designated hospitals in Chinle, Gallup, Shiprock, Ft. Defiance, and Tuba City [53].

This short review only provides a quick glance at the continuing legacy of long-lived health effects for many Native American populations due to uranium procurement in the United States. The reader is encouraged to explore some of these topics and become aware of the issues. Native American communities, those on and near reservations, consistently experience lower health status when compared with other Americans. To be able to set up medical geology studies as collaborations within these separate nations, it is important that traditional knowledge is incorporated into the study plans. The non-Native American exposure doses and other variables within each unique study may underestimate necessary values within a study related to Native American communities. Without weighting standard values differently in applied models, or considering different types of variables in GIS and other geospatial tools, the results of the studies may not truly represent the Native American or Alaska Native populations and the effects of the environment or toxic indicator which is studied.

Medical Geology has been shown to be an effective tool in many applications around the world. The sample size of many of the Native American and Alaska Native communities is small for large statistical studies, but increased homogeneity in the small sample sizes due to cultural and traditional values may provide good results, which can be implemented to improve health conditions of the people involved. Funding for projects will also need to be collaborative. Working with programs like the Tribal ecoAmbasadors Program, National Institute of Health, National Science Foundation, the

U.S. Geological Survey, IHS and Tribal colleges may yield productive studies that can be used to help improve the overall health of these communities. The use of community-based participatory research approaches that incorporate Native American social networks can be effective in helping to achieve policy changes to address health issues.

Acknowledgments

Funding for research: Alfred P. Sloan Graduate Scholarship Programs - Minority Ph.D. Component/Sloan Indigenous Graduate Partnership; Montana State University - Dennis and Phyllis Washington Foundation Native American Graduate Fellow; HOPA Mountain Program. Note: The content is solely the responsibility of the author; it has not been formally reviewed by any of the funders.

Conflicts of Interest

The author declares no conflict of interest

References

1. Moore-Nall, A.L.; Lageson, D.R. Lower health status on Indian Reservations a geologic or geographic correlation associated with natural resources? In *Proceedings of the 5th International Conference on Medical Geology*, Arlington, VA, USA, 25–29 August 2013.

2. Brugge, D.; Benally, T.; Harrison, P.; Austin-Garrison, M.; Begay, L.F. Memories come to US in the rain and the wind: Oral histories and photographs of Navajo Uranium miners and their families. In *The Navajo Uranium Miner Oral History and Photography Project*; Tufts School of Medicine: Boston, MA, USA, 1997; pp. 1–63.

3. Brugge, D.; Benally, T. Navajo Indian voices and faces testify to the legacy of uranium mining. *Cult. Surviv. Q.* **1998**, 22, 16–19.

4. Brugge, D.; Benally, T.; Harrison, P.; Austin-Garrison, M.; Stilwell, C.; Elsner, M.; Bomboy, K.; Johnson, H.; Fasthorse-Begay, L. The Navajo Uranium miner oral history and photography project. In *Dine Baa Hane Bi Naaltsoos: Collected Papers from the Seventh through the Tenth Navajo Studies Conferences*; Piper, J., Ed.; Navajo Nation Historic Preservation Department: Window Rock, AZ, USA, 1999; pp. 85–96.

5. Brugge, D.; Goble, R. The history of Uranium mining and the Navajo people. *Am. J. Public Health* **2002**, 92, 1410–1419.

6. Brugge, D.; Goble, R. A documentary history of Uranium mining and the Navajo people. In *The Navajo People and Uranium Mining*; Brugge, D., Benally, T., Yazzie-Lewis, E., Eds.; UNM Press: Albuquerque, NM, USA, 2007; pp. 25–47.

7. Yazzie-Lewis, E.; Zion, J. Leetso, the powerful yellow monster a Navajo cultural interpretation of Uranium mining. In *The Navajo People and Uranium Mining*; Brugge, D., Benally, T., Yazzie-Lewis, E., Eds.; UNM Press: Albuquerque, NM, USA, 2007; pp. 1–10.

8. Johnston, B.R.; Dawson, S.E.; Madsen, G.E. Uranium mining and milling, Navajo experiences in the American southwest. In *Half-Lives & Half-Truths, Confronting the Radioactive Legacies of the Cold War*; Johnston, B.R., Ed.; School for Advanced Research Press: Santa Fe, NM, USA, 2007; pp. 97–117.

9. Technical Report on Technologically Enhanced Naturally Occurring Radioactive Materials from Uranium Mining Volume 2: Investigation of Potential Health, Geographic, and Environmental Issues of Abandoned Uranium Mines, EPA 402-R-08-005, April 2008. Available online:

http://www.epa.gov/radiation/docs/tenorm/402-r-08–005-volii/402-r-08-005-v2.pdf (accessed on 20 December 2014).

10. Uranium Mining Wastes. What is the History of Uranium Mining in the U.S.? Available online: http://www.epa.gov/radiation/tenorm/uranium.html#history (accessed on 20 December 2014).

11. Abandoned Mine Lands Portal. Available online: http://www.abandonedmines.gov/wbd_um.html (accessed on 20 December 2014).

12. Brugge, D.; Buchner, V. Health effects of uranium: New research findings. *Rev. Environ. Health* **2011**, 26, 231–249.

13. Manhattan Project. Energy.gov Office of Management. Available online: http://energy.gov/management/officemanagement/operationalmanagement/history/manhattan-project (accessed on 28 December 2014).

14. Los Alamos National Laboratory. *Our History*. Available online: http://www.lanl.gov/about/history-innovation/index.php (accessed on 28 December 2014).

15. Churchhill, W. A breach of trust. In *Acts of Rebellion: The Ward Churchill Reader*; Routledge: London, UK, 2002; pp. 103–130.

16. Wright, Q. The law of the Nuremberg trial. *Am. J. Int. Law* **1947**, 41, 38–42.

17. Department of Energy Hanford. *Hanford Overview and History*. Available online: http://www.hanford.gov/page.cfm/HanfordOverviewandHistory (accessed on 28 December 2014).

18. Orem, W.; Tatu, C.; Pavlovic, N.; Bunnell, J.; Kolker, A.; Engle, M.; Stout, B. Health Effects of Energy Resources. U.S. Department of the Interior, U.S. Geological Survey, FS 2009-3096. Available online: http://pubs.usgs.gov/fs/2009/3096/ (accessed on 30 December 2014).

19. Ali, S.H. Mining, the Environment, and Indigenous Development Conflicts; The University of Arizona Press: Tucson, AZ, USA, 2003; p. 254.

20. Klauk, E. Impacts of Resource Development on Native American Lands. Available online: http://serc.carleton.edu/research_education/nativelands/navajo/humanhealth.html (accessed on 10 December 2014).

21. EPA Pacific Southwest Region 9. Addressing Uranium Contamination on the Navajo Nation. Contaminated Water Sources. Available online: http://www.epa.gov/region9/superfund/navajo-nation/contaminated-water.html (accessed on 8 December 2014).

22. Dawson, S.E.; Madsen, G.E. Uranium Mine Workers, Atomic Downwinders, and the Radiation Exposure Compensation Act (RECA). In *Half-Lives & Half-Truths, Confronting the Radioactive Legacies of the Cold War*; Johnston, B.R., Ed.; School for Advanced Research Press: Sante Fe, NM, USA, 2007; pp. 117–143.

23. Eichstaedst, P. If You Poison Us: Uranium and Native Americans; Red Crane Books: Santa Fe, NM, USA, 1994; p. 194 p.

24. Jackpile Mine (Jackpile-Paguate), Laguna District, Cibola Co., New Mexico, USA. Available online: http://www.mindat.org/loc-33622.html (accessed on 28 December 2014).

25. Native Sun News: Laguna Pueblo Still Affected by Uranium Mine. Available online: http://www.indianz.com/News/2014/014847.asp (accessed on 28 December 2014).

26. Schilmoeller, J. Decades of Environmental Injustice: Wyoming Indian Reservation Faces High Cancer Rates. Mint Press News. Available online: http://www.mintpress.net/decades-of-environmental-injustice-wyoming-indian-reservation-faces-deteramental-rates-of-cancer/ (accessed on 13 December 2012).

27. Cleanup of Midnite Mine on Reservation to Begin by 2015. The Spokesman-Review. Available online: http://www.spokesman.com/stories/2013/nov/21/cleanup-of-midnite-mine-on-reservation-to-begin/ (accessed on 8 December 2014).

28. Spokane Tribe Members Worked Gladly in Uranium Mines. The Spokesman-Review. Available online: http://www.spokesman.com/stories/2011/jun/05/i-watch-them-die-young-and-old/ (accessed on 8 December 2014).

29. Liebow, E. Hanford, tribal risks, and public health in an era of forced federalism. In Half-Lives & Half-Truths, Confronting the Radioactive Legacies of the Cold War; Johnston, B.R., Ed.; School for Advanced Research Press: Santa Fe, NM, USA, 2007; pp. 145–165.

30. Department of Energy Hanford. Hanford Cleanup. Available online: http://www.hanford.gov/page.cfm/HanfordCleanup (accessed on 28 December 2014).

31. Reynolds, T. Final Report of Hanford Thyroid Disease Study Released. *J. Natl. Cancer Inst.* **2002**, 94, 1046–1048.

32. Centers for Disease Control and Prevention, HTDS Guide—How the Study Was Conducted. Available online: http://www.cdc.gov/nceh/radiation/hanford/htdsweb/guide/conduct.htm (accessed on 16 January 2015).

33. Prados, J. Presidents' Secret Wars: CIA and Pentagon Secret Operations since World War II; William Morrow & Co.: New York, NY, USA, 1986; pp. 255–256.

34. Brugge, D.; de Lemos, J.L. The Sequoyah Corporation fuels release and the church rock spill: Unpublicized nuclear releases in American Indian communities. *Am. J. Public Health* **2007**, 97, 1595–1600.

35. Pasternak, J. Yellow Dirt: A Poisoned Land and a People Betrayed; Free Press: New York, NY, USA, 2010; 149 p.

36. Dixon, M.; Roubideaux, Y. Promises to Keep: Public Health Policy for American Indians and Alaska Natives in the 21st Century; American Public Health Association: Washington, DC, USA, 2001; p. 311.

37. Indian Health Service (IHS) Website. Available online: http://www.ihs.gov/index.cfm?module=ihsIntro (accessed on 11 March 2013).

38. Lillie-Blanton, M.; Roubideaux, Y. Understanding and addressing the health care needs of American Indians and Alaska natives. *Am. J. Public Health* **2005**, 95, 759–761.

39. Census 2010 Brief: The American Indian and Alaska Native population: 2010. Available online: http://www.census.gov/prod/cen2010/briefs/c2010br-10.pdf (accessed on 11 March 2013).

40. Indian Health Service (IHS) Environmental Health Services Fact Sheet. Available online: http://www.ihs.gov/factsheets (accessed on 11 March 2013).

41. Day, G.E.; Lanier, A.P. Alaska native mortality, 1979–1998. *Public Health Rep*. **2003**, 118, 518–530.

42. Hoover, E.; Cook, K.; Plain, R.; Sanchez, K.; Waghiyi, V.; Miller, P.; Dufault, R.; Sislin, C.; Carpenter, D.O. Indigenous peoples of North America: Environmental exposures and reproductive justice. *Environ. Health Perspect.* **2012**, 120, 1645–1649.

43. Kunitz, S.J. Changing patterns of mortality among American Indians. *Am. J. Public Health* **2008**, 98, 404–412.

44. Native American Health Care Disparities Briefing Executive Summary; Office of the General Counsel U.S. Commission on Civil Rights: 2004; p. 52. Available online: http://www.law.umaryland.edu/marshall/usccr/documents/nativeamerianhealthcaredis.pdf (accessed on 11 March 2013).

45. Rogers, D.; Petereit, D. Cancer disparities research partnerships in Lakota Country: Clinical trials, patient services, and community education for the Oglala, Rosebud, and Cheyenne River Sioux Tribes. *Am. J. Public Health* **2005**, 95, 2129–2132.

46. Nuclear War: Uranium Mining and Nuclear Tests on Indigenous Lands. Available online: http://www.culturalsurvival.org/publications/cultural-survival-quarterly/united-states/nuclear-war-uranium-mining-and-nuclear-tests- (accessed on 8 December 2014).

47. RECA Radiation Exposure Compensation Act: Radiation Exposure Compensation Program-About the Program United States Department of Justice. Available online: http://usdoj.gov/civil/torts/const/reca/about.htm (accessed on 30 December 2012).

48. Agencies Cite Progress, Work Still Remaining on Navajo Uranium Cleanup. Chronkite News, 24 January 2013. Available online: http://cronkitenewsonline.com/2013/01/agencies-cite-progress-work-still-remaining-on-navajo-uranium-cleanup/ (accessed on 8 December 2014).

49. EPA Pacific Southwest Region 9. Addressing Uranium Contamination on the Navajo Nation. Cleanup of Abandoned Mines. Available online: http://www.epa.gov/region9/superfund/navajo-nation/abandoned-uranium.html (accessed on 8 December 2014).

50. DeLemos, J.L.; Bostick, B.C.; Quicksall, A.N.; Landis, J.D.; George, C.C.; Slagowski, N.L.; Rock, T.; Brugge, D.; Lewis, J.; Durant, J.L.; Rapid dissolution of soluble Uranyl phases in arid, mine-impacted catchments near Church Rock, NM. *Environ. Sci. Technol*. **2008**, 42, 3951–3957.

51. CDC Navajo Uranium Impact Studies: Dr. Johnnye Lewis. Available online: https://lajicarita.wordpress.com/2012/08/31/cdc-navajo-uranium-impact-studies-dr-johnnye-lewis/ (accessed on 7 December 2014).

52. Navajo Health Research: Dr. Johnnye Lewis Continues. Available online: http://lajicarita.wordpress.com/2012/09/21/navajo-health-research-dr-johnnye-lewis-continues/ (accessed on 7 December 2014).

53. Southwest Research and Information Center. Available online: http://www.sric.org/nbcs/index.php (accessed on 7 December 2014).

© 2015 by the authors; licensee MDPI, Basel, Switzerland. This article is an open access article distributed under the terms and conditions of the Creative Commons Attribution license (http://creativecommons.org/licenses/by/4.0/).© 2015 by the authors; licensee MDPI, Basel, Switzerland. This article is an open access article distributed under the terms and conditions of the Creative Commons Attribution license (http://creativecommons.org/licenses/by/4.0/).

CHAPTER 3

POTENTIAL HEALTH RISKS FROM URANIUM IN HOME WELL WATER: AN INVESTIGATION BY THE APSAÁLOOKE (CROW) TRIBAL RESEARCH GROUP

Contribution of Authors and Co-Authors

Manuscript in Chapter 3

Co-Author: Margaret Eggers

Contributions: Margaret Eggers has served as a non-voting Crow Environmental Health Steering Committee (CEHSC) member since 2006, served as Project Leader including designing the research project in consultation with the CEHSC, local Project Coordinator and Dr. Camper, training local staff, overseeing fieldwork, preparing reports to homeowners, managing and analyzing the data, preparing GIS from project data and with the Project Coordinator communicating project results to community groups and local teachers; primary author on paper.

Co-Author: Anita Moore-Nall

Contributions: Anita Moore-Nall researched federal and state data on local water quality; suggested project test wells for uranium; prepared GIS map incorporating federal, state and project data on well water quality; researched the area's geology; wrote the Study Area description for paper.

Co-Author: John Doyle

Contributions: John Doyle has served on the CEHSC since 2006; served as local Project Coordinator for the past two years, conducting home visits to explain well test results, discussing project results in community and with Tribal officers, and conducting outreach to local teachers and school children; contributes local expertise to research; as the Director of the Apsaalooke Water and Wastewater Authority, coordinates efforts between the CEHSC and the AWWA. Contributed to and reviewed drafts of the paper.

Contribution of Authors and Co-Authors - Continued

Co-Author: Myra Lefthand

Contributions: Myra Lefthand has served on the CEHSC since 2006; reviewed and edited initial survey; contributed health education and cultural expertise to project; explained project results to community members; provided training for student interns, especially those conducting surveys; collaborates with the Executive Branch of the Crow Nation on water issues; reviewed drafts of the paper.

Co-Author: Sara Young

Contributions: Sara Young has served on the CEHSC since 2007; reviewed and edited the initial survey; recruited participants; coordinated this project with other related projects at MSU; reviewed drafts of the paper.

Co-Author: Ada Bends Ada Bends has served on the CEHSC since 2008; as a Community Organizer for the Crow Reservation has recruited participants and organized community meetings for presentation of project results; contributed data from the 2010 health disparities survey she conducted; reviewed drafts of the paper.

Co-Author: Anne Camper

Contributions: Ann Camper has participated in the CEHSC since 2008; oversaw research that provided testing for well and river water testing/survey collection; reviewed data analysis; contributed to the manuscript.

Co-Authors: CEHSC

Contributions: All CEHSC co-authors and additional CEHSC members have guided and advised the project, contributed local environmental, health and cultural expertise, and co-presented on the research at conferences and workshops.

Manuscript Information Page

Eggers, M.J.; Moore-Nall, A.L.; Doyle, J.T.; Lefthand, M.J.; Young, S.L.; Bends, A.L.; Committee, C.E.H.S.; Camper, A.K.
Journal name: GeoSciences
Status of Manuscript:
____ Prepared for submission to a peer-reviewed journal
____ Officially submitted to a peer-review journal
____ Accepted by a peer-reviewed journal
__X__ Published in a peer-reviewed journal

Published by MDPI AG, Basel, Switzerland
March 2015, Volume 5, Issue 1, Special Issue Medical Geology: Impacts of the Natural Environment on Public Health

With the exception of its publication in the peer reviewed Geosciences, this article has not been reproduced elsewhere.

COPYRIGHT

The following chapter has been published in the journal Geosciences. This is an open access article distributed under the Creative Commons Attribution License which permits unrestricted use, distribution, and reproduction in any medium, provided the original work is properly cited and is published here: doi:10.3390/geosciences5010067 in agreement with the journal's copyright policy. No written permission is needed. The full citation of the published article is:

Eggers, M.J.; Moore-Nall, A.L.; Doyle, J.T.; Lefthand, M.J.; Young, S.L.; Bends, A.L.; Committee, C.E.H.S.; Camper, A.K. Potential Health Risks from Uranium in Home Well Water: An Investigation by the Apsaálooke (Crow) Tribal Research Group. *Geosciences* **2015**, *5*, 67-94.

CHAPTER 3

POTENTIAL HEALTH RISKS FROM URANIUM IN HOME WELL WATER: AN INVESTIGATION BY THE APSAÁLOOKE (CROW) TRIBAL RESEARCH GROUP

Margaret J. Eggers 1,*, Anita L. Moore-Nall 2,5, John T. Doyle 3,5, Myra J. Lefthand 4,5, Sara L. Young 5,6, Ada L. Bends 3,5, Crow Environmental Health Steering Committee 3 and Anne K. Camper 1,7

[1] Center for Biofilm Engineering, Montana State University, P.O. Box 173980, Bozeman, MT 59717, USA

[2] Department of Earth Sciences, Montana State University, P.O. Box 173480, Bozeman, MT 59717, USA; E-Mail: amoorenall@yahoo.com or anita.moorenall@msu.montana.edu

[3] Little Big Horn College, P.O. Box 370, Crow Agency, MT 59022, USA; E-Mails: doylej@lbhc.edu (J.T.D.); bendsal@lbhc.edu (A.L.B.)

[4] Crow/Northern Cheyenne Hospital, P.O. Box 592, Crow Agency, MT 59022, USA; E-Mail: myra.lefthand@ihs.gov

[5] Crow Tribal Member(s)

[6] Montana Infrastructure Network for Biomedical Research Excellence (INBRE) Program, Montana State University Bozeman, 1246 Harvard Avenue, Billings, MT 59102, USA; E-Mail: slyoung@montana.edu

[7] Department of Civil Engineering, Montana State University, P.O. Box 173980, Bozeman, MT 59717, USA; E-Mail: anne_c@erc.montana.edu

***** Author to whom correspondence should be addressed; E-Mail: mari.eggers@biofilm.montana.edu; Tel.: +1-406-994-3064; Fax: +1-406-994-6098.

Abstract: Exposure to uranium can damage kidneys, increase long term risks of various cancers, and cause developmental and reproductive effects. Historically, home well water in Montana has not been tested for uranium. Data for the Crow Reservation from the United States Geological Survey (USGS) National Uranium Resource Evaluation (NURE) database showed that water from 34 of 189 wells tested had uranium over the Environmental Protection Agency (EPA) Maximum Contaminant Level (MCL) of 30 μg/L for drinking water. Therefore, the Crow Water Quality Project included uranium in its tests of home well water. Volunteers had their well water tested and completed a survey about their well water use. More than 2/3 of the 97 wells sampled had detectable uranium; 6.3% exceeded the MCL of 30 μg/L. Wells downgradient from the uranium-bearing formations in the mountains were at highest risk. About half of all Crow families rely on home wells; 80% of these families consume their well water. An explanation of test results; associated health risks and water treatment options were provided to participating homeowners. The project is a community-based participatory research initiative of Little Big Horn College; the Crow Tribe; the Apsaálooke Water and Wastewater Authority; the local Indian Health Service Hospital and other local stakeholders; with support from academic partners at Montana State University (MSU) Bozeman.

Keywords: uranium; drinking water; well water; risk assessment; risk communication; Native American; health disparity; community based participatory research; environmental justice; Crow Reservation; Crow Tribe

1. Introduction

Uranium contamination of groundwater is being increasingly recognized as a health threat to rural residents relying on home wells for their drinking water, not only in communities with a legacy of mining [1], but also where naturally occurring uranium is the source of contamination [2–5]. However, most of the key studies of health effects from drinking uranium contaminated water have been conducted in other countries [4,6–8]. In the United States, naturally occurring elevated uranium in groundwater has been identified as a widespread issue in Western states, as well as in scattered locations in Eastern states [2,9]. Native Americans in the Colorado Plateau area have been particularly impacted [10]. A recent comprehensive survey of well water contaminants conducted by the U.S. Geological Survey found that 1.7% of home wells tested nationwide exceeded the Environmental Protection Agency (EPA) Maximum Contaminant Level (MCL) for uranium contamination [11] and highlighted the need for data on well water consumption by rural residents. In this study, the Crow Tribal community in Montana recognized the potential for uranium contamination of their home wells, tested wells for inorganic and microbial contamination, simultaneously conducted surveys of well water use and treatment, assessed the risk of exposure to waterborne contaminants and conducted outreach to educate rural residents of the health risks of consuming contaminated well water.

1.1. The Crow Reservation

The Crow Reservation in south-central Montana is home to the Apsaálooke (Crow) people, and encompasses 2.3 million acres in the center of the Tribe's original homelands. Of the Tribe's approximate enrollment of 11,000 people, 7900 live on the Reservation [12]. The Reservation is rich in water resources, including the Little Bighorn River, Bighorn River, Pryor Creek and their tributaries, fed by the Wolf, Big Horn and Pryor Mountain ranges. The Apsaálooke people still maintain their language, ceremonial practices, and relationships to the rivers, springs and other natural resources. Water as a "giver of life," an "essence of life," has always been held in high respect by the Apsaálooke people and considered a source for health; water continues to be a sacred resource essential to many prayers, ceremonies and other traditional practices [13–15]. Water contamination-even well water contamination-has additional, unique impacts in Native American communities due to traditional values and practices [15]. Therefore, this project is a relevant case study for understanding health risks from water contamination in rural Native American communities.

Like many other tribes and minority communities, the Apsaálooke people also face health disparities and economic hardships which increase vulnerability to environmental contamination. Statistics for Big Horn County give some idea of the health status of the Reservation, as 64% of the county's land base is within the Reservation's boundaries and 66% of the county's population is Native American [16]. In a comprehensive and thoroughly cited analysis of county health and socioeconomic status, the local Community Health Center describes the confluence of: (1) disparities in physical health;

(2) disparities in mental health; (3) an ongoing cycle of poverty [17]; and (4) inadequate health care, as combining to contribute to health disparities [18]. These include an elevated infant mortality rate [19] cited in [18], a much higher age-adjusted death rate ([20,21], cited in [18]), and a *twenty year lower* life expectancy for Native Americans compared to Caucasian residents of the county [19] cited in [18].

One health statistic relevant to uranium contamination of well water is the high diabetes prevalence rate of 12.1% in Big Horn County, compared to 6.2% statewide. In a survey of 400 Crow Tribal members, diabetes was named as top local health disparity [22]. The impacts of this chronic disease on health are also elevated: the hospitalization rate for diabetes is 246.3 per 100,000, compared to 115.4 per 100,000 in Montana and 180.2 per 100,000 nationwide [23] cited in [18]. The death rate from diabetes is nearly twice the statewide rate (50.1 per 100,000 compared to 27.1 per 100,000 in Montana) and 143% of the national rate [24] cited in [18].

For rural Reservation residents, the challenge of obtaining safe, palatable drinking water is relatively new. Traditionally, people lived near rivers and springs, used this water for domestic purposes, knew they needed water to survive and kept these sources clean. Crow Elders reflect that there used to be a level of trust that the rivers and springs were clean. Until the 1960s, many families on the Crow Reservation hauled river water for home use, a practice most of the Tribal co-authors remember from their childhoods. At that time, agriculture was expanding and river water quality visibly deteriorating; wells and indoor plumbing finally became available and rural families switched to piped home well water. In many parts of the Reservation, this was a hardship, not a blessing:

the groundwater tapped for home wells was high in total dissolved solids, including so much sulfate, iron and manganese that it was undrinkable [25]. Widespread high alkalinity and excessive hardness resulted in scaling that ruined pipes and hot water heaters. There was no community education on how to protect one's well water or maintain and repair wells, plumbing and septic systems.

Today, about half of all local families rely on home well water [11]. In many parts of the Reservation, well water quality is poor, but is still used for drinking and/or cooking. Community members, increasingly concerned about potential health effects from their poor quality drinking water, partnered with Little Big Horn College and Montana State University Bozeman to tackle both well and river water contamination issues. Forming the Crow Environmental Health Steering Committee (CEHSC) in 2006, the partners initiated the Crow Water Quality Project and have been working together ever since to improve the health of Crow community members by assessing, communicating and mitigating the risks from local waterborne contaminants [13]. The CEHSC and their academic partners secured funding to assess waterborne contaminants through a free "full domestic analysis" of home well water to local residents who volunteered to participate. On learning from co-author geologist Moore-Nall that the United States Geological Survey (USGS) National Uranium Resource Evaluation (NURE) database showed 34 out of 189 wells tested had uranium concentrations exceeding the EPA MCL [26], and knowing about the old uranium mines in the Pryor and Bighorn Mountains adjacent to the reservation, the CEHSC added uranium to its home well water testing parameters.

1.2. Study Area

1.2.1. Physiography and Geology

The Crow Indian Reservation (Figure 3.1) lies within the unglaciated portion of the Missouri Plateau, a subdivision of the Great Plains physiographic province [27]. The Missouri Plateau on the Crow Reservation is described as a mature landscape consisting of flat to rolling plains dissected by rivers with scattered isolated mountains [28].

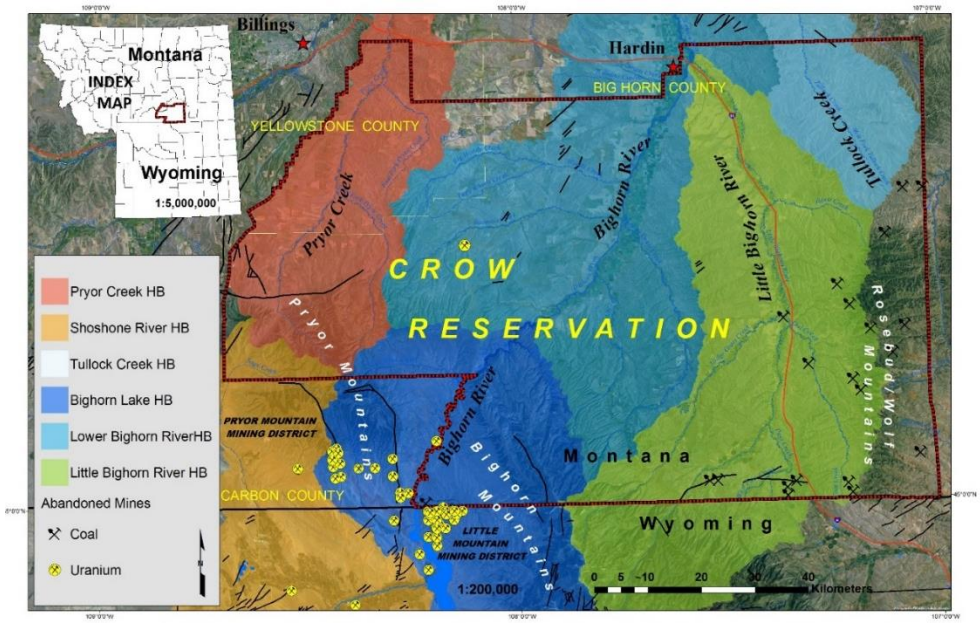


Figure 3.1. Study area, showing the Crow Reservation (outlined by the red and black border). Hydrologic basins (HB) for the major drainages, mountain ranges and the location of the two abandoned uranium mining districts southwest of the reservation are shown. The Bighorn/Yellowstone County line is delineated in yellow.

Elevations range from about 2822 m (9257 feet) in the Bighorn Mountains to about 884 m (2900 feet) at the confluence of the Bighorn and Little Bighorn Rivers at Hardin. The towns of Billings and Hardin, Montana, are near the northern edge of the reservation,

and the Montana-Wyoming border forms much of the southern edge. The reservation includes about 9324 km^2 (3600 mi^2) in the Big Horn and southeastern part of Yellowstone Counties, Montana [29]. The reservation is approximately 129 km (80 mi) wide and 85 km (53 mi) north to south.

1.2.2. Drainages

Three rivers create two major valleys and the natural divisions between the three mountainous areas of the reservation. On the northwest side of the reservation Pryor Creek is the main drainage which flows northwest through the Pryor mountains and then changes and flows to the northeast. The Bighorn River flows northeast from the southwestern edge of the reservation and defines the boundary between Carbon and Bighorn counties. The Little Bighorn River flows north across the reservation joining the Bighorn River at Hardin. All three drainages are tributary to the Yellowstone River [30]. The Tullock Creek drainage flows north joining the Bighorn. Drainage from the western half of the coal producing area on the reservation (Wolf/Rosebud mountainous area) flows into the Little Bighorn River. Drainage from the northeastern portion of the area is collected by the Rosebud Creek drainage system and flows east into the Tongue River [31]. The alluvial low lands located along the Bighorn River and Little Bighorn River are where uranium was found to exceed EPA's MCL in some tested home wells.

1.2.3. Mountain Ranges

The mountain ranges on the Crow Reservation include the Bighorn and the Pryor Mountains which are an outlying portion of the Rocky Mountains, to the southwest, and

the Wolf/Rosebud Mountains on the east. The northern end of the Bighorn range extends from north-central Wyoming into the southwestern corner of the reservation. The Dryhead-Garvin Basin, a flat floored syncline separates the northern Bighorn Mountains and the east side of the Pryors [32]. The northern portion of the Bighorn range ends in the canyon of the Bighorn River (Figure 3.2) just southeast of the Pryor Range. These ranges host two abandoned uranium mining districts [33–36] which border the reservation. These mining districts operated from about 1956 to the early 1980's [34]. The east side of the reservation is flanked by the Wolf and Rosebud Mountains. A narrow divide that separates the Davis Creek and Rosebud Creek drainages, separates the Wolf Mountains from the Rosebud Mountains to the north. These mountains are highly dissected with numerous outcroppings of Eocene Wasatch Formation and Paleocene Fort Union Formation coal deposits [27].



Figure 3.2. Northern portion of the Bighorn Mountains and the Bighorn River.

1.2.4. Geologic Setting

The geologic setting of the Crow Reservation includes the west flank of the Powder River basin, a northwest-trending synclinal feature at least 400 km long and as much as 160 km wide in eastern Wyoming and southeastern Montana; the south flank of the Bull Creek syncline, a large east-trending fold in central Montana; and the northern parts of the Bighorn and Pryor uplifts [37]. These features, and many subsidiary folds and faults associated with them, were formed in late Cretaceous to early Tertiary time [38] and account for the distribution of rock units in the reservation.

The geologic formations exposed at the surface on the Crow Reservation range from Cambrian units in the Big Horn Canyon to the younger Tertiary units on the eastern flank of the reservation [38] (Figure 3.3). With the exception of small structural fluctuations, the beds gently dip easterly. In general, erosion has exposed each geologic formation at or near the surface in a series of stacked inclined formations progressing from older beds on the west to younger beds on east side of the reservation [27]. The youngest exposed rocks, exclusive of surficial stream terrace deposits and alluvium, are the Tertiary Wasatch and Fort Union Formations which lie east of the Little Bighorn River on the flank of the Powder River basin in the Wolf Mountains [31].

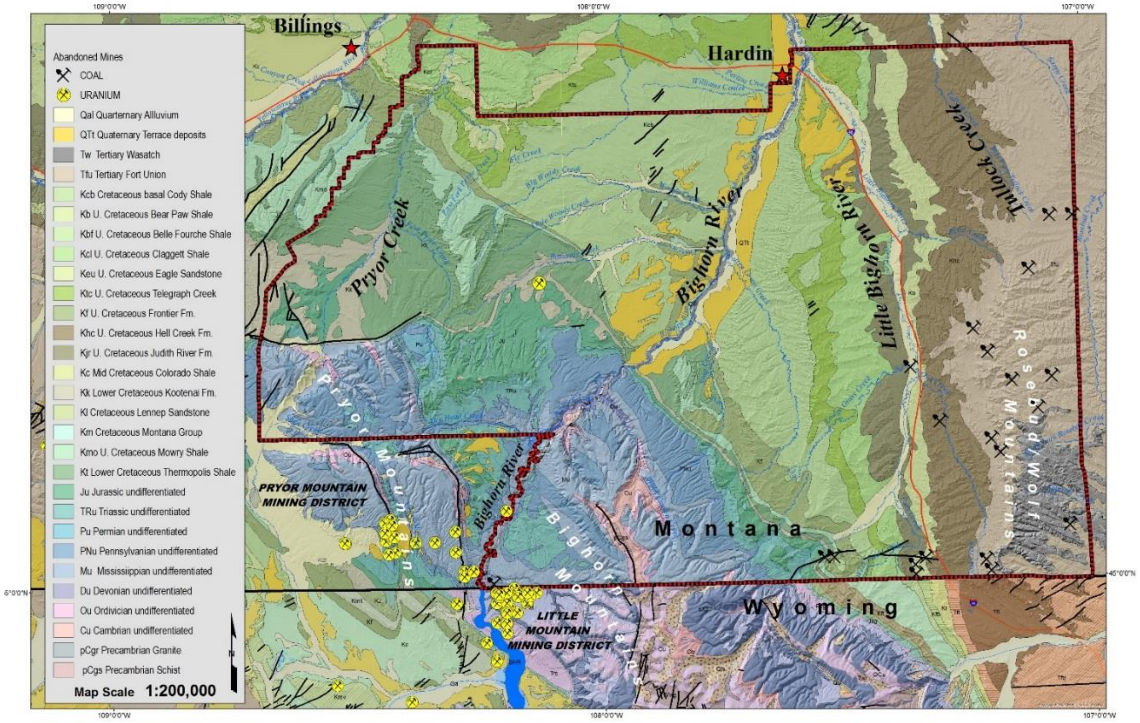


Figure 3.3. Geologic map of the reservation, showing locations of old uranium mines.

1.2.5. Description of the Uranium Mining Districts

An area spanning from the Big Pryor Mountain Mining District, in Montana to the Little Mountain Mining District in Wyoming has been prospected for uranium and other radioactive minerals since 1956 [34,35,39]. The Mississippian Madison Limestone outcrops extensively throughout the area. A paleokarst horizon in the top 58–73 m is the main zone for mineralization [35] (p. 1). Relatively small, high-grade (median grades of 0.26% U_3O_8, 0.23% V_2O_5) deposits in Montana and Wyoming combined, produced 133,810 kg (295,000 lb) of triuranium octoxide (U_3O_8) and 106,594 kg (235,000 lb) of vanadium oxide (V_2O_5) during 1956–1964 [35] (p. 1). The Madison displays zones of extensive brecciation that are both discordant and concordant to bedding. The upper 60 m

of the Madison Limestone are characterized by “solution cavities” along bedding planes, fractures and joints; angular limestone fragments of variable size (from several centimeters to a meter or more across) have filled the cavities, in addition to reddish clay silt from the overlying Amsden Formation and cryptocrystalline silica [34]. Uranium and vanadium minerals are also concentrated in the solution cavities and at the Madison-Amsden contact.

In addition to being stratigraphically localized, the uranium deposits in the area of Red Pryor Mountain show a structural relationship to a zone of fractures that trend N 65° W, on a trend that includes the East Pryor and Little Mountain group of mines [34] (p. 12); mineralization appears to be enhanced where northwest-striking fractures intersect the crest of a large south-plunging anticline [34]. Furthermore, the alignment of mines (Old Glory, Sandra, Lisbon, Dandy, and Swamp Frog) on the Red Pryor quadrangle is spatially coincident with a reverse fault in the basement that subtends the south-plunging anticline [36]. Deposits in the Little Mountain Mining district of Wyoming occur in the same stratigraphic units, within collapse breccia features and with the same ore minerals. Principal ore minerals are the calcium uranyl vanadates tyuyamunite and metatyuyamunite [34,35,38].

1.3. Uranium

Uranium is a very dense, radioactive metal. Of its three naturally occurring isotopes, U-238 is the most common, constituting more than 99% of natural uranium by mass. U^{4+} in uraninite and other minerals undergoes oxidative weathering, forming highly soluble U^{6+}. In this oxidized form, it is easily transported in groundwater and is found in rivers and lakes

[40]. As a radioactive element, U-238 has a decay chain which includes radium-226, the gas radon-222, polonium-210 and finally, the stable nuclide lead-206 (Figure 3.4).

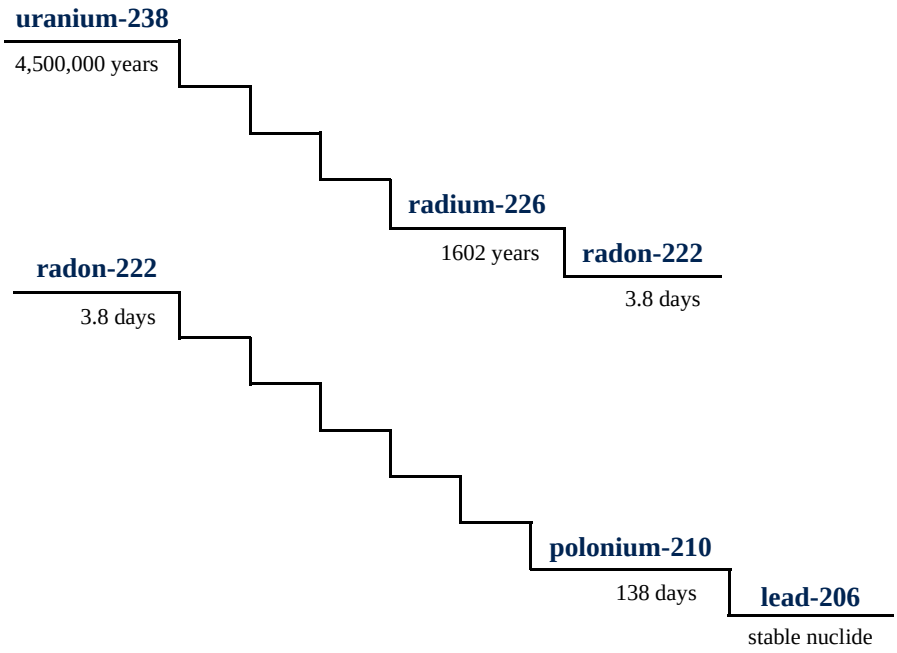


Figure 3.4. Greatly simplified Uranium-238 decay series showing radioactive decay products discussed in this report (adapted from [41]).

1.3.1. Uranium and Human Health

Uranium, a radionuclide which emits primarily alpha particles, has a variety of associated health risks. Although most of the uranium and daughter products consumed in drinking and cooking water are eliminated by the body, small amounts are absorbed from the digestive tract and enter the bloodstream. Uranium in the bloodstream is filtered by and deposited in the kidneys, where it targets the proximal tubules [42]. Uranium exposure has been found to be positively associated with cytotoxicity biomarkers: increases in urinary albumin [8], glucose and calcium [2], β_2-microglobulin and alkaline

phosphatase [6]. Absorbed uranium not excreted via urine, accumulates primarily in the skeleton and kidney [4,43]. Exposure can increase cancer risk and lead to liver damage [44]. Additional documented health outcomes of concern include effects on the brain, diminished bone growth, DNA damage and developmental and reproductive effects [45,46]. The health risks from uranium in drinking water are greatest for infants and young children, who can suffer lasting damage from exposure at critical times in their growth [47]. Drinking and cooking with uranium contaminated water is the primary route of exposure to uranium in well water, as absorption through skin is minimal [48].

1.3.2. Uranium in Well Water

Historically, home well water in Montana has not been tested for uranium [48]. By 2009, more than 600 wells had been drilled by the Indian Health Service for Crow Tribal members on the Reservation, but uranium was almost never included in the analysis. When the Crow Water Quality Project began home well water testing, and even now, a "full domestic analysis" of home well water through Montana's Well Educated Program at the nearest EPA certified laboratory does not include testing for uranium or any other radionuclide [49].

In 2009, the National Water Quality Assessment Program of the U.S. Geological Survey published the groundbreaking "Quality of Water from Domestic Wells in Principal Aquifers of the United States, 1991–2004". Sampling of domestic wells in 30 of the 60 principal aquifers found that 1.7% of wells exceeded the Environmental Protection Agency's Maximum Contaminant Limit (MCL) of 30 μg/L for uranium [11].

USGS National Uranium Resource Evaluation (NURE) collected well water data in 1976–1979 on the Crow Reservation. Almost all the samples were filtered, acidified then analyzed for uranium at the Department of Energy's Los Alamos National Laboratory in New Mexico, using fluorescence spectroscopy, methods LA6-FL, OR9-FL, with a detection limit of 0.5 µg/L. Well use was not recorded, except for six records which mention "livestock well." Nearly all the samples list "agriculture" or "none" as potential contaminant sources. 34 of 189 of these tested wells, or 18%, had uranium over the EPA regulated limit of 30 µg/L for drinking water. Eighteen of these 34 wells were in the lower Bighorn hydrological basin (HB), 14 were in the Little Bighorn HB, and only one was in the Pryor HB [26].

More recently, testing by the USGS in southwestern Montana found that 14.1% of 128 wells exceeded the MCL for uranium, while 29% exceeded the drinking water standard for uranium, radon, radium 226, radium 228 and/or alpha or beta particles [50]. Although this sampling was done in counties some 240 km (150 mi) west of the Reservation, these data illustrate that sampling for uranium alone could substantially underestimate the health risks from radionuclides in well water as decay products of uranium can also be present.

The presence of uranium and/or other radionuclides in well water alone is not sufficient to determine whether health risks exist. As the USGS noted, "Improved information is needed on the number of people consuming water from domestic wells in specific regions and aquifers… Such information is essential for evaluating the potential human health implications and possible mitigation approaches." [11].

2. Methods

This research addresses the limitations of previous well water quality studies by combining well water testing for uranium and other analytes, with homeowner surveys and secondary health and economic data. These methods have provided data on well water consumption, well and septic system maintenance practices and economic factors limiting well water treatment, which in conjunction with well water quality data, enable better assessment of health risks from well water contamination.

2.1. Community-Based Participatory Research

The collaboration follows the principles of community-based participatory research (CBPR), which has been defined as, "a partnership approach to research that equitably involves, for example, community members, organizational representatives, and researchers in all aspects of the research process and in which all partners contribute expertise and share decision making and ownership" [51]. The Crow Environmental Health Steering Committee (CEHSC) members, all of whom are Crow Tribal members, meet about ten times a year with academic partners who serve as non-voting Committee members. The CEHSC members guide, actively participate in and contribute vital local environmental, health, social and cultural expertise to the research. The local Project Coordinator, with various interning Little Big Horn College science majors and a Montana State University (MSU) graduate student, all Tribal members, conducted nearly all the well water sampling, survey work and follow-up visits with participating families. The data management and statistical analysis were conducted by a non-Tribal academic

partner; the geology expertise was provided by a Crow graduate student at MSU, who also took the lead on the geographic information system (GIS) maps (ArcMap™ 10.2.1, ESRI ©, Redlands, CA, USA). CEHSC members and academic partners including Crow graduate students co-presented project results locally, regionally and nationally, and collaborated on this publication. Applying CBPR principles to risk assessment research as well as risk communication and risk mitigation is an effective way to reduce health disparities in Crow Reservation communities. This approach has been found to be effective in other Tribal communities addressing environmental health issues [15], as well as internationally with communities experiencing environmental health disparities [52].

2.2. Volunteer Recruitment and Participation

Based on USGS, U.S. census and project data, it is estimated that 970 Crow families in Big Horn County use home wells. The northwest corner of the Reservation is in Yellowstone County, constituting about 10% of the Reservation's acreage; approximately 50 Crow families live in this region. Including both Counties, at least 1020 Crow families living on the Reservation rely on home wells for their domestic water supply.

In 2008 an Institutional Review Board approved a survey that covered treatment and uses of home well water; well water taste, color and odor; other sources of water for domestic, traditional and recreational uses; well and septic system knowledge and maintenance practices; potential sources of well water contamination and other factors. The survey drew from comprehensive environmental health surveys used in other studies [53,54] as well as on co-authors' knowledge of local conditions and practices, and was

edited by two Crow CEHSC members with graduate degrees in social science disciplines and lifetime knowledge of Crow Reservation communities.

Beginning in 2009, participants were recruited from throughout the Reservation. Random sampling was ruled out from the very beginning by the CEHSC as culturally inappropriate and hence ineffective. Flyers were posted in public locations, ads were placed in the local papers, staff set up tables at community health fairs and other events, and all involved recruited through word of mouth. Personal recruiting through friends, family and social networks proved to be by far the most effective strategy. The local project coordinator, a Tribal member, met each volunteer at their home, explained the project, answered questions and collected the water samples for microbial and chemical analyses. Participants chose either to complete the survey on their own, or completed it with the project coordinator. Each received a free comprehensive domestic analysis of their well water, a stipend and a follow up explanation of their well test results and treatment options. Recruitment was capped at 150 participants due to budget and time limitations and as this was a sufficient sample for analysis.

2.3. Sample Collection and Analysis

Water samples were collected from the home's kitchen tap. In the rare cases where the homeowner had installed a water treatment device, untreated water was collected from another point in the plumbing system or not included in the analysis. Water temperature, conductivity and pH were measured on site. Samples were placed on ice and delivered in less than 24 hours (usually within the same day) to Energy Laboratories, an EPA certified lab in Billings, Montana for a full domestic analysis on each water sample that included

physical properties (total dissolved solids (TDS), conductivity, corrosivity and pH); inorganics (alkalinity, bicarbonate, carbonate, chloride, sulfate, fluoride, nitrate + nitrite as N, hardness as $CaCO_3$ and sodium absorption ratio (SAR)); and metals (aluminum, arsenic, cadmium, calcium, chromium, iron, lead, magnesium, manganese, potassium, sodium and zinc). Corrosivity, hardness and SAR were calculated, all other analyte values including TDS were measured.

After about 50 wells had been tested, geologist and Crow Tribal member Anita Moore-Nall suggested adding testing for total uranium, an element not part of the Montana Well Educated Program's "full domestic analysis" [49]. Total dissolved uranium was included as an analyte in all subsequent wells tested, 97 in total, utilizing EPA Method E200.8 [55] per the recommendation of Energy Laboratories. The reporting limit for uranium with this method was 1 μg/L. (Energy Laboratories has been accredited by the National Environmental Laboratory Accreditation Program since 2001. Their quality assurance (QA) procedures, including how the Lab estimates method accuracy, are provided in their QA manual [56].

The decision was made not to return to homes previously sampled just to test for uranium, for several reasons. Most participants worked away from home during normal business hours, making sampling difficult; homes were as far as 120 km (75 mi) from our base of operation at Little Big Horn College, so each home visit was expensive. Given limited budget and staff time, the decision was made to limit uranium sampling to new participants, to maximize the number of families the project could serve.

2.4. Data Entry and Analysis

Mapping the spatial distribution of well water contaminants is vital for risk assessment, communication and mitigation. A GIS map was prepared to show both spatial patterns and the considerable variability in uranium contaminant levels even among neighboring wells. In the GIS a point and polygon overlay was used to look at well data and elements present in the wells and surface water samples and stream sediment samples from the National Uranium Resource Evaluation (NURE) Hydrogeochemical and Stream Sediment Reconnaissance (HSSR) Program's data base for Montana and Wyoming [26]. Additional water quality data was obtained and added to the GIS from the Montana Bureau of Mines and Geology's Ground Water Information Center (GWIC) [57], the Montana Natural Resources Information System [58], Natural Resource Conservation Service's Data Gateway [59], the University of Wyoming's Water Resources Data System [60], the Wyoming Geographic Information Center [61], USGS Water Quality Data for Wyoming [62] and the USGS National Geochemical Database Reformatted Data for Montana and Wyoming [63]. Data from all 97 wells tested for uranium by the Crow Water Quality Project was then entered into MS Excel™ and added to the GIS.

Well water contamination was also examined spatially using watershed boundaries, as each watershed has distinctive water contamination issues. The Reservation's three main river valleys, from west to east, are Pryor Creek, the Bighorn River and the Little Bighorn River, all of which flow south to north, separated by mountain ranges (Figure 1). Crow settlements have traditionally been along the rivers and creeks, and that pattern continues

today. Histograms of uranium concentrations in well water were plotted for each watershed, and the respective means and standard deviations were calculated, using Excel 2013.

As shown in Figure 3.5 (below), the traditional "Districts" of the Reservation correspond to watersheds, with the exception that the "Black Lodge District" encompasses portions of both the Bighorn and Little Bighorn River watersheds. Districts are well understood geographic, social and political regions of the Reservation, hence their utility for communicating risk.

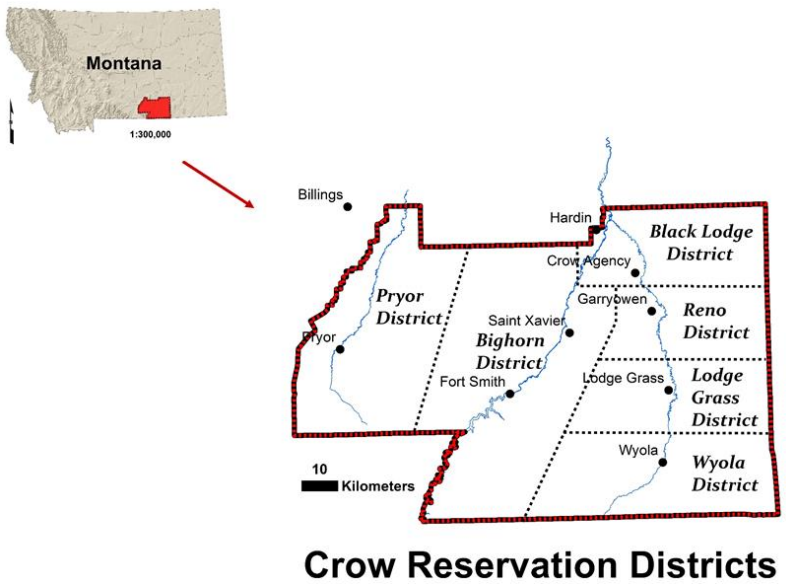


Figure 3.5. Maps of the Crow Reservation, showing location within Montana and major rivers, towns and traditional districts of the Reservation.

Contaminant concentrations were log transformed to improve normality. Correlations between or among contaminants (e.g., uranium concentration and TDS) were analyzed

using regression (for two contaminants) or multiple regression (for three or more contaminants), utilizing IBM SPSS™ Statistics 22 (IBM, Armonk, NY, USA). Surveys were completed by one hundred ninety-seven participants from 165 households. These data were entered into MS Access™ and subsequently analyzed using IBM SPSS™ Statistics 22. Comparisons of categorical variables were made using chi square ("cross-tabs" in SPSS). Comparisons of contaminant concentrations across categorical variables—such as uranium *vs.* water use group—were conducted with analysis of variance (ANOVA). When SPSS calculated that there was significantly unequal variance between contaminant concentration distributions, a non-parametric test (Dunnett T3) was used.

2.5. Risk Communication

Methods included risk communication and risk mitigation in addition to risk assessment. Well owners received a spreadsheet comparing their well water contaminant concentrations, including uranium, with EPA's primary and secondary standards, along with an individualized letter reviewing and explaining their well water test results. Follow up in person visits with as many well owners as could be reached were conducted in 2012–2013.

Ongoing project results, including the GIS maps of uranium and other well water contaminants, were discussed regularly at meetings of the CEHSC, and were presented to the Crow Tribe's Water Resources staff, the Pryor 107 Elders Committee, Messengers for Health and to the community at large through at least one open house a year. Copies of GIS maps showing the spatial distribution of each contaminant were also provided to the

Environmental Health Department of the local Indian Health Service Hospital, which contracts to drill wells for well owners. A poster displaying these maps and explaining the health risks was prepared and is being displayed at local health fairs and in the project office in Crow Agency.

Project data were provided to the Crow Tribe at the request of the Tribal Chairman, to the Crow Tribal Environmental Protection Department and to the Apsaálooke [Crow] Water and Wastewater Authority (AWWA). The AWWA subsequently was able to raise funds for and install a "water salesman," an automated dispensing system in the main Reservation town of Crow Agency, which allows rural residents to purchase municipal water at a very low cost. Other mitigation options for well owners with unpalatable or unsafe well water have been and are being explored. An article summarizing final water quality test results by watershed, with specific recommendations for well water testing for those contaminants of most concern, was submitted to the Tribal newspaper.

Several two day professional development workshops on local water quality were held for local K—12 teachers in conjunction with Montana State University or Little Big Horn College educators. Presentations have also been given in school classrooms and at several local health fairs.

3. Results

Uranium was detected in 68% of the 97 wells tested by the Crow Water Quality Project, with concentration of at least 1 μg/L of uranium (the reporting limit), exceeding EPA's Maximum Contaminant Level Goal (MCLG) for uranium of 0 μg/L [64] (Figure 3.6). The EPA sets the MCLG after reviewing studies of health effects, and describes the

MCLG as “the maximum level of a contaminant in drinking water at which no known or anticipated adverse effect on the health of persons would occur, and which allows an adequate margin of safety. MCLGs are non-enforceable public health goals”. [64] Low levels of uranium in water sources are common, so the public health goal of 0 µg/L is not only non-enforceable but practically speaking, also non-attainable. However, it is important to note that there are known adverse health effects at uranium concentrations lower than the MCL, the municipal drinking water standard, which considers economics as well as health.

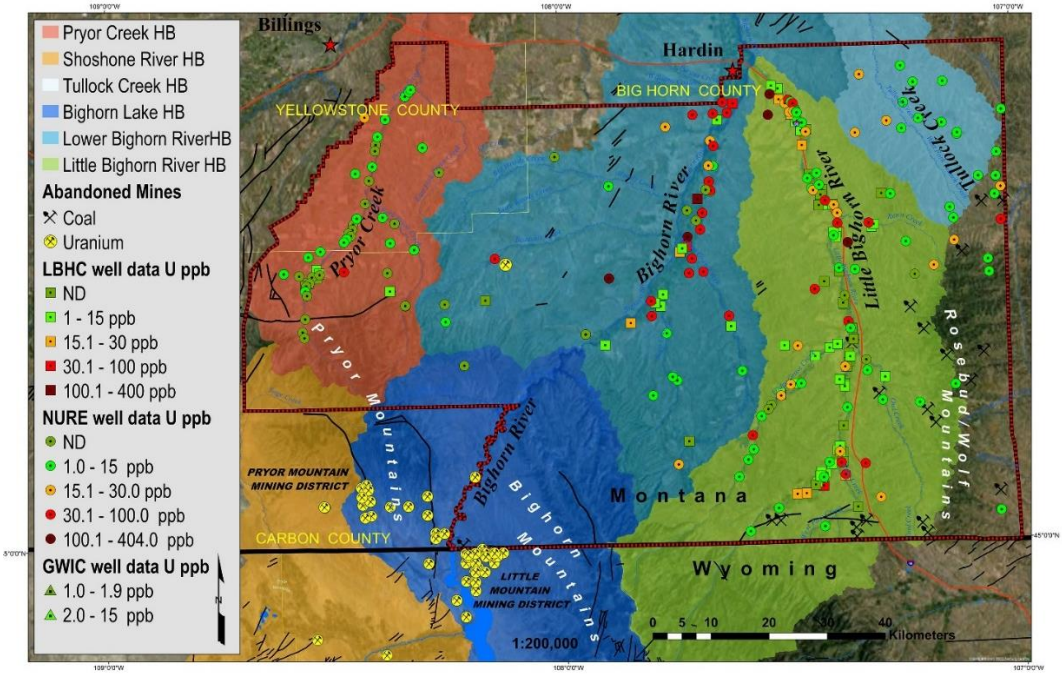


Figure 3.6. Geographic information system (GIS) generated map showing hydrologic drainage basin units, old uranium mines (yellow dots) and well water data from the United States Geological Survey (USGS) National Uranium Resource Evaluation (NURE) Hydrogeochemical and Stream Sediment Reconnaissance (HSSR) data base; the Montana Bureau of Mines and Geology Ground Water Information Center (GWIC) data base and the Crow Water Quality Project data base.

EPA's MCL of 30 μg/L (ppb) was exceeded in 6.3% of wells. Other national and international standards for uranium in drinking water are stricter. In Canada, the "maximum acceptable concentration" is 20 μg/L [65], which was the standard initially proposed for the U.S. EPA, but rejected based on a cost-benefit analysis [45]. Some states, such as Vermont, have also opted for the more conservative standard of 20 μg/L [5]. 10.3% of wells tested on the Reservation by this Project exceeded this stricter standard.

Averaging well water uranium concentrations by river valley shows that residents in the Bighorn River Valley (n = 12) are most at risk for contaminated wells, with an average uranium concentration of 25 ± 29 μg/L (Figure 7). Uranium concentrations in Little Big Horn River valley home wells (n = 75) averaged 6 ± 9 μg/L; Pryor Creek home wells (n = 10) had the lowest uranium concentrations, averaging 3 ± 3 μg/L (Figure 3.7).

Given the considerable variability in uranium concentrations, how would a homeowner decide whether well water testing is worth the cost? Uranium in water is colorless, tasteless and odorless [66], so there are no sensory clues. High TDS, which imparts a taste that families can recognize, was found to be a potential indicator for the occurrence of uranium. pH, easily measured by Project staff, was also investigated as a potential indicator. Regression analysis found that TDS was significantly associated with uranium in the Bighorn River Valley (R^2 = 0.828) and in Pryor (R^2 = 0.719). In the Little Bighorn River valley, multiple regression analysis found that both TDS (p < 0.001) and pH (p < 0.001) were predictive of uranium (R^2 = 0.446) [67].

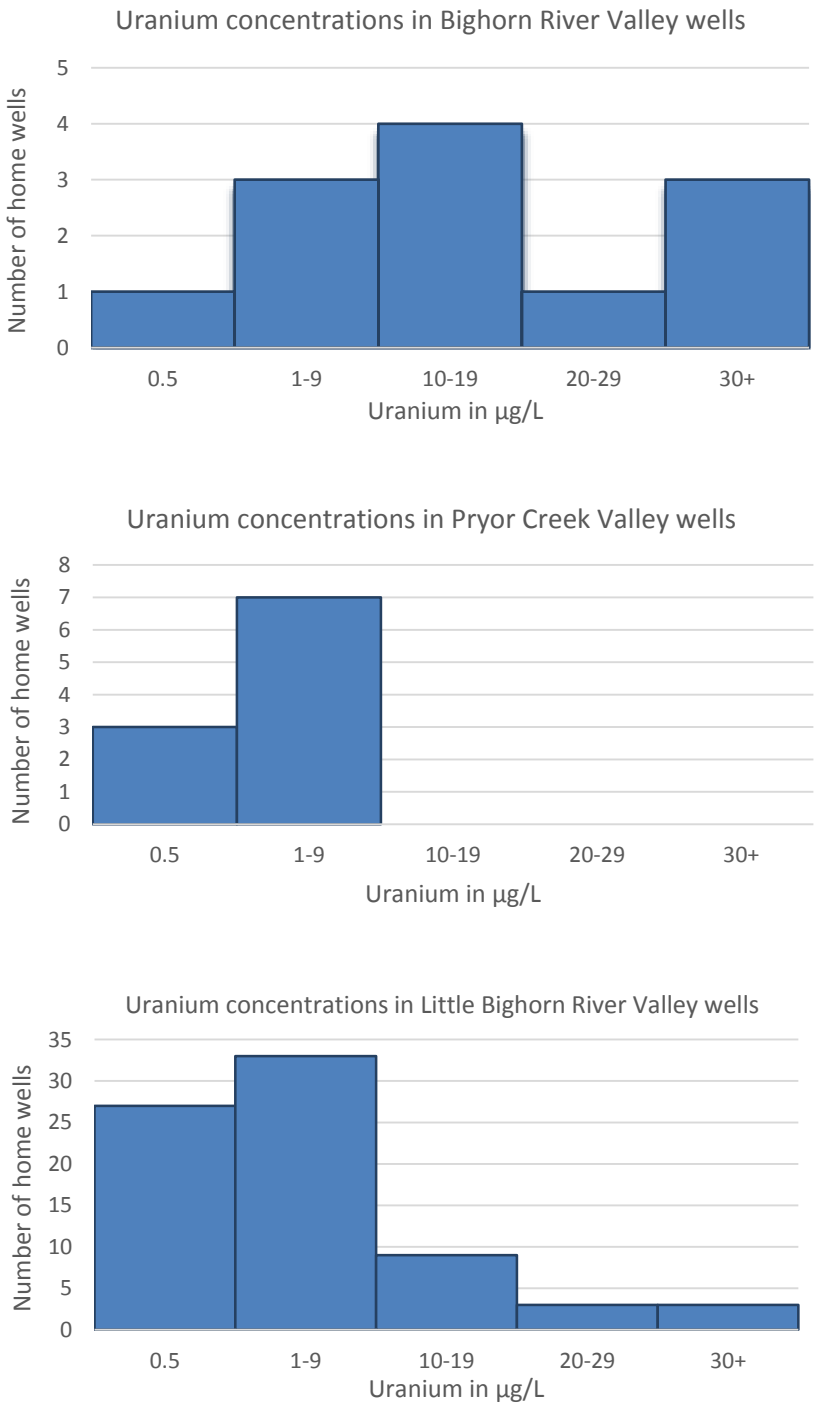


Figure 3.7. Histograms of uranium concentrations in well water (in µg/L) by river valley, Crow Reservation. The reporting limit is 1.0 µg/L, hence 0.5 µg/L represents non-detection.

These results agree with an analysis of nationwide data, which found a correlation between uranium and oxic waters with a pH in the range of 6.5 to 8.5 as well as high carbonate levels. In these conditions, high uranium also corresponded with high TDS levels [68]. These correlations can be explained: in oxic conditions in shallow groundwater and surface water, uranium most commonly exists as U(VI) in the uranyl ion (UO_2^{2+}); this ion typically complexes with the ligand carbonate (or phosphate), which greatly increases the solubility of uranium in water [69].

Similar pH, carbonate and TDS conditions were all found in the home wells tested on the Crow Reservation: (1) wells with elevated uranium were all in the pH range of 7.0 to 8.0, (2) bicarbonate levels were high in all three river valleys, ranging from a mean of 350 mg/L in Pryor to a mean of 495 mg/L in the Little Bighorn River Valley, and (3) high TDS was significantly correlated with high uranium concentrations in all three river valleys. Redox conditions are unknown, as neither oxidation reduction potential nor well depth was measured. However, most homeowners reported that their wells are in relatively shallow groundwater, due to the cost of drilling deeper wells; shallower groundwater is more likely to be oxic.

As the USGS acknowledged in its nationwide study, both well water quality data and well water consumption data are needed to assess the health risks from groundwater contamination [11]. Survey results (Table 1) document that 20% of well owners neither drink nor cook with their well water (Group I), 20% only consume their well water through cooking (Group II) and 60% of well owners both drink and cook with their well

water (Group III). All well owners who participated in this study use their well water for bathing, washing dishes and cleaning their house, regardless of the water quality.

Families who drink and cook with their well water (Group III) have an average TDS level of 959 mg/L in their water—almost double the EPA's secondary standard of 500 mg/L. Although their well water is thus on average considered "objectionable" for consumption [49], they have significantly better well water quality, based on TDS, than families who consume well water only through cooking (Group II, mean TDS 1970 mg/L, standard deviation (SD) of 1466 mg/L) ($p = 0.002$) or don't consume it at all (Group I, mean TDS 2262 mg/L) ($p = 0.001$) (Table 3.1).

Well Water Use	Number of Families	Drink Well Water?	Cook with Well Water?	Mean and SD of TDS in mg/L	Mean and SD of [U] in µg/L*
Group I	30	No	No	2262 ± 1726	14 ± 15
Group II	31	No	Yes	1970 ± 1466	13 ± 23
Group III	91	Yes	Yes	959 ± 578	4 ± 6

Note: * For families whose wells were tested for uranium: Group I, $n = 21$; Group 2, $n = 21$; Group 3, $n = 52$. Water use data lacking for three participating households.

Table 3.1. Relationship of well water quality to consumption.

This analysis shows that families whose well water is good enough to drink untreated (Group III) have significantly lower concentrations of total dissolved solids in their water, including generally low levels of uranium. Families who neither drink nor cook with their water (Group I) are not at risk of exposure to uranium, as absorption through skin is minimal [46]. Families who still cook with their well water, despite its unpleasant taste

(Group II), are most at risk of consuming water with unsafe uranium concentrations. Families in both Groups II and III should also consider testing their home air for radon [70].

Despite the widespread poor quality of well water, very few families have home water treatment systems. Although 77% of all wells tested have unacceptably hard water (in excess of the EPA secondary standard), only 3.3% of families had installed a water softener. While 85% of all wells tested exceed the EPA secondary standard for TDS, only 4% of families had a reverse osmosis system. Despite the generally high levels of iron and of manganese, no participating family had an iron/manganese removal unit [67]. The hard water requires softening before treating it by reverse osmosis, and water softeners require purchasing treatment chemicals regularly. While the U.S. and the Montana per capita incomes for 2010 were $27,334 and $23,836 respectively, the per capita income for the four largest Crow Reservation communities a third or less of this, ranging from only $7,354 to $8,130 [17]. Crow Environmental Health Steering Committee (CEHSC) members explain that the cost of installing and maintaining treatment technology, including the monthly cost of chemicals, is simply prohibitive for most families. Most families with unpalatable well water cope by purchasing and hauling bottled water and/or filling gallon jugs at homes of friends and relatives. A few collect and use spring or river water.

As the two most populated local communities—Hardin and Crow Agency—use the Bighorn and Little Bighorn Rivers respectively for their municipal water supplies, water samples were collected monthly from both rivers over an eight month period, delivered to

the EPA-certified lab in Billings and tested for the same parameters as well water, including uranium. The Big Horn River at Hardin averaged about 4 μg/L uranium, and the Little Big Horn River even less.

4. Discussion and Conclusions

4.1. Potential Sources of Uranium in Local Groundwater

Both project data and the NURE data indicate that uranium contamination of wells is most serious in the Bighorn River valley and also of concern in the Little Bighorn River valley, while only one well tested in the Pryor Creek valley (by NURE) exceeded 30 μg/L.

Mapping the uranium concentration in well water in relation to the geology of the Crow Reservation shows that the highest uranium values appear to be associated with Quaternary Terrace deposits in the lower Bighorn River Valley (Figure 3.6) [71]. These valley fill sediments could have eroded from the uranium bearing upland bedrock, as is the case elsewhere in Montana [46]. Other possible uranium sources may be from the Jurassic Morrison Formation or the Fort Union Formation. In 1952, the Atomic Energy Commission made an airborne radiometric survey over portions on the east flank of the Bighorn Mountains covering about 647 km^2 (250 mi^2), including part of the Crow Reservation [29]. The only anomaly found on the Crow Reservation by the aerial survey was in the Morrison Formation in Section 34, Township 4 South, Range 29 East, and Section 3, Township 5 South, Range 29 East [29]. Investigation on the ground revealed a very weak radioactive zone within the shales of the Morrison Formation. Radioactivity

was also noted in dinosaur bone fragments embedded in a sandstone facies of the Morrison Formation; results from chemical assays on samples of bones showed the highest radioactivity indicated was 0.23 percent triuranium octoxide (U_3O_8, a form of yellowcake) [29]. Later a NURE investigation of the Billings Quadrangle was conducted from 1978–1981 [33]. Geologic units were investigated for favorable uranium deposits that could contain at least 100 tons of U_3O_8 in rocks with an average grade of not less than 100 parts per million (ppm) U_3O_8. A thin, radioactive, carbonaceous claystone bed from an outcrop of Fort Union was sampled and found to contain 50 ppm U_3O_8, and this was considered unfavorable for uraniferous lignite-type deposits [33]. These formations may be a source of naturally occurring uranium on the Crow Reservation.

Historic uranium and vanadium mining directly to the southwest of the Reservation, just outside of the Reservation boundary, might also be contributing to well water contamination down gradient in the Bighorn River Valley. The two abandoned mining districts in the Mississippian-aged Mission Canyon formation which hosts the mineralized uranium/vanadium deposits are represented as mining symbols in the southwest corner of the map (Figure 3.6).

Agricultural fertilizer is a third potential source of uranium in groundwater, as the radionuclide occurs in phosphate mined for fertilizer production [72]. Research in Germany has found that the uranium concentrations in groundwater below agricultural land are three to 17 times higher than under forested land [73] cited in [72]. Hence, extensive irrigated and dry land farming on the Reservation, particularly in the Bighorn River valley [74], could be contributing uranium from fertilizer to the groundwater.

In short, uranium contamination of home well water is likely to be coming from natural sources, and might be exacerbated by mining in the upper Bighorn River watershed and/or fertilization of agricultural lands in the Bighorn and Little Bighorn River valleys. Future research employing isotopic analysis of uranium in well water could help elucidate contamination source(s).

4.2. Sources of Uncertainty

The "snowball" sampling strategy for participation in this study—based on volunteers—could have biased results, as one might suspect that families with poor quality well water would have been more likely to volunteer to participate. However, comparing project data with the non-georeferenced Indian Health Service well water database showed that families with poor quality well water were *underrepresented* [67]. Perhaps families who neither drank nor cooked with their water had less reason to take the time to participate?

One might ask whether the subset of 97 families whose wells were tested from uranium differed from the overall sample of 151 families. There is no evidence to suggest a difference: the sampling strategy did not change after the project added uranium as an analyte, nor did the proportion of families in the three water use Groups (no consumption, cooking only, cooking and drinking) change at this point in the study (Table 3.1). Both the overall sample of 151 families and the subset of 97 families whose wells were tested for uranium are drawn primarily from the Little Big Horn River Valley, with lesser representation of the Bighorn River and Pryor Creek valleys; this accurately reflects the distribution of the Tribal population on the Reservation.

Well water was tested only for total dissolved uranium. It is possible that particle-bound uranium is also present in well water. If this is the case, a higher percentage of home wells might exceed the MCL, presenting a health risk to families consuming the water.

In the Little Big Horn River Valley, the presence of two aquifers—a shallower one with poor water quality and a deeper one with better water [75]—probably contributes to the variability in well water uranium concentrations. Many families participating in this study were unsure of the exact depth of their well, hence it was not possible to correlate uranium with well depth. Measuring well depth would improve the ability to predict uranium concentrations based on aquifer as well as to assess the impacts of land use practices on contamination of shallow groundwater.

Simply measuring uranium concentrations in home well water might underestimate the risks from exposure to radionuclides, as the USGS found in western Montana [50]. Elevated levels of uranium progeny such as radium and radon (along with uranium) have been found to occur in groundwater where there is uranium mineralization [76]. Higher concentrations of radium have been found to be associated with manganese or iron-rich anoxic groundwater [68]. Wells in both the Bighorn and Little Bighorn River valleys are relatively high in manganese, with average concentrations well exceeding EPA's secondary standard of 0.05 mg/L [67]. Additionally, average iron concentrations in well water substantially exceeded the EPA secondary standard of 0.30 mg/L in every zip code in the Big Horn and Little Big Horn River valleys, with the exception of Fort Smith in the

upper Big Horn River watershed. Hence, the conditions may exist for radium to also be found in higher concentrations in home well water.

Nationally, radon is also a relatively common well water contaminant: the USGS found 4.4% of home wells tested in 48 states exceeded the EPA's proposed MCL of 4,000 pCi/L for radon, and 65% exceeded the alternate proposed MCL of 300 pCi/L [9]. Bighorn County is classified as "Zone 1" for the highest risk of radon in homes [77]. While testing well water for radon contamination might be advisable, it is expensive and radon released from soil into home air and inhaled is a more significant health risk (lung cancer) [78]. The limited radon data for Bighorn County shows that of homes tested, 34% had radon levels at or above 4 pCi/L, requiring mitigation [79]. Testing home air for radon is needed, but was deemed beyond the scope of this risk assessment.

In sum, although there are numerous sources of uncertainty, particularly with regards to whether other potential (radionuclides and pesticides) and known (inorganic and microbial [80,81]) contaminants are contributing to the health risks, the potential for error in this study is primarily in having *underrepresented* the health risks to families using wells.

4.3. Uranium Contamination of Home Well Water is a Priority Public Health Issue

Based on the following recognized criteria for prioritizing and addressing exposures to environmental chemical mixtures [82], contamination of home well water on the Crow Reservation should be addressed as a high priority public health issue:

(1) *Breadth of exposure.* Roughly 50% of Crow families rely on home wells for their domestic water supply [11]; 80% of these families drink and/or cook with their well water. Uranium and possibly other radionuclides in well water are widespread in the Bighorn and Little Bighorn River valleys on the Reservation.

(2) *Nature of exposure.* People consume well water daily for many years. Survey data document that people who drink their well water consume about eight cups per day [67]. Half of families whose well water is so high in TDS that it is unfit for drinking, nevertheless still use it for cooking.

(3) *Severity of effects.* The nephrotoxic effects of uranium [83] are a particular concern given the high diabetes prevalence rate of 12.1% in Big Horn County, compared to 6.2% statewide, as well as the downstream effects of seriously elevated rates of hospitalization and death from diabetes [18]. While many factors, including physical activity level, diet, obesity, metabolic factors and possibly genetics increase risk of diabetes [84,85], exposure to the nephrotoxin lead is another known factor [84]. Decline in kidney function associated with blood lead and tibia lead levels is significantly more rapid in middle aged and older men with diabetes than in men without this disease [86]. Uranium, like lead, is nephrotoxic [83,87]. While the effects of uranium exposure on diabetic kidney disease incidence and progression is unknown, this possibility is of concern to the project team.

(4) *Interactions.* Interactions as understood in an ecological framework include natural, built and sociopolitical factors [88], all of which contribute to local health impacts from water contamination. The interactive direct health effects of uranium

> with other potentially co-occurring inorganic, organic, radioactive, and/or microbial contaminants in well water are unknown. Community members burdened by existing health conditions are likely to be more vulnerable to the impacts of well water contamination. Any health effects from exposure to contaminated drinking water are likely to both contribute to and be exacerbated by the existing health disparities that underlie the twenty year difference in life expectancy between Native American and non-Native residents of Big Horn County [19] cited in [18]. Lack of environmental health literacy is also viewed by the CEHSC as contributing to health disparities. One Crow Elder compared the arrival of indoor plumbing in the 1960s with the earlier arrival of watermelons: not knowing how to prepare watermelons, people boiled them as they did squash. Indoor plumbing was equally unfamiliar as there was no community education on how to protect one's well water or maintain and repair wells, plumbing and septic systems.

Inequity could arguably be considered a fifth criteria for recognizing an environmental exposure as a priority public health issue. Well owners nationwide lack the regulatory oversight that safeguards public health via enforcement of standards for municipal water quality. Uranium is an especially insidious well water contaminant as it cannot be detected by taste, smell or discoloration. In absence of any governmental regulation of or environmental health community education on well water quality, community members frequently stated, "Oh my well water tastes fine, it doesn't need to be tested". In Bighorn County, residents of the two most populous communities are provided with municipal water from surface water sources with lower average concentrations of uranium, as noted

above. Hence local well owners are at higher risk of uranium exposure through their drinking water than residents of towns which use surface water sources for their supply.

Unsafe well water and the limited financial resources of most families also interact to increase exposures to contaminants. As noted above, some families cook with water which tastes so unpleasant they aren't drinking it, as they can neither afford to install and maintain water treatment technology, nor purchase and haul sufficient bottled water for both drinking and cooking [89].

4.4. Future Research, Community Education and Risk Mitigation

The Crow Environmental Health Steering Committee and project staff continue to work on assessment, communication and mitigation of health risks from contaminated well water. A new EPA grant includes limited funding for additional home well water testing—free to community members. The project team has also applied for National Institutes of Health (NIH) funding to be able to offer free health screenings for adults with a history of consuming contaminated well water.

Mitigating contaminated well water is a complex challenge for which the CEHSC is seeking solutions. It will require additional resources to expand the project's free well water testing, as well as increased community awareness of the risks, greater understanding of how to protect and maintain wells, plumbing and septic systems, and more affordable alternatives for homeowners with bad well water. Mitigating home well water with unsafe levels of inorganic contaminants such as uranium is challenging, as nearly all these wells have such hard water that both a water softener and a reverse osmosis unit would be required. Even if a grant for installing all this treatment equipment

could be obtained, many families could not afford the monthly costs of chemicals and regular filter replacements.

A new collaboration led by a Crow Tribal member on MSU's faculty, has been funded and is planning an environmental health literacy campaign with fourth graders, focused on surface and groundwater stewardship, and well and septic system care.

The project team is also working to understand how climate change impacts on water resources could affect health risks from waterborne contaminants [90]. Funding is being sought for additional home well water testing, including measurements of well depth, to allow for better spatial analysis of contaminant distributions and relationships to land uses, using a geographic information system (GIS). The CEHSC, including academic partners, continues to explore ways to improve community health by reducing exposures to waterborne contaminants, increasing access to safe drinking water and promoting environmental health literacy.

4.5. Conclusions

In conclusion, for families on the Crow Reservation who rely on home wells, exposure to uranium and potentially other waterborne contaminants may both contribute to and be exacerbated by existing health disparities. Limited financial resources restrict families' options for either treating well water or purchasing and hauling sufficient safe water for consumption. Conducting such research and education as a true partnership between community and academic researchers will help to ensure that the science is sound, the community is increasingly empowered to address environmental health disparities, and that the work is effective in reducing health risks. In a state where home well water has

not historically been tested for uranium and 88% of counties are at Level 1 risk for radon in homes, many rural and impoverished Montana families may be similarly at risk. Additional risk assessment research, risk communication and risk mitigation measures are warranted to ensure families have access to safe drinking water. Limited or lack of access to safe drinking water for these families likely contributes to existing health disparities and is a priority public health issue.

Acknowledgments

Current members of the Crow Environmental Health Steering Committee (CEHSC) are: John Doyle, Myra Lefthand, Sara Young, Ada Bends, Brandon Good Luck, Alma Knows His Gun McCormick and Robin Stewart. All are Crow Tribal members. They represent the Apsaalooke (Crow) Water and Wastewater Authority, Little Big Horn College (the local Tribal College), the Crow Tribal government, the Crow/Northern Cheyenne Indian Health Service Hospital, the Bureau of Indian Affairs, the local non-profit Messengers for Health, the Crow Legislature and education.

Funders: Center for Native Health Partnerships' Grant #P20MD002317 from National Institute of Minority Health & Health Disparities; NIH Grant #P20 RR-16455-04 from the Infrastructure Network of Biomedical Research Excellence (INBRE) Program of National Institute of General Medical Science National Institutes of Health; Award #RD83370601-0 from the National Center for Environmental Research, Environmental Protection Agency; EPA STAR Fellowship Research Assistance Agreement #FP91674401. Alfred P. Sloan Graduate Scholarship Programs—Minority

PhD Component/Sloan Indigenous Graduate Partnership; Montana State University—Dennis and Phyllis Washington Foundation Native American Graduate Fellow.

Note: The content is solely the responsibility of the authors; it has not been formally reviewed by any of the funders and does not necessarily represent the official views of the National Institutes of Health or of the Environmental Protection Agency. The EPA does not endorse any of the products mentioned.

Dr. Tim Ford, then Montana INBRE Principal Investigator and Microbiology Department Chair at Montana State University Bozeman (MSU), provided initial academic support from MSU and was instrumental in securing NIH and EPA funding for testing well water and conducting surveys. Advice on statistical analysis was provided by Dr. Al Parker (MSU). Dr. David Roberts (MSU) consulted on database management. Dr. Margaret Hiza (USGS; Crow) and Dr. Cliff Montagne (MSU) and their colleagues provided inspiring examples of community-based participatory research and were always available for consultation. Dr. David Yarlott, President of Little Big Horn College, has supported this project from its inception. This research would not have been possible without the contributions of previous CEHSC members and Project Coordinators Gail Whiteman, Crescentia Cummins and Tamra Old Coyote as well as more than a dozen student interns. We especially thank the more than 200 Crow community members who gave of their time and expertise as participants in this research project. Anonymous reviewers provided excellent suggestions for improving the article.

Author Contributions

Margaret Eggers: Has served as a non-voting CEHSC member since 2006, served as Project Leader including designing the research project in consultation with the CEHSC, local Project Coordinator and Dr. Camper, training local staff, overseeing fieldwork, preparing reports to homeowners, managing and analyzing the data, preparing GIS from project data and with the Project Coordinator communicating project results to community groups and local teachers; primary author on paper. Anita Moore-Nall: Researched federal and state data on local water quality; suggested project test wells for uranium; prepared GIS map incorporating federal, state and project data on well water quality; researched the area's geology; wrote the geologic Study Area description for paper. John Doyle: Has served on the CEHSC since 2006; served as local Project Coordinator for the past two years, conducting home visits to explain well test results, discussing project results in community and with Tribal officers, and conducting outreach to local teachers and schoolchildren; contributes local expertise to research; as the Director of the Apsaalooke Water and Wastewater Authority, coordinates efforts between the CEHSC and the AWWA. Contributed to and reviewed drafts of the paper. Myra Lefthand: Has served on the CEHSC since 2006; reviewed and edited initial survey; contributed health education and cultural expertise to project; explained project results to community members; provided training for student interns, especially those conducting surveys; collaborates with the Executive Branch of the Crow Nation on water issues; reviewed drafts of the paper. Sara Young: Has served on the CEHSC since 2007; reviewed and edited the initial survey; recruited participants; coordinated this project

with other related projects at MSU; reviewed drafts of the paper. Ada Bends: Has served on the CEHSC since 2008; as a Community Organizer for the Crow Reservation has recruited participants and organized community meetings for presentation of project results; contributed data from the 2010 health disparities survey she conducted; reviewed drafts of the paper. Anne Camper: Has participated in the CEHSC since 2008; oversaw research that provided testing for well and river water testing/survey collection; reviewed data analysis; contributed to the manuscript. CEHSC: All CEHSC co-authors and additional CEHSC members have guided and advised the project, contributed local environmental, health and cultural expertise, and co-presented on the research at conferences and workshops.

Conflicts of Interest

The authors declare no conflict of interest

References

1. DeLemos, J.L.; Burgge, D.; Cajero, M.; Downs, M.; Durant, J.L.; George, C.M.; Henio-Adeky, S.; Nez, T.; Manning, T.; Rock, T.; Seschillie, B.; Shuey, C.; Lewis, J. Development of risk maps to minimize uranium exposures in the Native Churchrock Mining District. *Environ. Health* **2009**, *8*, 29, doi:10.1186/1476-069X-8-29.

2. Arzuaga, X.; Rieth, S.H.; Bathija, A.; Cooper, G.S. Renal effects of exposure to natural and depleted uranium: A review of the epidemiologic and experimental data. *J. Toxicol. Environ. Health B Crit. Rev.* **2010**, *13*, 527–545.

3. Caldwell, R. *Uranium and Other Radioactive Elements in Jefferson County Ground Water*; U.S. Geological Survey: Helena, MT, USA, 2008.

4. Kurttio, P.; Auvinen, A.; Salonen, L.; Saha, H.; Pekkanen, J.; Makelainen, I.; Vaisanen, S.B.; Penttila, I.M.; Komulainen, H. Renal Effects of Uranium in Drinking Water. *Environ. Health Perspect.* **2002**, *110*, 337–342.

5. Vermont Department of Health. Uranium. Available online: http://healthvermont.gov/enviro/rad/Uranium.aspx (accessed on 10 December 2014).

6. Zamora, M.L.; Tracy, B.L.; Zielinski, J.M.; Meyerhof, D.P.; Moss, M.A. Chronic Ingestion of Uranium in Drinking Water: A Study of Kidney Bioeffects in Humans. *Toxicol. Sci.* **1998**, *43*, 68–77.

7. Selden, A.I.; Lundhom, C.; Edlund, B.; Hogdaul, C.; Ek, B-M.; Bergstrom, B.E.; Ohlson, C.-G. Nephrotoxicity of uranium in drinking water from private drilled wells. *Environ. Res.* **2009**, *109*, 486–494.

8. Mao, Y.; Desmeules, M.; Schaubel, D.; Berube, D.; Dyck, R.; Brule, D.; Thomas, B. Inorganic components of drinking water and microalbuminuria. *Environ. Res.* **1995**, *71*, 135–140.

9. Orloff, K.G.; Mistry, K.; Charp, P.; Metcalf, S.; Marino, R.; Shelly, T.; Melaro, E.; Donohoe, A.M.; Jones, R.L. Human exposure to uranium in groundwater. *Environ. Res*. **2004**, *94*, 319–326.

10. Moore-Nall, A. The legacy of uranium development on or near Indian reservations and health implications rekindling public awareness. *Geosciences* **2015**, *5*, 15–29.

11. DeSimone, L.A. *Quality of Water from Domestic Wells in Principal Aquifers of the United States, 1991–2004*; U.S. Geological Survey Scientific Investigations Report 2008-5227; U.S. Geological Survey: Reston, VA, USA, 2009.

12. Montana Department of Public Health and Human Services. Big Horn County Health Profile. Available online: http://www.docstoc.com/docs/86526062/2006-Montana-County-Health-Profiles-Department-of-Public-Health (accessed on 3 December 2014).

13. Cummins, C.; Doyle, J.T.; Kindness, L.; Lefthand, M.J.; Bear Don't Walk, U.J.; Bends, A.; Broadaway, S.C.; Camper, A.K.; Fitch, R.; Ford, T.E.; *et al*. Community-Based Participatory Research in Indian Country: Improving Health Through Water Quality Research and Awareness. *Fam. Community Health* **2010**, *33*, 166–174.

14. Lefthand, M.J.; Eggers, M.J.; Old Coyote, T.J.; Doyle, J.T.; Kindness, L.; Bear Don't Walk, U.J.; Young, S.L.; Bends, A.L.; Good Luck, B.; Stewart, R.; *et al*. Holistic community based risk assessment of exposure to contaminants via water sources. In *Proceedings of the American Public Health Association Conference*, San Francisco, CA, USA, 10 October 2012.

15. U.S. Environmental Protection Agency. A Decade of Tribal Environmental Research: Results and Impacts from EPA's Extramural Grants and Fellowship Programs. In *Tribal Environmental Health Research Program*; NCER, ORD, EPA: Washington, DC, USA, 2014. Available online: http://epa.gov/ncer/tribalresearch/news/results-impacts-010714.pdf (accessed on 12 February 2014).

16. U.S. Census Bureau. DP-1-Geography-Big Horn County, Montana: Profile of General Population and Housing Characteristics: 2010. Available online: http://factfinder2.census.gov/ (accessed on 25 November 2013).

17. U.S. Census Bureau. Montana locations by per capita income. Available online: http://en.wikipedia.org/wiki/Montana_locations_by_per_capita_income (accessed on 2 April 2014).

18. Mark, D.; Byron, R. *Bighorn Valley Health Center Program Narrative*; Bighorn Valley Health Center (BVHC): Hardin, MT, USA, 2010, unpublished.
United States Census. 2000. Available online: http://www.census.gov/main/www/cen2000.html (accessed on 11 January 2010).

19. The Centers for Disease Control and Prevention (CDC), National Center for Health Statistics, Division of Vital Statistics, National Vital Statistics Report Volume 58, Number 19, May 2010, Table 29. Available online: http://www.cdc.gov/nchs/data/nvsr/nvsr58/nvsr58_19.pdf (accessed on 7 June 2010).

20. Montana Department of Public Health and Human Services. 2004–2008 Statistics.

21. Bends, A.L. *Health Disparities on the Crow Reservation*; Center for Native Health Partnerships, Montana State University: Bozeman, MT, USA, 2010, unpublished data.

22. Montana Hospital Association. Age-adjusted rates calculated based on the primary diagnosis by the Montana Hospital Discharge Data System, based on data provided by the Montana Hospital Association, Population denominators: NCHS bridged race estimates of the resident population of Montana for 1 July 2000–1 July 2008 (Vintage 2008).

23. National Vital Statistics System, Center for Disease Control and Prevention, U.S.: Death certificate Montana resident data from 2004–2008.

24. Eggers, M.J.; Lefthand, M.J.; Young, S.L.; Doyle, J.T.; Plenty Hoops, A. When It Comes to Water, We Are All Close Neighbors. EPA Blog It All Starts With Science. Available online: http://blog.epa.gov/science/2013/06/when-it-comes-to-water-we-are-all-close-neighbors/ (accessed on 30 June 2013).

25. National Uranium Resource Evaluation (NURE) Hydrogeochemical and Stream Sediment Reconnaissance (HSSR) Program's data base for Montana and Wyoming. Available online: http://tin.er.usgs.gov/nure/water/ (accessed on 18 February 2013).

26. Bureau of Land Management Montana State Office. *Crow Indian Tribe: Geology and Minerals Resources Report*; BLM: Billings, MT, USA, 2002; pp. 67–73. Available online: http://www.blm.gov/style/medialib/blm/mt/field_offices/miles_city/og_eis/crow.Par.79832.File.dat/minerals.pdf (accessed on 10 December 2014).

27. Perry, E.S. *Montana in the Geological Past. Montana Bulletin 26*; Montana Bureau of Mines and Geology: Montana Tech of the University of Montana, Butte, MT, USA, 1962.

28. Mapel, W.J.; Roby, R.N.; Sarnecki, J.C.; Sokaski, M.; Bohor, B.F.; McIntyre, G. Status of Mineral Resource Information for the Crow Indian Reservation, Montana. Available online: https://www1.eere.energy.gov/tribalenergy/guide/pdfs/crow_7.pdf (accessed on 10 December 2014).

29. Lopez, D.A. *Geologic Map of the Bridger 30' × 60' Quadrangle, Montana: Montana Bureau of Mines and Geology Geologic Map 58, 2000, Scale 1:100,000*; Montana Bureau of Mines and Geology: Montana Tech of the University of Montana, Butte, MT, USA, 2000.

30. BLM. *Crow Natural, Socio-Economic and Cultural Resources Assessment and Conditions Report, Hydrology*; BLM: Billings, MT, USA, 2002; pp. 74–84.

Available online: http://www.blm.gov/style/medialib/blm/mt/field_offices/miles_city/og_eis/ crow.Par.48024.File.dat/hydrology.pdf (accessed on 10 December 2014).

31. Stewart, J.C. *Geology of the Dryhead-Garvin Basin, Bighorn and Carbon Counties, Montana: Map G-2*; Montana Bureau of Mines and Geology Special Publication 17; Montana Bureau of Mines and Geology: Montana Tech of the University of Montana, Butte, MT, USA, 1958.

32. Warchola, R.J.; Stockton, T.J. *National Uranium Resource Evaluation, Billings Quadrangle, Montana. PGJ/F-015(82)*; Morris & Warchola, Inc., Bendix Field Engineering Corporation, U.S. Department of Energy: Grand Junction, CO, USA, 1982.

33. Patterson, C.G.; Toth, M.I.; Kulik, D.M.; Esparza, L.E.; Schmauch, S.W.; Benham, J.R. *Mineral Resources of the Pryor Mountain, Burnt Timber Canyon, and Big Horn Tack-On Wilderness Study Areas, Carbon County, Montana and Big Horn County, Wyoming*; U.S. Geological Survey Bulletin 1723; U.S. Geological Survey: Denver, CO, USA,1988; pp. 1–15.

34. Van Gosen, B.S.; Wilson, A.B.; Hammarstrom, J.M. *Mineral Resource Assessment of the Custer National Forest in the Pryor Mountains, Carbon County, South-Central Montana*; U.S. Geological Survey Open-File Report 96-256; U.S. Geological Survey: Denver, CO, USA, 1996.

35. Blackstone, D.L., Jr. *Preliminary Geologic Map of the Red Pryor Mountain 7.5' Quadrangle, Carbon County, Montana: Montana Bureau of Mines and Geology Open File Report 68, 1:24,000*; Montana Bureau of Mines and Geology: Montana Tech of the University of Montana, Butte, MT, USA, 1974.

36. Klauk, E. Impacts of Resource Development on Native American Lands, Geology and Physiography of the Crow Reservation. Available online: http://serc.carleton.edu/research_education/nativelands/ crow/geology.html (accessed on 10 December 2014).

37. Richards, P.W. *Geology of the Bighorn Canyon-Hardin Area, Montana and Wyoming*; U.S. Geological Survey Bulletin 1026; U.S. Geological Survey: Helena, MT, USA, 1955; pp. 1–93. Available online: http://pubs.er.usgs.gov/publication/b1026 (accessed on 10 December 2014).

38. Hauptman, C.M. Uranium in the Pryor Mountain area of southern Montana and northern Wyoming. *Uranium Mod. Min.* **1956**, *3*, 14–21.

39. Florentine, C.; Krause, T.; Eggers, M.J. Biogeochemical Cycling of Uranium. Presented at Montana State University, Bozeman, MT, USA, April 2013.

40. U.S. Environmental Protection Agency. Radiation Protection: Decay Chains: Uranium-238 Decay Chain. Available online: http://www.epa.gov/radiation/understand/chain.html#u_decay (accessed on 3 August 2013).

41. World Health Organization. Uranium in drinking water: Background document for development of WHO Guidelines for drinking-water quality. Available online: http://www.who.int/water_sanitation_health/dwq/chemicals/en/uranium.pdf (accessed on 25 September 2012).

42. Wrenn, M.E.; Durbin, P.W.; Lipsztein, H.B.; Rundo, J.; Still, E.T.; Willis, D.L. Metabolism of ingested U and Ra. *Health Phys*. **1985**, *48*, 601–633.

43. U.S. Environmental Protection Agency. Uranium. Available online: http://www.epa.gov/radiation/radionauclides/uranium.html (accessed on 25 September 2012).

44. Brugge, D.; de Lemos, J.L.; Oldmixon, B. Exposure pathways and health effects associated with chemical and radiological toxicity of natural uranium: A review. *Rev. Environ. Health* **2005**, *20*, 177–193.

45. Brugge, D.; Buchner, V. Health effects of uranium: New research findings. *Rev. Environ. Health* **2011**, *26*, 231–249.

46. Georgia Department of Human Resources. Radium and Uranium in Public Drinking Water Systems. Available online: http://www.gaepd.org/Documents/radwater.html (accessed on 2 August 2013).

47. Montana Department of Environmental Quality (MTDEQ). Uranium in Drinking Water. Available online: http://deq.mt.gov/wqinfo/swp/Guidance.mcpx (accessed on 6 August 2013).

48. Montana State University Well Educated Program. Well Educated Parameter List. Available online: http://waterquality.montana.edu/docs/WELL_EDUCATED/ParameterPackageList2014.pdf (accessed on 23 December 2014).

49. Caldwell, R. Technical Announcement. USGS Samples for Radioactive Constituents in Groundwater of Southwestern Montana. Available online: http://mt.water.usgs.gov/ (accessed on 7 August 2013).

50. Minkler, M.; Wallerstein, N. *Community-Based Participatory Research for Health*; Jossey-Bass: San Francisco, CA, USA, 2008.

51. Collman, G.W. Community-based approaches to environmental health research around the globe. *Rev. Environ. Health* **2014**, *29*, 125–128.

52. Riederer, A.M.; Thompson, K.M.; Fuentes, J.M.; Ford, T.E. Body weight and water ingestion estimates for women in two communities in the Philippines: The importance of collecting site-specific data. *Int. J. Hyg. Environ. Health* **2006**, *209*, 69–80.

53. Butterfield, P.G.; Hill, W.; Postma, J.; Butterfield, P.W.; Odom-Maryon, T. Effectiveness of a household environmental health intervention delivered by rural public health nurses. *Am. J. Public Health* **2011**, *101*, S262–S270.

54. Creed, J.T.; Brockhoff, C.A.; Martin, T.D. *Method 200.8. Determination of Trace Elements in Waters and Wastes by Inductively Coupled Plasma-Mass Spectrometry, Revision 5.4., EMCC Version*; U.S. Environmental Protection Agency: Cincinnati, OH, USA. Available online: http://water.epa.gov/scitech/methods/cwa/bioindicators/upload/2007_07_10_methods_method_200_8.pdf (accessed on 5 March 2015).

55. Energy Laboratories. Certifications/quality control. Available online: http://www.energylab.com/why-us/certifications-quality-control/ (accessed on 5 March 2015).

56. Montana Bureau of Mines and Geology's Ground Water Information Center. Available online: http://mbmggwic.mtech.edu/ (accessed on 4 February 2013).

57. Montana Natural Resources Information System. Available online: http://nris.mt.gov (accessed on 4 February 2013).

58. Natural Resource Conservation Service's Data Gateway. Available online: http://datagateway.nrcs.usda.gov/ (accessed on 4 February 2013).

59. University of Wyoming's Water Resources Data System. Available online: http://www.wrds.uwyo.edu/ (accessed on 4 February 2013).

60. Wyoming Geographic Information Center. Available online: http://wygl.wygisc.org/wygeolib (accessed on 4 February 2013).

61. USGS. Water Quality Data for Wyoming. Available online: http://waterdata.usgs.gov/wy/nwis/qw (accessed on 4 February 2013).

62. Little Big Horn College Library. Map of the Crow Reservation. Available online: http://lib.lbhc.edu (accessed on 2 August 2013).

63. U.S. Environmental Protection Agency. Regulating Public Water Systems and Contaminants under the Safe Drinking Water Act. What are the drinking water standards? Available online: http://water.epa.gov/lawsregs/rulesregs/regulatingcontaminants/basicinformation.cfm#What%20are%20drinking%20water%20standards? (accessed on 5 March 2015).

64. Health Canada. Water talk-Uranium in drinking water. Available online: http://www.hc-sc.gc.ca/ewh-semt/pubs/water-eau/uranium-eng.php/ (accessed on 25 September 2012).

65. Arnold, C. Once upon a mine: The legacy of uranium on the Navajo Nation. *Environ. Health Perspect.* **2014**, *122*, A44–A49.

66. Eggers, M.J. Community Based Risk Assessment of Exposure to Waterborne Contaminants on the Crow Reservation, Montana. Ph.D. Thesis, Montana State University, Bozeman, MT, USA, May 2014.

67. Szabo, Z. Geochemistry as a critical factor in defining radionuclide occurrence in water from principal drinking-water aquifers of the United States. In Proceedings of the 5th International Conference on Medical Geology, Arlington, VA, USA, 27 August 2013.

68. Farrell, J.; Bostick, W.D.; Jarabek, R.J.; Fiedor, J.N. Uranium removal from ground water using zero valent iron media. *Groundwater* **1999**, *37*, 618–624.

69. Schiller, R. Radon Program Contact, U.S. Environmental Protection Agency, Region 8, Denver, CO, USA. Personal communication, 2013.

70. Moore-Nall, A.; Eggers, M.J.; Camper, A.K; Lageson, D. Elevated Uranium and Lead in Wells on the Crow Reservation, Big Horn County-A Potential Problem. Presented at the Earth Science Colloquium, Bozeman, MT, USA, 12–13 April 2013.

71. Schnug, E.; Lottermoser, B.G. Fertilizer-deirved uranium and its threat to human health. *Environ. Sci. Technol.* **2013**, *47*, 2433–2434.

72. Schnug, E. Uran in Phosphor-Dungemitteln und dessen Verbleib in der Umwelt. *Strahlentelex* **2012**, *26*, 3–10. (In German)

73. Montana Department of Revenue. 2013 Agricultural Land Classification and fallow adjustment zones. Available online:

https://revenue.mt.gov/Portals/9/committees/Ag_LandValuation/map_summer_fallow_adj_zones.jpg (accessed on 6 March 2015).

74. Tuck, L. *Ground-Water Resources along the Little Bighorn River, Crow Indian Reservation, Montana*; Water-Resources Investigations Report 03-4052; U.S. Department of the Interior and the U.S. Geological Survey: Helena, MT, USA, 2003.

75. Pelizza, M. Uranium and uranium progeny in groundwater associated with uranium ore bearing formations. In *Proceedings of the 5th International Conference on Medical Geology*, Arlington, VA, USA, 27 August 2013.

76. U.S. Environmental Protection Agency. Montana—EPA Map of Radon Zones. Available online: http://www.epa.gov/radon/pdfs/statemaps/montana.pdf (accessed on 6 August 2013).

77. U.S. Environmental Protection Agency. Radiation Protection: Radon. Available online: http://www.epa.gov/radiation/radionuclides/radon.html (accessed on 6 August 2013).

78. Montana Department of Environmental Quality. Big Horn County Radon Information. Available online: http://county-radon.info/MT/Big_Horn.html (accessed on 6 August 2013).

79. Richards, C.; Broadaway, S.; Eggers, M.J.; Doyle, J.T.; Pyle, B.H.; Camper, A.K.; Ford, T.E. Detection of Pathogenic and Non-pathogenic Bacteria in Drinking Water and Associated Biofilms on the Crow Reservation, Montana, USA. *Microb. Ecol.* **2015**, accepted for publication.

80. Hamner, S.; Broadaway, S.C.; Berg, E.; Stettner, S.; Pyle, B.H.; Big Man, N.; Old Elk, J.; Eggers, M.J.; Doyle, J.; Kindness, L.; *et al*. Detection and source tracking of *Escherichia coli*, harboring intimin and Shiga toxin genes, isolated from the Little Bighorn River, Montana. *Int. J. Environ. Health Res.* **2014**, *24*, 341–362.

81. Sexton, K.; Hattis, D. Assessing cumulative health risks from exposure to environmental mixtures-Three fundamental questions. *Environ. Health Perspect.* **2007**, *115*, 825–832.

82. Agency for Toxic Substances and Disease Registry, U.S. Department of Health and Human Services. *Toxicological Profile for Uranium*; ATSDR: Atlanta, GA, USA, 2013.

83. Young, T.K. Diabetes mellitus among Native Americans in Canada and the United States: An epidemiological review. *Am. J. Hum. Biol.* **1993**, *5*, 399–413.

84. Sullivan, P.W.; Wyatt, H.R.; Morrato, E.H.; Hill, J.O.; Ghushchyan, V. Obesity, inactivity, and the prevalence of diabetes and diabetes-related cardiovascular comorbidities in the U.S., 2000–2002. *Diabetes Care.* **2005**, *8*, 1599–1603.

85. Tsaih, S.-W.; Korrick, S.; Schwartz, J.; Amarasiriwardena, C.; Aro, A.; Sparrow, D.; Hu, H. Lead, Diabetes, Hypertension, and Renal Function: The Normative Aging Study. *Environ. Health Perspect.* **2004**, *112*, 1178–1182.

86. Agency for Toxic Substances and Disease Registry, U.S. Department of Health and Human Services. *Toxicological Profile for Lead*; ATSDR: Atlanta, GA, USA, 2007.

87. Balazs, C.L.; Ray, I. The drinking water disparities framework: On the origins and persistence of inequities in exposure. *Am. J. Public Health* **2014**, *104*, 603–611.

88. Lefthand, M.J.; Eggers, M.J.; Crow Environmental Health Steering Committee; Camper, A.K. *Community-Based Cumulative Risk Assessment of Well Water Contamination: A Tribal Environmental Health Disparity*. Presented at the NIH Native American Research Centers for Health's Tribal Environmental Health Summit, Pablo, MT, USA, 24 June 2014.

89. Doyle, J.T.; Redsteer, M.H.; Eggers, M.J. Exploring effects of climate change on Northern Plains American Indian health. *Clim. Chang.* **2013**, *120*, 643–655.

© 2015 by the authors; licensee MDPI, Basel, Switzerland. This article is an open access article distributed under the terms and conditions of the Creative Commons Attribution license (http://creativecommons.org/licenses/by/4.0/).

CHAPTER 4

STRUCTURAL CONTROLS AND GEOCHEMICAL CHARACTERIZATION OF BRECCIAS IN PALEOKARST IN THE NORTHERN BIGHORN BASIN

Abstract:

The Bighorn Basin is well known for oil and gas production with most of the primary oil production from structures such as anticlines that formed during the Laramide Orogeny. Past productive U and V deposits in the northern Bighorn Basin, Montana and Wyoming are hosted in structures that likely hosted oil until they were breached. Tectonic hydrothermal breccia have been recognized in Madison Group limestone in several reservoir characterization studies in the Bighorn and Wind River Basins, Wyoming. Both U-V mining districts have tectonic breccias associated with the deposits. Geochemistry and field relations indicate tectonic breccias associated with these deposits were episodic and hydrothermal. Isotopically depleted fluids with $\delta^{18}O$ compositions between -24.8 and -11.99‰ VPDB, indicate fluids with elevated temperatures cemented the breccias in the U and V deposits supporting a hydrothermal source for their origin. Groups of minerals from different mines have similar $^{87}Sr/^{86}Sr$ compositions while within each mine site the $^{87}Sr/^{86}Sr$ composition of minerals vary. Field surveys of silica cemented tectonic breccias indicate they are only present on the hanging wall of the Crooked Creek fault in the Pryor Mountain Mining District. Both mineralized and unmineralized silica cemented breccias are present in the same area of the district. Structural data of the siliceous tectonic breccias indicate that along with structural

position the density of the fractures was the controlling attribute that influenced U-V mineralization. The mineralized breccia data sets have a greater frequency of fractures from 4 out of 6 orientations than the unmineralized data. This difference allowed for more fluid migration along fractures and vugs that had available Fe-V oxides to form metal uranyl vanadates, the primary ore minerals in the deposits. The structural position where the tectonic hydrothermal breccias occur likely had the greatest influence on U-V mineralization by creating more fractures that provided pathways for fluid migration.

Introduction

Two past productive U-V mining districts, the Pryor Mountain Mining District (PMD) and the Little Mountain Mining District (LMD), are located along the northeast rim of the Bighorn Basin. Oil and gas production in the Bighorn Basin has primarily been from structural traps such as anticlines with primary oil production from Permian- and Pennsylvanian-age reservoir rock (Wyoming State Geologic Survey, 2016). In the northern Bighorn Basin primary oil production has also been from Mississippian Madison Group and Mississippian to Pennsylvanian Amsden Formation carbonates (Wyoming State Geologic Survey, 2016). The location (Figure 4.1) and presence of bitumen suggest that both U-V mining districts occur in structures within Madison Group paleokarst similar to actively producing oilfields in the Bighorn Basin. It is likely that structures hosting U-V mineralization served as oil reservoirs until they were breached. Bitumen is often a residual by product of water biodegradation in oil reservoir rocks that have been invaded by oxygenated water (Hollerbach, 1997; Meyer et al., 2007).

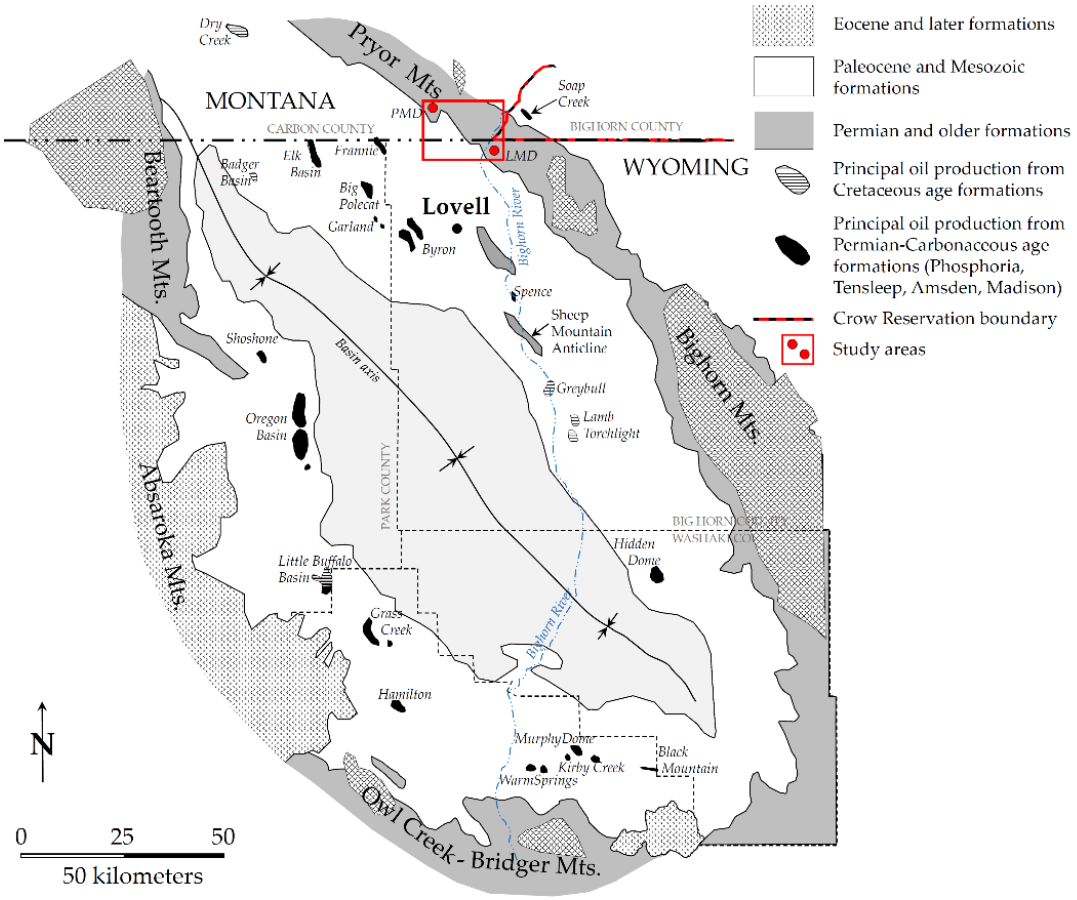


Figure 4.1 Location of the U-V mining districts in Montana and Wyoming showing location relative to oil producing fields in the northern Bighorn Basin, Wyoming.

Both U-V mining districts occur in fault propagated folds that were formed during the Laramide Orogeny. Tectonic hydrothermal breccias (THB) and associated hydrothermal dolomite are recognized in the Wind River Basin and along the eastern, western and southern rims of the Bighorn Basin, Wyoming in fault propagation folds in the Madison Limestone (Katz et al., 2006; Westphal et al, 2004; Kislak et el., 2001). Thus tectonic breccias recognized in this study in the northern Bighorn Basin in the Madison Limestone likely formed by the same process.

Hydrothermal dolomite, associated with the process of tectonic hydrothermal brecciation, is recognized as a fault-related, structurally controlled, type of carbonate diagenesis that often increases porosity in carbonate reservoir rocks (Sibson et al., 1975; Davies and Smith, 2006). Episodic bursts of pressurized fluid migration are thought to drive some of the diagenesis (Sibson et al., 1975; Davies and Smith, 2006); these bursts may be triggered by fault activation and/or reactivation (Sibson, 1986; Katz et al., 2006). Figure 4.2 is an illustration of the formation of THB and hydrothermal dolomite modified from Jeffery (2014).

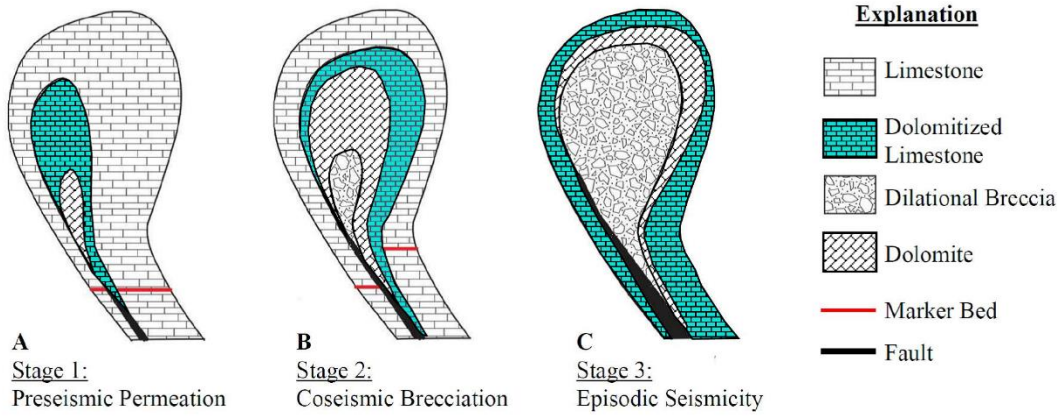


Figure 4.2 Model for the formation of hydrothermal breccia pipes. Hydrofracturing at the fault tip results in three stages of progressively damaged and mineralized zones: (A) zone of permeation at the propagating fault tip, causing extensive hanging wall dolomitization; (B) a region of hydraulic fracturing and brecciation of the previously dolomitized halo, resulting in the precipitation of hydrothermal minerals; and (C) the repetition of seismic events, allowing the brecciated area to become progressively more vertical with continued activity (Figure modified from Jeffery, 2014)

The purpose of this study was to characterize the nature of the fluids that cemented the different types of breccias that host the U-V deposits in the mining districts. These include: 1) the silica cemented hematite- and limonite-stained breccias in the

PMD; 2) the lithified collapse breccias that many of the silica cemented tectonic breccias occur in on Red Pryor Mountain; and 3) the tectonic breccias in the LMD. The field based fracture analysis focuses on the PMD because the tectonic breccias in the PMD differ from other recognized hydrothermal tectonic breccias in the Bighorn Basin.

Pryor Mountain Study Area

The expression of topography in the Pryor Mountains is due to movement of the underlying Archean basement blocks. Movement along an E-W trending sinistral strike-slip fault separating the N and S blocks of the Pryor Mountains was accompanied by approximately (040º- 060°) NE-SW directed regional horizontal compression produced during the Laramide Orogeny (Bird, 2002; Neely and Erslev, 2009). This stress resulted in each block being tilted up in the NE corner as stress was relieved in two directions (Figure 4.3). Fault propagation folds formed on the surface of each block. The PMD is hosted in folds on Big Pryor and East Pryor Mountains (Figure 4.3 and 4.4).

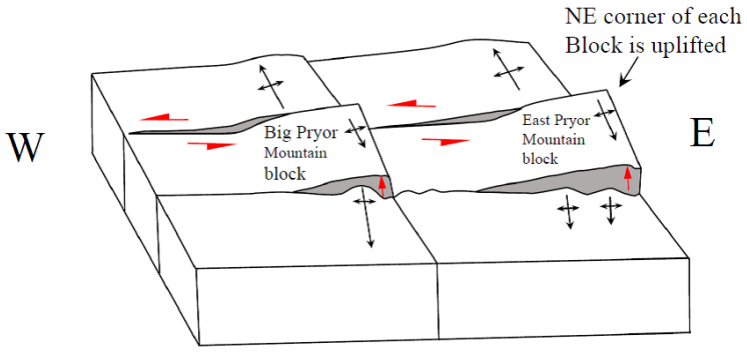


Figure 4.3 Block diagram of the Pryor Mountains. Big Pryor Mountain and East Pryor Mountain blocks are bounded on the N by the sinistral Sage Creek fault. The E edge of both blocks are bound by faults. These faults core the folds that are on the surface of each block depicted by the arrows drawn on each block in the diagram.

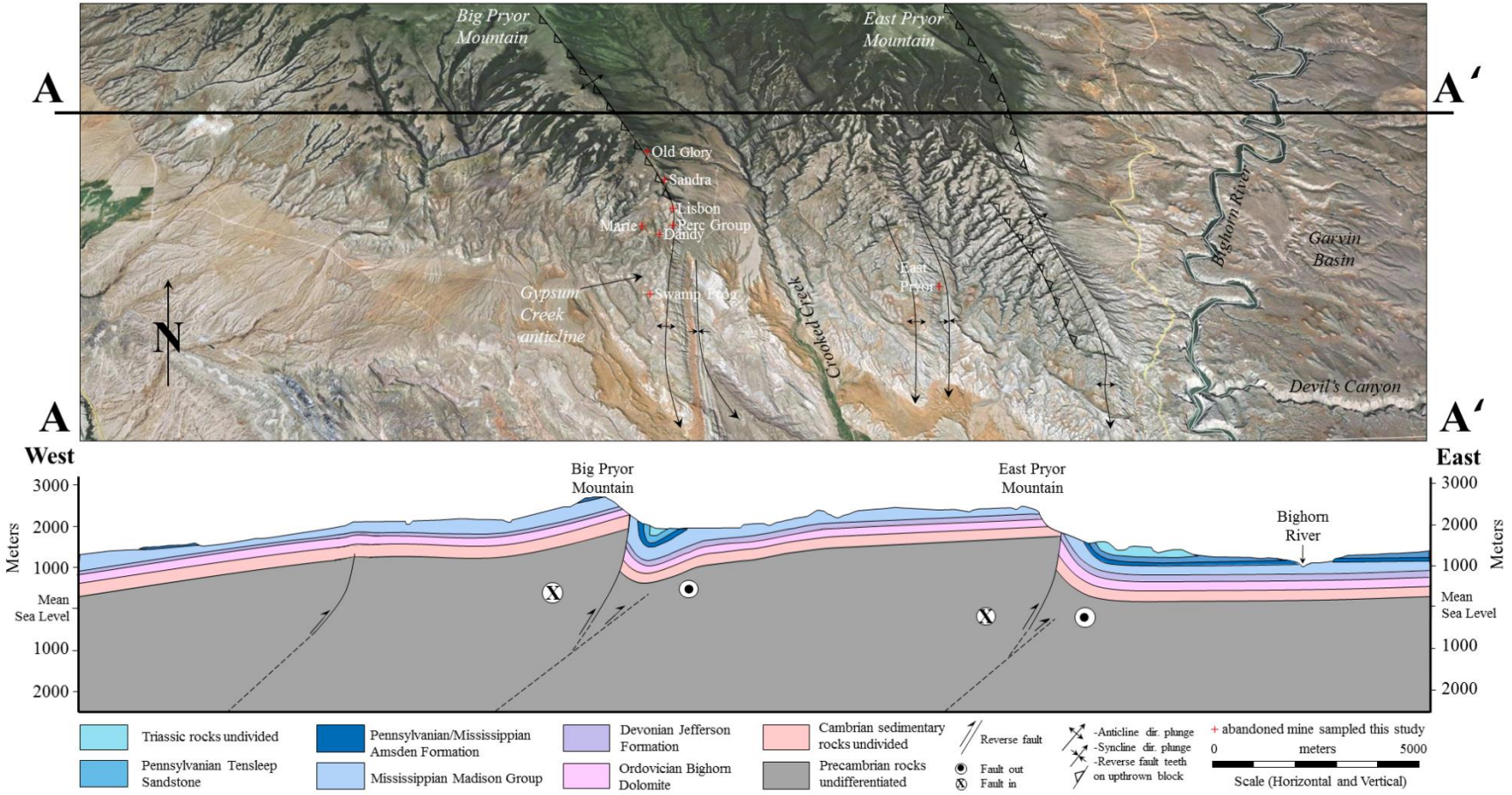


Figure 4.4 Location of the Pryor Mountain Mining District in Montana. The labeled mines (+) were sampled in this study. The cross-section was constructed using the Geologic Map of the Bridger Quadrangle, Montana (Lopez, 2000) for the profile elevations, dip of the mapped sedimentary bedding, and structural data. Google Earth image on top shows location of cross-section.

The E-W cross-section (Figure 4.4) is drawn across Big Pryor and East Pryor Mountain. The cross-section illustrates the style of faulting that produced the E-W to N-S orientation of the Pryor Mountains that formed in a sinistral accommodation zone. The cross-section runs approximately parallel to the Sage Creek fault that is an extension of the Nye Bowler lineament. The Nye Bowler lineament is interpreted to be a sinistral strike slip fault at depth (Wilson, 1936; Blackstone, 1940). The reactivation of this fault during the Laramide Orogeny resulted in movement along each of the Pryor Blocks.

The location of the U-V mining districts on Big Pryor Mountain, coincides with the axis of the Gypsum Creek anticline and the Crooked Creek Fault. The Gypsum Creek anticline is the southern plunging fold shown in Figures 4.3 and 4.4 located on the southern portion of the Big Pryor Mountain block. The Crooked Creek fault propagated up from the Precambrian basement through the Mississippian-age Madison Group and ruptured between the Lisbon and Old Glory mines on Big Pryor Mountain (Figure 4.4). The Dryhead fault is a similar feature associated with the East Pryor Mountain block. The Dryhead fault propagated eastward and ruptured bringing Precambrian Archean gneiss and granite to the surface on the NE corner of the East Pryor Mountain block. The East Pryor Mountain block was elevated the most of the Archean cored blocks in the Pryor Mountains.

The original structure of the Pryor Mountains was mapped by Donald L. Blackstone for his doctoral dissertation, completed in 1936. Blackstone described the Pryor Mountains as asymmetric "trap-door" type uplifts (Blackstone, 1940). The description applies to the style of faulting that produced the asymmetric anticlines, which

Blackstone concluded was due to tangential compression acting on curved fault planes in the basement complex.

Breccias in the Districts

Collapse Paleokarst Breccias

Several types of breccias occur in both U-V mining districts. Collapse paleokarst is the most common type in both districts. U-V mineralization is concentrated in the top 55–75 m of the paleokarst horizon of the Madison Limestone. The collapse paleokarst breccias developed during a maximum 34 m.y. hiatus at the top of the Madison Limestone and was overlain by the diachronous Pennsylvanian Amsden Formation (Maughan, 1983; Sando, 1988; Eldam, 2012). The collapse paleokarst breccias within which the U-V deposits occur vary in degree of lithification. Most collapse paleokarst breccias are filled with angular limestone fragments of variable size (from several cm to several meters across) and reddish clay silt from the overlying Amsden Formation (Figure 4.5). Some of these collapse features also have secondary fine sandstone and silty sediments filling in portions of the zones. The mineralization in the collapse paleokarst breccias are concentrated as fine coatings on the surfaces and along fractures. The main alteration present in the collapse paleokarst breccias is staining from the Amsden Formation. If tectonic breccias are present in these zones they have a random orientation that follow fractures and occasionally follow bedding planes.



Figure 4.5 Typical paleokarst collapse breccia observed in both mining districts.

Lithified Collapse Breccia

Other collapse breccias have a lithified, more consolidated matrix and appear to have formed after the original collapse paleokarst breccias. These breccias probably formed once ground water or surface water invaded the paleokarst. These breccias have very little staining related to the Amsden Formation, possibly the iron may have been mobilized and redistributed (Figure 4.6). These breccias are likely related to changes in the level of groundwater in the region as the Bighorn Basin was exhumed.



Figure 4.6 Typical lithified collapse paleokarst breccia lacks the Amsden Formation staining of less consolidated paleokarst in the area.

Silica Cemented Tectonic Breccia

The tectonic breccias observed in the PMD differ from other recognized THB in the Bighorn Basin because the breccias are cemented with silica. THB that are primarily silica cemented have not been described in the Bighorn Basin but have been described in the U-V mining districts near Cameron, Arizona in collapse breccias similar to these deposits. The Arizona breccias were attributed to the activity of ascending thermal solutions which caused localized collapse in the Permian Kaibab Limestone and overlying Triassic formations by the removal of carbonates (Barrington and Kerr, 1963).

The THB observed in the East Pryor and Big Pryor Mountain areas are heavily hematite- and limonite-stained silica cemented breccias. These breccias follow bedding

or fractures and have clasts of limestone and dolomite that have been partially or completely replaced by silica (Figure 4.7).



Figure 4.7 Typical silica cemented tectonic breccia observed in the PMD. This breccia is located north of Lisbon mine area and partially follows bedding that is dipping 20 ° and has a dip direction of approximately 220°.

The matrix within silica cemented tectonic breccias is composed of cryptocrystalline silica and local microscopic Fe-oxide inclusions. Both unmineralized and mineralized silica cemented tectonic breccias have barite, local fluorite, minor oxides, and sulfides along fracture surfaces and in vugs. The mineralized silica cemented tectonic breccias have U-V minerals filling vugs and fractures in addition to the other minerals. In some of the deposits, silica cemented tectonic breccias appear to follow sets of fractures through lithified type collapse breccia (Figure 4.8).



Figure 4.8 Mineralized hematite- and limonite-stained silica cemented tectonic breccia appears to follow sets of fractures (red and blue dashed lines) in a lithified collapse paleokarst breccia. The collapse breccia is bleached. Mineralization is concentrated in the vugs and fractures in the stained tectonic breccia. Near the Sandra Mine, PMD, Montana.

Alteration of the host rocks is greatest in areas where silica cemented tectonic breccias are present. Alteration other than the staining attributed to the Amsden Formation includes bleaching of the limestone; silicification; replacement by fluorite; and liesegang banding, especially the northern extent of the 6.4 km zone that the mineralization on Big Pryor Mountain is concentrated. The alteration does not extend very far into the host rocks.

Lag Deposits

Silica cemented tectonic breccias on the top of Big Pryor Mountain are found as lag deposits several kilometers away from the U-V mines near the northern end of the ruptured portion of the Crooked Creek fault. These tectonic breccias lack the hematite- and limonite-staining characteristic of the silica cemented tectonic breccias in the mineralized zone. The clasts in the matrix of these breccias appear to have only Pennsylvanian Tensleep and possibly Permian Phosphoria clasts. The matrix is grey or

white microcrystalline quartz. This suggests that the brecciation extended beyond the Madison Limestone at least through the top of the Tensleep Formation and possibly the bottom of the Permian Phosphoria Formation (Figure 4.9). The thickness of Tensleep Sandstone in this part of the Pryor Mountains was approximately 60 m and only small isolated outcrops remain near the top of Red Pryor Mountain (Lopez, 2000). White barren "bull" quartz vein material occurs in a few areas on Big Pryor Mountain. It is generally observed as broken fragments (e.g. near the Dandy and Sandra mines). In a few locations it appears to be in place but may also be a lag deposit (Figure 4.9C).

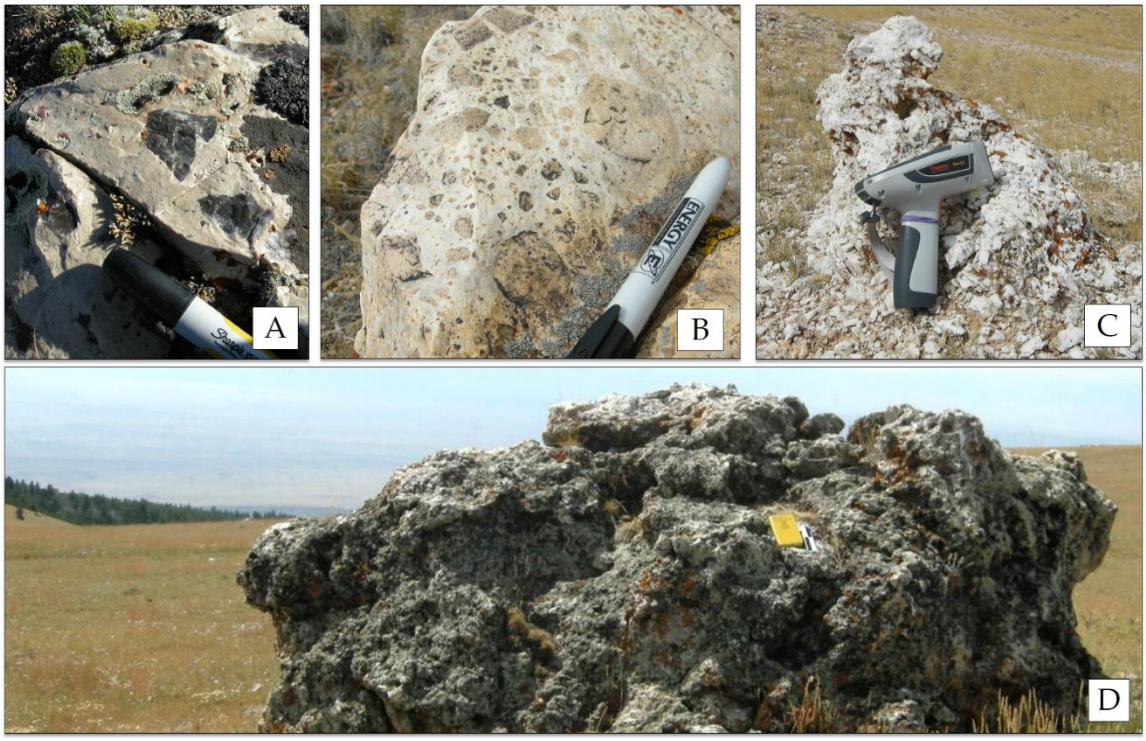


Figure 4.9 (A) THB lag deposit with black chert clasts of lower Permian Park City Formation or upper Pennsylvanian Tensleep Formation, Big Pryor Mountain, PMD **(**B) White quartz cemented THB with Tensleep quartzite clasts. (C) Quartz vein material on Big Pryor Mountain, portable XRF for scale is about 30 cm long. (D) Lag deposits on top of Big Pryor Mountain, yellow field notebook for scale is about 20 cm long.

Tectonic Breccias, LMD

In the Little Mountain study area, the tectonic breccias occur along fractures, occasionally follow bedding planes, and are concentrated in collapse paleokarst breccias in the top 58–73 m of the Madison Limestone. There is very little alteration of the host rock in the LMD and very little silica in the tectonic breccias (Figure 4.10).



Figure 4.10 Mineralized tectonic breccia follows fracture cutting across bedding. The wall rock is slightly bleached and mineralization is concentrated in the fracture with the tectonic breccia, near the Lisbon Mine, LMD, Wyoming.

Methods

In order to understand the structural influence and controls on fluid migration in the Pryor Mountain and Little Mountain study areas a geochemical analysis of stable and radiogenic isotopes was conducted (Appendix B, Tables B1 and B2). The Pryor Mountain area, specifically Big Pryor Mountain, differs from the other study areas with the presence of silica cemented tectonic breccias. In order to understand how structure

may have controlled the distribution of the “mineralized” versus “unmineralized” siliceous tectonic breccias a field-based fracture analysis was conducted. Prior to the field-based fracture analysis, a computer aided lineament analysis of the Pryor Mountain area was conducted and field reconnaissance was made in the areas to investigate the distribution and type of breccias present in the study areas.

Computer Aided Lineament Analysis

Google Earth Pro (GEP) version 7.2.1 was used to identify dominant lineament orientations at the macroscale on Big Pryor Mountain, the southwestern block of the Pryor Mountains (Appendix B, Table B3). Lineaments were extracted from GEP as described in Lageson et al. (2012). After compilation of lineament measurements in GEP, the data was imported in ESRI ArcGIS as a KML file and converted to a polyline feature shapefile. By running GIS geometry tools, the length and orientation of lineaments were calculated and added to the attribute table. To classify the lineaments based on their orientation the table was exported to Excel and basic command lines were used to automatically determine each lineament set. The lineaments were divided into six directions based on observation.

Rockware StereoStat version 1.6.1 was used to plot and compare the lineament and field data orientation data on rose diagrams. A 5 degree class was selected and the data was split into six groups based on orientation observed. Field data was compiled and plotted on equal-area lower-hemisphere projections. Poles to fracture planes were plotted using the Kamb method described in Marshak and Mitra (1988) to analyze the distribution and density of fractures in the field data.

Fieldwork

A Thermo Scientific™ RadEye™ PRD Personal Radiation Detector was used to identify elevated radiation sources in the study areas. Rock samples included breccia clasts and matrix samples, altered and unaltered host rock, generations of cements from veins, and mineralized samples from dumps and outcrops. Two speleothem calcite samples from Big Pryor Mountain were collected for analyses and comparison with vein fill calcite and breccia cements to test meteoric and hydrothermal theories.

A field survey showed that tectonic breccias are most concentrated along the NE side of the Big Pryor Mountain block. The breccias were only observed on the hanging wall of the Crooked Creek thrust block. Fifty-five siliceous tectonic breccias were recorded on Big Pryor Mountain between the Lisbon mine and the Old Glory mine, a distance of approximately 1.8 km; and 6 more tectonic breccias were recorded approximately 1.5 km NW of the Old Glory mine near the top of Red Pryor Mountain (Appendix B, Table B4). A fracture analysis was performed focusing on that area. The "selection" method, as described in Marshak and Mitra (1988) for rock outcrops, was used to collect fracture orientations. This method seemed most viable as the breccias varied in size and shape and fracture spacing varied greatly between the outcrops. The number of fractures measured at each station depending on the size of the breccia. Fractures were classified by their mode of opening, although more than 90% of fractures appeared to be mode I tensile fractures (Ramsay and Huber, 1987). A total of 2083 fractures were collected from 61 fracture stations; 28 stations were silica cemented tectonic breccias. Evidence of shearing or tearing parallel to the plane of the fractures

was sparse, only 17 slickenlines were observed and recorded from 11 fracture stations. Fracture attributes were recorded on a spreadsheet created by our structure group lab at MSU. Attributes included: orientation, length, spacing, aperture, crosscutting relationships, slip indicators, and vein fill information if present. In the note section the host rock and orientation were also described and also the orientation of the tectonic breccia if that could be determined. The locations were recorded in UTM NAD 27 Zone 12 datum using a Garmin Rino 120 Global Positioning System (GPS) receiver (Appendix B, Table B4).

Geochemical Characterization

Powdered samples were prepared for stable C, O, and radiogenic Sr isotope geochemistry at Montana State University, Bozeman, Montana. Most samples were broken into chips and then pulverized in a Plattner's diamond mortar and pestle set while a few required micro drilling with a diamond tipped Dremel® bit. Some samples were stained for carbonate identification using a mixture of alizarin red and potassium cyanide solution (Dickson, 1965; Tucker, 1988). Staining aided in identifying Fe-rich carbonate and in delineating the different generations of calcite fill for powder x-ray diffraction (XRD) spectroscopy examination prior to preparation of isotope samples. Carbonates were analyzed for stable C and O isotopes at the University of Michigan, Department of Earth and Environmental Sciences, Stable Isotope Laboratory, Ann Arbor, Michigan. Sr was separated from late stage calcites, carbonate host rock, matrix material from breccia samples, and fluorite in the clean labs at the University of Wyoming and $^{87}Sr/^{86}Sr$ was measured using a Neptune Plus Multicollector-Inductively Coupled Plasma Mass

Spectrometer (MC-ICPMS) at the Wyoming High-Precision Isotope Laboratory at the University of Wyoming, Laramie, Wyoming. Sr was separated from barite and $^{87}Sr/^{86}Sr$ was measured on a NEPTUNE MC-ICPMS at the Institute of Marine Sciences, University of California, Santa Cruz, California (Paytan, pers. com.). Isotope methodology and data is in Appendix B.

Results and Discussion

Stable Isotopes (C and O)

Mississippian (Mm) limestone and dolomite host rock samples (blue squares) plot in or near the expected Mississippian seawater (dashed box) carbonate composition (Veizer et al, 1999) and the most depleted $\delta^{18}O$ and $\delta^{13}C$ compositions of this study plot in the oval (Figure 4.11). The strongly depleted $\delta^{18}O$ composition of the vein fill and breccia samples suggests increased temperatures during fluid circulation events, giving strong evidence for the presence of hydrothermal fluids (Hardie, 1987; Allan and Wiggins, 1993). The wide range of C and O isotope compositions suggests that there were multiple episodes of fluid migration through the host rocks with varying temperatures; thus, more depleted values are interpreted to represent episodes with higher temperature fluids (and vice versa). Additionally, later stage cementation becomes progressively lighter in both C and O signatures; therefore, successive generations of cementation will display increasingly more depleted isotopic signatures (Hoefs, 2009).

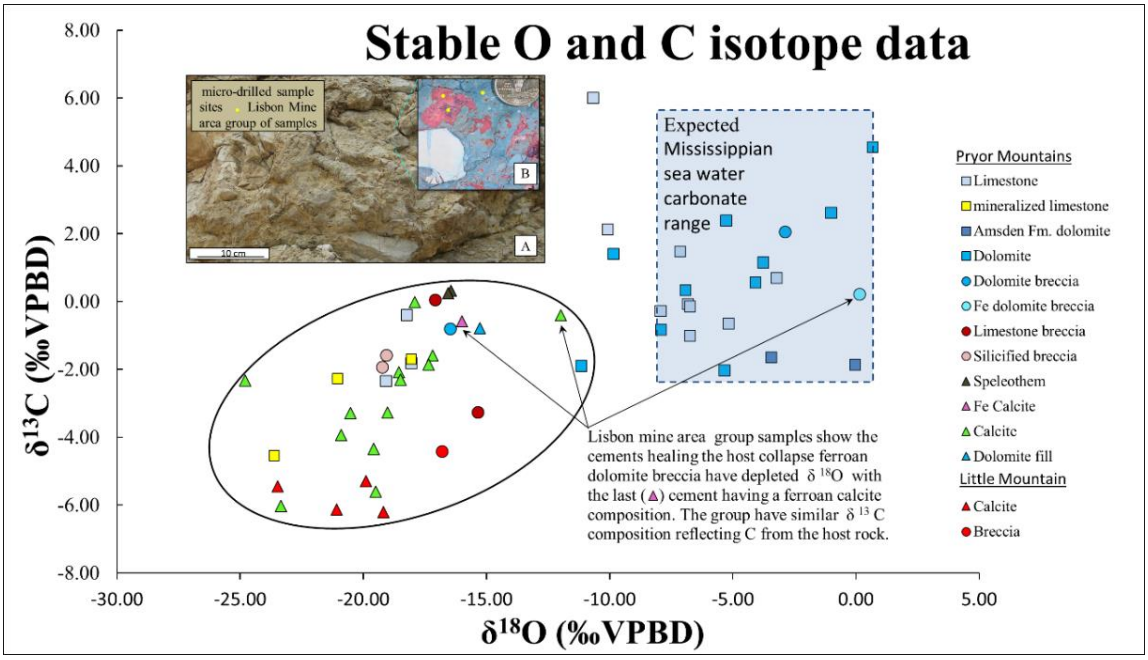


Figure 4.11. Stable C and O isotope cross-plot. Triangles = calcite; circles = breccias; and squares = limestone and dolomite. Blue dashed box represents approximate expected Mm seawater carbonate compositions. Oval shape encloses the more depleted $\delta^{18}O$ and $\delta^{13}C$ compositions with respect to VPBD. (A) Inset photo of ferroan dolomite collapse breccia outcrop that Lisbon mine area group of samples were collected from (B) Stained sample: turquoise = ferroan dolomite; red = calcite; and purple = ferroan calcite. Samples were drilled from the unstained half of the sample corresponding to the yellow dots in the stained sample: Lisbon001A (breccia matrix), Lisbon001B (red calcite), and Lisbon001C (purple calcite). Samples are color coded in Appendix B, Table B1.

The $\delta^{13}C$ compositions vary between the samples of this study. The heavier $\delta^{13}C$ of the samples near the top of the oval reflect contributions of the Mm host limestone. Calcite with lighter $\delta^{13}C$ compositions, for example the samples from LMD (bright red symbols) that have the most depleted $\delta^{13}C$ in this study, may reflect carbon derived from organic material such as oil. Some breccias have saddle (baroque) dolomite within the matrix, which is another indication that the cement is probably hydrothermally influenced (Spotl, 1998). Saddle dolomite is associated with hydrothermal dolomite facies (Davies and Smith, 2006).

The chaotic, floating-clast ferroan dolomite breccia (inset photo in Figure 4.11) was micro-drilled to assess the evolution of the fluids that cemented the breccia and precipitated the late-stage calcite that healed fractures. Analytical results show the breccia host to be in the range of Mm seawater carbonate. This sample in the field did not exhibit radioactivity. Mineralized zones of silica cemented tectonic breccias and the Lisbon mine are located near this site. The late-stage calcites from the sample have depleted $\delta^{18}O$ and $\delta^{13}C$ composition compared to the Mm host (arrows in Figure 4.11). The ferroan calcite symbolized by the lilac colored triangle inside and near the top of the oval outline shape, was the last calcite to form. It had the most depleted compositions of both $\delta^{18}O$ and $\delta^{13}C$ (-15.99‰ and -0.59‰) respectively of this sample group. This chaotic breccia is representative of the "lithified" collapse breccias that are present in the area.

The speleothem calcite samples, shown as brown triangles that plot at the top of the oval, have the most enriched $\delta^{13}C$ of the calcite samples. The depleted $\delta^{18}O$ composition of these samples is likely related to surface or rainwater derived from higher elevations that migrated (likely down) through fractures into the cave rather than increased temperature (Hoefs, 2009).

The range of isotopic composition of carbonate samples in this study indicates a long, complex history of fluid migration and vein filling. The isotopic compositions are complicated by the many episodes of karst that have affected the Madison Group ranging from Mississippian time through the present.

Radiogenic Sr Isotopes

Radiogenic $^{87}Sr/^{86}Sr$ isotope analysis was conducted to determine if fluids sourcing breccia cements, vein fill precipitation, and/or barite and fluorite formation interacted with high Rb source rocks, such as basement granite and gneiss. Table 4.1 shows a range and average $^{87}Sr/^{86}Sr$ composition for geologic reference materials from locations near the study area and an average for continental volcanics compiled from many studies.

Geologic material	$^{87}Sr/^{86}Sr$		Reference
	average	range	
Archean rock, eastern Beartooth Mountains, MT	0.732565	0.70708-0.78304	Wooden and Mueller, 1988
Archean Granite from the Bighorn batholith, N. Bighorn Mountains, WY	0.73755	0.70728-0.82309	Frost et al., 2006
Mississippian Madison Group, Bighorn Basin		0.70823-0.70907	Katz et al., 2006
Mississippian Madison Limestone, Bighorn Basin	0.70809		Frost and Toner, 2004
Mississippian Madison Group paleokarst, Bighorn Basin	0.70875		Frost and Toner, 2004
Pennsylvanian Tensleep Formation, Bighorn Basin	0.71123		Frost and Toner, 2004
Pennsylvanian-Permian Casper Fm. SS and LS, Powder River Basin, WY		0.71150-0.71924	Frost and Toner, 2004
Permian Reservoir rocks in the NE flank of the Rock Springs uplift, central WY		~0.71550-0.71912	McLaughlin et al., 2014
Continental volcanics	0.704	0.702-0.707	Faure, 1998

Table 4.1. Ranges and average $^{87}Sr/^{86}Sr$ composition of some reference geologic materials.

Comparing the $^{87}Sr/^{86}Sr$ composition data based on sample type reflects episodic precipitation throughout the districts (Figure 4.12). All of the barite, fluorite, and silica cemented breccias plot outside the blue shaded portion of the graph that represents the expected $^{87}Sr/^{86}Sr$ composition of the Mississippian Madison Group in the Bighorn Basin (Frost et al., 2006; Katz et al., 2006). This suggests that the Sr source was not the Madison Limestone for these samples.

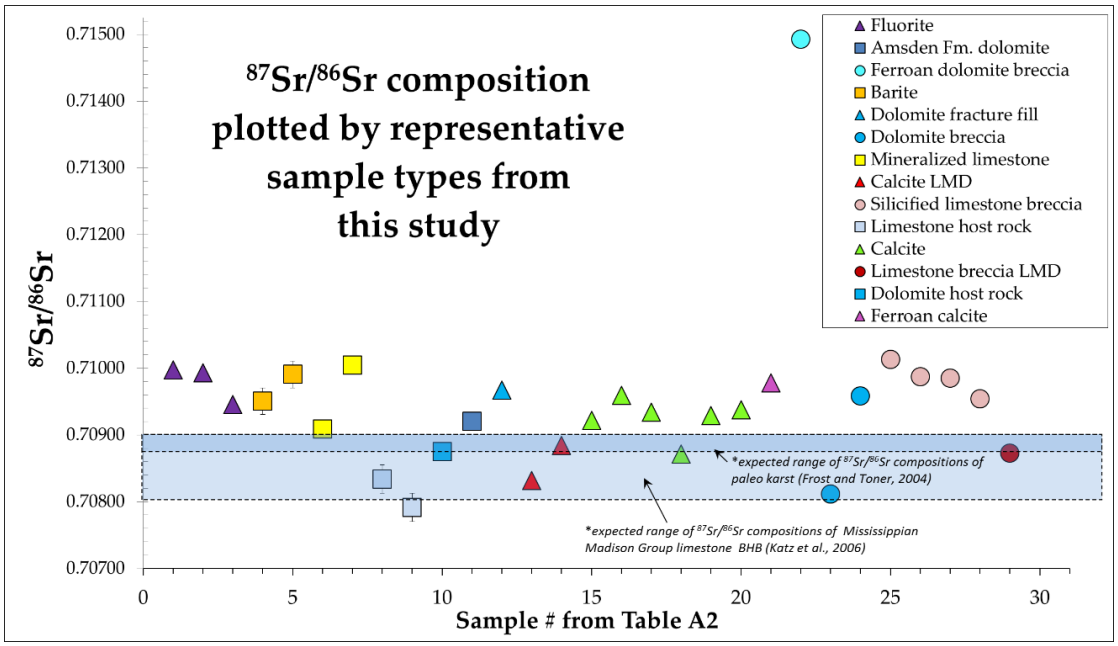


Figure 4.12. Cross-plot of $^{87}Sr/^{86}Sr$ composition of different sample types. The sample $^{87}Sr/^{86}Sr$ compositions are in Appendix B, Table B4. The shaded blue box represents expected values of Madison Group $^{87}Sr/^{86}Sr$ composition in the Bighorn Basin (Katz et al., 2006; Frost and Toner, 2004). Standard deviation error bars (30 ppm) are about the width of the plotted symbols and are plotted with the barite and limestone for scale.

Comparing groups of samples collected from different mines and locations reflects episodic precipitation of cements and minerals differing both at the individual mines and also varying between mines (Figure 4.13).

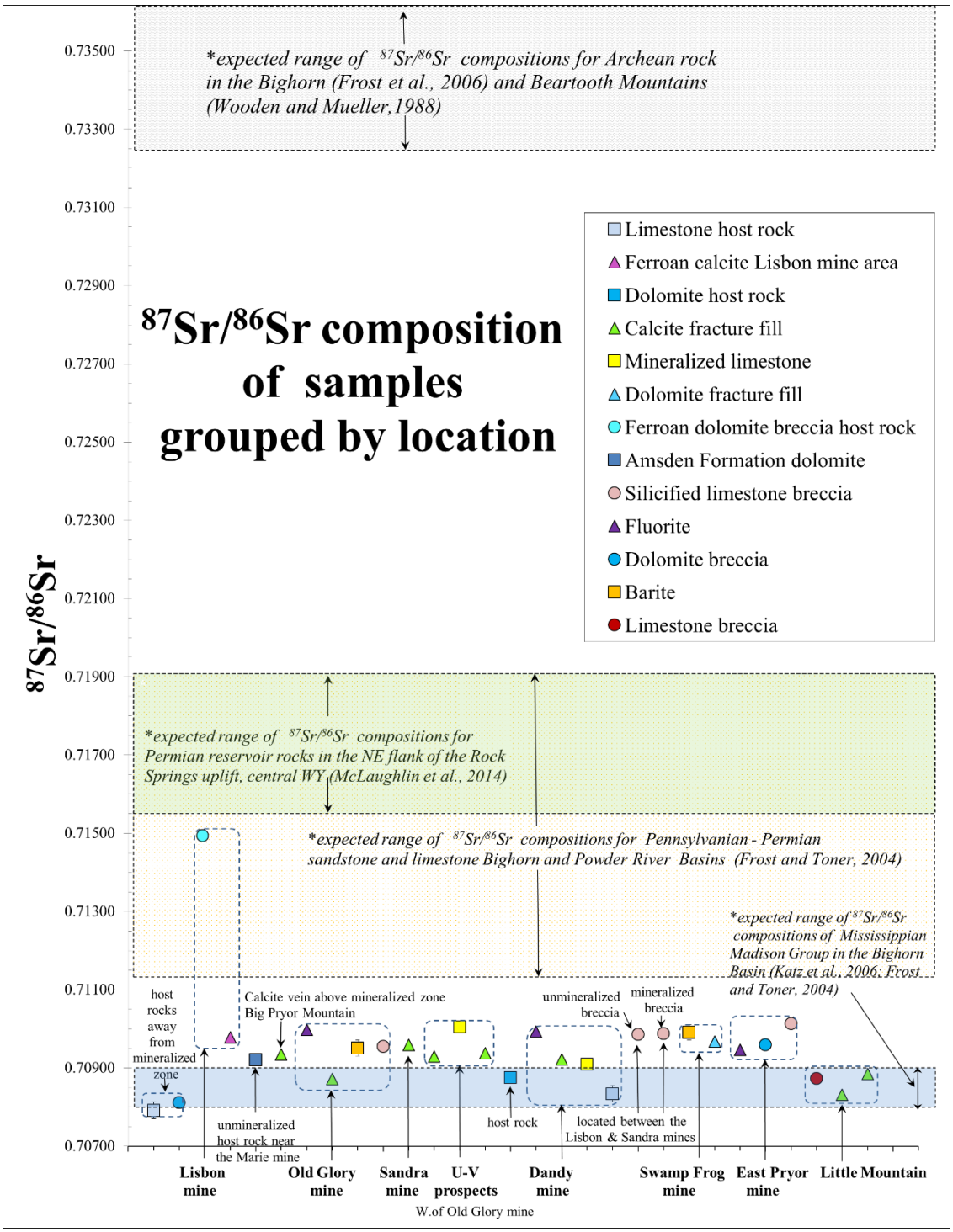


Figure 4.13. Cross-plot of $^{87}Sr/^{86}Sr$ composition from different locations in the mining districts. The shaded boxes represent expected $^{87}Sr/^{86}Sr$ compositions of rocks from nearby areas in WY and MT using values from Table 4.1. Most samples in the PMD plot between the expected $^{87}Sr/^{86}Sr$ composition for Pennsylvanian rock and the expected $^{87}Sr/^{86}Sr$ composition for Mississippian host rock in the Bighorn Basin.

Plotting the samples with the expected ranges of $^{87}Sr/^{86}Sr$ composition of rocks from areas near this study (Table 4.1) shows that most of the samples plot between the expected $^{87}Sr/^{86}Sr$ compositions of the Madison Group (blue shaded box at bottom of figure) and the expected range of $^{87}Sr/^{86}Sr$ composition of Pennsylvanian to Permian sandstone and carbonate in the Bighorn and nearby Powder River basins (Frost and Toner, 2004).

The $^{87}Sr/^{86}Sr$ compositions of the samples are more similar to Pennsylvanian Tensleep sandstone in Bighorn Basin (Frost and Toner, 2004) than they are to nearby Archean sources. This may suggest that fluids sourced from the Pennsylvanian Tensleep Sandstone migrated through fractures, likely during folding, into Madison Group. Another possibility is that meteoric sourced fluids such as groundwater, interacted and mixed with fluids that had migrated along faults that originated from the Archean basement (Katz et al., 2006).

Carbonates that were measured for both $\delta^{18}O$ and $^{87}Sr/^{86}Sr$ composition were compared (Figure 4.14). All vein fill material and mineralized samples have depleted $\delta^{18}O$ compositions compared with limestone and dolomite host rock which are denoted by the black oval. The unmineralized ferroan dolomite chaotic-floating-clast breccia has the most radiogenic composition of all the samples (inset photo) and also the some of the heaviest $\delta^{18}O$ composition (0.15‰). The ferroan calcite, sample Lisbon001C, from the Lisbon Group of samples also included in this plot has less radiogenic composition than the breccia host rock. The ferroan breccia is located between the Lisbon mine and the Perc Group of mines (Figure 4.2). The differences in $\delta^{18}O$ compositons of the calcite

cements that healed fractures in the ferroan breccia suggest separate calcite precipatation events, reflecting episodic or repeated fracturing and cementing in the area. The cross-cutting relationships establish several episodes of fracturing and carbonate cements. The ferroan collapse breccia host was intially cemented by $\delta^{18}O$ enriched fluids.

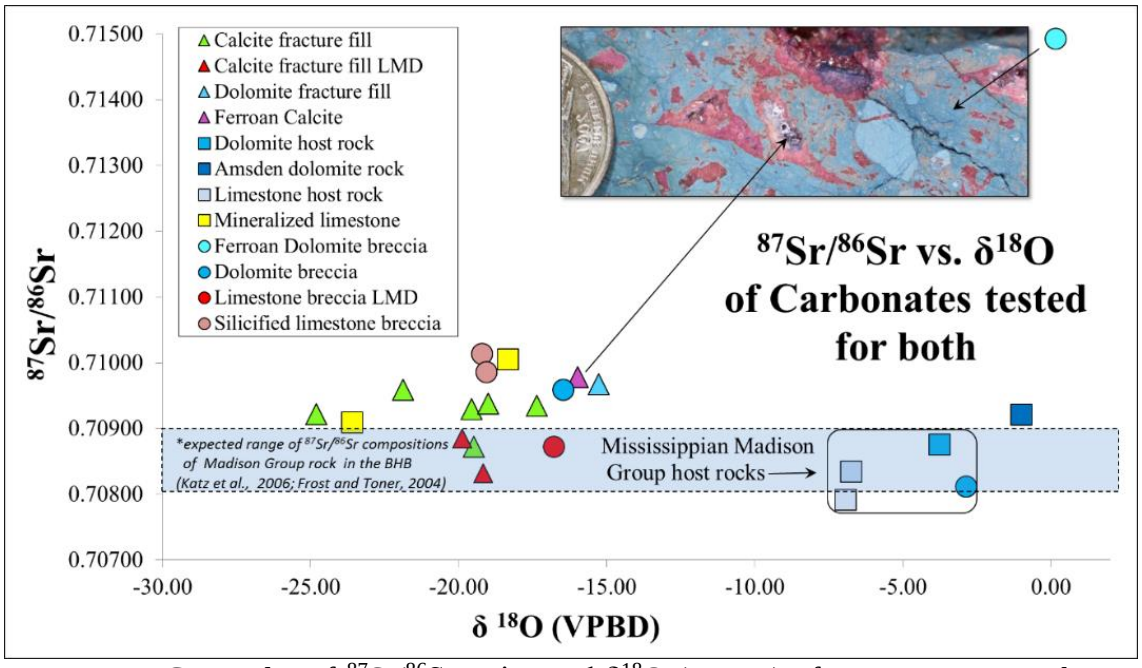


Figure 4.14. Cross-plot of $^{87}Sr/^{86}Sr$ ratios and $\delta^{18}O$ (VPBD) of representative carbonate sample types from the mining districts. Inset photo shows ferroan dolomite breccia sample again for reference to the samples described in the following text.

The heavier $\delta^{18}O$ composition of the breccia cement suggests the collapse breccia was invaded by cool, likely meteoric waters. The meteoric waters may have originated from surface waters such as a lake or river with a $^{87}Sr/^{86}Sr$ composition suggesting interaction with either exposed bedrock or down through fractures in bedrock that had a more radiogenic composition than the Madison Limestone. The water migrated into the collapse breccia and was impounded creating a slurry that incorporated iron from the

Amsden Formation, later lithifying to produce the well cemented ferroan dolomite cemented collapse breccia. The breccia was subsequently fractured and healed by at least two episodes of calcite that precipitated from warmer ascending hydrothermal fluids along a fractures or a fault that served as a conduit. The latest fluid in this set of samples was ferroan calcite (purple calcite in figures 4.11 and 4.14).

The variable $^{87}Sr/^{86}Sr$ and $\delta^{18}O$ compositions of samples from this study indicates that the precipitation the minerals in the deposits did not form simultaneously suggesting multiple episodes of fluid migration. More extensive sampling and analyses at each mine and prospect site might reveal coeval fluid migration events throughout the district.

GEP Lineament Analysis

Lineament mapping conducted using Google Earth Pro satellite imagery revealed six dominant orientations. These orientations (n=2613) were subjectively split up into six 30° groups of orientations based on observation. The orientation groups are as follows:

N-S orientations ranging from (355°- 025° and 175°- 205°)

NNE-SSW orientations ranging from (025°- 055° and 205°- 235°)

NE-SW orientations ranging from (055°- 085° and 235°- 265°)

E-W orientations ranging from (085°- 115° and 265°- 295°)

SE-NW orientations ranging from (115°- 145° and 295°- 325°)

SSE-NNW orientations ranging from (145°- 175° and 325°- 355°)

The lineament orientation groups were plotted on a rose diagram divided into 5° class intervals. The orientations were plotted on an ARC GIS image and mines were added as black and white filled circles to veiw the lineaments present in the study area (Figure 4.15). The data for the orientations recorded are found in Appendix B, Table B3.

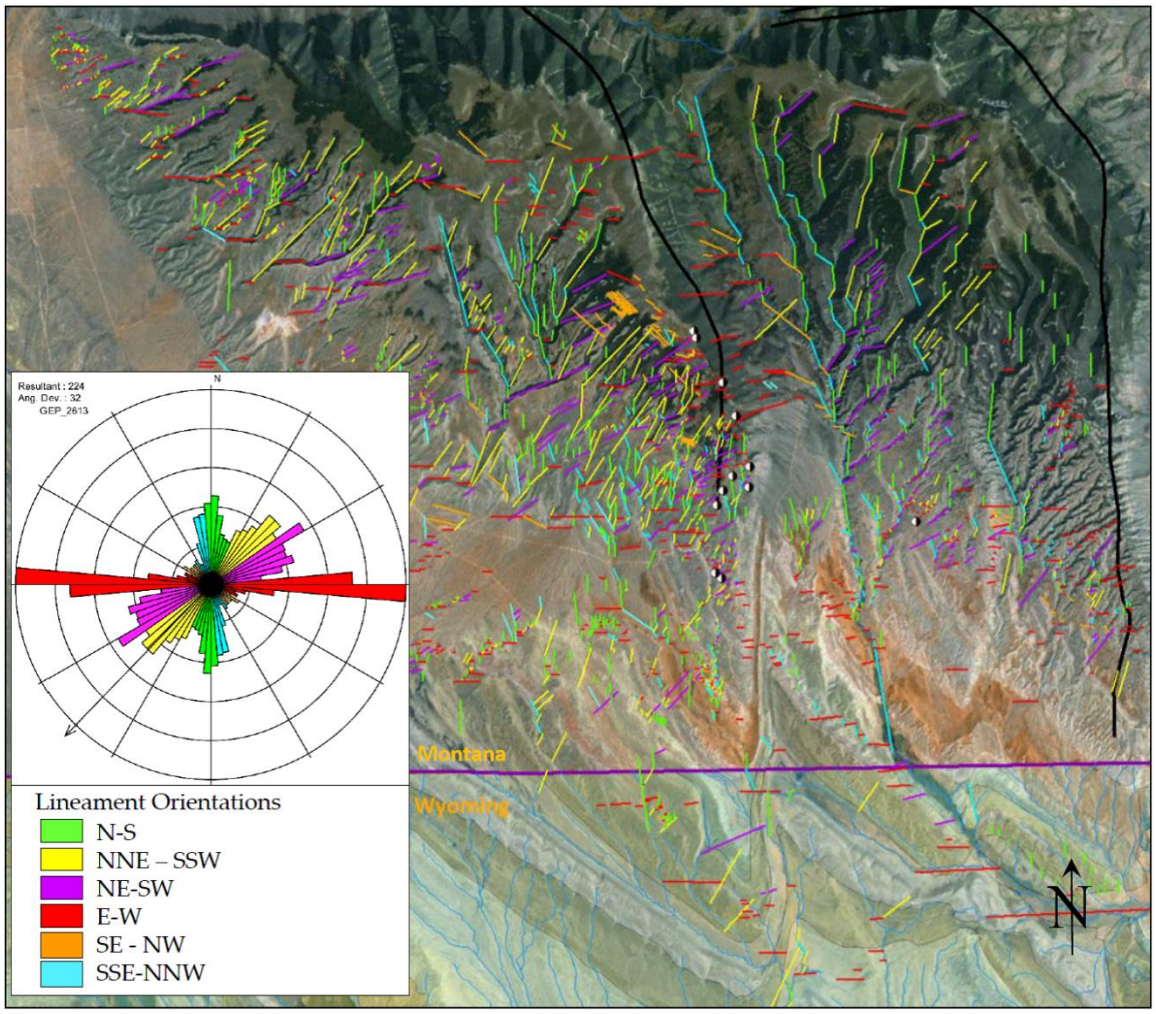


Figure 4.15. GEP lineament analysis of Pryor Mountain study area, Montana. Data was divided into 5° class intervals into six dominant directions and plotted on a rose diagram with lineament orientations weighted according to length.

Linear scaling was used to show the frequency of lineaments in each orientation. Thus, for example a segment of the rose that has 5 observations is five times longer (extending outward from the origin) than a segment corresponding to a class containing only 1 observation. The rose diagram constructed from GEP lineament orientations shows the E-W (085°- 105° and 265°- 295°) orientations were recorded the most. The rose diagram suggests that there are five main orientations. The NNE (yellow) and NE (purple) orientations are the dominant group of lineations recorded, reflected by the resultant NNE-SSW (044° - 244°) azimuth generated from the total data base. Analyzing the data this way does not reflect the longest orientations; though visually displaying both the rose diagram and the raw data plotted on either a GEP image or on an image using GIS allows the viewer to visually see the variations in length.

The DEM was overlaid with geology, field data was added as a layer, and scale of view was zoomed in to produce a visual, color coded GIS image of the area where the silica cemented breccias are concentrated (Figure 4.16). The GIS map shows that the breccias are concentrated in the area that corresponds with the southern exposure of the ruputured Crooked Creek fault trace that also coresponds with the axis of the anticline as it wraps around to the south. The GEP lineaments in this view show dominantly NNE (yellow), NE (violet), and E-W (red) trending lineaments in the area delineated by the black oval. These do correspond with the rose diagram generated with the GEP lineament data shown to the right of the figure.

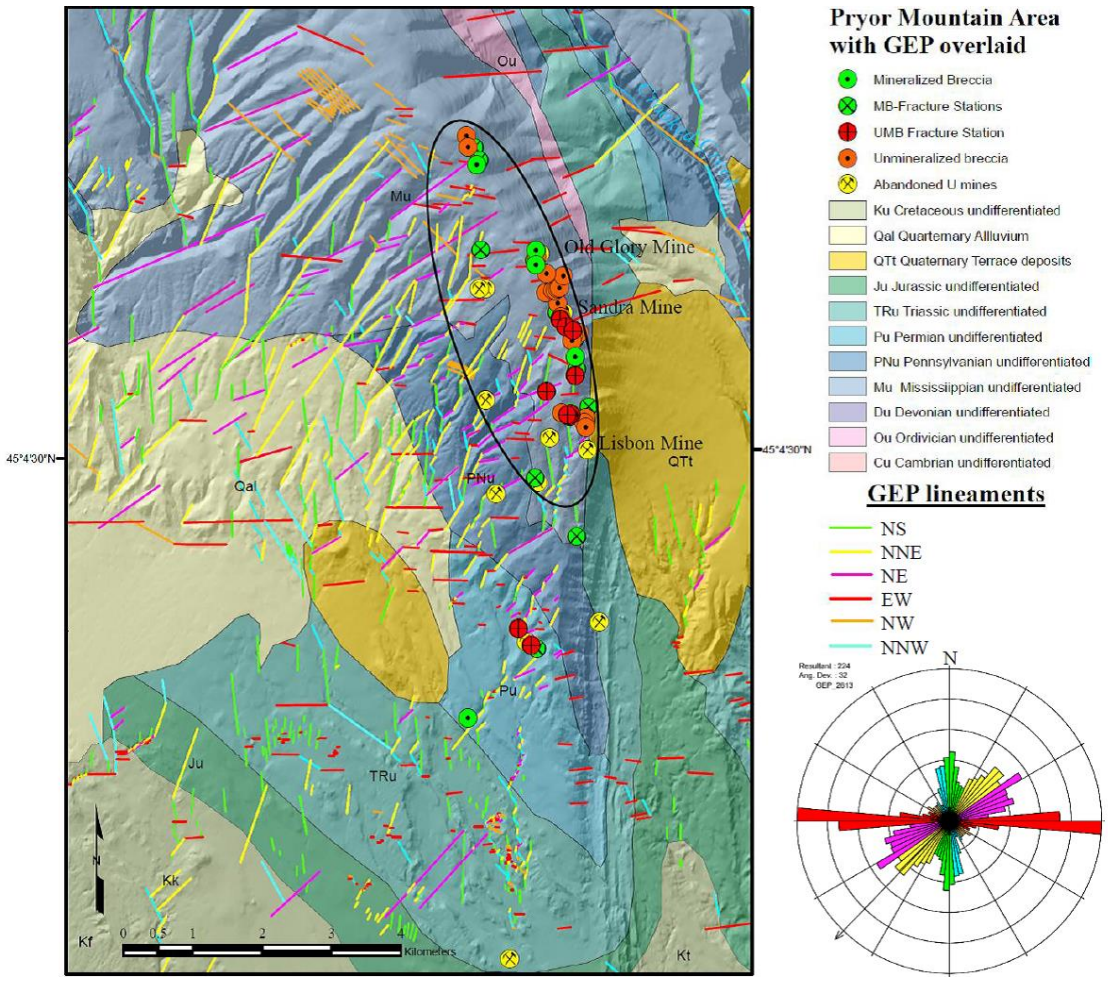


Figure 4.16. GEP data added to GIS. Mineralized and unmineralized breccias, plotted in red and green symbols are concentrated between the Lisbon and Old Glory mines, denoted by the black oval. Rose diagram to left is the GEP lineament data for the entire study area. Localized area appears to correspond visually to the same density of fracture orientations plotted in the rose diagram.

The mineralized breccias(n=30) and unmineralized breccias (n=41) locations were plotted on DEMs. Fracture orientation data for mineralized breccias (n=14 stations; 486 fractures) and unmineralized breccias (n=14 stations; 470 fractures) were plotted on lower hemisphere stereographic projections and rose diagrams were produced from the data for side by side comparison (Figure 4.17).

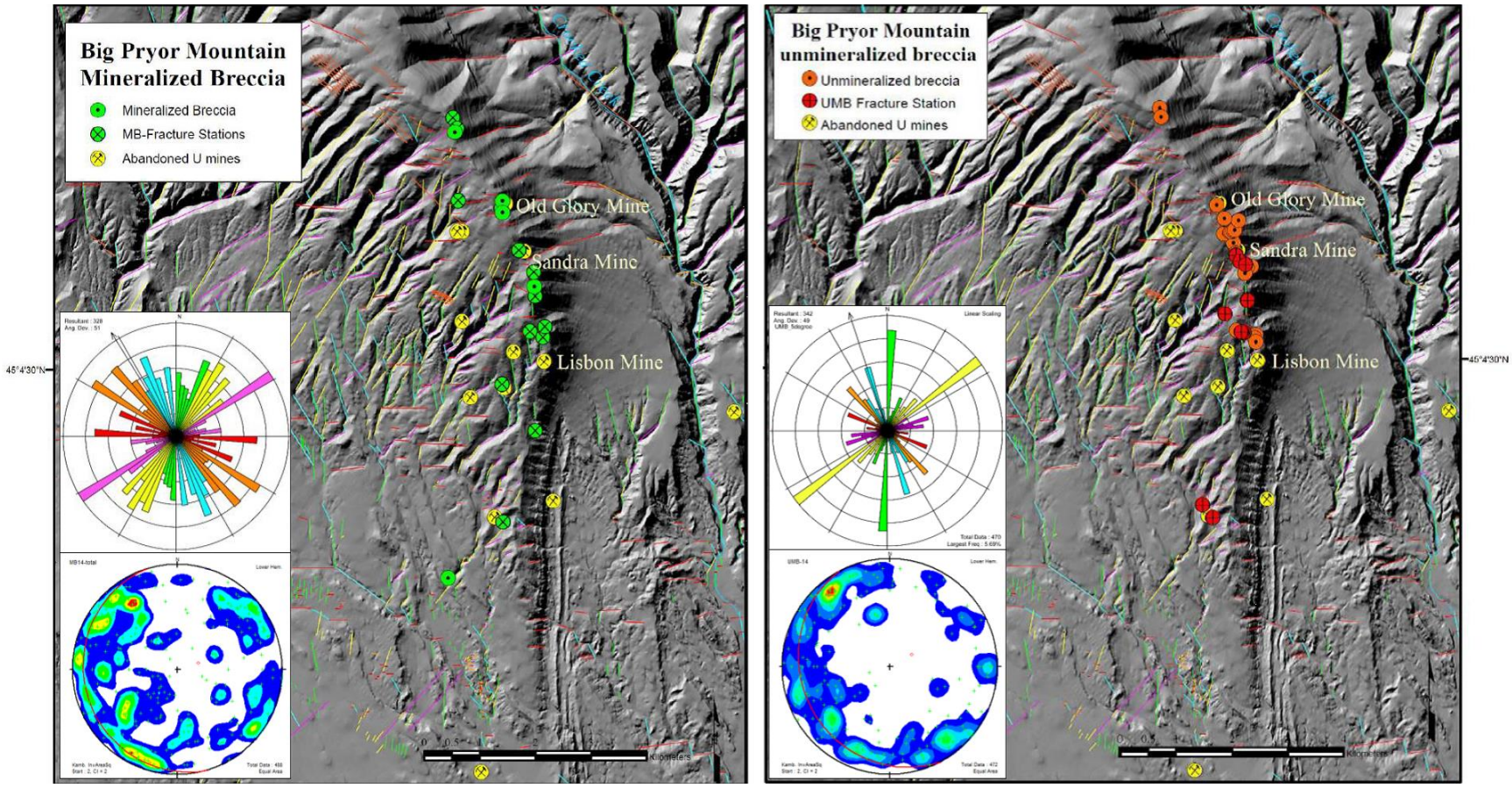


Figure 4.17. Mineralized breccia are plotted in green symbols in the left hand image and red symbols in the right hand figure. Rose diagram and equal area filled contoured poles to planes diagrams from the mineralized breccia fracture station data show a dominance of NE-SW (purple) and NNW-SSE (orange) fractures. The mineralized data have more fractures from all directions than the unmineralized breccia. The unmineralized breccia have few E-W fractures compared to the mineralized breccia.

The rose diagrams created from the fracture station data using linear scaling were divided into the same 5° class intervals and color theme as the GEP lineation data for comparison. The rose and equal area contoured poles to planes show slightly different distribution of dominant fractures in mineralized versus unmineralized fracture data. The rose diagram produced from the mineralized fracture data shows NE (055°- 060°) (purple) and SE-NW orientations (120°- 125° and 140°- 145°) (orange) oriented fractures were recorded the most. NS (000°- 005°) (green) and NNE-SSW (050°-055°) (yellow) oriented fractures were recorded the most in the unmineralized breccias. The rose diagram from the mineralized data is similar to the GEP lineation rose diagram. The rose diagram for the mineralized fracture data show a greater frequency of fractures in all directions.

Movement and Mineralization along Fracture Planes

Movement was recorded at some of the fracture stations that had some type of indicators such as offset fractures or slickenlines on fracture planes (slickesides). Slickenlines were observed more frequently in the mineralized than the unmineralized breccia. A few fractures had mineralization preferentially along some orientations though this was not common. Equal area poles to planes and rose diagrams were used to show fracture orientations that had mineralization or movement along fracture planes, sometimes coincident. Mineralized breccias showed movement along NE-SW, NW-SE, E-W, and N-S striking slickenside planes (red) (Figure 4.18). Mineralization (yellow lines) along preferred orientations was observed at four fracture stations (FS114, FS132, FS137, and FS118) shown in Figure 4.18.

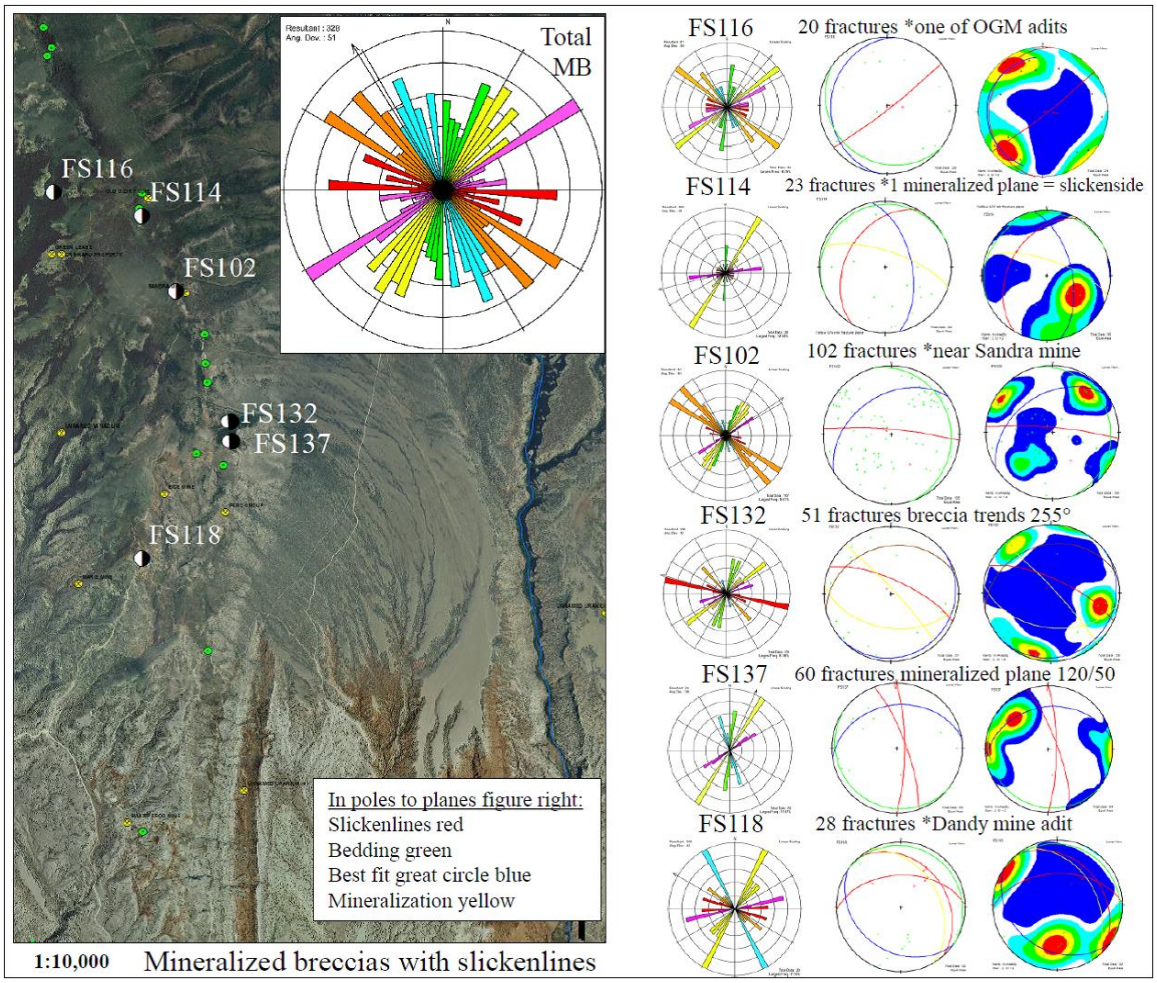


Figure 4.18. Mineralized breccia fracture stations with slickenlines are shown by the black and white symbols on the map. Equal area poles to planes diagrams from fracture station data show movement along NE-SW, E-W, NW-SE, N-S and NNW-SSE (red lines) and mineralization along fracture planes in FS114, FS132, and FS118 (yellow lines). Bedding = green; mineralization = yellow; slickenside plane = red; red arrows on slickenside plane show direction of movement; best fit great circle = blue; breccia trend = brown in FS 132.

Mineralization in the fraction stations (yellow lines) above showed preferred orientations along a few fractures. Mineralization at fracture station FS114 was recorded on fractures oriented nearly E-W. Mineralization at fracture station FS132 was recorded on fractures oriented NW and coincides with one nearly E-W bedding plane (dip direction of 188°). Mineralization at fracture station FS118 was intersected by E-W

oriented fractures with movement down to the SW. This may suggest that E-W fractures intersecting other fractures contributed to mineralization in the PMD.

Unmineralized breccias show movement (NW) along NE-SW striking, movement to the N in N-S striking, and east movement along E-W slickenside planes (Figure 4.19). Direction was not determined along some slickensides at FS130, though slickenlines on a plane oriented nearly NS showed movement to the NW.

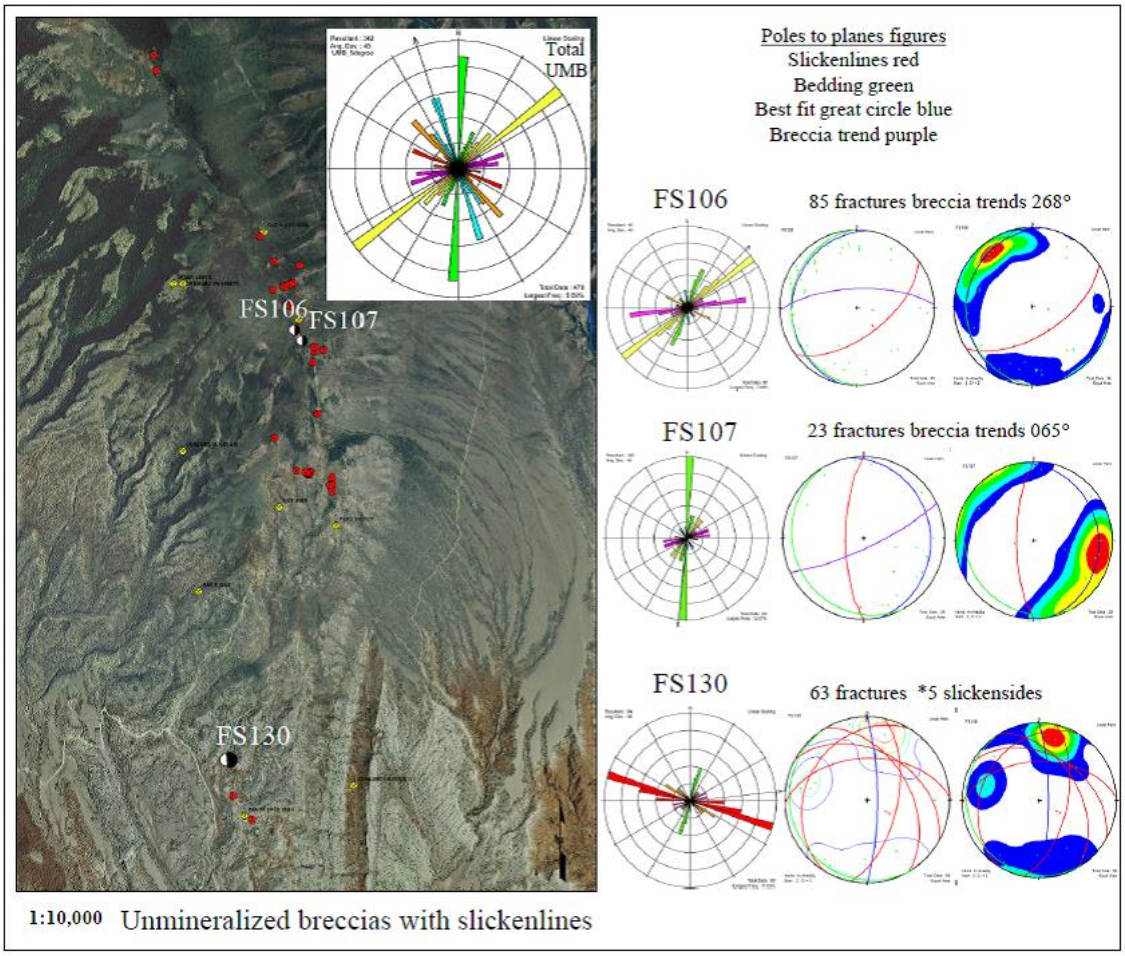


Figure 4.19. Unmineralized breccia fracture stations with slickenlines are shown by the black and white symbols on the map. Equal area poles to planes diagrams show movement along NE-SW, N-S, NW-SE, and E-W trending fracture planes. Red arrows on slickenside plane show orientaton of slickenlines. Bedding = green; slickenside plane = red; Best fit great circle = blue; purple = trend of breccia in FS106 and FS107.

The dominant fracture orientations for fracture stations FS106 and FS107 which are located in the area where the fault has erupted are N (050°- 055°) E and N (000°-010°) S. These coincide with directions for movement. The trend of the breccias in these two fracture stations are likely along fractures. The breccia trends EW at fracture station FS106 and is cut by a NE oriented fracture with movement to the NW. The breccia trend at fracture station FS107 is NE and it is cut by a fracture trending N with movement to the N. Fracture station FS130 reflects multiple episodes of movement with dominant movement in the E (090°-110°)W (red) sriking slickensides. Movement to the NW was observed on a N-S slickenside plane.

Expected Laramide Stress Field

The dominance of E-W trending lineaments in the GEP data suggests that movement along the E-W trending Sage Creek sinistral fault influenced the fracture pattern in the Pryor Mountain range. Looking the DEM many of the lineaments are linear and drainages are offset either to the E or NE likely reflecting the movement along the reactivated Sage Creek sinistral fault at depth.

By overlying the expected Laramide stress field model (after Brown 1993) on the DEM, some of the major lineaments correspond to the expected geometry and kinematics of the model. For example, using the most frequent purple NE (055° - 060°) orientation recorded in the total data set for the mineralized breccias and positioning the direction of Laramide shortening in that orientation, the Sage Creek fault lines up with the expected E-W sinistral fault with the north side dropped down as predicted in the model. The Big Pryor Mountain block is on the upside of the Sage Creek fault. Similarly the orange N-

NW oriented fault predicted in Brown's model lines up with the Sage Creek drainage which has been appears to have been slightly offset to the NE. The expected thrusting in the SE pie (aqua) of the circle or the thrust faulting associated with the orange orientation would corresponds to the thrusting of the East Pryor Mountain block that is cored by the Dry Head thrust fault (Figure 4.20). The expected orientation (aqua) of the fault also appears to line up with a main draingage along the East Pryor block that parallels Crooked Creek.

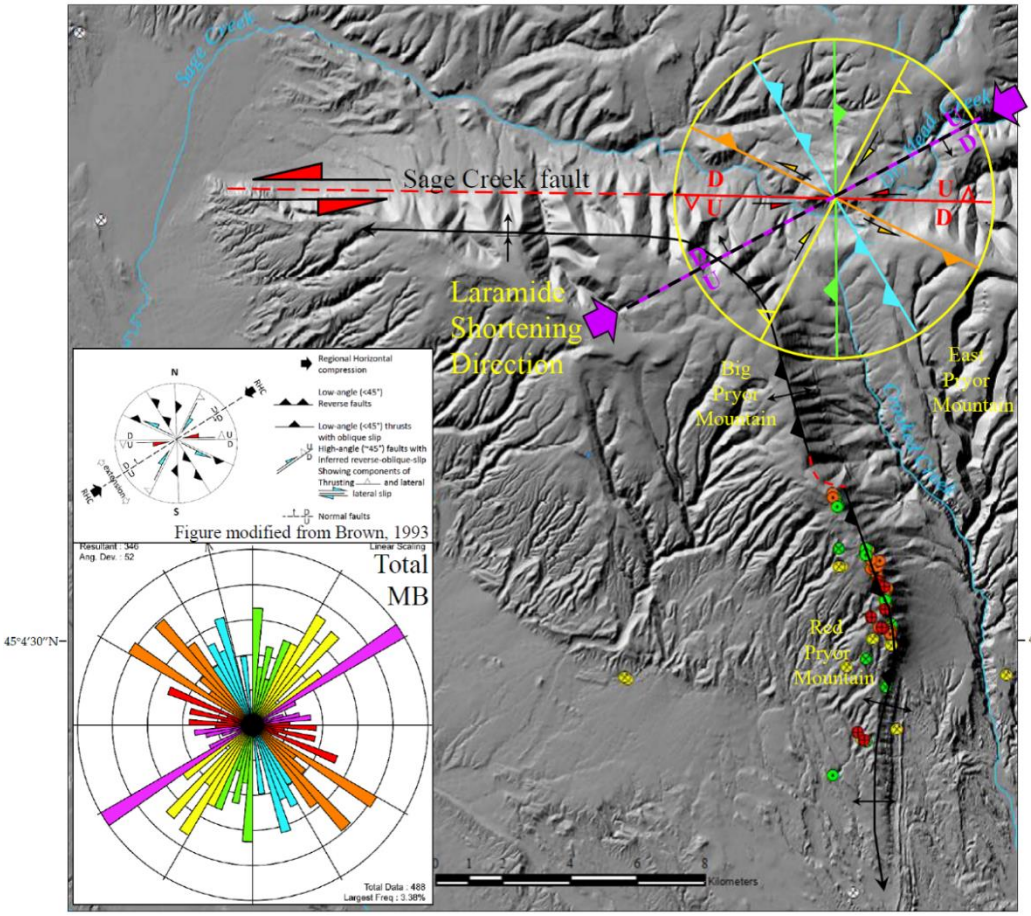


Figure 4.20. DEM with expected Laramide Stress field and expected geometry and kinematics after Brown (1993). Fracture data for total mineralized breccia are shown in the rose diagram. The red dashed line along the fault in the figure is the author's interpretation suggesting offset of the axis of the structure by W-E movement.

Thus, in the Pryor Mountains, a Laramide Shortening direction of (055-060°) is suggested. The lineations likely reflect the brittle deformation of the sedimentary rocks as fractures were produced during folding in the Laramide Orogeny.

Discussion

Geochemical data from this study supports an ascending hydrothermal source of fluids for the cement of the tectonic breccias in both districts. Both radiogenic Sr and stable C and O isotope data presented in this study suggest that the mineralization in the U-V mining districts was episodic.

Structural field data from siliceous tectonic hydrothermal breccias, only present in the Pryor Mountain Mining District, suggest that the location of the fractures along the ruptured portion of the Crooked Creek fault had the greatest control on mineralization. The mineralized tectonic hydrothermal breccias had an overall more even distribution of fractures in four of the six dominant orientations and had more NW-SE (orange) and NE-SW (yellow) oriented fractures than the unmineralized breccia.

The structural position of the tectonic hydrothermal breccias along the intersection of the hanging wall of the Crooked Creek thrust block and the curved axis of the Gypsum Creek anticline was the most fractured and subsequently provided more pathways for fluid migration. Because this area was so intensely fractured and U-V deposits were concentrated in collapse paleokarst, suggests collapse of paleokarst breccias that coincided with fractures was enhanced. This allowed for more fluid migration into the paleokarst along both new and existing fractures.

The dominant W-E fractures and lineaments recorded suggest episodic eastward movement of the Big Pryor Mountain block. This created more fluid migration paths in the mineralized area of the mountain. Some fractures oriented in other directions were likely opened by this movement. Episodic movement directed in the direction of Laramide shortening likely followed preexisting weakness. Fluid pressure that built up between and accompanied episodic movements would be explosively directed along fractures; some of the same fractures that tectonic breccias were emplaced. This process would re-fracture the silica cemented breccias. Later oxidized fluids carrying mobilized U^{6+} as uranyl ions would migrate through the fractures and U and V mineralization would occur where Fe-V oxides were available.

Other breccias present in the mining districts are associated with the overall hydrologic processes of exhumation of the Bighorn Basin. The lithified collapse breccias likely formed in response to cool, meteoric fluids invading earlier collapse paleokarst that may have experienced more collapse during folding; possibly with fluids derived from a lake or an ancestral tributary to the Bighorn River. This is supported in this study by the difference in radiogenic Sr and stable C and O isotope composition of the cements.

Origin of the Tectonic Breccias

Several studies concentrating on oil and gas reservoir characteristics of the Mississippian Madison Group in the Bighorn Basin documented the presence of tectonic hydrothermal breccias (Katz et al., 2006; Kislak et al., 2001; Westphal et al., 2004). This study adds to that data base and also documents another type of tectonic hydrothermal breccia, the silica cemented breccia of the PMD, that hasn't been recognized previously

in the Bighorn Basin. The THB observed throughout the Bighorn and Wind River basins were determined to be hydrothermal in nature based on their morphology, distribution, and geochemical signature (Katz et al., 2006). The distribution of the THB in these basins is along the basin margins that are dominated by groundwater chemistry (Katz et al., 2006). The interaction of groundwater in these settings suggests mixing of meteoric waters with basin brines to account for the geochemical signatures of the late-stage calcite that cemented the tectonic hydrothermal breccias observed in these studies. Katz et al. (2006) presented a fluid flow model to explain the origin and geochemical signature for the THB. These studies may serve as an analogue for similar occurrences of tectonic hydrothermal breccias in basin margin settings such as the structures in this study. The model might also be applied to the PMD and the LMD with a few modifications that could possibly account for the silica in the cement of the breccias in the PMD and the hematite- and limonite-staining of the THB along the mineralized zone.

One proposal would be that the Bighorn Basin was occupied by a lake or lakes. An Eocene age uraniferous phosphatic lake may have occupied the area above the heavily fractured areas on Big Pryor Mountain, similar to those described by Love (1964) in the Green River basin of Wyoming and areas in Utah. The lake may have concentrated silica derived from the volcanic ash that was deposited in the lake. Eocene age volcanic centers near the PMD include the Absaroka/Gallatin (53-47 Ma) volcanic field (Hiza, 1998) or the Crazy Mountain (51-49 Ma) volcanics (Skipp and McGrew, 1977). Sliderock Mountain volcano (DuBray and Harlan, 1998) would be an older volcanic center (78-75 Ma) near the PMD or a younger volcanic event such as the

Yellowstone (2.6-0.64 Ma) eruptions (Lanphere et al., 2002) may also have contributed large volumes of ash and volcanic materials to lakes that may have been present during different stages of exhumation of the Bighorn Basin. Rivers or streams may have originated from the lake or lakes. Ancestral river terraces from former levels of the Bighorn River and its tributaries are present in the area, with a major one directly below the Lisbon mine area extending up to the area below the Sandra mine (see Figure 4.16). The region just to the north of the Lisbon mine area in the PMD may also lend some support to this idea (Figure 4.21).



Figure 4.21. View looking west from Crooked Creek toward the Lisbon mine area. The Lisbon mine is located at the top of the ridge to the left of the access road that switches back and forth across the curved tree lined drainage (possibly a fault trace?). The area of heavy hematite- and limonite-staining extends across the ridge from the middle third of the image a little passed the border of the photo, a distance of approximately 1-2 km.

The region is approximately 1-2 km long and has extensive hematite- and limonite-staining. The area appears to be a collapse feature that could have been occupied

by a lake or simply a large ponded collapse karst system. Evidence supporting this would be the pervasive silicified and hematite- limonite-stained zone. This area coincides with the intersection of the erupted southern portion of the Crooked Creek thrust block and the curved axis of the Gypsum Creek anticline. If a lake or river were present here fluids could have migrated down into fractures and invaded paleokarst. Water migrating and interacting with the fractured silica cemented tectonic breccia would oxidize and mobilize available iron and vanadium. The fluids would thus be iron rich and this could account for the ferroan dolomite cement in the lithified collapse breccia and also for the hematite- limonite-staining of the silica cemented breccias in this region. It would also provide a possible explanation for the silica cemented lag deposits present above the zone of mineralization on the top of Big Pryor Mountain that lack the hematite-staining. If a lake or river were not present in that area, then the iron would not have been oxidized to the extent that it has been in the breccias in the mineralized zone.

The silica cemented breccias and the lithified collapse breccias that were later episodically fractured and cemented with calcite are likely related to episodes of tectonic pumping associated with the Laramide Orogeny. A fluid flow model proposed by Katz et al. (2006) may also serve as a model in the Pryor Mountain District. Adding lakes to the model may account for some of the silica present in the hydrothermal breccia and or the pervasive hematite- limonite-staining of the THB. Lakes may have periodically been positioned over the most fractured fault zone as the Bighorn Basin was exhumed.

Fluid Flow Model

The fluid migration model of Katz et al. (2006), patterned after Huntoon (1993) and Sonnenfeld (1996) is useful for explaining the variable chemistry of late-stage calcites in Laramide basins. The model helps to explain the recharge of the aquifers in the Bighorn Basin from different structures surrounding the basin. The model applied to the Pryor Mountains would include fluids migrating down into fractures and faults below the lakes and ponds and also have the structural complexity of the sinistral strike slip fault that separates the N and S blocks of the Pryor Mountains (Figure 4.22).

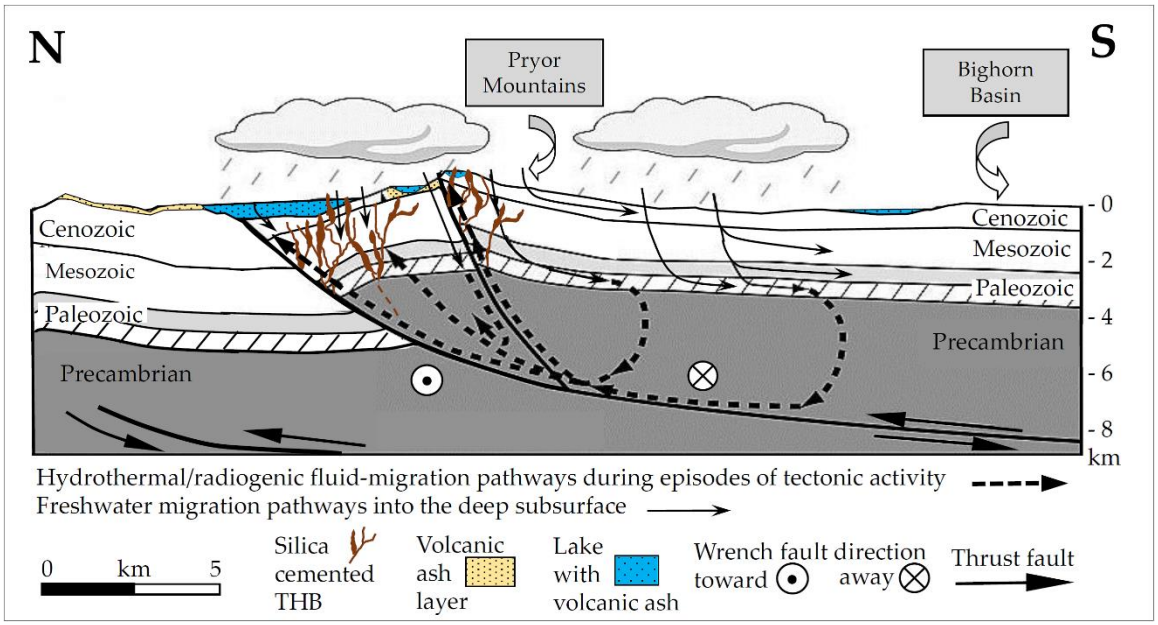


Figure 4.22. Schematic figure showing fluid flow in the PMD. Volcanic ash blanketed the surface and was deposited in ponds and lakes (size is greatly exaggerated) during early BHB formation (exhumation). Downward-percolating fresh waters recharge the aquifers on the basin side of the faults mixing with radiogenic basement derived fluids through fractures. Hot waters were later expelled and cycled along basement-rooted thrusts that brecciated and hydro-fractured the overlying strata during shortening episodes of the Laramide orogeny. Figure modified from Katz et al., 2006.

In the Bighorn Basin model of Katz et al. (2006) the fluids that contribute to the mineralization originated from under saturated meteoric groundwater that migrated into the burial environment while dissolving and incorporating Ca^{2+}, CO_3^{2-} and radiogenic Sr from the dissolution of the surrounding carbonates and the felsic basement, respectively.

The geochemistry of this study also suggests a mixing of fluids; likely fluids from Pennsylvanian and Permian aquifers which are more radiogenic than the Mississippian age host rock (Frost and Toner, 2004) but less radiogenic than the felsic basement (Wooden and Mueller, 1988; Frost et al., 2006). The Pennsylvanian Tensleep Sandstone may have held oil and brines that migrated into fractures, paleokarst, and permeable portions of the Mississippian Madison Limestone before the structure was totally breached by propagating fractures as folding and faulting proceeded during the latter part of the Laramide Orogeny (Stone, 1967; Sheldon, 1967). This could explain the Sr composition that is present in the PMD. The Pennsylvanian Tensleep would be a closer, more logical source than the Archean basement for the values of Sr that are present in the PMD. As the structure was breached, fractures could have provided pathways for either meteoric waters or fluids from the Pennsylvanian Tensleep Sandstone to invade the paleokarst and as in the model of Katz et al. (2006) dissolve and incorporate Ca^{2+}, CO_3^{2-} and radiogenic Sr from the dissolution of the surrounding carbonates.

In the model, the fluids that migrated into the burial environment were heated and mixed with hypersaline brines from deeply buried parts of the basement and were forcefully injected into the overlying strata by hydrofracturing (Katz et. al., 2006). The

$\delta^{18}O$ composition of calcite cements that healed fractures in the silica cemented and the lithified breccia support this model.

The Katz et al. (2006) study also included 11 modern speleothems as a proxy for Laramide age meteoric calcite in equilibrium with meteoric groundwater to compare the possibility of the late-stage calcite fluids being derived strictly from a Laramide age meteoric source (Katz et. al., 2006). The speleothem were analyzed and found to have the second most depleted $\delta^{18}O$ compositions (-17.4 to -16.8‰) with $\delta^{13}C$ compositions also depleted (-6.4 to -2.5‰). The $\delta^{18}O$ values of the speleothem were used with empirical formulas based on the temperature equation of Epstein and Mayeda (1953) to derive the $\delta^{18}O$ values the late-stage calcite would have had if Laramide-age meteoric groundwater were the sole source for precipitating the late-stage calcite (Katz et. al., 2006). Their derived $\delta^{18}O$ values (-47.6 to -42‰) were significantly more depleted than the measured values indicating that the late-stage calcites were likely the product of an intermediate mixture of downward percolating meteoric waters and hot subsurface brines (Katz et. al., 2006). Their conclusions were also supported by fluid inclusion data (Katz et. al., 2006).

In our study only two speleothems from the area were analyzed and found to have similar depleted values for $\delta^{18}O$ (-16.55 to -16.44‰) and slightly heavier $\delta^{13}C$ compositions (0.24 to 0.32‰). Though only two speleothem were analyzed in our study and have not been dated, we feel that the late-stage calcite in our study area is hydrothermal in origin and likely formed in a mixing model similar to the model proposed by Katz et al. (2006).

Conclusions

The intent of this study was to characterize the nature of the fluids that cemented the breccias in the two districts and to identify the structural control on mineralization. The geochemical data presented in this chapter supports an ascending hydrothermal source of fluids for the cement of the tectonic breccias in both districts. The "lithified" collapse breccias of the districts are not of hydrothermal origin based on the stable O composition of the cement. The radiogenic composition could support either a basement or meteoric derived source. Based on the stable O isotope data the source was likely a river or lake which interacted with a nearby exposed Archean source, such as the Bighorn or Beartooth Mountains as they were being exhumed. Some of the Sr composition may have been derived from Pennsylvanian to Permian rock that was present as well. The later calcites that healed the breccias are of hydrothermal origin based on O isotope compositions.

Structural control of the deposits based on field data from siliceous tectonic hydrothermal breccias only present in the PMD, suggests that the location of the fractures along the ruptured portion of the Crooked Creek fault had the greatest control on mineralization. All the deposits, including those without silica cemented breccias, in the PMD were located on the hanging wall of the Crooked Creek fault and mineralization was concentrated in the areas of Red Pryor Mountain that coincided with the ruptured portion of the fault. The greater intensity and quantity of fractures in this area allowed for more fluid migration that resulted in U-V mineralization in the district.

The fluid flow model is as suggested a model. It could offer an explanation for some of the observed and geochemical results of this study. Some of the U and silica may have been derived from the devitrification of a large ash source such as the Yellowstone or Absaroka volcanics if lakes or the collapse paleokarst served as impounding features to enable this process. More extensive data would be needed to characterize each deposit as each deposit displays some individual differences likely related to not only structural position (intersection of fractures, proximity to faults etc.) but also the sedimentological and later diagenetic changes that have affected the Mississippian Madison Limestone in the study area.

References

1. Allan, J. R; Wiggins, W. D. Dolomite reservoirs, geochemical techniques for evaluating origin and distribution: *AAPG* Continuing Education Course Note Series 36, **1993**, 129.

2. Arthur, M.A.; Anderson, T.F.; Kaplan, I.R.; Veizer, J.; Land, L.S. Stable isotopes in sedimentary geology: *SEPM Short Course*, **1983**, 10, 5–54.

3. Barrington, J.; Kerr, P.F. Collapse Features and Silica Plugs near Cameron, Arizona: *Geol. Soc. Am. Bull.* **1963**, 74, 1237-1258.

4. Bird, P. Stress direction history of the western United States and Mexico since 85 Ma. *Tectonics* **2002**, 21, 3, 1-12.

5. Blackstone, D. L., Jr. Structure of the Pryor Mountains, Montana: *J Geol*, **1940**, 48, 6, 590-618.

6. Blackstone, D.L., Jr. Structural geology, northwest margin, Bighorn Basin, Park County, Wyoming and Carbon County, Montana. In *Geology of the Beartooth uplift and adjacent basins; Montana Geological Society and Yellowstone Bighorn Research Association, joint Field conference and Symposium*; Montana Geological Society: Billings, MT, USA, 1986, pp. 125-135.

7. Broadhead R.F.; Robertson, J.M. Introduction to the atlas. In *Atlas of major Rocky Mountain gas reservoirs*; Robertson, J.M., Broadhead, R.F., Eds.; New Mexico Bureau of Mines and Mineral Resources, 1993, 206 p.

8. Brown, W.G. Structural style of Laramide basement-cored uplifts and associated folds. In *Geology of Wyoming*; Snoke, A. W., Steidtmann, J.R., Roberts, S.M., Eds.; Geological Survey of Wyoming Memoir, 1993, no. 5, pp. 312-371.

9. Davies, G.R.; Smith, L.B. Structurally controlled hydrothermal dolomite reservoir facies: An overview: *AAPG Bull* **2006**, 90, 1641–1690.

10. Dicken, A.P. Radiogenic Isotope Geology, Second Edition, Cambridge University Press: New York, 2005, 492 p.

11. Dickson, J.A.D. A modified technique for carbonates in thin section. *Nature* **1965**, 205, 587- 587.

12. Dickinson, W.R.; Klute, M.A.; Hayes, M.J.; Janecke, S.U.; Lundin, E.R.; McKittrick, M.A.; Olivares, M.D. 1988, Paleogeographic and paleotectonic setting

of Laramide sedimentary basins in the Rocky Mountain region. *Geol. Soc. Am. Bull.* **1988**, 100, 1023–1039.

13. Du Bray, E.A.; Harlan, S.S. Geology and tectonic setting of the Cretaceous Sliderock Mountain volcano, Montana. U.S. Geological Survey professional paper 1602, 1998, 19 p. Available online: http://pubs.er.usgs.gov/publication/pp1602 (Accessed: 10 December 2015).

14. Egemeier, S. J. Cave development by thermal waters with a possible bearing on ore deposition, Ph.D. dissertation: Stanford University, 1973, 88 p.

15. Egemeier, S. J. Cave development by thermal waters, National Speleological Society Bulletin, 1981, 43, 2, 31–51.

16. Eldam, N.S. Structural Controls on Evaporite Paleokarst Development: Mississippian Madison Formation, Bighorn Canyon Recreation Area, Wyoming and Montana [Master's thesis]: University of Texas at Austin, 2012, 170 p.

17. Engel, A.S.; Stern, L.A.; Bennett, P.C. Microbial contributions to cave formation: new insight into sulfuric acid speleogenesis: *Geology*, **2004**, 32, 369-372.

18. Engel, A.S.; Engel, S.A.; Moore, P.J.; DuChene, H. Eds., *Carbonate Geochemistry: Reactions and Processes in Aquifers and Reservoirs*, Selected papers and abstracts of the symposium held in Billings, Montana, August 6-9, 2011, Karst Waters Institute Special Publication 16: Leesburg, Virginia, Karst Waters Institute, 2011, 84 p.

19. Epstein, S.; Mayeda, T. Variation of O18 content of waters from natural sources. *Geochim Cosmochim Acta*, **1953**, 4, 213-224.

20. Epstein, S.; Buchsbaum, R.; Lowenstam, H.A.; Urey, H.C. Revised carbonate-water isotopic temperature scale. *Geol. Soc. Am. Bull.* **1953**, 64, 1315-1326.

21. Faure, G. *Principles and Applications of Geochemistry*, *ed. 2*. Prentice Hall: N.J., USA, 1998, 544 p.

22. Foose, R.M.; Wise, D.U.; Garbarini, G.S. Structural geology of the Beartooth mountains, Montana and Wyoming, *Geol. Soc. Am. Bull.* **1961**, 72, 1143-1172.

23. Frost, C.L.; Toner, R.N. Strontium Isotopic Identification of Water-Rock Interaction and Ground Water Mixing. *Groundwater* **2004**, 42, 418-432.

24. Frost, C.D.; Frost, B.R.; Kirkwood, R.; Chamberlain, K.R. 2006. The tonalite-trondhjemite granodiorite (TTG) to granodiorite-granite (GG) transition in the Late

Archean plutonic rocks of the central Wyoming province. *Can J Earth Sci* **2006**, 43, 1419-1444.

25. Hardie, L.A. Dolomitization: A critical view of some current views. *J. Sediment. Petrol.* **1987**, 57, 166-183.

26. Hauptman, C.M. Uranium in the Pryor Mountain area of southern Montana and northern Wyoming. *Uranium and Modern Mining*, **1956**, 3, 11, 14-21.

27. Hiza, M. The Geologic History of the Absaroka Volcanic Province, *Yellowstone Science*. **1998**, 6, 2, 2-7. Available online: https://www.nps.gov/yell/learn/upload/YS_6_2_sm.pdf (Accessed 7, December 2016).

28. Hollerbach, A. Influence of Biodegradation on the Chemical Composition of Heavy Oil and Bitumen: Characterization, Maturation, and Degradation. In *Section II Exploration for Heavy Crude Oil and Natural Bitumen*; Meyer, R.F., Ed.; *AAPG*, Studies in Geology: Tulsa, OK, USA, 1997, 243-247.

29. Hoefs, J. *Stable Isotope Geochemistry* 6th ed., Springer: Berlin, 2009, 285 p.

30. Huntoon, P.W. The influence of Laramide foreland structures on modern ground-water circulation in Wyoming artesian basins. In *Geology of Wyoming*; Snoke, A.W., Steidtmann, J.R., Roberts, S.M., Eds.; Geological Survey of Wyoming: 1993, Memoir No. 5, pp. 756-789.

31. Katz, D.A.; Eberli, G.P.; Swart, P.K.; Smith, L.B. Tectonic-hydrothermal brecciation associated with calcite precipitation and permeability destruction in Mississippian carbonate reservoirs, Montana and Wyoming. *AAPG Bull* **2006**, 90, 1803-1841.

32. Kislak, J.; Smith, L.; Peacock, D.; Eberli, G.; Swart, P. Classification, distribution, and origin of hydrothermal breccia, Madison Formation, Wyoming (abs.): AAPG Annual Meeting Program, 2001, 10, p. A105.

33. Lageson, D.R.; Larsen, M.C.; Lynn, H.B.; Treadway, W.A. Applications of Google Earth Pro to fracture and fault studies of Laramide anticlines in the Rocky Mountain foreland. In *Google Earth and Virtual Visualizations in Geoscience Education and Research*. Whitmeyer, S.J., Bailey, J.E., De Paor, D.G., Ornduff, T., Eds.; Geological Society of America Special Paper 492, 2012, p. 1–12.

34. Lanphere, M.A.; Champion, D.E.; Christiansen, R.L.; Izett, G.A.; Obradovich, J.D. Revised ages for tuffs of the Yellowstone Plateau volcanic field: Assignment of the Huckleberry Ridge Tuff to a new geomagnetic polarity event. *Geol. Soc. Am. Bull.* **2002**, 114, 5, 559-568.

35. Laznicka, P. Breccias and coarse fragmentites; petrology, environments, associations, ores: Developments in Economic Geology. Elsevier Science & Technology Books: University of California, USA, 1988, v. 25, 832 p.

36. Lopez, D.A. *Field guide to the northern Pryor Bighorn structural block, south central Montana*. Open-File Report 330. Montana Bureau of Mines and Geology: Butte, Montana, USA, 1995, 22 p.

37. Lopez, D.A. Geologic Map of the Bridger 30' × 60' Quadrangle, Montana: Montana Bureau of Mines and Geology Geologic Map 58, 2000, Scale 1: 100,000; Montana Bureau of Mines and Geology: Montana Tech of the University of Montana, Butte, MT, USA, 2000.

38. Love, J.D. Uraniferous phosphatic lake beds of Eocene age in intermontane basins of Wyoming and Utah. *U.S. Geol. Surv. Prof. Pap.* 474- E, 1964, 66 p.

39. Marshak, S.; Mitra, G. *Basic Methods of Structural Geology* Prentice Hall: NJ, USA, 1988, 446 p.

40. Marshall, D. J. *Cathodoluminescence of Geological Materials*. Unwin Hyman, Boston, MA, USA, 1988, 146 p.

41. Maughan, E.K. Tectonic setting of the Rocky Mountain region during the late Paleozoic and early Mesozoic. In *Proceedings of the Symposium on the Genesis of Rocky Mountain Ore Deposits: Changes with Time and Tectonics*; J.W. Babcock, Ed.; Regional Exploration Geologists Society, Denver, CO, USA, 1983, p. 39-50.

42. McLaughlin, J.F.; Quillinan, S.A.; Bentley, R.; Deiss, A.; Jiao, Z. (Carbon Management Institute, University of Wyoming) Geologic Controls on Sealing Capacity; Defining Heterogeneity Relative to Long-Term CO2 Storage Potential in Wyoming, poster presented at The Thirteenth Annual Carbon Capture, Utilization & Storage Conference, Pittsburgh, PA, 28 April 2014 - 1 May 2014. Available online: http://www.uwyo.edu/cmi/_files/images/posters/2014-ccus-poster_fred.pdf (Accessed November, 2016).

43. Meyer, R.F.; Attanasi, E.D.; Freeman, P.A. Heavy oil and natural bitumen resources in geological basins of the world: U.S. Geological Survey Open-File Report 2007-1084, 2007. Available online: http://pubs.usgs.gov/of/2007/1084/ (Accessed October, 2016).

44. Neely, T.G.; Erslev, E.A. The interplay of fold mechanisms and basement weaknesses at the transition between Laramide basement-involved arches, northcentral Wyoming, U.S.A. *J Struct Geol* **2009**, 31, 1012–1027.

45. Paytan, A. Performed the Sr separation and analysis of the barite from the Pryor Mountains using the strontium methodology of Scher et al., 2014. Personal communication by e-mail, 6 August 2014.

46. Phillips, W.J. Hydraulic fracturing and mineralization: *J Geol Soc* **1972**, 128, 337–359.

47. Piper, D.Z.; Perkins, R.B.; Rowe, H.D. Rare-earth elements in the Permian Phosphoria Formation: Paleo proxies of ocean geochemistry. *Deep Sea Res. Part II* **2007**, 54, 1396-1413.

48. Ramsay, J. G.; Huber, R. M. *The techniques of modern structural geology*, Volume 2: folds and fractures, Academic Press An Imprint of Elsevier Science, London, UK, 1987, 697 p.

49. Sando, W.J.; Gordon Jr., M.; Dutro Jr., J.T. Stratigraphy and geologic history of the Amsden Formation (Mississippian and Pennsylvanian) of Wyoming. *U.S. Geol. Surv. Prof. Pap.* **1975**, 858A, 78 p.

50. Sando, W. J., 1976, Mississippian history of the northern Rocky Mountains region: *U.S. Geol. Surv. J Res.* **1976**, 4, 317-338.

51. Sando, W. J. Madison Limestone (Mississippian) paleokarst: a geologic synthesis. In *Paleokarst*; James, N. P., Choquette, P.W., Eds.; Springer-Verlag, New York, USA, 1988, pp. 256-277.

52. Scher, H. D.; Griffith, E. M.; Buckley, W. P. Accuracy and precision of $^{88}Sr/^{86}Sr$ and $^{87}Sr/^{86}Sr$ measurements by MC-ICPMS compromised by high barium concentrations. *Geochem, Geophy, Geosys* **2014**, 15, 499–508.

53. Serc.carleton website http://serc.carleton.edu/research_education/geochemsheets/index.html accessed: October 29, 2014.

54. Sheldon, R.P. Long distance migration of oil in Wyoming: *The Mountain Geologist* **1967**, 4, 53-65.

55. Sibson, R.H.; Moore, J.; McM.; Rankin, A.H. Seismic pumping - a hydrothermal fluid transport mechanism. *J. Geol. Soc. London* **1975**, 131, 6, 653-659.

56. Sibson, R.H. Brecciation processes in fault zones – Inferences from earthquake rupturing. *Pure Appl. Geophys*. **1986**, 124, 159-175.

57. Sims, P. K.; Finn, C.A.; Rystrom, V.L. Preliminary Precambrian Basement Map Showing Geologic-Geophysical Domains, Wyoming. U.S. Geological Survey Open-File Report 2001-199, 2001, 199 p.

58. Skipp, B.; McGrew, L.W. The Maudlow and Sedan Formations of the Upper Cretaceous Livingston Group on the west edge of the Crazy Mountains Basin, Montana. (Contributions to stratigraphy), Geological Survey Bulletin 1422-B, 1977.

59. Smith, L.B.; Davies, G.R. Structurally controlled hydrothermal alteration of carbonate reservoirs: Introduction: *AAPG Bull*, **2006**, 90, 1635–1640.

60. Smith, L. B. Jr.; Eberli, G.P.; Sonnenfeld, M.D. Sequence stratigraphic and paleogeographic distribution of reservoir quality dolomite, Madison Formation, Wyoming and Montana. In *Integration of outcrop and modern analogues in reservoir modeling;* G. M. Grammer, G. P. Eberli, P. M. Harris, Eds.; *AAPG Memoir* **2004**, 80, 94–118.

61. Sonnenfeld, M.D. Sequence evolution and hierarchy within the Lower Mississippian Madison Limestone of Wyoming. In *Paleozoic Systems of the Rocky Mountain Region*; Longman, M.W., Sonnenfeld, M.D., Eds.; Society for Sedimentary Geology, Rocky Mountain Section, 1996, pp. 165-192.

62. Stone, D.S. Theory of Paleozoic oil and gas accumulation in Bighorn Basin, Wyoming. *AAPG Bull.* **1967**, 51, 10, 2056-2114.

63. Tucker, M. E.; Wright, V. P. Radiogenic isotopes. In *Carbonate sedimentology*; Tucker, M. E., Wright, P. V., Dickson, J. A. D., Eds.; Blackwell Science Publishing (GBR): Oxford, United Kingdom, 1990, 312 p.

64. Tucker, M. Techniques in Sedimentology, Blackwell Scientific Publications: Oxford, England, 1988, 408 p.

65. Van Gosen, B.S.; Wilson, A.B.; Hammarstrom J.M. *Mineral Resource Assessment of the Custer National Forest in the Pryor Mountains, Carbon County, South-Central Montana*. U.S. Geol. Surv. Open-File Report 96-256, 1996, 69 p.

66. Veizer, J.; Compston, W. 87Sr/86Sr composition of seawater during the Phanerozoic, *Geochim Cosmochim Acta*, **2004**, 38, 1461–1484.

67. Westphal, H., Eberli, G.P., Smith, L.B., Grammer, G.M., and Kislak, J., 2004, Reservoir characterization of the Mississippian Madison Formation, Wind River Basin, Wyoming. *AAPG Bull* **2004**, 88, 4, 405–432.

68. Warchola, R.J.; Stockton, T.J. *National Uranium Resource Evaluation, Billings Quadrangle, Montana. PGJ/F-015(82)*; Morris & Warchola, Inc., Bendix Field Engineering Corporation, U.S. Department of Energy: Grand Junction, CO, USA, 1982.

69. Wilson, C.W. Geology of the Nye-Bowler lineament, Stillwater and Carbon Counties, Montana: *AAPG Bull* **1936**, 20, 9, 1161-1188.

70. Wingate, L. Results for C and O isotope analysis of most of the carbonate samples from the study and provided methodology, University of Michigan Stable Isotope Laboratory, Ann Arbor, Michigan. Personal communication by e-mail, 2014.

71. Wooden, J.L.; Mueller, P.A. Pb, Sr, and Nd isotopic compositions of a suite of Late Archean, igneous rocks, eastern Beartooth Mountains: implications for crust-mantle evolution. *Earth Planet. Sci. Lett.* **1988**, 87, 59-72.

72. Wyoming State Geological Survey website, Oil and Gas map. Available online: http://www.wsgs.wyo.gov/products/wsgs-2016-ms-103.pdf (Accessed: 8 October, 2016).

CHAPTER 5

REE DATA SUPPORT OIL WITH A PERMIAN PHOSPHORIA FORMATION SOURCE AS A SOURCE OF METALS FOR U AND V MINERALIZATION IN THE NORTHERN BIGHORN BASIN

Contribution of Authors and Co-Authors

Manuscript in Chapter 5

Co-Author: Anita L. Moore-Nall

Contributions: primary author on paper.

Co-Author: Ranalda Tsosie

Contributions: Researched and did the chemistry for the silica polyamine composites; contributed to the manuscript.

Manuscript Information Page

Moore-Nall, A.L.; Tsosie, R.L.
Journal name: Minerals
Status of Manuscript:
__X_ Prepared for submission to a peer-reviewed journal
____ Officially submitted to a peer-review journal
____ Accepted by a peer-reviewed journal
___ Published in a peer-reviewed journal

Published by: MDPI AG, Basel, Switzerland
Submitted:

Abstract: Past productive abandoned U-V mines in the northern Bighorn Basin, Montana and Wyoming have a close association with hydrocarbons. Geochemical and mineralogical data support a Permian Phosphoria Formation source of metals for the deposits hosted in Mississippian Madison Limestone and paleokarst of the northern Bighorn Basin. The REE plus Y composition of Madison Limestone and limestone breccia hosted bitumen reflect similar patterns to both mineralized samples from this study and to U.S. Geological Survey rock samples from studies of the Phosphoria Formation. As, Hg, Mo, Pb, Tl, U, and Zn, often metals of environmental concern occur in high concentrations in Phosphoria Formation samples and were detected in anomalous concentrations in ore minerals analyzed from both mining districts. Maximum values of 1295 ppm As, 12.8 ppm Hg, 791 ppm Mo, 146 ppm Pb, 490 ppm Tl, 86,800 ppm U, and 2230 ppm Zn, were detected in mineralized samples from this study. Geochemical and field data were used to investigate past theories for mineralization of these deposits to determine if U present in home wells and Hg content of fish from rivers on the proximal Crow Indian Reservation may have been derived from these deposits or related to their mode of mineralization. Collaborative research related to U contaminated drinking water on the Navajo and Crow Indian reservations is being conducted at the University of Montana, University of New Mexico and Montana State University. Part of this research is developing silica polyamine composites to aid in removal of U and other toxic metals from contaminated drinking water.

Keywords: uranium; vanadium; As, Hg, Mo, Pb, Tl, Zn, REE; Permian Phosphoria Formation; abandoned mines; silica polyamine composites; SPC

1. Introduction

Uranium was discovered in the Pryor Mountains, Montana (MT) in September 1955 and several months later in the northern Bighorn Mountains, Wyoming (WY) [1-5]; subsequently, both U and V were mined. Mines produced U-V ore from underground operations in both the Pryor Mountain Mining District (PMD), MT and the Little Mountain Mining District (LMD), WY. Some mining was by open pit in the LMD [6]. Most production occurred 1955-1959, after the Atomic Energy Commission opened a U buying station in Riverton, WY [1]. This station closed in the mid 1960's [4]. Some mining continued until 1970 in the LMD [6] and until 1974 in the PMD [6]. The relatively small, high-grade (median grades of 0.26% U_3O_8, 0.23% V_2O_5) deposits in MT and WY combined, produced 133,810 kg triuranium octoxide (U_3O_8) and 106,594 kg of vanadium oxide (V_2O_5) during 1956-1964 [1]. The primary ore minerals in MT/WY are the Ca-uranyl vanadates tyuyamunite ($Ca(UO_2)_2(VO_4)_2 \cdot 5\text{-}8H_2O$) and metatyuyamunite ($Ca(UO_2)_2(VO_4)_2 \cdot 3\text{-}5H_2O$) [1,2,6-8].

The U.S. Bureau of Land Management reclaimed ten mines in the PMD in 2006 [9]. They removed ore for reprocessing and re-graded waste rock and overburden to discourage recreational use on the piles. Mine entrances were closed and some of them were fitted with bat gates to maintain bat populations [9]. The LMD is closed to the public for safety.

The LMD borders the SW corner of the Crow Reservation (outlined in red and black line) (Figure 5.1). The Bighorn River flows north through WY. It is superimposed across

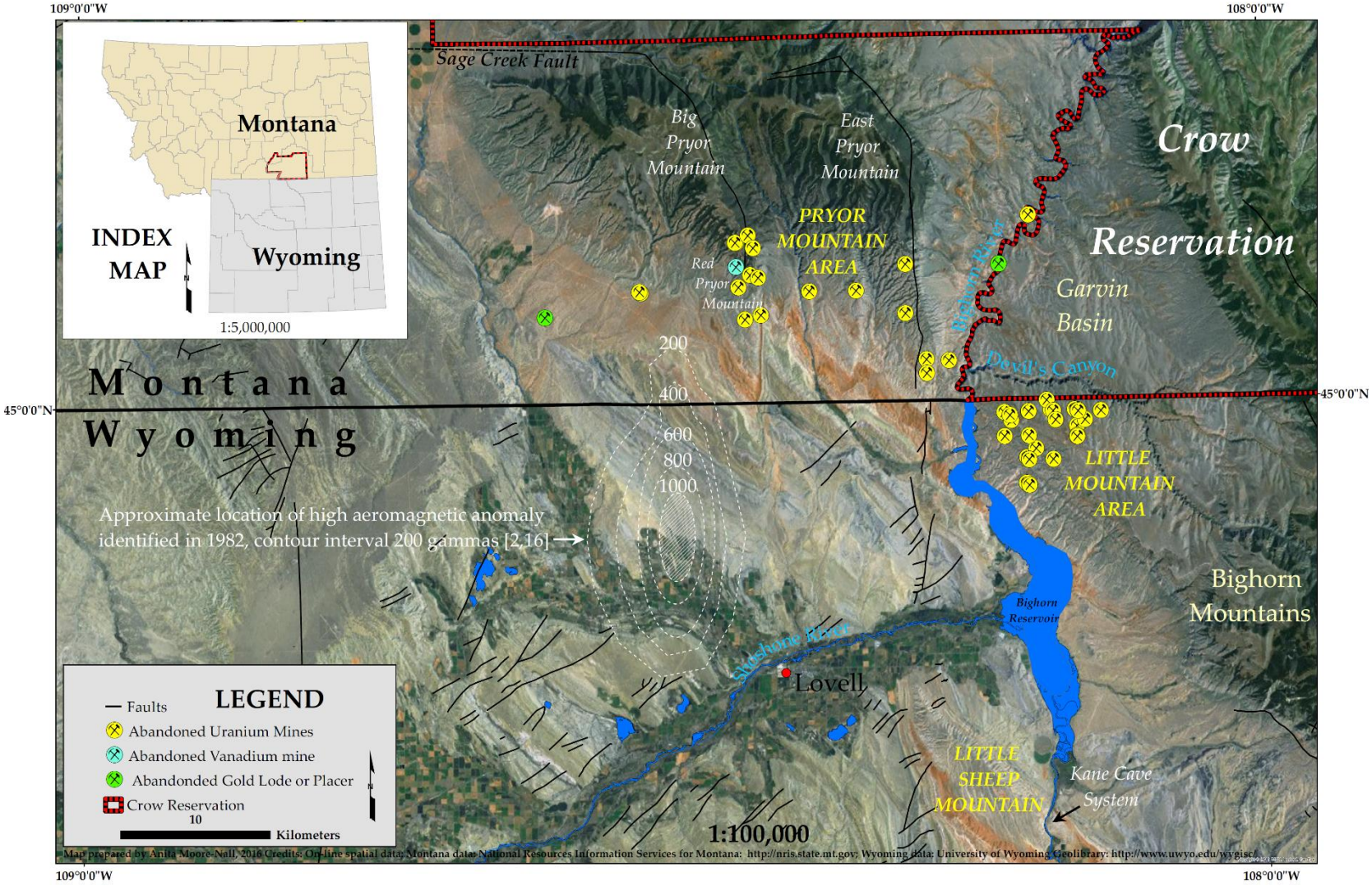


Figure 5.1. Map showing the location of the PMD, MT and the LMD, WY. Yellow symbols represent abandoned U-V mines. The Bighorn River flows N from WY , then NE through MT, there forming the SW border of the Crow Indian Reservation.

Little Sheep Mountain, WY, shown at the bottom of the map. The river then flows NE into MT, between the two mining districts, there forming the SW border of the Crow Indian Reservation. Approximate location of high aeromagnetic anomaly identified in 1982 [2] discussed later in the text, is shown to the southwest of Red Pryor Mountain. The green symbols represent abandoned gold deposits.

The impetus for this study was to test theories proposed for mineralization in the two districts. This was to see if U present in home wells on the Crow Reservation [10] and Hg detected in fish from the Bighorn Reservoir and from rivers of the Crow Reservation [11,12] might have been derived from erosion of or possibly related to the mode of mineralization of the deposits.

Also of interest, is Pb detected in the Bighorn River. In 1995, the Bighorn River was listed as a 303d impaired water body downstream of the Crow Indian Reservation due to elevated Pb and Hg [13]. It remains on the latest (July 2015) water quality integrated report submission to the U.S. Environmental Protection Agency for the State of MT and the source of contamination is unknown [13]. The Bighorn River and its tributaries drain both the PMD and LMD U-V districts.

1.1 Theories for Origin of Deposits

Several models have been proposed for the origin of the MT/WY U-V deposits. [1]. One model proposed that U-bearing meteoric water leached U from tuffaceous material or ash that once covered the region during the Tertiary [7], which was deposited in preexisting karst solution cavities. Other researchers suggested that the deposits occur along previous routes for major drainages of the Bighorn Basin [1,3]. Some workers

proposed that structurally controlled, ascending hydrothermal fluids were the source of the U and V based on identification of davidite [$(La,Ce)(Y,U,Fe)(Ti,Fe)_{20}(O,OH)_{38}$] a high temperature U-REE oxide mineral and associated fluorite [14,15].

The abundance of caves, especially in the LMD [7,16], may support a hypogenic karst origin with groundwater mixing. Support for this model is the nearby Kane Cave system in the Little Sheep Mountain anticline, WY. The Lower Kane cave, hosted in Mississippian-age Madison Group limestone in the core of the anticline, is actively forming by hypogenic sulfuric acid speleogenesis, at the level of the Bighorn River [17,18]. The cave contains radioactive mud and water with U, V, Pb, other metals, hydrogen sulfide gas, and a microbial community of Fe- and sulfate-reducing bacteria [17]. Gypsum ($CaSO_4 \cdot 2H_2O$), a product of limestone and sulfuric acid in the hypogenic sulfuric acid speleogenesis process [17,18], is associated with the U-V mineralization in both districts.

In 1982, a dozen years after mining ceased, the U.S. Department of Energy identified a N-S trending, 30 km long magnetic high anomaly located to the SW of the Big Pryor Mountain block [2,19]. The estimated depth of 3-3.6 km to the anomaly suggests the buried magnetic body occurs at or near the top of the Precambrian basement [2]. An inferred intrusion, a potential source of the magnetic anomaly (Figure 5.1), could provide ascending hydrothermal fluids and a heat source for the MT/WY deposits [1,16]. An intrusion may also account for the abandoned gold workings to the west of Big Pryor Mountain, Au detected in samples in this study (Appendix C, Table C1, Figure C1), and silicification in the PMD.

Potential V sources are the Permian Park City Formation (Phosphoria Formation equivalent in MT) [20-22] or V-rich, Phosphoria Formation-sourced oil from the Bighorn Basin [23,24].

This paper will present observations of hydrocarbons and bitumen in samples. REE and Y data from samples from this study, bitumen collected from the river cut at Little Sheep Mountain, and from Phosphoria Formation samples will be compared. Geochemical similarities of data from this study and to data from Phosphoria Formation samples will be presented to support a hydrothermal source of metals from the Bighorn Basin.

2. Study Areas

2.1 Physiography

The study area lies along the eastern side of the Middle Rocky Mountain Physiographic Province in the northeast margin of the Bighorn Basin. The study area includes the two mining districts and the river cut area of Little Sheep Mountain. The Bighorn Basin is a structural basin bounded by the Bighorn Mountains to the east, the Owl Creek/Bridger Mountains to the south, the Absaroka and Beartooth Mountains to the west and the Pryor Mountains to the north. The areal extent of the basin is approximately 25,900 km^2 within the outcrop of upper Cretaceous rock exposed in the basin [25-26]. Topographically the Pryor Mountains are moderately dissected block faulted mountains with gentle slopes and flat rolling plateaus of Mississippian-age limestone to the west and steep scarp slopes to the east [27]. The range rises to an approximate elevation of 2675 m

above sea level. The LMD, WY, is characterized by gently rolling tablelands immediately east of Bighorn Canyon and south of Devil's Canyon [27,28] (Figure 5.1). The area has an elevation of approximately 1500 m above sea level. Little Sheep Mountain has a similar elevation of approximately 1568 m above sea level. There are no incorporated towns in the area. Lovell, WY, is the closest town to the study areas.

2.2 Stratigraphy

Rocks in the region range from Archean to Quaternary in age (Figure 5.2). Approximately 760-915 m of Paleozoic rock overlie Archean gneiss and schist in the study areas [29]. The main formations of exposure relevant to the U-V deposits in the mining districts include limestones and dolomites of the Mississippian-age Madison Group (Madison Formation in WY), which host the U-V deposits.

Extensive regional paleokarst features at the top of the Madison Group locally host collapse breccia [30-31]. In this horizon, zones of brecciation are both discordant and concordant to bedding. The horizon is characterized by solution cavities along bedding planes, fractures and joints, and collapse breccia filled with angular limestone fragments of variable size (from several cm to several meters across) and reddish clay silt from the overlying Amsden Formation [2]. Red sandstones and shales of Mississippian-Pennsylvanian-age Amsden Formation disconformably overlie the Madison Group. Any of the three members of the Amsden Formation may be found directly overlying or filling in collapse features of the Madison Group in the northern Bighorn Basin (Figure 5.2B) [31]. The in filling with Amsden Formation imparts a red to purple matrix to many of the

breccia units. The U-V deposits of both mining districts occur in the top 60-75 m of the paleokarst horizon [1,2,6,7].

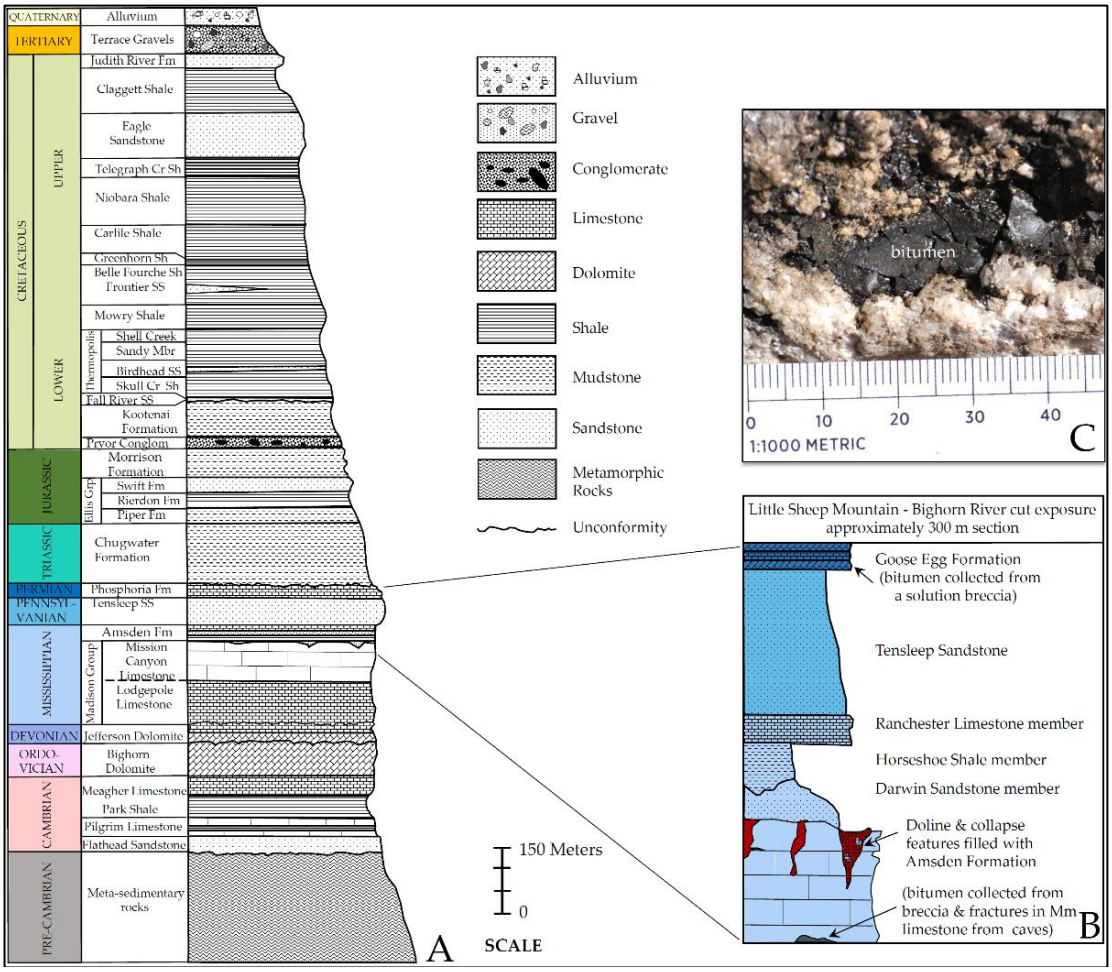


Figure 5.2. (A) Generalized stratigraphic column of the Pryor Mountain area, MT, modified from Lopez, 1995 [28]. (B) Generalized stratigraphic column of the river cut exposure in Little Sheep Mountain anticline is shown to the right with arrows indicating stratigraphic position of bitumen collection sites for this study. (C) Bitumen collected in Mm limestone breccia from upper Kane Cave, Little Sheep Mountain, WY.

In the PMD the Permian Phosphoria and Pennsylvanian Tensleep Sandstone formations were eroded from the top of Big Pryor Mountain leaving Madison Group as the most prominent rocks exposed on the anticlines. In the Little Sheep Mountain

anticline south of both U-V mining districts these formations are preserved. Bitumen was collected for this study from fractures in Madison Group limestone and limestone breccia from two caves and from a solution breccia in Permian Goose Egg Formation limestone exposed in a river cut in the Little Sheep Mountain anticline (Figures 5.2B and 5.2C).

2.3 Structural Setting

During the Laramide Orogeny (80-35 Ma), the central Rocky Mountain region experienced a general NE-SW (40°- 55°) transpressional strain regime as a result of the low-angle subduction of the Farallon plate at its western continental margin [32,33]. Beginning in the late Cretaceous, Laramide shortening was accommodated by uplift of broad basement arches that eventually isolated the Bighorn Basin (Figure 5.3) [34]. The Bighorn Basin has a generally NW-SE sinuous axis [26]. Smaller scale folds in the form of anticlines and synclines formed along the basin margins and served to accommodate regional shortening [34-36]. These folds host most of the oil fields of the Bighorn Basin [37]. The structures hosting the U-V mining districts and the Little Sheep Mountain anticline are all folds created during this time and were likely structural traps for oil until they were breached. Estimates of present-day maximum burial of the Madison Group at the basin center are 6-7 km and 5-6 km near the basin flanks [34,36]. Structurally the Pryor Mountains are divided into N and S segments by the Sage Creek fault zone, the eastern extension of the Nye-Bowler lineament. The lineament is interpreted to be the expression of a left-lateral wrench fault at depth and defines the northern end of the Bighorn Basin [38-39]. The Lake Basin Fault zone is a similar feature to the north. The U-V deposits in the PMD occur in the southern portion of the Pryor Mountains, MT.

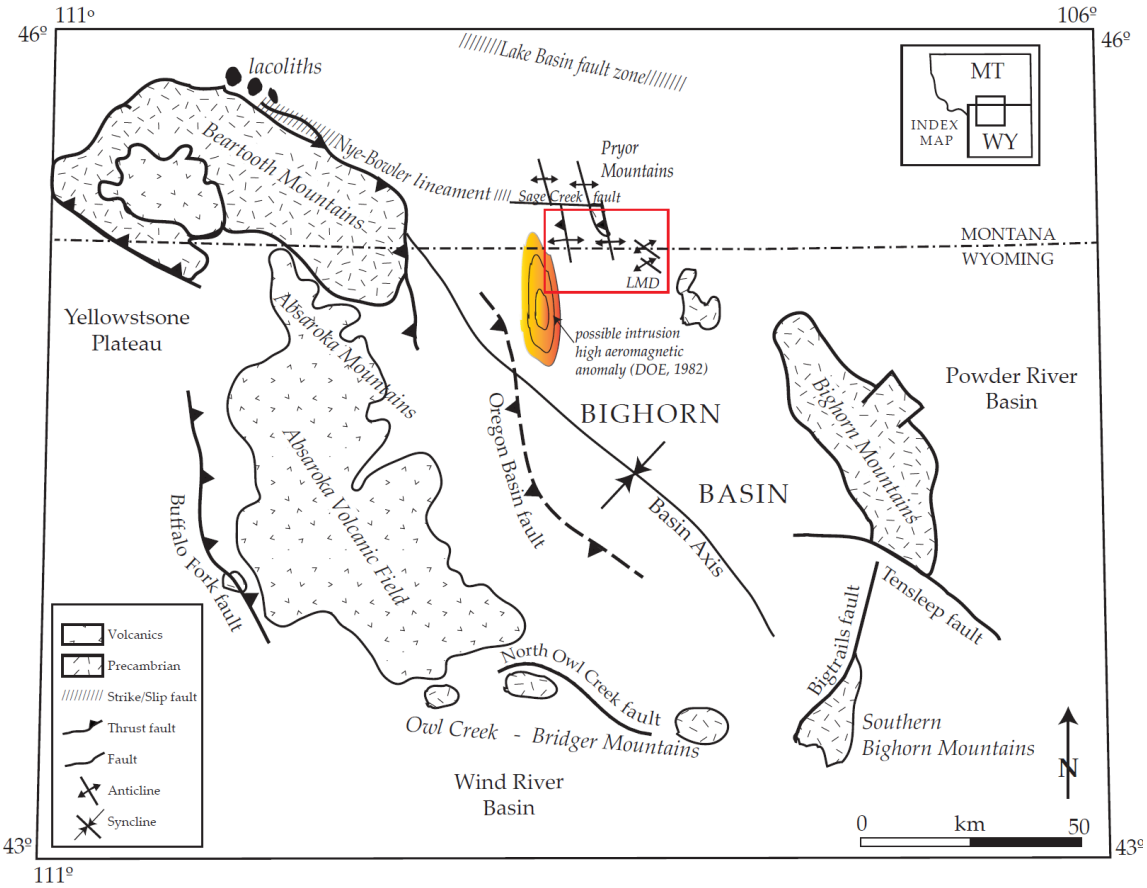


Figure 5.3. Map showing the tectonic features of the Bighorn Basin. Precambrian cored arches and volcanics are represented by stipled patterns. The Lake Basin fault zone, volcanic domes (lacoliths) of the Nye-Bowler lineament, Sage Creek fault zone are shown in the top portion of the figure. The location of the mining districts is outlined by the red rectangle. Map modified from Blackstone [26] and Stahl [40].

2. 4 Mineralization and Alteration

Mineralization is concentrated in Madison Group collapse paleokarst breccia and limestone in both mining districts. The main difference in the ore of the two districts is the silica content. The silica content of the PMD was high and the LMD was low [1,5,10]. The U-V ore minerals of MT/WY are easy to recognize in outcrop due to their bright yellow color (Figure 5.4A-5.4G).

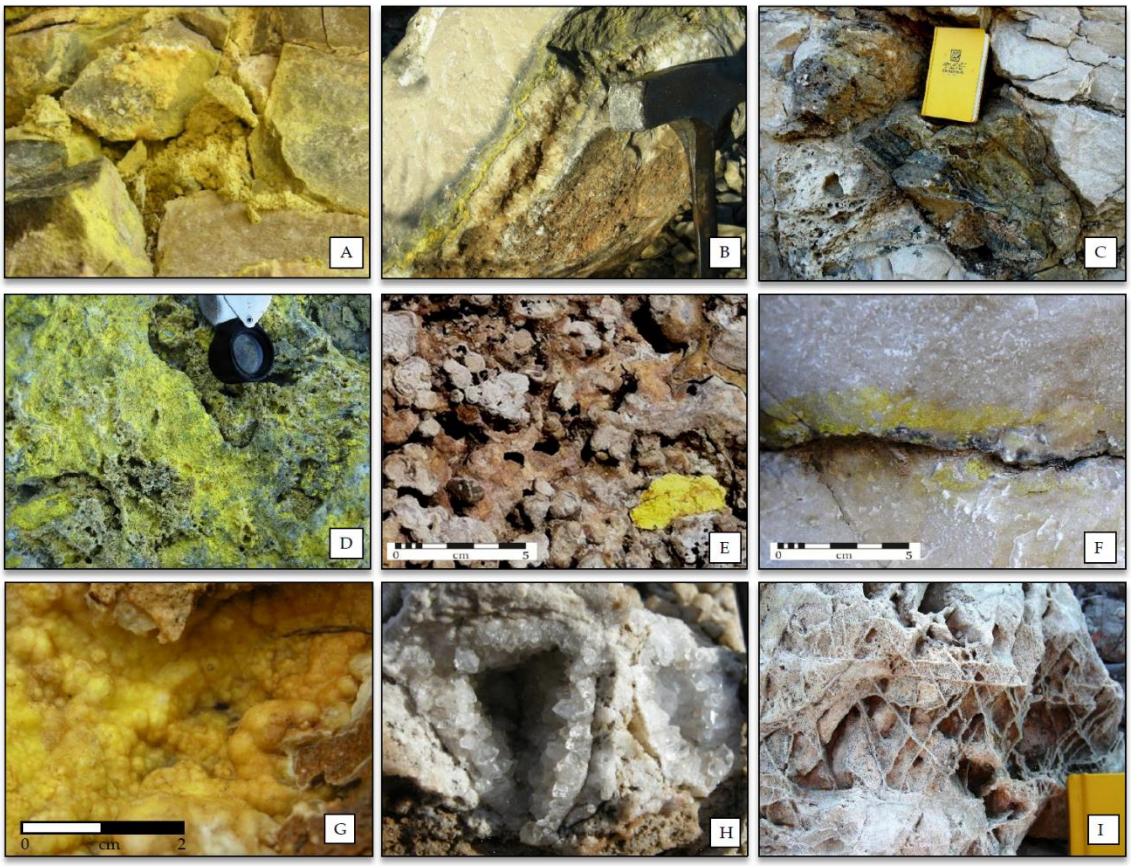


Figure 5.4. Outcrop photos of U-V mineral occurrences and boxwork the MT/WY deposits: (A) Silt-size and powdery coatings, PMD (B) Boulder with U-V minerals lining fractures filled with calcite, LMD (C) Fracture hosted tectonic hydrothermal breccia with boxwork formed in host limestone, LMD (D) Calcite cemented surface coatings, LMD (E) Cave floor type occurrence, PMD (F) U-V minerals along sprung stylolites, PMD. (G) Silica and U minerals coating breccia clasts, PMD; (H) Quartz-lined boxwork, PMD; and (I) Systematic fractures preserved as boxwork, LMD.

Some U-V minerals are still forming. Liebigite ($Ca_2(CO_3)_3 \cdot 11H_2O$), a triuranium carbonate mineral, was observed in other studies of the PMD [2]. Because U^{6+} is very mobile in water, it is likely that triuranium carbonate minerals, which are generally the most soluble [41], are being dissolved in the deposits. As surface water percolates through the deposits these minerals are likely dissolved and reprecipitated as the relatively insoluble metal-uranyl vanadates when encountering a V source such as

material from sprung stylolites (Figure 5.4F). U minerals are also present on the surfaces of burned wooden supports of some worked prospects in the PMD, indicating on-going mineral precipitation.

Abundant silica observed in the PMD is concentrated in and around siliceous tectonic hydrothermal breccias. These were emplaced in fractures along the crest of the Gypsum Creek anticline which forms the southern portion of the Big Pryor Mountain block (Figure 1). The literature describes silica being most pervasive along relict cavern floors and walls in the PMD [3]. Authors described breccia fragments coated with tyuyamunite and metatyuyamunite that were subsequently coated by dense microcrystalline quartz [3]. Underground workings are no longer accessible so this was not observed in this study although breccia clasts coated with mammillary quartz and U minerals and quartz lined boxwork were observed (Figure 5G-5I). Boxwork is common in both districts. At many of the deposits, the host rock appears fresh and unaltered within a few feet of the mineralization. The wallrock in the PMD has the most alteration of the three areas studied including bleaching, liesegang banding, silicification, hematite-, and limonite-staining.

2.5 Tectonic Hydrothermal Breccias, PMD

Siliceous tectonic hydrothermal breccias only observed in the PMD, are relatively small, 0.5 to 5 m wide, hematite- and limonite-stained dike-like features (Figure 5.5A). The tectonic breccias were determined to be hydrothermal by stable C, O and radiogenic Sr data [42]. Although bleaching does not extend far from the tectonic hydrothermal

breccias, the wall rock is generally bleached where the breccias cut through. Wallrock around some of the features is liesegang banded (Figure 5.5B).

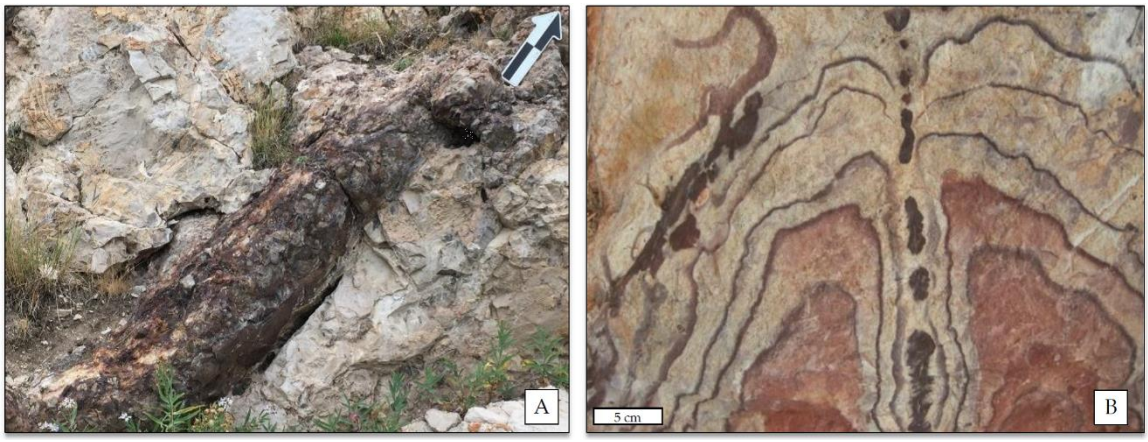


Figure 5.5. (A) Mineralized hematite- and limonite-stained, silicified tectonic hydrothermal breccia cuts through bleached collapse paleokarst breccia along a fracture, Sandra mine area, PMD, 20 cm arrow for scale (B) Liesegang banding developed in lower Amsden Formation adjacent to the Old Glory mine, PMD.

The matrices of the tectonic hydrothermal breccias are composed of cryptocrystalline silica and local microscopic Fe-oxide inclusions. The tectonic hydrothermal breccias in the mineralized zone have clasts of Madison Group and Amsden Formation. Both unmineralized and mineralized tectonic hydrothermal breccias have barite, local fluorite, minor oxides, and sulfides along fracture surfaces and in vugs. The mineralized tectonic hydrothermal breccias have U-V minerals filling in vugs and fractures in addition to the other minerals.

3. METHODS

3.1 Field work

Samples were chosen to test theories proposed for the origin of these deposits. A Thermo Scientific™ RadEye™ Personal Radiation Detector was used to identify elevated radiation sources in the study area. Rock samples included breccia clasts and matrix samples, altered and unaltered host rock, generations of cements from veins, and mineralized samples from dumps and outcrops. A bentonite sample was collected from an operating bentonite mine approximately 20 km southeast of the LMD to use to test the theory that U leached from volcanic ash that once covered the region. Dried bitumen was collected from fractures in Mississippian Madison Group limestone and limestone breccia in two caves as well as from fractures in a limestone solution breccia in the Permian Goose Egg Formation exposed in the river cut of Little Sheep Mountain (Figure 1). The bitumen samples were collected to compare the REE and Y composition of our U-V mineralized samples for an association between oil in the brines from the BHB and hydrothermal mineralization. Two speleothem calcite samples from Big Pryor Mountain were collected to compare REE and assay analyses with calcite cement of breccia samples and calcite fracture fill to test the meteoric theory.

3.2 Mineralogical and Geochemical Characterization

Work performed to complete analyses in the study areas included: standard petrography, cathodoluminescence (CL), scanning electron microscopy (SEM) utilizing energy dispersive x-ray spectrometry (EDS) and backscatter electron imaging (BSE),

powder x-ray diffraction (XRD) spectroscopy and minor fluid inclusion work. Most of the analytical work was performed using instrumentation in the Imaging and Chemical Analysis Laboratory (ICAL) facility at Montana State University (MSU) in Bozeman, MT. XRD work was performed on a SCINTAG X1 Diffraction Spectrometer and computer-aided mineral identification system at ICAL. SEM work was conducted at ICAL using a JEOL JSM-6100. CL was performed at the Department of Earth Sciences, MSU using a RELIOTRON CL luminoscope instrument attached to a Nikon microscope.

Assays were performed by two different commercial laboratories: American Analytical Services (AAS) Inc., in Osborn, Idaho and an Australian Laboratory Services (ALS) Global branch out of Reno, Nevada. Data from the commercial labs is shown in Appendix C.

3.2.1 Sample Preparation

Samples were prepared for chemical assay and REE analyses at MSU. Most samples were broken into chips and then pulverized in a Plattner's diamond mortar and pestle set while a few required micro drilling with a diamond tipped dremel bit. Some of the samples for REE analysis were pulverized in a shatter box. The mineralized U-V breccias were selected to try to get mainly the yellow U-V minerals, samples included part of the breccia host as the U-V minerals were disseminated throughout the samples. Fluorite was microdrilled. Barite was collected as individual crystals in the field and pulverized at MSU. Thin sections and some hand samples were stained for carbonate identification using a mixture of alizarin red and potassium cyanide solution [43].

4. Results, Mineralogy and Geochemistry

Samples examined by multiple methods revealed the episodic nature of mineralization in both districts. Bitumen was observed at all scales in this study; in outcrop along fractures and bedding planes, petrographically in interparticle porosity, and as inclusions in cement and minerals. Oxides, hydroxides and sulfides were closely associated with U-V minerals in both districts. The white card petrographic method, placing a piece of white paper beneath a petrographic slide, differentiated bitumen from sulfides and oxides [44]. It was also useful for viewing U-V minerals. CL revealed zoning in carbonates, fluorites, and highlighted U-V minerals and Fe-V oxides. The EDS and BSE modes of the SEM revealed compositional variations in minerals. The Secondary Electron Image (SEI) mode of the SEM aided in viewing morphology of minerals with the same composition. BSE mode discriminates between different phases as a function of the mean atomic number (Z) [45]. Minerals with larger Z appear brighter than minerals with smaller Z. This mode was useful for seeing zonation in some of the sulfides and for identifying elements present in minerals. Some results are presented in figures in Appendix C.

4.1 Mineralogy: Ore and Gangue Minerals

4.1.1 Ore Minerals

Ore and gangue minerals reported in the literature and new minerals identified in this study are shown in Table 5.1. The primary ore minerals in the two districts are metal-uranyl vanadate minerals. Tyuyamunite ($Ca(UO_2)_2(VO_4)_2 \cdot 5\text{-}8H_2O$) and metatyuyamunite

($Ca(UO_2)_2(VO_4)_2 \cdot 3\text{-}5H_2O$), Ca-uranyl vanadates, which have been reported in the literature, were confirmed in both districts in this study by XRD and EDS. These minerals are the only U minerals observed or previously described in the LMD.

Ore minerals reported in the districts *PMD only			
uranyl-vanadates		uranyl (silicate , carbonate, phosphate)	
metatyuyamunite $Ca(UO_2)_2(VO_4)_2 \cdot 3\text{-}5H_2$	[1,2,3,6,7,14]	*uranophane $Ca(UO_2)_2Si_2O_7 \cdot 6H_2O$	[1,2]
tyuyamunite $Ca(UO_2)_2(VO_4)_2 \cdot 5\text{-}8H_2O$	[1,2,3,6,7,14]	*green liebigite $Ca_2(UO_2)(CO_3)_3 \cdot 11H_2O$	[2]
*francevillite $Ba(UO_2)_2(VO_4)_2 \cdot 5H_2O$	[this study]	*autunite $Ca(UO_2)_2(PO_4)_2 \cdot 10\text{-}12H_2O$	[2]
*francevillite $(Ba,Pb)(UO_2)_2(VO_4)_2 \cdot 5H_2O$	[this study 46]	Crichtonite Group	
*carnotite $K_2(UO_2)_2(VO_4)_2 \cdot 3H_2O$	[this study]	*davidite $(Fe^{+2},La, U, Ca)_6 (Ti,Fe^{+3})_{15}(O,OH)_{36}$	[14]
*Unidentified thallium uranyl-vanadates	[this study]		
Gangue minerals reported in the districts [1] *PMD only [1,2,4,14-15]			
hematite	iron-oxides	green radioactive calcite	*celestite
limonite	iron-hydroxides	dogtooth calcite	*dark purple fluorite
pyrite	clay minerals	dolomite	*golden and white barite
marcasite	gypsum	quartz	*opal
Gange minerals identified in this study *PMD only			
*witherite $BaCO_3$	*halloysite $Al_2(Si_2O_5)(OH)_4$	saddle dolomite	herkimer style quartz
pyrobitumen and or bitumen found as inclusions in minerals and coating fractures and bedding plane [this study]			

Table 5.1. Ore and gangue minerals reported in the literature and identified in this study for the Pryor Mountain and Little Mountain mining districts of Montana and Wyoming.

Two mineral phases of metal-uranyl vanadates in the Curienite-Francevillite Series ($Pb(UO_2)_2(VO_4)_2 \cdot 5H_2O$ to $Ba(UO_2)_2(VO_4)_2 \cdot 5H_2O$) [46] were identified by XRD and EDS in the PMD in this study [47]. These minerals are francevillites with varying amounts of Ba and Pb. Carnotite ($K_2(UO_2)_2(VO_4)_2 \cdot 3H_2O$), a K-uranyl vanadate, was identified by EDS in this study (Figure C2). Carnotite, occurs locally as 2-10 µm grains in dark purple fluorite (Figure C3). EDS detected thallium (Tl) in an unidentified uranyl vanadate from a prospect site, in the PMD (Figure C4). A mineral with the same morphology was found with tyuyamunite from the Dandy mine, which had the highest Tl

(490 ppm) concentration of the study in analyses performed by ALS (Appendix C, Table C2). The only Tl-uranyl vanadate found in Mindat.org is thallian carnotite $(K,Tl)_2(UO_2)_2[VO_4]_2 \cdot 3H_2O$ [48]. This mineral did not contain K. The mineral may represent a mineral phase of the Curienite-Francevillite Series. It may be a Tl-bearing phase of curientite, with Tl substituting for some of the Pb because Tl and Pb have similar atomic and covalent radii: Tl (1.71.6 Å and 1.45 +/- 7 Å) and Pb (1.75 Å and 1.46 +/- 5 Å) [49]. EDS detected Tl in another Tl-bearing uranyl vanadate from a sample collected from a stockpile area near the Dandy mine (Figure C5). The weight percent of the elements are similar to francevillite; the mineral may be a Tl-bearing francevillite with Tl substituting for Pb.

Minerals were cross-referenced with information in the volume *Reviews in Mineralogy, Uranium: Mineralogy, Geochemistry and the Environment* [50] and internet sources such as Mindat.org, handbookofmineralogy.org, rruff.info and webmineral.com. The U-V minerals locally occur together. In the mines that have abundant barite, the Ba phase followed by the (Ba,Pb) phase, then the (Ba,Tl) phase of francevillite occur together with metatyuyamunite and tyuyamunite in the deposits and probably reflect the changes in available metals in the fluids sourcing the deposits. Carnotite is found only in trace amounts with fluorite. Metatyuyamunite and tyuyamunite represent approximately 80-90% of the U-V minerals in the PMD and are the only U-V minerals indentified in the LMD. The Tl-bearing uranyl vanadates have similar morphologies to the francevillites observed in this study. The morphologies of some of the metal-uranyl vanadates observed in this study are shown in Figure 5.6.

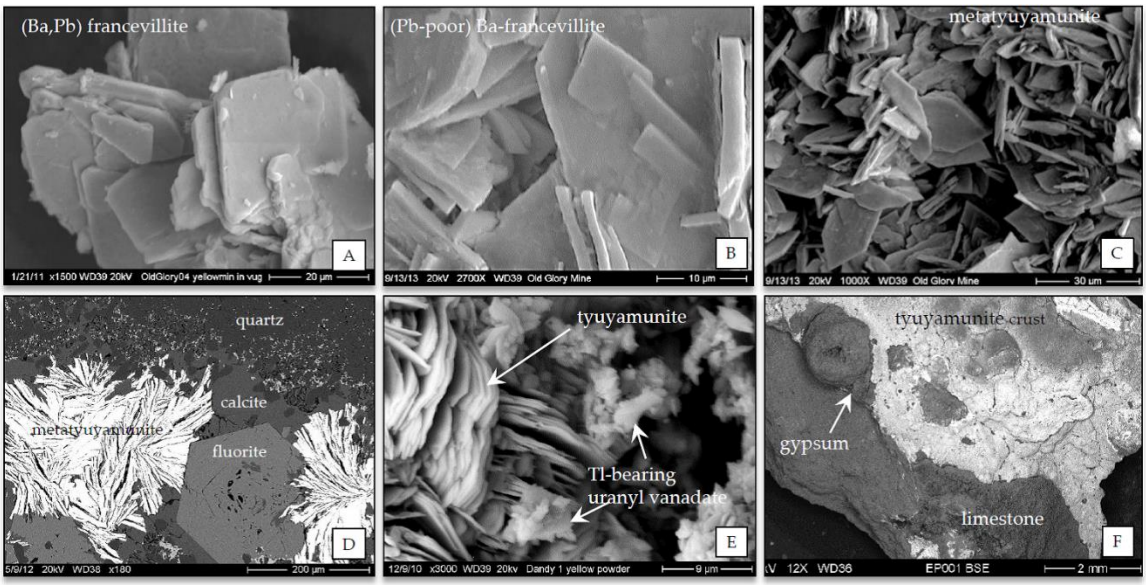


Figure 5.6. (A) (Ba,Pb) francevillite, Old Glory mine, SEI, 1500x magnification. (B) Ba francevillite, Old Glory mine, SEI, 2700x mag. (C) Metatyuyamunite, Old Glory mine, SEI, 1000x magnification. (D) Metatyuyamunite with fluorite intergrown, with late calcite filling in porosity in a vug of a silicified breccia, Old Glory mine, BSE, 180x magnification. (E) Tyuyamunite (left) and unidentified Tl-uranyl vanadate mineral, Dandy mine, SEI, 3000x magnification. (F) Cavern type deposit, tyuyamunite coating limestone with secondary gypsum, BSE, 12x magnification.

5.1.2 Gangue Minerals Associated with Hydrothermal Dolomitization

Tectonic hydrothermal brecciation with associated hydrothermal dolomite [51] and calcite has been documented in the Madison Group in the Bighorn Basin and nearby Wind River Basin [52-56]. Gangue minerals in both deposits associated with hydrothermal dolomitization include sulfides, oxides, hydroxides, hydothermal “saddle” dolomite [57], and herkimer style, double terminated, quartz [58]. Pyrobitumen and bitumen, though not minerals, are also associated with hydrothermal dolomitization and are included in Table 1 having been observed in this study. Fluorite and barite, only observed in the PMD, are also associated with hydrothermal dolomitization [50]. Other

gangue minerals in the PMD that may have hydrothermal origins are halloysite and witherite, identified by XRD and EDS in this study [59,60].

5.1.3 Bitumen, Sulfides, FeV Oxides, and Vugs

Bitumen lines clasts, fills interparticle porosity, and is found as inclusions in samples (Figure 5.7A-5.7E). Bitumen is often a product of water biodegradation of hydrocarbons. “Water washing” of a hydrocarbon reservoir invaded with water likely mobilizes metals. The minerals present in vugs and along fractures may have formed after oxygenated fluids were introduced to the system once the structures were breached. For example, Fe-sulfides (pyrite and marcasite) containing variable trace elements are found in the interparticle porosity or in fractures (Figure 5.7F-5.7H). Round pyrobitumen preserved in late-stage calcite (Figure 5.7E) may serve as an analogue for spherical shaped vugs found in cements of both districts. Vugs likely formed after hydrocarbon or volatiles were released or possibly dissolved in other episodes of fluid migration. Spherical vugs with sulfides (Figure 5.7F), barite, clay coatings (Figure 5.7I-5.7J), witherite, fluorite, Fe-V oxides (Figure 5.7I-5.7N), or a combination of these minerals are found in samples from the PMD. In mineralized silicified tectonic hydrothermal breccia of the PMD, vugs lined with Fe-V oxides often have U-V minerals in the centers surrounded by bleached quartz rims (Figure 5.7M). Spherical, cubic, and hexagonal vugs are present in quartz cements of breccia in the PMD (Figure 5.7F, 5.7I, 5.7K, 5.7L). The cubic and hexagonal minerals were likely oxides possibly magnetite, apatite, or barite, based on petrography and SEM; no sulfides were observed in the matrix only in fractures.

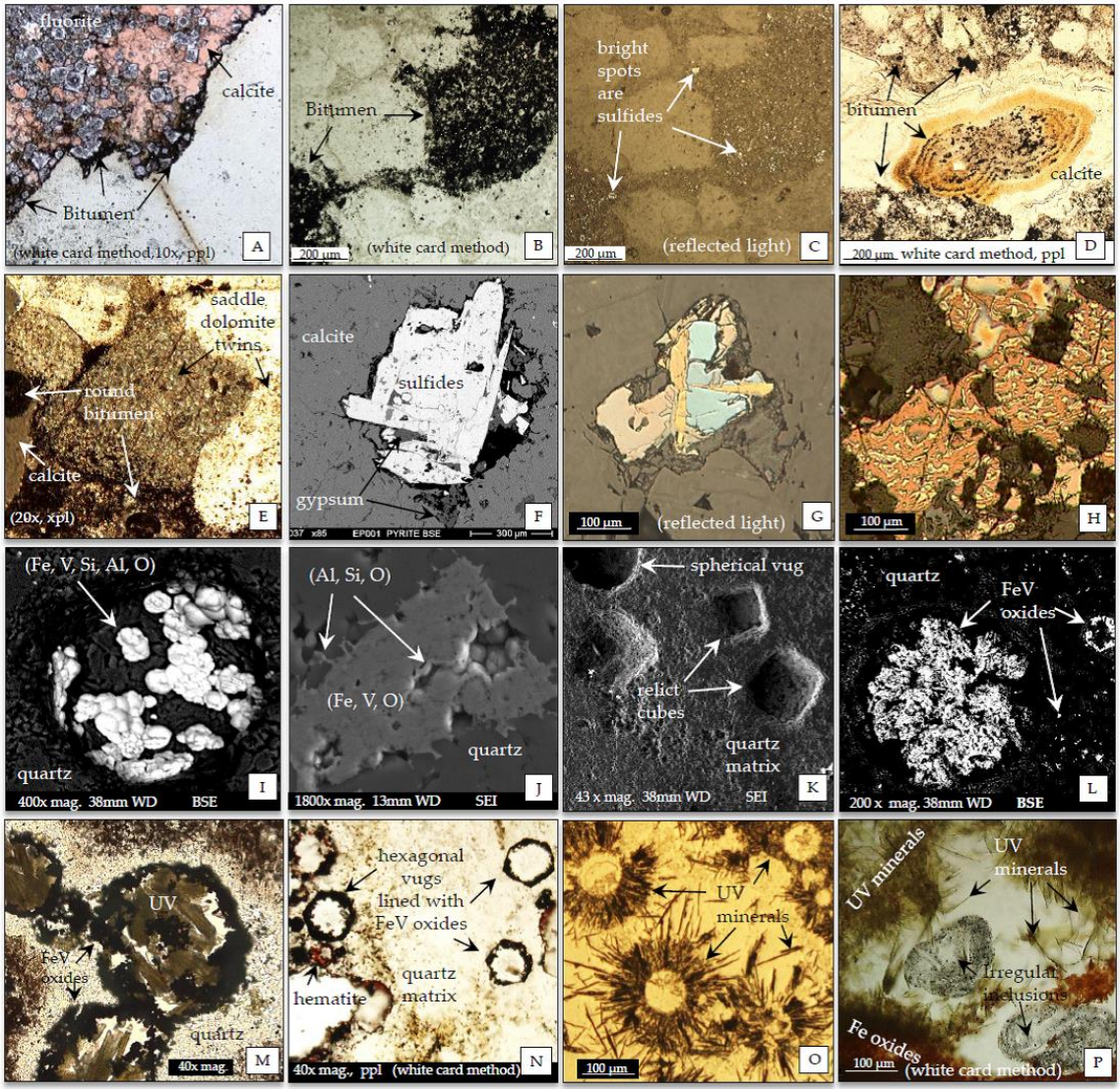


Figure 5.7. Images of bitumen and vugs: (A) bitumen lining clast of silicified limestone. Red stained calcite fills in porosity of oolites metasomically replaced by fluorite, Dandy mine, PMD, ppl. (B) Bitumen filled in porosity of East Pryor mine breccia, ppl, white card method (C) Sulfides appear bright in reflected light view of B. (D) Calcite filling in fracture with bitumen inclusion "bleeding" out in concentric rings, Dandy mine, PMD, ppl, white card method. (E) Round bitumen is preserved in late-stage calcite of breccia and saddle dolomite twins show up in xpl., 20x mag, E. Pryor Mountain Group, PMD. (F) Sulfides and gypsum formed in round vug, E. Pryor mine, PMD, BSE, 85x mag. (G) Isotropic Fe-sulfides in reflected light; four different isotropic minerals are shown in this view, blue may be Ni-bearing pyrite and pinkish brown may be bornite Cu_5FeS_4, E. Pryor mine, ppl (H) Two isotropic Fe-sulfides in reflected light exhibiting myrmekite texture, pyrite may be the yellow mineral, E. Pryor mine, ppl (I) Fe-V oxides with clay mineral coating, BSE, 100x mag. (J) Another portion of sample in 10I shows Fe-V oxides with clay mineral coating, 1800x mag., SEI (K) Spherical and cubic shaped vugs in quartz

matrix, Old Glory mine, SEI, 43x mag. (L) BSE of K, microscopic Fe-V oxides visible in large vug, lining smaller vug and between microcrystalline quartz crystals, 200x mag. (M) Tyuyamunite or metatyuyamunite crystals in FeV oxide lined, bleached circular vugs (N) Clear quartz matrix with hexagonal FeV oxide rimmed vugs and red hematite along edge, Old Glory mine, PMD, ppl, 40x mag., white card method. (O) Spherical and cubic shaped vugs in quartz matrix, Old Glory mine, SEI, 42x mag. (P) Tyuyamunite or metatyuyamunite crystals radiating out from circular vugs in fracture appear dark due to Ir coating on slide used for SEM work, LMD, ppl, white card method.

In the LMD, tyuyamunite or metatyuyamunite crystals that radiate from round vugs in calcite cements are closely associated with Fe-oxides and or Fe-hydroxides (Figure 5.7O). Irregular shaped inclusions were observed in calcite cement from LMD samples. Some of the inclusions had U-V minerals growing into them (Figure 5.7P); these were closely associated with Fe-oxides or Fe-hydroxides.

Fe-V oxides, identified by EDS (Figures C6-C9) in samples are found in association with bitumen. EDS spectra of the Fe-V oxides show a high percentage of Fe which varies from around 32% to 70% weight percent. The EDS spectra from the PMD samples also show moderately strong V, Si, Al, O, and no S peaks, suggesting that the metals are iron oxides (magnetite, goethite, or hematite) coated with silicate minerals (probably clays). Zn was detected in Fe-V oxide samples from the LMD (Figure B9). The Fe-V oxides may represent an isomorphous substitution of trace elements with Fe-oxides and hydroxides rather than a specific mineral phase. Using EDS, Zn , Cu, and Ni were detected in a mineral from the East Pryor mine area (Figure C10) likely reflecting metals derived from hydrocarbons based on chemical analyses of the bitumen from this study (Table C2).

4.2 Cathodoluminescence

CL revealed the episodic nature of calcite and fluorite formation. It highlighted U-V minerals and Fe-V oxides showing the close relationship of bitumen or hydrocarbons in the samples. The UV minerals and Fe-V oxides fluoresce bright green due to V; these minerals occur along fractures and interparticle pore space (Figure 5.8A). REE are common activators in fluorite [61,62]. A strong blue CL signal is generally attributed to the LREE fraction, with Eu^{2+}, Sm^{3+}, and Dy^{3+}, serving as the main activators [61] while

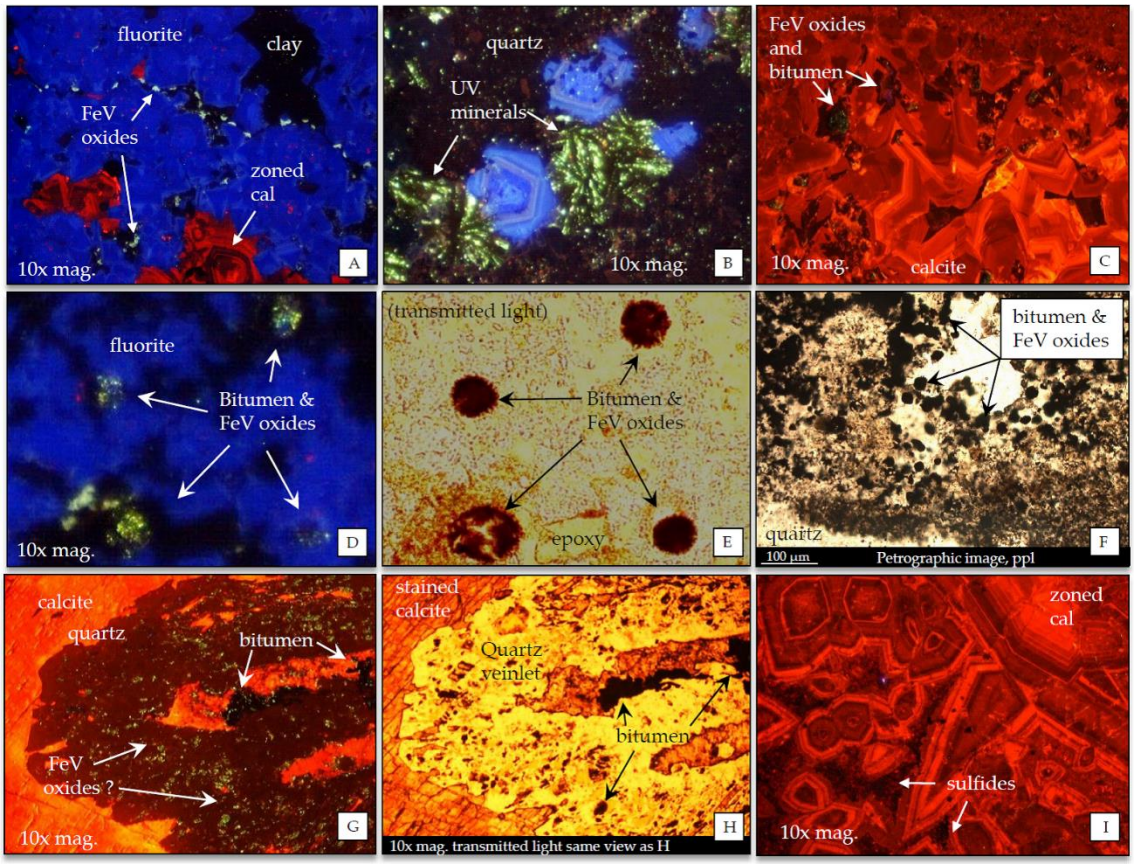


Figure 5.8. CL images of samples from the Pryor Mountain district. (A) Blue fluorite with zoned calcite and Fe-rich clay coating calcite filling in the porosity. Green luminescing Fe-V oxides follow fracture and occupy pore space, Marie mine, PMD. (B) U-V minerals luminesce bright green with hexaoctahedral blue and lilac zoned fluorite in

vug of a silicified breccia from the Old Glory mine. (C) Zoned calcite with bitumen and FeV oxides filling in the porosity, Lisbon mine, LMD (D) Fluorite and with Fe-V oxides and bitumen spheres, Marie mine, PMD (E) Transmitted light view of D. (F) Spheres of bitumen and Fe-V oxides in quartz, Old Glory mine, PMD (G) Corroded quartz veinlet filled in by calcite and bitumen. Fe-V oxides luminesce green in the bitumen. (H) Quartz appears white and bitumen black in the transmitted light view of G. (I) Zoned calcite. Sulfides appear black in the pore space between calcite crystals.

Dy^{3+} and Tb^{3+} are usually the activators in HREE environments, which impart a lilac color [61]. Hexaoctahedral fluorite from the Old Glory mine, PMD, alternates between blue and lilac colored zones (Figure 5.8B). Spheres of Fe-V oxides fluoresce green in the interparticle porosity of calcite and fluorite (Figure 5.8C-5.8D). In transmitted, plane polarized light, the spheres are clearly visible in the same view of Figure 4.8D and in a standard petrographic image in quartz (Figure 5.8E). Luminescence in carbonates is generally due to Mn^{2+} in the crystal and quenching by Fe^{2+} [63]. The calcite cements from this study fluoresce bright red orange alternating with dark zones, which is indicative of episodic Fe-rich hydrothermal sourced fluids [64]. REE-activated luminescence in sedimentary calcite is much lower than hydrothermal influenced carbonates, which often crystalize from REE-enriched solutions [63,64]. A corroded and fractured quartz veinlet from the Marie mine, PMD, reflects episodic fluid interactions. Calcite and bitumen filled in the pore spaces of the quartz veinlet. Inclusions in the bitumen along the edges of the quartz luminesce green, likely indicating V content (Figure 5.8G). In transmitted light view of the same image the quartz appears white (Figure 5.8H). Sulfides are also common in the interparticle porosity of calcite and

dolomite breccia in both mining districts and also in fluorite in the PMD. The sulfides appear black in Cl images (Figure 5.8I).

5.3 *Fluid Inclusions*

Fluid inclusions in several samples from the PMD were analyzed by FLUID INC., Denver, Colorado. A barite sample from the Swamp Frog mine contained yellow fluorescing primary inclusions; these were too small to study. Hydrocarbon (HC) inclusions are usually yellow and usually imply some sort of low API gravity [65] e.g. relatively heavy liquids - consistent with the HCs generated from Phosphoria source rocks for oil of the Bighorn Basin [66]. Jim Reynolds (pers. comm.) noted that the quartz and fluorite he examined from our study area appeared hydrothermal in origin, typical of what he observes in low-temperature (<200°C) epithermal systems. The quartz and fluorite samples with H_2O fluid inclusion assemblages had highly variable liquid to vapor ratios due to necking and were too small to obtain reliable homogenization temperatures. This is typical for low-temperature quartz in hydrothermal environments, because of the short-lived pulses of warm fluids, there is not enough geological time for maturation of the inclusions at low (<200°C) temperatures [66].

5.4 REE and Geochemical Assay Data

5.4.1 Rare Earth Elements REE Plus Y

Spidergram plots of REE plus Y normalized to NASC (North American Shale Composite) were produced from the data (Figure 5.9) using the values of Gromet et al.,

1984 [67]. Plots were split up by similar REE plus Y patterns. The data from the bitumen, bentonite, and the average upper continental crust [68] are plotted together (Figure 5.9A). This plot shows the bitumen have a low concentration of REE compared to the average continental crust and the bentonite.

Most of the patterns plotted from the data of mineralized and gangue minerals resemble portions of the bitumen patterns. The bentonite sample data plotted with the bitumen and average crustal abundance data, has a negative Eu anomaly. This likely reflects its volcanic origin when plotted normalized to shale. The Permian Goose Egg hosted bitumen differs from the Mississippian Madison Group hosted bitumen. It has lower REE concentration, no Eu, no Lu, and a flatter, irregular HREE and Y pattern. Many of the patterns from the samples in this study reflect portions of the Mississippian Madison Group hosted bitumen patterns (Figures 5.9B-E). These patterns were split up based on the steepness of the LREE patterns and similar patterns to each other.

Some samples from both districts have patterns similar to both the Permian Goose Egg hosted and Mississippian Madison Group hosted bitumen (Figures 5.9F-G). Other samples have patterns more similar to the Permian Goose Egg hosted bitumen than to the Mississippian Madison Group hosted bitumen (Figure 5.9H-I). The Tensleep Sandstone (TS53) hosted quartz (Figure 5.9H) differs the most of the quartz samples. It lacks Eu and has a LREE composition similar to the Permian Goose Egg carbonate hosted bitumen, but differs from the bitumen and other quartz samples (Figures 5.9F, H and I) with a positive sloping HREE pattern.

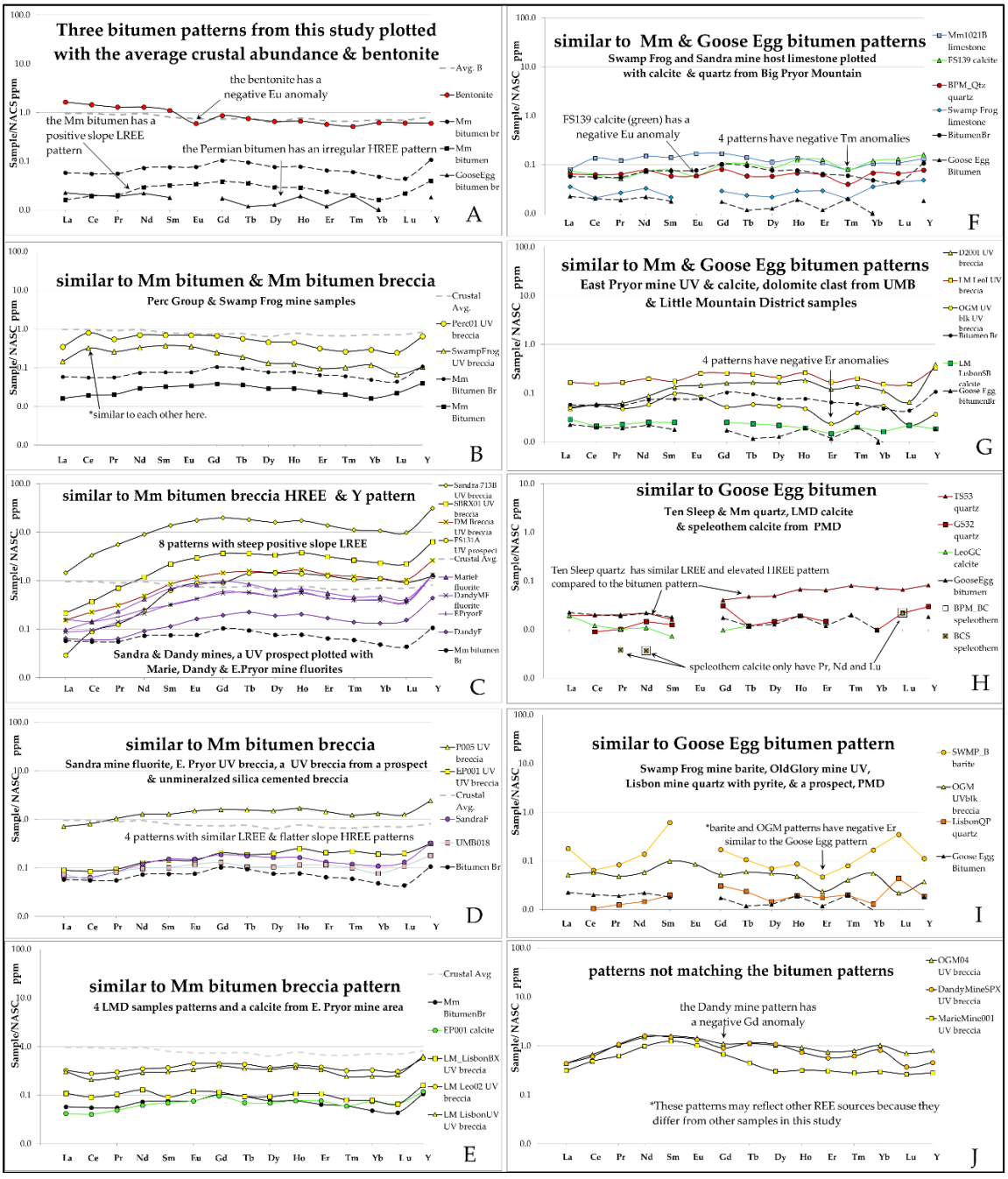


Figure 5.9. Spidergram plots of REE plus Y data from NASC-normalized samples. Each graph is plotted using a log base 10 scale (range is 0.01 ppm – 100 ppm). Plots are split up by similar REE and Y patterns. The bitumen data are plotted in Figure 5.9A with the bentonite and the average crustal abundance. Many of the mineralized and gangue minerals resemble portions of the bitumen patterns. Mississippian Madison Group is abbreviated Mm in the plots.

All the samples have greater REE plus Y concentrations than the bitumen except for two spleothem calcite samples from Big Pryor Mountain (Figure 5.9H). The speleothem calcite have the least concentration of REE of all the samples reflecting the typical low REE concentrations in natural waters [68]. The fluorites are the most enriched in REE plus Y of the gangue minerals and are more enriched than many of the U-V mineralized samples (Figures 5.9C-D). The Sandra Mine U-V samples are the most enriched in REE plus Y (Figure 5.9C).

The REE and Y pattern for barite from the Swamp Frog mine differs most from other data patterns in this study though is similar to the HREE portion of the Goose Egg bitumen pattern between Dy and Tm (Figure 5.9I). The pattern is similar to the quartz with pyrite from the Lisbon mine sample pattern (Figure 5.9I). The Old Glory mine sample (solid black line and yellow filled symbols) is similar to the barite sample in the from Ho-Yb in the HREE portion of the pattern. Both the Old Glory sample and the barite sample are somewhat enriched in Sm relative to the other REE in each sample. The Old Glory sample has Eu where the rest of the samples in this group do not.

Three U-V breccia data patterns from the Dandy, Old Glory and Marie mines do not match the bitumen patterns. These patterns have convex light and middle REE with flat to irregular HREE patterns (Figure 5.9J). The patterns in this set as well as those from Figure 5.9I and the Tensleep Sandstone hosted quartz (Figure 5.9H) may reflect a contribution from a different source, possibly the inferred intrusion to the west of the PMD (Figure 5.1)[1,16], or some other fractionation process during mineral formation.

5.4.2 REE Analyses of Permian Phosphoria Formation Data

The U.S. Geological Survey (USGS) studied the Permian Phosphoria Formation and related rock units in the Western U.S. Phosphate Field in southeast Idaho, southwest Wyoming, and southwest Montana (Figure 5.10) throughout much of the twentieth

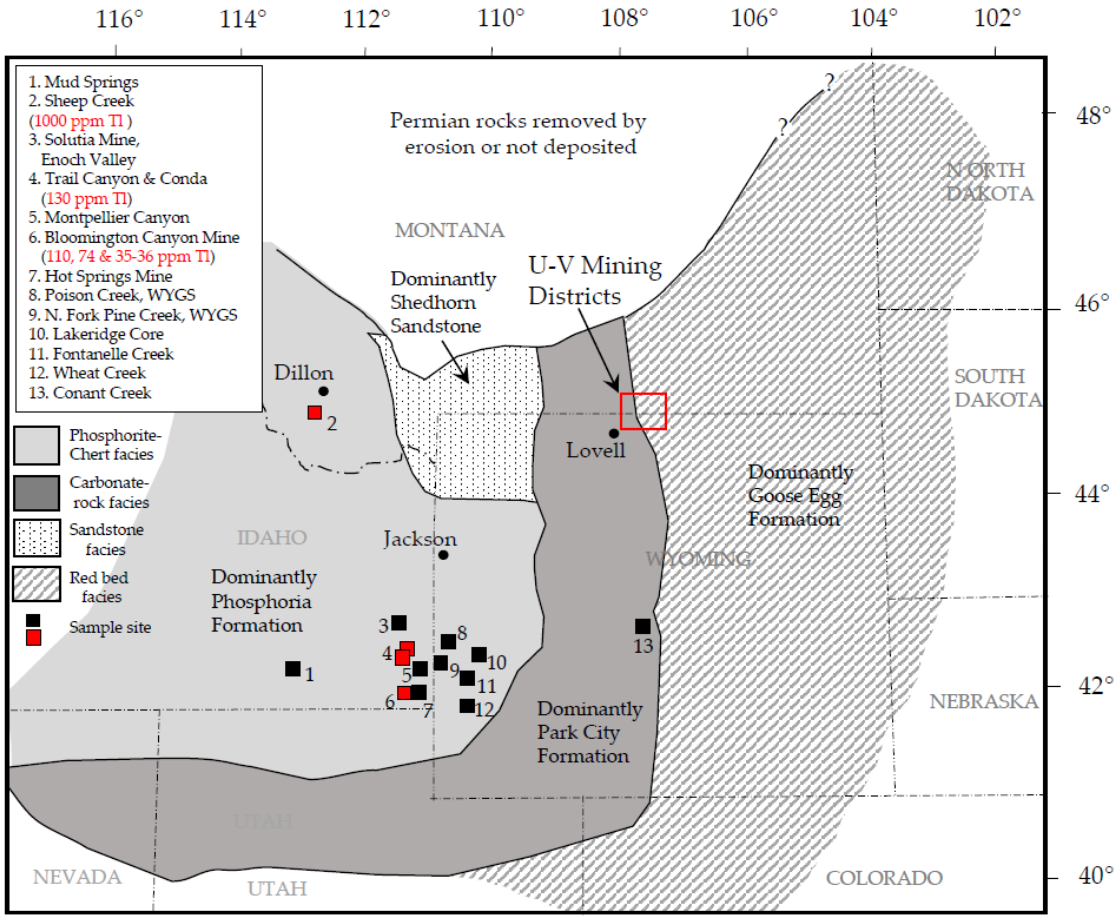


Figure 5.10. Index map showing location of dominant facies of rocks of Permian age samples by the USGS. The numbered sites (filled squares) give the approximate location of the sample sites for which samples have been analyzed for major-element oxides and trace elements in previous studies [71,72,74,75,79,80,82]. Red filled squares are sites that had samples with greater than 100 ppm concentration of Tl. The map is adapted from Sheldon, 1963 [70] and locations from the different studies.

century [20-22,69-80]. The deposit has been a major phosphate resource for agricultural fertilizer [75]. Early studies were to evaluate the economic resources of this deposit which is enriched in many metals, define its origin, and aid in exploration for similar deposits [75]. REE and trace element data were used in many of the studies to define the origin [74-76, 78,79]. Later studies focused on reaction pathways, transport, and fate of potentially toxic trace elements (Se, Cd, Tl, Hg, As, etc.) associated with the occurrence, development, and societal use of phosphate [76-77]. A recent study has shown that phosphorite deposits including the Phosphoria Formation are enriched in REE that would be easily recoverable as a byproduct of phosphate production [80]. The REE occur in the francolite ($Ca_5(PO_4)_3F$) portion of the Phosphoria phosphorite rock, a carbonate-rich fluorapatite, which is beneficiated or physically concentrated and dissolved in sulfuric acid to produce fertilizer [81]. In the study, dilute H_2SO_4 and HCl, extracted nearly 100% of the total REE content of the phosphorite samples in leaching experiments [80].

For this study, data from several studies carried out by the USGS and the Wyoming State Geological Survey of the Phosphoria Formation in ID, WY and MT [69-72,78,79,80] was examined. Figure 5.10 shows the locations of samples sites and the approximate location of this study; map shows approximate location of the Permian age rock. Also noted are the locations of samples that had greater than 100 ppm Tl. Not all of the studies included Tl as one of the analytes.

Data from analyses of rock samples studied by the USGS from MT, ID, and WY was normalized to NASC (North American Shale Composite) using the values of Gromet et al., 1984 (Figure 5.11) [67].

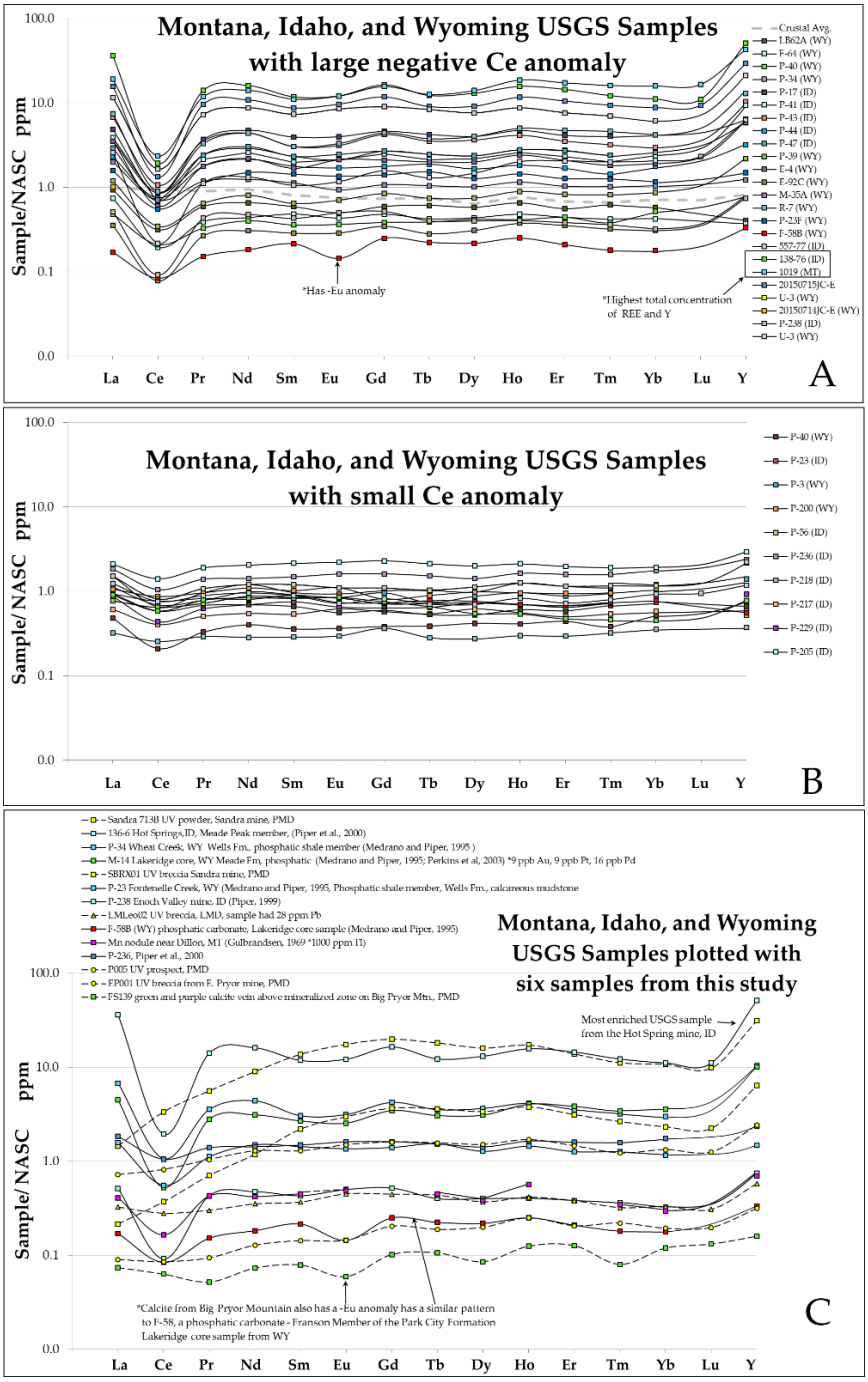


Figure 5.11. NASC-normalized REE and Y Permian Phosphoria Formation rock sample data (A) with strong negative Ce anomaly, slightly elevated Y (B) with smaller negative Ce anomally and flatter HREE and Y pattern. (C) Six samples from this study plotted with USGS samples. The mosted enriched PMD sample has similar, slightly higher concentration of REE and Y from Sm-Y. The only PMD sample with a negative Eu anomaly is similar to a phosphatic carbonate from the USGS Lakeridge core, WY that also has a negative Eu anomaly.

Two main patterns are present in the USGS data: (1) a strong negative Ce anomally with HREE patterns showing slightly elevated Gd and Y (Figure 5.11A) and (2) patterns with little or no Ce anomally and flatter HREE and Y patterns compared to the average crustal abundance pattern (Figure 5.11B). Most of the data reviewed (approximately 90 %) in the USGS studies had the strong negative Ce anomaly. Six sample analyses from this study plotted with data from the USGS studies show similar REE and Y concentrations and patterns (Figure 5.11C). Samples from the Sandra mine are comparable in concentration of HREE and Y to the most enriched of the USGS samples (Figure 5.11C).

Fractionation of Ce in the marine environment has been attributed to the oxidation of Ce^{3+} to Ce^{4+} and subsequent removal by suspended Fe and Mn particles in the water column or solid phases residing on the sea floor [83-85]. This results in REE patterns with the distinctive negative Ce anomally characteristic of seawater [83-85]. The negative Ce anomally is often associated with the precipitation of Mn nodules [85]. For an example, Mn nodules occur in a fine grained argillaceous sandstone bed of the Franson Tongue Member of the Park City Formation, Dillon, MT [71]. The depletion of Ce and the REE content of the U.S. Geological Survey samples, including the Permian nodules, were attributed mainly to the apatite fraction present in the samples as the mineral francolite [74-76,80]. All the samples in our study lack the Ce anomaly, although they display similar HREE and Y patterns to the Phosphoria rock sample REE patterns. The difference in the REE patterns from this study and those of the USGS rock samples likely represents the fractionation of the REE as a group due to the maturation and migration of

the hydrocarbons and brines from the Phosphoria Formation as the depth of the overlying sediments increased in the Bighorn Basin. REE are mobilized in hot reducing conditions typical of deep basin brines [68].

5.4.2 Concentration of Metals in the datasets

Geochemical analyses from the vanadiferous portions of the Phosphoria Formation of WY, ID and MT have anomalous high values of many metals. Some maximum values include: 857 ppm As, 22 ppm Ag, 3000 ppm Ba, 3000 ppm Cd, 150 ppm Co, 30,800 ppm Cr, 1.6 ppm Hg, 16000 ppm Mn, 280 ppm Mo, > 1000 ppm Ni, 668 ppm Pb, 1200 ppm Se, 130 ppm Tl, 328 ppm U, 35,840 ppm V, 1600 ppm Y, 15,000 ppm Zn and 2158 REE ppm [20,21,69-80]. Analyses of the Mn nodule used in Figure 5.11 above from a U.S. Geological Survey study near Dillon, MT had low total REE but high compositions of other metals: 400 ppm As, 1200 ppm Cd, 2200 ppm Co, 70 ppm Mo, 13000 ppm Ni, 1 ppm Te, 1000 ppm Tl, 700 ppm V, and 25000 ppm Zn [71].

U-V samples from this study contain anomalously high concentrations of many of the same metals supporting derivation from this source (Table 5.2). The bitumen do not have high concentrations but do have many of the elements of concern in this study. Analyses for all the samples are included in Appendix C, Table C2 and Table C3. All these elements present in these samples would not stoichiometrically fit into the structure of the minerals that they have been identified with this study. As hydrocarbons and brines migrated into the structures hosting the U-V deposits, it is likely many of these metals were incorporated as inclusions in minerals or breccia cement.

District	Sample	As	Ba	Hg	Mo	Ni	Pb	Tl	U	V	W	Zn
*avg. crustal abund. (McLennan, 2001) ppm		0.8-1.5	150-500	0.067	0.8-1.5	44-156	5.0-17	0.2-0.8	0.5-3	107-271	0.7-2	71-83
PMD	FS131A UV breccia	262	1230	2.84	53	<1	<2	180	86800	18900	94	16
PMD	Sandra713B UV powder	99	6550	1.485	29	167	44	20	21400	8730	24	804
PMD	SBRX Sandra UV breccia	49	5460	0.333	11	38	7	10	2600	1950	71	136
PMD	Perc Group UV breccia	329	5170	1.21	52	19	51	170	20700	6700	30	95
PMD	OGM04 UV breccia	1295	2310	0.354	152	2	13	100	10600	4410	105	26
PMD	P005 UV breccia	1080	1305	1.255	386	80	18	340	9000	6010	19	165
PMD	Swamp Frog UV breccia	556	1320	0.396	791	11	<2	340	6100	4160	81	44
PMD	DandyMSP UV breccia	94	2470	na	20	<1	35	490	8600	2220	382	9
PMD	MarieMine UV breccia	87	533	1.715	319	15	<2	30	2100	6740	40	57
PMD	D2001 UV breccia	87	79.5	6.32	9	2	35	50	17700	6310	16	849
PMD	DandyMSPF UV breccia	30	39.6	3.4	4	21	8	10	3000	3320	12	76
PMD	DandyMBr UV breccia	130	61.3	12.8	28	102	55	20	28100	10500	26	1110
LMD	Lisbon UV breccia	89	42.6	0.197	25	421	146	30	31100	8520	11	1300
LMD	LeoIncline02 UV breccia	726	255	0.179	137	517	57	230	16000	10300	11	2230
PMD	OGM UV blk UV breccia	46	1530	na	21	<1	2	50	4900	1240	107	7
PMD	EP001 UV breccia	50	27.6	na	2	63	11	10	907	25	6	143
LMD	LeoIncline UV breccia	116	183	na	98	191	28	20	>1000	4330	13	970
LMD	LisbonBX UV breccia	212	140	na	93	122	4	10	1300	1850	12	569
LSM	Mm bitumen	0.2	10	0.01	1.63	14.1	0.9	0.02	6.8	73	8.6	5
LSM	Mm breccia bitumen	<0.1	20	<0.01	0.12	1.5	0.5	<0.02	4.04	7	2.4	2
LSM	Goose Egg bitumen	1	630	0.01	0.46	3.2	1.5	0.03	11.6	8	21	9

PMD = Pryor Mountain District LMD = Little Mountain District LSM = Little Sheep Mountain na = not analyzed

Table 5.2 U-V breccia samples contain elevated concentrations of many of the same elements detected in the Permian Phosphoria Formation samples collected by the USGS. Elements that are elevated greater than the average crustal abundance are shown in red and blue highlighted text in the table. Highest values are outlined in black boxes.

6. Discussion

This study has found that U-V mineralization in the districts has a close association to hydrocarbons and fracture induced permeability. Bighorn Basin oilfield brines with Phosphoria Formation-sourced oil likely provided a transporting fluid and source of V and other metals to the deposits. This conclusion is based on similar REE and other trace element geochemistry of: 1) the bitumen from Little Sheep Mountain 2) the

U-V breccia and gangue minerals from this study and 3) the data from Phosphoria Formation studies conducted by the USGS.

The Bighorn Basin has produced oil and gas for over a century [40]. Fracturing and faulting accompanied folding during the Laramide Orogeny. This is when the Phosphoria Formation sourced oil has been determined to have migrated from stratigraphic traps into the structures hosting oil and gas in the Bighorn Basin [23,24,86].

6.1 Phosphoria Oil Migration and Oilfields in the Bighorn Basin

Originally, Phosphoria Formation-sourced hydrocarbons accumulated in the Bighorn Basin in stratigraphic traps created primarily by up dip facies change, pinch out and truncation of reservoir carbonates, and by uneven Phosphoria Goose Egg truncation of the underlying Pennsylvanian Tensleep Sandstone [23,24]. The timing of the first migration of Phosphoria sourced oil ranges from Jurassic to late Cretaceous in time [86]. The Cottonwood Creek oil field in the southeastern Bighorn Basin produces from a stratigraphic trap **(**Figure 5.12).

The oil produced in the field is from a Phosphoria Formation reservoir with a seal formed by impermeable Permian Goose Egg shales and anhydrites [40], similar to the original pre-Laramide stratigraphic traps. Most principal oil production in the Bighorn Basin, however, has been from structural traps such as anticlines with primary oil production from Permian- and Pennsylvanian-age reservoir rock (Figure 5.12) [40].

Seven of the top ten producing oilfields in WY are in the Bighorn Basin. These are highlighted in red in Figure 5.12. The primary oil production in the northern Bighorn

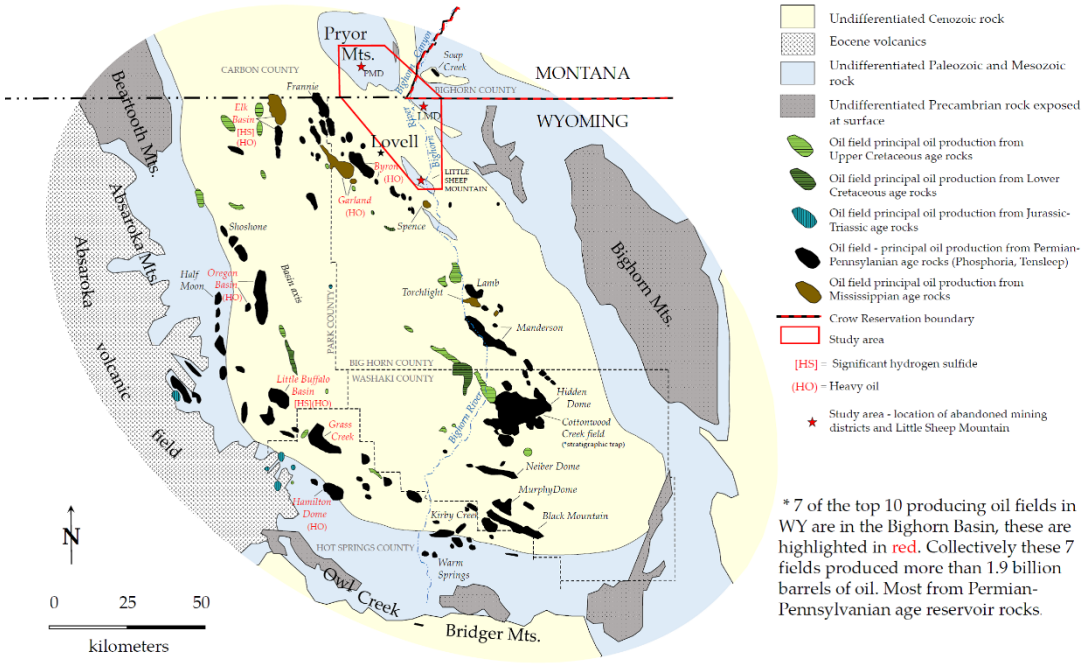


Figure 5.12. Map showing the oilfields in the Bighorn Basin. The study areas are shown by the red stars. Oil field locations and reservoir rock designation are based on the Wyoming Geologic Survey's Wyoming Oil and Gas Field map, 2016 [40].

Basin was from Mississippian age reservoir rock in two of the top seven fields show in Figure 5.12. These fields, Elk Basin and Garland, may serve as analogues for the structures hosting the U-V deposits in the two districts. Both Elk Basin and Garland produce heavy oil and significant hydrogen sulfide is associated with the Elk Basin oilfield [40]. Heavy oil and bitumen are both produced by water biodegradation [87].

6.2 Origin of Bitumen and Heavy Oil

Most heavy oil and natural bitumen is thought to be the residue of formerly light oil that has lost its light-molecular-weight components through degradation by bacteria, water-washing, and evaporation [87, 88]. Meteoric water is the commonly accepted

vehicle for bringing dissolved oxygen and microbes into contact with oil reservoirs, either along faults or fractures or by aquifers in hydrodynamic connection with the surface [88]. Generally, this is under aerobic conditions at depths of about 5,000 feet or less and temperatures below 176°F [87]. Hydrocarbons are oxidized completely to carbon dioxide and water without intermediate products by many bacteria [88]. This results in the remaining residue of solid bitumen and asphalt which are enriched in N-S-O compounds [88]. Some average chemical variations in conventional oil and bitumen have been observed in many studies from oil and bitumen producing basins around the world. Based on studies from approximately 8,500 deposits there is an increase in the metal concentration in bitumen compared to conventional oil [87]. For example, conventional oils have average concentrations of approximately 1 ppm Pb, 16 ppm V, 6 ppm Fe, 1 ppm Al, 8ppm Ni, and 0.5 ppm Cu and bitumen has concentrations of approximately 5 ppm Pb, 335 ppm V, 4290 ppm Fe, 21,000 ppm Al, 89 ppm Ni, and 44 ppm Cu [87]. Hg however, is less concentrated in bitumen 0.019 ppm compared to an average of about 19 ppm in conventional oil [87]. This may suggest that Hg is being mobilized in the biodegradation process. The combination of aerobic and anaerobic heterotrophic bacteria metabolic processes and subsequent water washing likely results in mobilization of some metals during biodegradation and enrichment or a sink for others.

6.3 Style of Breaching of Oil Traps in the Study Areas

We suggest that the structures hosting the U-V deposits likely had Phosphoria sourced oil in structural traps until they were breached based on the presence of bitumen in most of the samples studied. Breaching of the structures in each district was not

synchronous or of the same style. The folds hosting the deposits are of different scales, maturity, and elevation. We suggest that breaching of the structure and subsequent U mineralization in the PMD was earlier than in the LMD based on elevation and structural maturity of the folds. The availability of oxidized fluids in both districts was related to the exhumation of the Bighorn Basin and the adjustment of the water table in response. Because the PMD district is about 1000 m higher than the LMD oxidizing fluids were available to the district while the LMD was still buried. The oxidizing fluids in the PMD were likely groundwater but possibly lakes and ancestral rivers. The PMD is hosted in a more structurally mature fold than the folds hosting the LMD. The Gypsum Creek anticline, the main fold hosting the U-V deposits in the PMD, was breached as the Crooked Creek fault propagated through its core. Hydrocarbons held in structural traps were likely released as far up as the fault propagated. Strata younger than the Madison Group have been eroded from the top of Big Pryor Mountain leaving little evidence for the termination of the fault.

The folds hosting the deposits in the Little Mountain area are smaller in scale and less structurally mature than those in the PMD in the sense that the master faults did not fully propagate through the structures. The Porcupine Creek anticline, one of the main structures hosting the U-V deposits in the LMD, was breached by the superposition of the ancestral Bighorn River across its axis, forming part of the Bighorn Canyon.

6.4 Paragenesis of U Minerals in the Two Districts

The paragenesis of U minerals in the two districts is slightly different due to the structure, elevation and position in the Bighorn Basin. The initial evolution of the U-V

mineralization in both districts is related to the migration of the oil and brines from the Bighorn Basin into structural traps as folding proceeded in the two areas. Simplified conditions for mobilizing metals in a basin environment are increased temperature, lower pH, and increased salinity. U would be stable in a reduced U^{4+} state in the basin environment and would likely form F and Cl complexes, which stabilize U^{4+} in solution [89]. Abundant F would have been available from the apatite of the Permian Phosphoria Formation. These complexes could have migrated with oil and been in solution in the traps until the structure was breached. Once oxidized meteoric water was available U^{+4} would oxidize to U^{+6} to stabilize the uranyl ion, UO_2^{2+}, and its complexes [90-91]. The uranyl ions would bind with available metals and precipitate out as various uranyl minerals. All the identified U minerals in the districts are uranyl minerals with the Ca-uranyl vanadates being the most common.

The uranyl silicates, phosphates, and vanadates are relatively insoluble and require Si, P, and V^{5+}, respectively to precipitate [90]. These elements can be derived from a variety of sources. In many U deposits, metal-uranyl vanadates are derived from the oxidation of U^{+4} minerals such as uraninite [89-91]. In this study, however no U^{+4} minerals have been observed. This suggests that the metal-uranyl vanadates are primary (did not oxidize from a reduced U mineral such as uraninite). We suggest that the metals necessary for the formation of the metal-uranyl vanadates were derived from the biodegradation of the oil once the basin fluids mixed with the meteoric groundwater after the structures were breached rather than oxidizing from a reduced form mineral such as uraninite.

6.4.1 Mineral Paragenesis Red Pryor Mountain Group, PMD

The two mining districts are hosted in the same paleokarst horizon with nearly identical ore minerals but differ in gangue minerals; notably fluorite, barite and abundant quartz present only in the PMD. Two episodes of siliceous fluid migration are apparent in the PMD. The first significant siliceous fluid migration was the emplacement of silica cemented tectonic hydrothermal breccia. We suggest these were emplaced as a result of earthquake induced seismic pumping during the Laramide Orogeny that hydrofractured the host rock [52, 92-93]. The resulting fractures and brecciation were healed by the rapid precipitation of quartz in the earlier episodes and later by calcite cement during subsequent and sudden decrease in the partial pressure of CO_2 [92]. As the master faults propagated in the structures fluids would episodically migrate along the same faults and the process would be repeated forming new or following previous fractures [92]. The earlier siliceous tectonic hydrothermal breccia had abundant Fe-oxides with trace amounts of V, Tl, Pb, and Ti present in the matrix (Figure 5.13A).

Early barite was associated with the first pulses of siliceous tectonic hydrothermal breccia evident by the inclusions of barite in the siliceous cement of the tectonic hydrothermal breccia (Figure 5.13B). Later barite precipitated along fractures and in vugs (Figure 5.13C). U-V mineralization followed emplacement of the siliceous tectonic hydrothermal breccia based on petrographic and field observations. No U minerals were observed in the quartz cement matrices of siliceous tectonic hydrothermal breccia; only secondary precipitation in vugs (Figure 5.13D), interparticle porosity, or along fractures. Heavily corroded subhedral quartz fractured in mosaic patterns healed by calcite and

accompanied by hydrocarbons reflect hydrofracturing associated with multiple brecciation events following emplacement of the siliceous tectonic hydrothermal breccia (Figure 5.13E-5.13G).

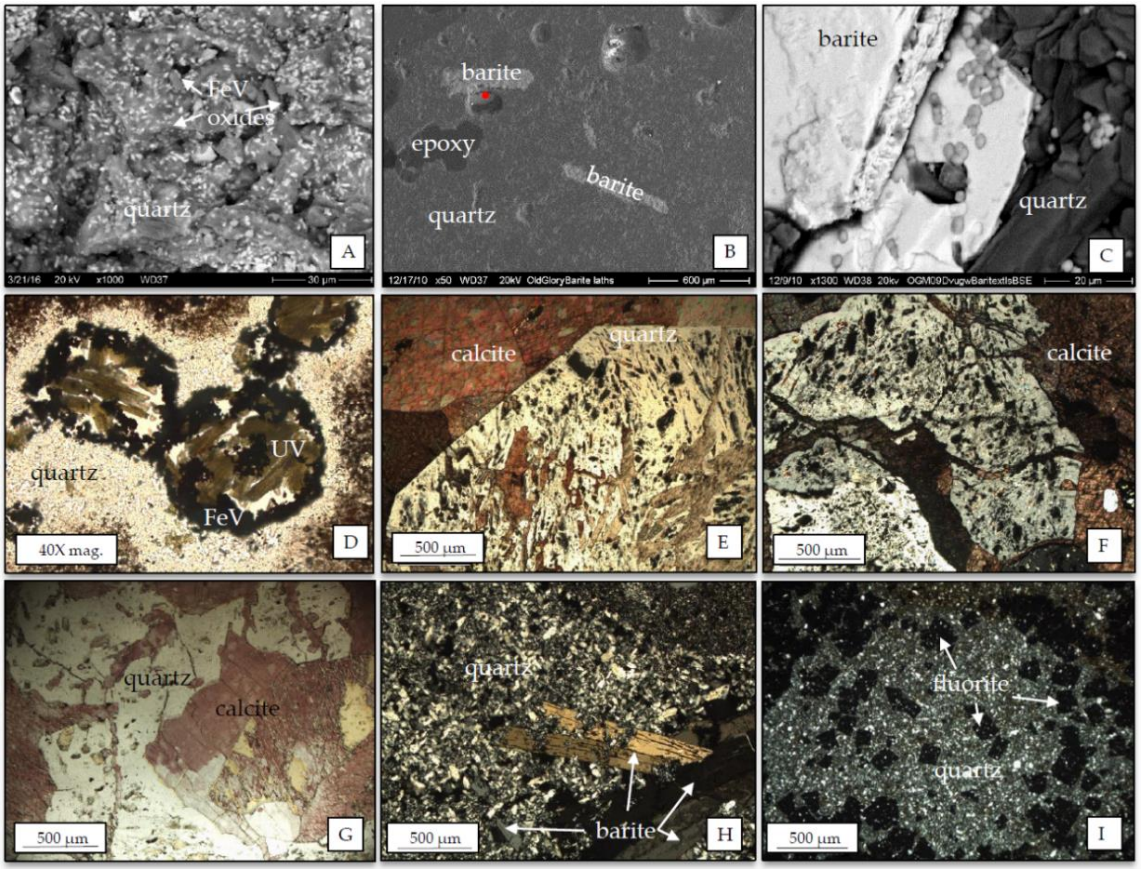


Figure 5.13. Barite and quartz in the PMD. (A) Fe-V oxides with trace amounts of Tl, Pb and Ti in quartz matrix of a tectonic hydrothermal breccia from the Old Glory mine, PMD, BEI, 1000x mag. (B) Barite laths in quartz matrix with barite in vug marked by red dot, SEI, 50x mag. (C) Barite from vug in G formed around spherical minerals with Fe, Si, Al, Ba and S, BEI, 1200x mag. (D) Tyuyamunite or metatyuyamunite crystals in Fe-V oxide lined, bleached circular vugs. (E) Sharp euhedral crystal boundary of corroded quartz grain and and red stained calcite fill in irregular vugs in quartz, Marie mine, PMD, xpl, white card method (F) Quartz veinlet, micro fractured with mosaic pattern, healed by calcite, Marie mine, PMD, xpl (G) Quartz veinlet, micro fractured with mosaic pattern, healed by red stained calcite, Marie mine, PMD, ppl, white card method. (H) Grey and white euhedral microcrystalline quartz filling in void space around earlier barite, Swamp Frog mine, PMD, xpl. (I) Cryptocrystalline quartz filling in around isotropic fluorite cubes, Dandy mine, PMD, xpl.

The quartz cement in the tectonic hydrothermal breccia may be related to the inferred intrusion. It may have formed in a similar time frame as the Late Cretaceous 78-75 Ma. diorite to granodiorite Sliderock stratovolcano and the Lodgepole intrusive [94,95]. These two features are part of an extensive NW-trending volcanic field that lies astride the folds and faults of the Nye-Bowler lineament [94,95] (Figure 5.3, laccoliths). The alignment of these volcanic intrusives along the Nye-Bowler lineament strongly suggests the fault zone controlled the emplacement of the volcanic centers of the field [94]. Thus, it would not be unreasonable to have another intrusion to have formed along the same NW-trending lineament because of low-angle subduction of the Farallon plate. The igneous products of the Sliderock Mountain stratovolcano were interpreted to be the products of continental arc-related magmatism based on geochemistry [94]. Evidence supporting the inferred intrusion near the PMD include:

- High aeromagnetic anomaly identified in 1982 by the Department of Energy [16] south of the Big Pryor Mountain block.
- Gold detected in samples from this study by commercial assays (Appendix C, Table C1) and using the SEM. An abandoned gold deposit south of the PMD may have been associated with an intrusion (Figure 5.1).
- High concentrations of Tl (up to 490 ppm) in the PMD. Tl is not common but is commonly associated with Carlin-type gold deposits that have a close proximity to Eocene volcanic centers or plutons [96-100]. Thus the Tl and Au detected in the PMD could support an intrusion.

- Proximity of the Late Cretaceous 78-75 Ma. diorite to granodiorite Sliderock stratovolcano and the Lodgepole intrusive [94,95] that is suggested to have been controlled by the E-W trending Nye Bowler lineament.
- Abundant fluorite and barite in the PMD. High concentrations of Ba in the PMD samples with the highest values excluding the barite samples ranging from (5460 – 6550 ppm).
- High silica content of the tectonic breccias, highly fractured zones with white "bull" quartz and a few outcrops or lag deposits of the same, and high silica content (95%) in reported ore during the years that the mines were operating [1].

6.5 Mineral Paragenesis LMD

The LMD deposits are hosted in smaller folds than the Gypsum Creek and East Pryor Mountain anticlines. The close association of bitumen and Fe-oxides and hydroxides with the U-V minerals in the LMD suggests that oilfield basin brines and hydrocarbons were present in the structures until the down cutting of the Bighorn River breached the Porcupine Creek anticline. Gypsum, dogtooth calcite, bitumen, sulfides and speleothem type occurrences from waste piles and outcrops suggest that hypogenic sulfuric acid speleogenesis [22,23] may have contributed to concentrating ore forming minerals in the LMD. Underground mines are no longer safely accessible though descriptions in the literature of the caves encountered and actually mined out in the LMD [2,12] support this interpretation. REE data show good correlation with the Mississippian Madison Group hosted bitumen (Figure 5.9E) support this interpretation. Hypogenic

caves likely developed after oxygen rich water and microbes were introduced to the system. Hydrogen sulfide that was produced by microbes consuming the light fraction of the hydrocarbons likely contributed to the initiation of sulfuric acid speleogenesis in the LMD and to the mobilization of the metals needed to form the U-V minerals. The bitumen that was the residuum of the microbial process as well as the caves support this interpretation. The Lower Kane Cave is actively forming by sulfuric acid speleogenesis [18,19]. It has an artesian geothermal spring emanating from fractures at the core of the anticline that are mixing basin derived fluids with the groundwater at the level of the Bighorn River. The presence of Fe- and S-reducing bacteria in the Lower Kane Cave system [18] as well as U and V and other metals present in the mud [19] and water of the geothermal artesian spring may serve as an analogue for the LMD.

Timing of U mineralization and active sulfuric acid speleogenesis in the LMD likely coincided with the timing of formation of Spence Cave in Sheep Mountain, WY, upper Kane Cave in Little Sheep Mountain, WY and the Horsethief cave formed near the mining district. Sheep Mountain and Little Sheep Mountain are anticlines that have been superposed by the Bighorn River. Each of these caves is proposed to have developed by hypogenic sulfuric acid speleogenesis [101]. Windblown sand and volcanic ash that were deposited in the Spence and Horsethief caves by wind were dated using cosmogenic nuclide concentrations [101]. A cosmogenic $^{26}Al/^{10}Be$ burial date for eolian sand in the entrance to Spence Cave yielded a burial date of 0.31+/- 0.19 million years. Tephrochronology constrains the age of Horsethief Cave which contains a deposit of the Lava Creek B fallout ash, erupted from the Yellowstone Plateau volcanic field ca. 0.64

million years [101]. These dates may provide minimum estimates for the timing of cave development in the northern Bighorn Basin and for the U-V mineralization in the LMD.

The LMD lacks the strong silica component, barite, and fluorite that the PMD has. If the oilfield brines that originally migrated into structures had F from the abundant apatite it would seem likely that there should have been some present also in the LMD. This may reflect more F and Ba available from the inferred intrusion in the PMD and not as much concentration in either Ba or F to form barite and fluorite in the LMD. It may also reflect less sampling in the LMD than in the PMD due to accessibility, though no barite or fluorite was observed in this study or documented in previous studies. Ba was detected in high (4300 ppm) concentration (Appendix C, Table C2, No. 19) in one sample from the LMD though barite was not observed in the field, petrographically or using the SEM.

Although the paragenesis of each deposit examined varies, the geologic events and processes affecting Madison Limestone in the two districts have some consistent similarities. The origin of the deposits reflects a close but complex relationship with the migration of hydrocarbons, hydrology, and the exhumation of the Bighorn Basin. A broad summary of the fluid migration and geologic events or processes affecting the Madison Limestone in the northern Bighorn Basin and the mining districts, and timing of volcanic events is presented in Table 5.3.

Our interpretation is that oil migration occurred at least three times. The first was pre-Bighorn Basin, the second during the Laramide Orogeny, and a third time was after the structures were breached when the oil migrated out of the traps (Table 5.3). The last

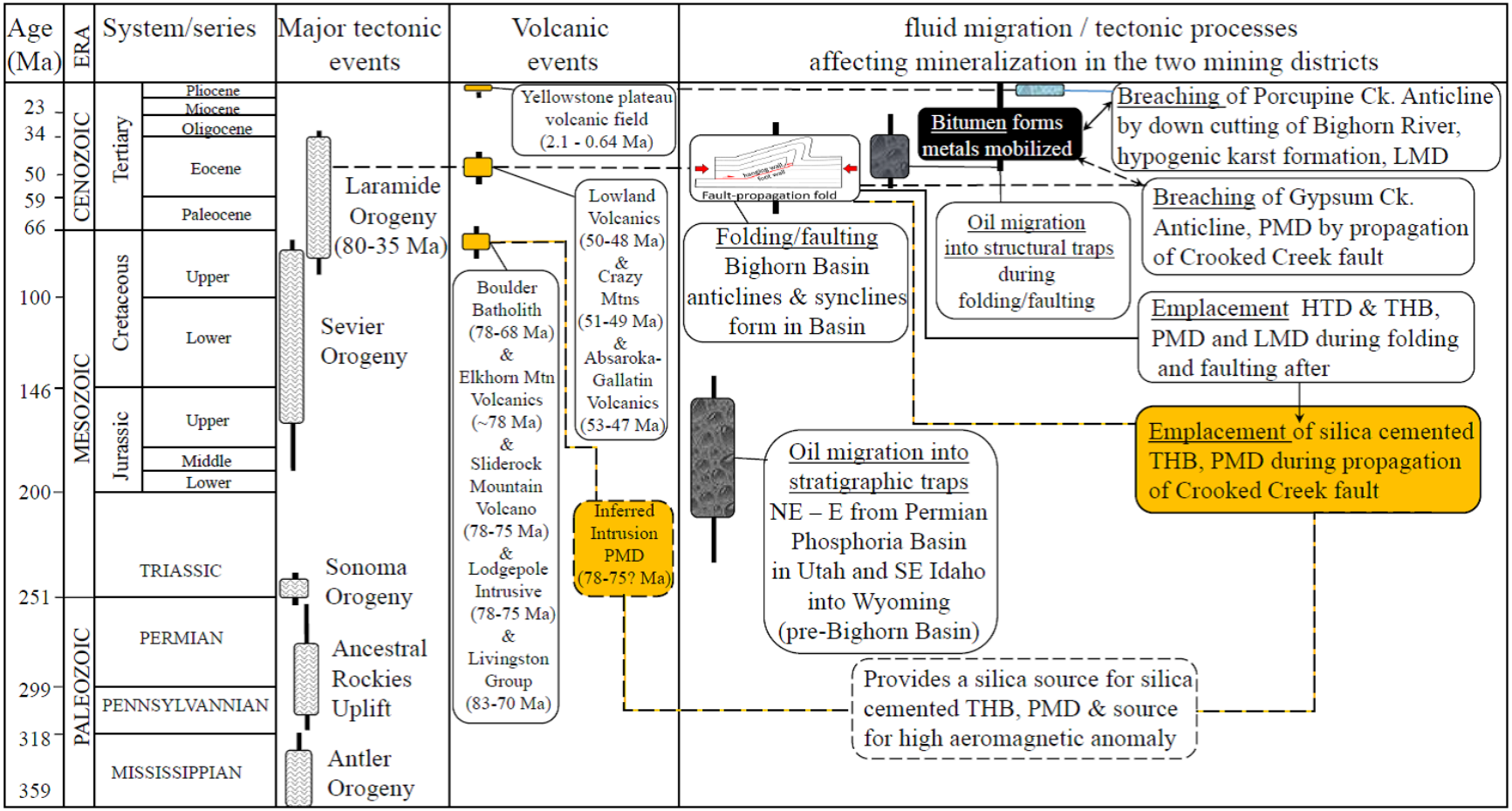


Table 5.3. Geologic timescale and table correlating events affecting the mining districts in the northern Bighorn Basin. Major tectonic events patterned boxes denote orogenies: Antler Orogeny [101]; Ancestral Rockies [102]; Sonoma Orogeny [103] Sevier Orogeny [104]; Laramide Orogeny [105]. Shaded orange boxes denote volcanic events [94,95,101,106-110]; In the fluid migration column: the fault propagation figure denotes Laramide folding; grey bubble filled boxes oil migration [23,24]; a black shaded box bitumen formation; and a blue patterned box denotes breaching of the Porcupine Creek anticline by the down cutting of the Bighorn River.

migration was earlier in the PMD than in the LMD. Bitumen formed likely earlier in the PMD than in the LMD as well and was related to available oxidized water and microbes. Major tectonic events affecting the region are shown in the column with patterned filled boxes. Several orogenies may have contributed to fracturing in the Madison Limestone which later influenced paleokarst development. Though most of the processes affecting mineralization in the two districts are related to the Laramide Orogeny. The folds hosting the deposits and the subsequent episodic fracturing that provided fluid migration paths were likely a result of the subduction of the Farallon Plate and the resulting Laramide Orogeny. The inferred intrusion depicted by the black dashed outlined orange box is likely the source of silica for the cement of the breccia in the PMD and may represent a time-equivalent subduction related intrusion to the Sliderock volcano complex thus was likely emplaced 78-75 Ma. The emplacement of the intrusion would possibly be similar to the time of migration of oil into the folds through fractures produced during the Laramide Orogeny. The other fault blocks may have impeded silica rich fluid migration into the LMD.

7. Future Directions

After elevated U was identified in home water wells on the Crow Reservation collaborative research related to U contaminated drinking water on the Navajo and Crow Indian Reservations was established with the University of New Mexico, the University of New Mexico and Montana State University. All three Universities are working on projects related to U and the health of people on reservations. Part of the research being conducted at the University of Montana, is the development of silica polyamine

composites to aid in removal of U and other toxic metals from contaminated drinking water.

7.1 Selective Solid Phase Extraction of U from Contaminated Water

A variety of methods such as precipitation, solvent extraction, electrolysis and ion exchange have been employed to remove dissolved metals from aqueous samples. Most of these have disadvantages such as poor removal efficiency, high cost, and generation of secondary pollutants and ineffectiveness for low concentration removal [111]. In an effort to address the long-standing health hazards imposed by abandoned uranium mines and mills, naturally occurring U, and trace metal contamination we propose the use of Silica Polyamine Composites (SPC). SPCs filter, isolate, and remove unwanted metals.

Since the mid-20th century amorphous silica gels have been a favored solid-state matrix for applications in chromatography, catalysis, colloid chemistry and as drying agents [112]. SPCs are solid phase hybrid materials that consist of an inorganic matrix combined with an organic polymer developed by the Rosenberg Research Group at the University of Montana [113,114]. These hybrid materials bring together the best properties of each component in order to enhance functionality. These silica based organic-inorganic materials offer a rigid matrix with high porosity and good thermal stability [115]. Furthermore, the polar nature of the silica polyamine surface also makes for better mass-transfer kinetics in the case of aqueous solutions, and the polyamine can be easily modified with metal selective functional groups. [116,117] SPCs act as chelating agents for a range of metal ions and can also be useful for toxic metal immobilization and disposal [117]. They have led to a wide range of metal-selective

materials that in most cases provide a high loading, rigid, surface that does not shrink or swell [115]. These patented materials are currently being used in medium to large-scale recovery of metals and the remediation of toxic anionic and cationic pollutants [114,115]. Acid stripping is the primary method of extracting immobilized metals from SPCs. Without the acid strip, metals can remain on the SPC and can be used as a medium for long-term disposal [117]. These composites have been previously found to maintain activity over more than 7000 test cycles that consist of treating a packed column of SPCs with a metal ion solution and then acid stripping. These composites showed no visible signs of degradation and negligible loss in metal ion adsorption capacity under a variety of conditions [113].

SPC's are engineered, patented, and commercially produced (Johnson Matthey Ltd.) materials that are designed to bond with a specified metal and extract the metal from aqueous solutions for later recovery [113-115,118,119]. SPCs have the ability to be modified with a variety of metal selective ligands which is vital to an effective remediation processes. Previously the Rosenberg research group has synthesized a number of different SPCs that are selective for Cu^{2+}, divalent transition metals, Fe^{3+}, Ni^{2+}, Ga^{3+}, divalent and trivalent metals (Figure 5.14).

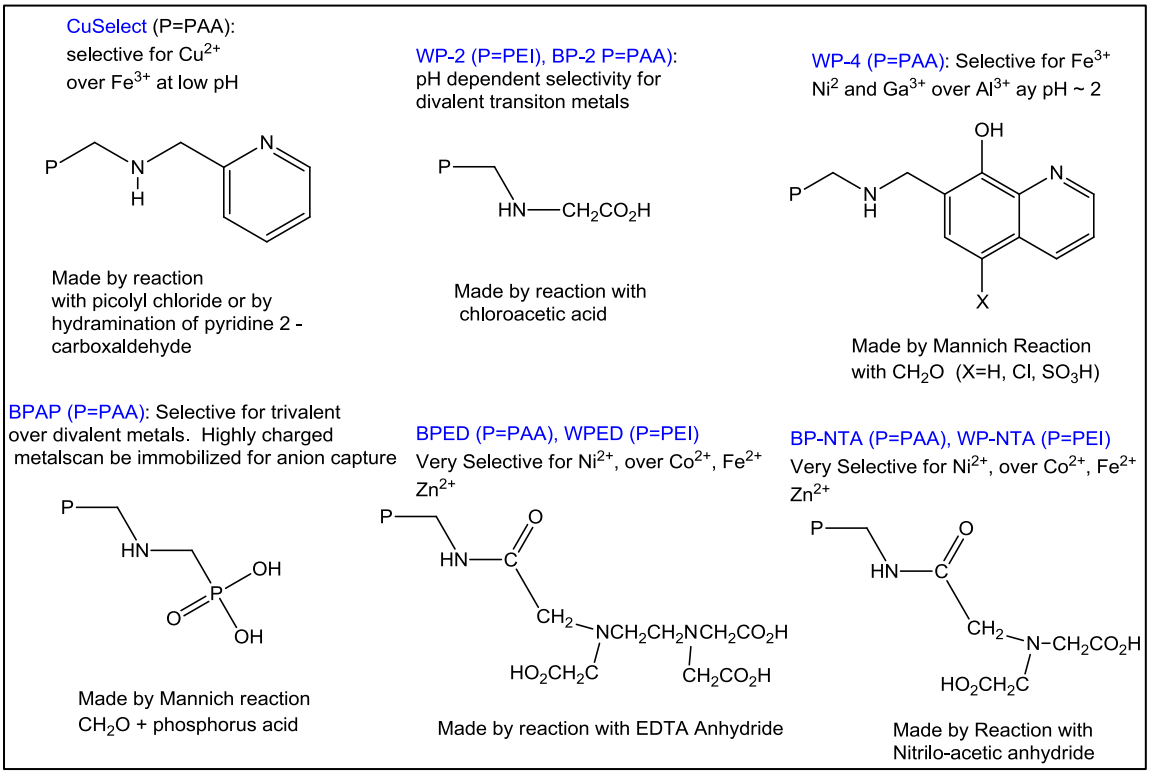


Figure 5.14. Ligands modified SPCs and their applications to date.

In addition, earlier studies have evaluated the ability of SPCs to separate REE from mine leachates from Mt. Weld in Laverton, Australia. These studies separated Ce(III), La(III), Nd(III), Sm(III), and Pr(III) from the solution matrix that contained Fe(III), Mn(II), Ca(II), Mg(II), Al(III), Zn(II), Ti(IV), and other lower concentration trace metals [120]. This separation required first the use of WP-4 followed by BPAP. The WP-4 removed the large excess of iron and BPAP selectively removed the entire family of lanthanides from mixtures of transition metals, alkali and alkaline earth metals at low pH [120]. This study demonstrates the feasibility to separate REE metals from a metal matrix like that of mine leachates. Thus if the concentration of REE or other desirable metals

was economical they might be recovered using SPCs possibly offsetting the cost of remediation efforts.

8. Conclusions

U-V mineralization is complex in the two districts. Our proposed model for paragenesis is a simplified sequence of mineralization. Both districts are hosted in the same paleokarst horizon but are in slightly different structural positions in the Bighorn Basin. The structures in both mining districts likely held hydrocarbons in structural traps until they were breached. The presence of bitumen throughout the study area suggests there is a strong association of microbes. Microbes likely mobilized many of the metals that formed the U-V minerals in both districts. More research would be necessary to determine the specific metabolic processes involved and the fate of the metals involved.

We conclude that the source of the metals in the deposits of this study was Permian Phosphoria Formation oil introduced through fluid migration in fractures as folding proceeding during the later stages of the Laramide Orogeny. The process of tectonic hydrothermal brecciation accompanied folding and provided both a mechanism and fluid source for metals in both districts. The exhumation of the Bighorn Basin affected each area differently and mineralization style and gangue minerals reflect this difference.

This study does not support a direct source of U, Hg or Pb as a source of contamination in the Bighorn River or home wells on the reservation. It is possible that during the formation of bitumen by biodegradation of oil, metals such as Hg and Pb were mobilized; this may be the source of these metals in the hydrologic system. Oil that is

still migrating up along faults such as the fault coring Little Sheep Mountain at the level of the Bighorn River may be being consumed and episodically contributing Pb, Hg and other metals to the hydrologic system. Material derived from the erosion of the deposits may also be a contributing factor. Future work may warrant additional areas of research in both of these areas.

U^{6+} is very mobile in water and is still being mobilized evident by U-V minerals found on the surfaces of burned wooden supports of worked prospects in the PMD, on surfaces of reclaimed materials, along sprung stylolites and along open fractures. The triuranium carbonate minerals are generally the most soluble [89] and some are still present in the deposits. As surface water percolates through the deposits these minerals are likely dissolved and reprecipitated as the relatively insoluble metal-uranyl vanadates when encountering a V source such as material from sprung stylolites. Thus, surface waters flowing through these deposits probably do not contribute many of these elements to the hydrologic system. Hydrothermal springs ascending from faults that are crossed by the Bighorn River do contribute some metals to the hydrologic system though are probably not of a concentration that would impact human health.

6.1 Elements of Environmental Concern

Alluvial low lands of the Crow Reservation, MT, located along the Bighorn and Little Bighorn Rivers are where U was found to exceed EPA's MCL in some tested home wells [10]. The source of the U has not been determined but it is likely that material eroded from the Wolf, Big Horn and Pryor Mountain ranges may have had U minerals present either from the U-V deposits, or thin Permian Phosphoria or equivalent

sediments. If the U was derived from erosion of materials associated with the U-V deposits or from Phosphoria Formation sediments, then there is a possibility other metals of environmental concern e.g. As, Cd, Hg, Pb, Se, and Tl may be present. Tl is not found in many rock types and Tl minerals are rare. The average crustal abundance of Tl is 0.75 ppm [121]. Tl is one of the metals found in anomalous high concentrations in both the Phosphoria Formation and in the U-V deposits of this study. All the mineralized samples from this study contained anomalous concentrations (10-490 ppm) Tl. Tl is more toxic to mammals than Cd, Pb, Cu, or Zn [122,123]. Tl is associated with hydrothermal sourced fluids in sediment hosted gold deposits [97-100]. Tl in these deposits was likely mobilized and transported with hydrocarbons and brines though could be related to the inferred intrusion that might also account for the Au and Ag present in the U-V deposits. Tl disperses readily and accumulates in soil, water transport and food crops such as cabbage, affecting the health of people [124]. Tl forms highly volatile complexes with halides and can enter the crystal lattices of sulfides and sulfosalts [125]. Drinking water wells on the Crow Reservation, MT, were analyzed for Tl because U was found some of the wells tested and might be associated with the eroded material sourced from deposits in WY and MT. Initial well water samples (n=29) from the Crow Reservation tested for Tl at the University of New Mexico did not show elevated concentrations of Tl. The results ranged from 0.01 to 0.36 µg/L well below the maximum contaminant level (MCL) of 0.002 mg/L and the EPA's MCLG (goal) of 0.0005 mg/L [126].

Water quality on many reservations will undoubtedly continue to be an issue. Research will continue to develop a way to remove U and other metals from the water to

ensure the most important need on the Navajo, Crow, and other reservations, clean water for good health.

Acknowledgments: We thank employees of the Bureau of Land Management, Cody, Wyoming, who granted permission for the work in the Little Mountain area; the Custer Gallatin National Forest who granted permission for work in the Pryor Mountain area; Lauren Kay, Janet Barkow, and Thomas H. Nall for fieldwork assistance; and Chris Gammons and Gary Wyss, Montana Tech, Butte, MT, for use of their facilities and analytical work and discussions related to this project. Funding for research: ZERT II (Zero Emissions Research) DOE Award #: DE-FE0000397; Alfred P. Sloan Indigenous Graduate Partnership; Montana State University-Dennis and Phyllis Washington Foundation; HOPA Mountain Program. Note: The content is solely the responsibility of the authors; it has not been formally reviewed by any of the funders.

Author Contributions:

Anita L. Moore-Nall: Researched the area's geology, did the field work, submitted samples, interpreted the geological and geochemical data, produced most of the figures and is primary author on paper; Ranalda A. Tsosie: Researched, did the chemistry and wrote the Selective Solid Phase Extraction of Uranium portion of the paper; reviewed drafts of the paper; contributed to the manuscript.

Conflicts of Interest: The authors declare no conflict of interest. The founding sponsors had no role in the design of the study; in the collection, analyses, or interpretation of data; in the writing of the manuscript, and in the decision to publish the results.

References

1. Van Gosen, B.S.; Wilson, A.B.; Hammarstrom, J.M. *Mineral Resource Assessment of the Custer National Forest in the Pryor Mountains, Carbon County, South-Central Montana*, U.S. Geological Survey Open-File Report 96-256; U.S. Geological Survey: Denver, CO, USA, 1996, 76 p. Available online: https://pubs.er.usgs.gov/publication/ofr96256

2. Patterson, C.G.; Toth, M.I.; Kulik, D.M.; Esparza, L.E.; Schmauch, S.W.; Benham, J.R. Mineral Resources of the Pryor Mountain, Burnt Timber Canyon, and Big Horn Tack-On Wilderness Study Areas, Carbon County, Montana and Big Horn County, Wyoming; USGS Bulletin 1723; U.S. Geological Survey: Denver, CO, USA, 1988; pp. 1–15. Available online: https://pubs.er.usgs.gov/publication/b1723

3. Hauptman, C.M. Uranium in the Pryor Mountain area of southern Montana and northern Wyoming. *Uranium Mod. Min.* **1956**, *3*, 14–21.

4. Hart, O.M. Uranium deposits in the Pryor-Big Horn Mountains, Carbon County, Montana, and Big Horn County, Wyoming. In *United Nations 2nd International Conference on Peaceful Uses of Atomic Energy, Proceedings*; 1958, pp. 523-526.

5. Harris, R.E., Uranium and thorium in the Bighorn Basin. In *Geology of the Bighorn Basin, Wyoming Geological Association, 34th annual field conference*; Boberg, W.W., Ed., Guidebook: Wyoming Geological Association, Casper, WY, USA, 1983; pp. 171-177.

6. Hurley, G. Geology and Mineralogy of the Devil Canyon/Little Mountain Area, Northern Big Horn Mountains, Wyoming. In *Resources of the Bighorn Basin*; 47th Annual Field Conference Guidebook; Wyoming Geological Association: Casper, WY, USA, 1996, pp. 281-295.

7. McEldowney, R.C.; Abshier, J.F.; Lootens, D.J. Geology of uranium deposits in the Madison Limestone, Little Mountain area, Big Horn County, Wyoming, in Veal, H.K., ed., Exploration frontiers of the Central and Southern Rockies: Rocky Mountain Association of Geologists, 1977, pp. 321-336.

8. Wilson, W.H. *Radioactive Mineral Deposits of Wyoming Geological Survey of Wyoming*; Report of Investigations; Wyoming Geologic Survey: Laramie, WY, USA, 1960, 7, 41 p.

9. Abandoned Mine Lands Portal. Available online: http://www.abandonedmines.gov/wbd_um.html (accessed on 20 December 2014).

10. Eggers, M.J.; Moore-Nall, A.L.; Doyle, J.T.; Lefthand, M.J.; Young, S.L.; Bends, A.L.; Committee, C.E.H.S.; Camper, A.K. Potential Health Risks from Uranium in Home Well Water: An Investigation by the Apsaalooke (Crow) Tribal Research Group. *Geosciences*, **2015**, 5, 67-94. . doi:10.3390/geosciences5010067 Available online: http://www.mdpi.com/2076-3263/5/1/67

11. Barnhart, E. Differentiating natural vs. anthropogenic mercury inputs and subsequent Se/Hg interactions and biogeochemical cycling in Bighorn Lake, Bighorn Canyon National Recreation Area, Montana and Wyoming. NOROCK EcoLunch and webinar, 24 March 2016; Montana State University, Bozeman, MT, USA.

12. Cummins, C.; Eggers, M.; Hamner, S.; Camper, A.; Ford TE. Mercury levels detected in fish from rivers of the Crow Reservation, Montana. SCREES National Water Conference, 8–11 February; St. Louis, MO., USA, 2009.

13. Montana's Clean Water Act Information Center (MCWAC). Available online: http://deq.mt.gov/wqinfo/cwaic/reports.mcpx (accessed on 14 November, 2015).

14. Warchola, R.J.; Stockton, T.J. *National Uranium Resource Evaluation, Billings Quadrangle, Montana. PGJ/F-015(82)*; Morris & Warchola, Inc., Bendix Field Engineering Corporation, US DOE: Grand Junction, CO, USA, 1982, 33 p.

15. Sahinen, U.M. Fluorspar deposits in Montana. *MBMG Bull.* **1962**, 28, 34-35.

16. US Department of Energy, Billings quadrangle-Residual intensity magnetic anomaly contour map: US Department of Energy, GJM-096, pl.4, 1982.

17. Schultz, R.L. Caves of the Bighorn-Pryor Mountains of Montana and Wyoming. *NSS* **1969**, 10, 1-28.

18. Engel, A.S.; Stern, L.A.; Bennett, P.C. Microbial contributions to cave formation: new insight into sulfuric acid speleogenesis. *Geol.* **2004**, 32, 369-372.

19. Egemeier, S.J. Cavern development by thermal waters with a possible bearing on ore deposition, Ph.D. Dissertation, Stanford University, Stanford, CA, USA, 1973, 88 p.

20. Love, J.D. Vanadium and associated elements in the Phosphoria Formation in the Afton area, western Wyoming: U.S. Geological Survey Professional Paper 424C, 1961, pp. C279-C282.

21. Love, J.D. Vanadium deposits in the Lower Permian Phosphoria Formation, Afton area, Lincoln County, western Wyoming: U.S. Geological Survey Professional Paper 1637, 2003, 28 p.

22. Rubey, W.W. Vanadiferous shale in the Phosphoria Formation, Wyoming and Idaho. (Abstract) *Econ. Geol.*, **1943**, 38, 1, 87.

23. Stone, D.S. Theory of Paleozoic Oil and Gas Accumulation Bighorn Basin Wyoming. *AAPG Bull*. **1967**, 51, 10, 2056-2114.

24. Sheldon, R.P. Long distance migration of oil in Wyoming. *The Mountain Geologist*, **1967**, 4, 53-65.

25. Blackstone, D.L., Jr. Foreland deformation, compression as a cause. *Rocky Mountain Geology* **1980**, 18, 2, 83-100.

26. Blackstone, D.L., Jr. Foreland compressional tectonics: southern Bighorn Basin and adjacent areas, Wyoming. Geological Survey of Wyoming Report of Investigations; Wyoming Geological Survey: Laramie, WY, USA, 1986, 34, 1-27.

27. Blackstone, D.L. Structure of the Pryor Mountains Montana. *J. Geol.* **1940**, 48, 6, 590-618.

28. Blackstone, D.L., Jr. Structural geology, northwest margin, Bighorn Basin, Park County, Wyoming and Carbon County, Montana. In *Geology of the Beartooth uplift and adjacent basins;* Montana Geological Society and Yellowstone Bighorn Research Association, joint Field conference and Symposium; Montana Geological Society: Billings, MT, USA, 1986, pp. 125-135.

29. Stewart, J.C. *Geology of the Dryhead-Garvin Basin, Bighorn and Carbon Counties, Montana: Map G-2*; Montana Bureau of Mines and Geology Special Publication 17; Montana Bureau of Mines and Geology: Montana Tech of the University of Montana, Butte, MT, USA, 1958.

30. Lopez, D. A. Field guide to the northern Pryor Bighorn structural block, south central Montana. Open-File Report 330. Montana Bureau of Mines and Geology, Butte, Montana, USA, 1995.

31. Richards, P.W. *Geology of the Bighorn Canyon-Hardin Area, Montana and Wyoming*; USGS Bull. 1026; USGS: Helena, MT, USA, 1955; pp. 1–93. Available online: http://pubs.usgs.gov/bul/1026/report.pdf

32. Sando, W.J. Madison Limestone (Mississippian) paleokarst: a geologic synthesis. In *Paleokarst*, James, N.P.; Choquette, P.W., Eds.; Springer-Verlag: New York, 1988, pp. 256-277.

33. Sando, W.J. Ancient solution phenomena in the Madison Limestone (Mississippian) of north-central Wyoming. *USGS Journal of Research* **1974**, 2, 133-141.

34. Sando, W.J.; Mamet, B.L. New evidence on the age of the top of the Madison Limestone (Mississippian), Big Horn Mountains, Wyoming and Montana. *USGS Journal of Research* **1974**, 2, 5, 619-624.

35. Bird, P. Stress direction history of the western United States and Mexico since 85 Ma. *Tectonics* **2002**, 21, 3, 1-12.

36. Neely, T.G.; Erslev, E.A. The interplay of fold mechanisms and basement weaknesses at the transition between Laramide basement-involved arches, north-central Wyoming, USA. *J. Struct. Geol.* **2009**, 31, 1012-1027.

37. Brown, W.G. Structural style of Laramide basement-cored uplifts and associated folds. In *Geology of Wyoming*, Snoke, A.; Steidtmann, J.; Roberts, S. Eds. Geological Survey of Wyoming Memoir No. 5, The Geological Survey of Wyoming: Laramie, WY, USA, 1993, pp. 312-371.

38. Dickinson, W. R.; Klute, M. A.; Hayes, M. J.; Janecke, S. U.; Lundin, E. R.; McKittrick, M. A.; Olivares, M.D. Paleogeographic and paleotectonic setting of Laramide sedimentary basins in the central Rocky Mountain region. *Geol. Soc. Am. Bull.* **1988**, 100, 1023-1039.

39. Erslev, E.A. Thrusts, back-thrusts, and detachment of the Rocky Mountain foreland arches. In *Laramide Basement Deformation in the Rocky Mountain Foreland of the Western United States*, Schmidt, C.J., Chase, R.B., Erslev, E.A., Eds.; *Geol. Soc. Am.* Special Paper 280: Boulder, Colorado, USA, 1993, pp. 339-358.

40. Wyoming State Geological Survey website, Oil and Gas map. Available online: http://www.wsgs.wyo.gov/products/wsgs-2016-ms-103.pdf (Accessed: 8 October, 2016).

41. Langmuir, D. Uranium solution-mineral equilibria at low temperatures with applications to sedimentary ore deposits. *Geochim Cosmochim Acta* **1978**, 42, 547-569.

42. Moore-Nall, A.L.; Lageson, D.R.; Uranium Vanadium Mineralization in Mississippian Aged Paleokarst, Northern Bighorn Basin, Montana and Wyoming, Indicates a Hydrothermal Permian Phosphoria Formation Source of Metals

Including REE and Tl. Presented at the GSA Annual Meeting, Denver, Colorado, USA, 9-12 October 2011. Available online: https://gsa.confex.com/gsa/2016AM/webprogram/Paper287959.html (Accessed 13 October 2016).

43. Dickson, J. A. D. A modified technique for carbonates in thin section. *Nature* **1965**, 205, 587- 587.

44. Folk, R.L. Detection of organic matter in thin sections of carbonate rock using a white card. *Sediment. Geol.*, **1987**, 54, 193-200.

45. Serc.Carleton website. Available online: http://serc.carleton.edu/research_education/geochemsheets/bse.html (Accessed: 17 November 2015).

46. Moore-Nall, A.L.; Lageson, D.R. Francevillite [$(Ba,Pb)(UO_2)_2(V_2O_8)\bullet 5H_2O$] identified in the Uranium Vanadium deposits in the Pryor Mountain Mining District, Montana and the Little Mountain Mining District, Wyoming may provide a link to the elevated lead in the Bighorn River and be related to fluid migration of the Lower Kane Cave, Wyoming. Presented at the GSA Annual Meeting, Denver, CO, USA, 27-30 October 2013. Available online: http://www.geosociety.org/meetings/2013/documents/13AM-progALL.pdf (Accessed 10 December, 2015).

47. Francevillite. Available online: http://www.handbookofmineralogy.org/pdfs/francevillite.pdf (Accessed: 21 December 2015).

48. Thallian carnotite. Available online: http://www.mindat.org/min-32379.html (Accessed: 21 December 2015).

49. Carnotite Group. Available online: http://www.mindat.org/min-32551.html (Accessed: 21 December 2015).

50. Burns, P.C.; Finch, R., Eds. Reviews in Mineralogy, Uranium: Mineralogy, Geochemistry and the Environment. Mineralogical Society of America: Washington, D.C., USA, 1999, vol. 38, 680 p.

51. Davies, G.R.; Smith, L.B., Jr. Structurally controlled hydrothermal dolomite reservoir facies: An Overview, *AAPG Bull*. **200**6, 90, 1641-1690.

52. Katz, D.A.; Eberli, G.P.; Swart, P.K.; Smith, L.B. Tectonic-hydrothermal brecciation associated with calcite precipitation and permeability destruction in

Mississippian carbonate reservoirs Montana and Wyoming: *AAPG Bull.* **2006**, 90, 1803–1841.

53. Smith, L. B. Jr.; Eberli, G.P.; Sonnenfeld, M.D. Sequence stratigraphic and paleogeographic distribution of reservoir quality dolomite, Madison Formation, Wyoming and Montana. In *Integration of outcrop and modern analogues in reservoir modeling* Grammer, G.M.; G. P. Eberli, G.P.; Harris, P.M., Eds., *AAPG Memoir* **2004**, 80, 94–118.

54. Westphal, H.; Eberli, G.P.; Smith, L.B.; Grammer, G.M.; Kislak, J. Reservoir characterization of the Mississippian Madison Formation, Wind River Basin, Wyoming. *AAPG Bull.* **2004**, 88, 4, 405–432.

55. Kislak, J.; Smith, L.; Peacock, D.; Eberli, G.; Swart, P. Classification, distribution and origin of hydrothermal breccias, Madison Formation, Wyoming. *AAPG* Annual Meeting Program; **2001**, 10, A105.

56. Beaudoin, N.; Bellahsen, N.;Lacombe, O.; Emmanuel, L. Fracture-controlled paleohydrogeology in a basement-cored, fault-related fold: Sheep Mountain Anticline, Wyoming, United States. *Geochem. Geophys. Geosyst*. **2011**, 12, 6, 1-15.

57. Spötl, C.; J. K. Pitman Saddle (Baroque) Dolomite in Carbonates and Sandstones: A Reappraisal of a Burial-Diagenetic Concept. In *Carbonate Cementation in Sandstones: Distribution Patterns and Geochemical Evolution*, Morad, S., Ed.; Blackwell Publishing Ltd.: Oxford, UK, 1998, ch 19, pp. 437-460.

58. Moore-Nall, A.L.; Lageson, D.R.; Herkimer diamonds in the Pennsylvanian Tensleep Formation may indicate hydrothermal influences for mineralization of the Red Pryor Mountain uranium/vanadium deposits. Presented at the GSA Annual Meeting, Minneapolis, Minnesota, USA, 9-12 October 2011. Available online: https://gsa.confex.com/gsa/2011AM/finalprogram/abstract_198138.htm (Accessed 10 December 2015).

59. Witherite. Available online: http://www.mindat.org/min-4299.html (Accessed: 17 February 2016).

60. Halloysite. Available online: http://www.mindat.org/min-1808.html (Accessed: 17 February 2016).

61. Mariano, A.N. Some further geological applications of cathodoluminescence. In *Cathodoluminescence of Geological Materials*, Marshall, D. J., Ed.; Boston, Unwin Hyman, 1988, 146 p.

62. Cherniak, D.J.; Zhang, X.Y.; Wayne, N.K.; Watson, E.B. Sr, Y, and REE diffusion in fluorite. *Chem. Geol.* **2001**, 181, 99-111.

63. Marshall, D. J. *Cathodoluminescence of Geological Materials*. Boston, Unwin Hyman, 1988, 146 p.

64. Habermann, D.; Neuser, R.D.; Richter, D.K. REE-activated cathodoluminescence of calcite and dolomite: high-resolution spectrometric analysis of CL emission (HRS-CL), *Sed. Geol*. **1996**, 101, 1-7.

65. Summa, L. Results of fluid inclusion work from Pryor Mountains performed at Fluid Inc., Denver, CO. Personal communication via e-mail, 6 December 2011.

66. Reynolds, J.A. In *Description of fluid inclusion work done on Pryor Mountain samples at Fluid Inc.*, submitted for the author by Lori Summa, Senior Technical Consultant, ExxonMobil Upstream Research Company for the authors. Personal communication via e-mail, 2 December 2011.

67. Gromet, P.L., Dymek, R.F., Haskin, L.A., and Korotev, R.L., 1984, The "North American shale composite"—its compilation, major and trace element characteristics: *Geochim Cosmochim Acta* **1984**, 48, 2469–2482.

68. Taylor, S.R.; McLennan, S.M.; Rare Earth Elements in Sedimentary Rocks: Influence of Provenance and Sedimentary Processes. In *Geochemistry and Mineralogy of Rare Earth Elements*, Lipin, R.R.; McKay, G.A., Eds.; Mineralogical Society of America: Washington D.C., USA, 1989; vol. 21, pp. 169-200.

69. McKelvey, V.E.; Williams, J.S.; Sheldon, R.P.; Cressman, E.R.; Cheney, T.M.; Swanson, R.W. The Phosphoria, Park City, and Shedhorn Formations in the Western Phosphate Field: U.S. Geological Survey Professional Paper 313-A, 1959, 47 p.

70. Sheldon, R.P. Physical Stratigraphy and Mineral Resources of Permian Rocks in Western Wyoming: U.S. Geological Survey, Professional Paper 313-B, 1963, 273 p.

71. Gulbrandsen, R.A.; Reeser, D.W. An occurrence of Permian manganese nodules near Dillon, Montana. U.S. Geological Survey Professional Paper 650-C, 1969, pp. C49-C57.

72. Gulbrandsen, R.A. Analytical data on the Phosphoria Formation Western United States. U.S. Geological Survey Open-file report 75-554: US Gov. Printing office, Washington, D.C., USA, 1975, 45 p. Available online: http://pubs.usgs.gov/of/1975/0554/report.pdf (Accessed: 17 February 2016).

73. McKelvey, V.E; Strobell, J.D., Jr.; Slaughter, A.L. The vanadiferous zone of the Phosphoria Formation in western Wyoming and southeastern Idaho: U.S. Geological Survey, Professional Paper 1465, 1986, 27p.

74. Medrano, M. D.; D. Z. Piper Partition of minor elements and major-element oxides between rock components and calculation of the marine-derived fraction of the minor elements in rocks of the Phosphoria Formation, Idaho and Wyoming: U.S. Geological Survey Open-File Report 95-270, 1995, 79 p.

75. Piper, D.Z. Trace elements and major-element oxides in the Phosphoria Formation at Enoch Valley, Idaho; Permian sources and current reactivities: U.S. Geological Survey Open File Report 99-0163, 1999, 66 p.

76. Piper, D.Z.; Skorupa, J.P.; Presser, T.S.; Hardy, M.A.; Hamilton, S.J.; Huebner, M.; Gulbrandsen, R.A. The Phosphoria Formation at the Hot Springs mine in Southeast Idaho: a source of selenium and other trace elements to surface water, ground water, vegetation, and biota. U.S. Geological Survey Open-File Report 00-050, 2000, 73 p.

77. Moyle, P.R.; Causey, D.J. Chemical Composition of Samples Collected from Waste Rock Dumps and Other Mining-Related Features at Selected Phosphate Mines in Southeastern Idaho, Western Wyoming, and Northern Utah. U.S. Geological Survey Open-File Report 01-411, 2001, 46p.

78. Hein, J.R.; McIntyre, B.; Perkins; R.B.; Piper, D.Z.; Evans, J. Composition of the Rex Chert and associated rocks of the Permian Phosphoria Formation: Soda Springs area, SE Idaho, U.S. Geological Survey Open File Report 02-345, 2002, 30 p.

79. Perkins, R.B.; McIntyre, B.; Hein, J.R.; Piper, D.Z. Geochemistry of Permian rocks from the margins of the Phosphoria Basin: Lakeridge core, Western Wyoming, U.S. Geological Survey Open File Report 03-21, 2003, 60 p.

80. Emsbo, P.; McLaughlin, P.I.; Breit, G.N.; du Bray, E.A.; Koenig, A.E. Rare earth elements in sedimentary phosphate deposits: Solution to the global REE crisis? *Gondwana Res*, **2015**, 27, 776–785. Available online: http://www.sciencedirect.com/science/article/pii/S1342937X14003128 (Accessed: 27 March 2016).

81. Jasinski, S.M. Phosphate rock. U.S. Geological Survey Mineral Commodity Summaries, 2011, pp. 118–119.

82. Carnes, J.D. Phosphate rock in Wyoming: Wyoming State Geological Survey Report of Investigations No. 68, 2015, 34 p.

83. Goldberg, E.D. Chemistry in the Oceans. In *Oceanography*, Sears, M., Ed.; *Am. Assoc. Advance. Sci. Publ.* **1961**, 67, 583-597.

84. Elderfield, H.; Greaves, M. The rare earth elements in seawater. *Nature* **1982**, 296, 214–219.

85. Sholkovitz, E.R. Ocean particle chemistry: the fractionation of rare earth elements between suspended particles and seawater. *Geochim Cosmochim Acta* **1994**, 58, 1567–1579.

86. Lillis, P.G.; Selby, D. Evaluation of the rhenium–osmium geochronometer in the Phosphoria petroleum system, Bighorn Basin of Wyoming and Montana, USA. *Geochim. Cosmochim. Acta* **2013**, 118, 312–330.

87. Meyer, R.F.; Attanasi, E.D.; Freeman, P.A. Heavy oil and natural bitumen resources in geological basins of the world: U.S. Geological Survey Open-File Report 2007-1084, 2007, Available online: http://pubs.usgs.gov/of/2007/1084/ (Accessed October, 2016).

88. Hollerbach, A. Influence of Biodegradation on the Chemical Composition of Heavy Oil and Bitumen: Characterization, Maturation, and Degradation. In Section II Exploration for Heavy Crude Oil and Natural Bitumen, Meyer, R.F., Ed.; AAPG Studies in Geology: Tulsa, OK, USA, 1997, pp. 243-247.

89. Langmuir, D. Uranium solution-mineral equilibria at low temperatures with applications to sedimentary ore deposits. *Geochim Cosmochim Acta* **1978**, 42, 547-569.

90. Finch, R.; Murakami, T. Systematics and Paragenesis of Uranium Minerals. In Reviews in Mineralogy, Uranium: Mineralogy, Geochemistry and the Environment, Burns, P.C.; Finch, R., Eds.; Mineralogical Society of America: Washington, D.C., USA, 1999, vol. 38, pp. 91-179.

91. Garrels, R.M.; Christ, C.L. Behavior of uranium minerals during oxidation. In Geochemistry and Mineralogy of the Colorado Plateau Uranium Ores, Garrels, R.M., Larsen, E.S., Eds.; USGS Prof. Paper 320: Washington, D.C., USA, 1959, pp. 81-90.

92. Phillips, W.J. Hydraulic fracturing and mineralization. *J. Geol. Soc.* **1972**, 128, 337-359.

93. Sibson, R.H.; Moore, J. McM.; Rankin, A.H. Seismic pumping-a hydrothermal fluid transport mechanism. *J. Geol. Soc. of London* **1975**, 131, 6, 653-659.

94. Du Bray, E.A.; Harlan, S.S. Geology and tectonic setting of the Cretaceous Sliderock Mountain volcano, Montana. U.S. Geological Survey professional paper 1602, 1998, 19 p. Available online: http://pubs.er.usgs.gov/publication/pp1602 (Accessed: 10 December 2015).

95. Brozdowski, R.A. Geologic setting and xenoliths of the Lodgepole intrusive area - Implications for the northern extent of the Stillwater Complex, Montana: Philadelphia, Pa., Temple University, unpublished Ph.D. dissertation, 1983, 322 p.

96. Stock, G.M.; Riihimaki, C.A.; Anderson, R.S. Age constraints on cave development and landscape evolution in the Bighorn Basin of Wyoming, USA. J *Cave Karst Stud* **2006**, 68, 2, 76–84.

97. Ikramuddin, M.; Asmeron, Y.; Nordstrom, P.M.; Kinart, K.P.; Martin, W.M.; Digby, S.J.M.; Elder, D.D.; Nijak, W.F.; Afemari, A.A. Thallium: a potential guide to mineral deposits. *J. Geochem. Explor.* **1983,** 19, 465--490.

98. De Albuquerque, C.A.R.; Shaw, D.M. Thallium. In Wedepohl, K.H., Ed.; Handbook of geochemistry, Berlin: Springer-Verlag, 1972, 81-D-1–81-D-18.

99. Berger, B.R. Descriptive model of carbonate-hosted Au-Ag. In Cox, D.P.; Singer, D.A., Eds.; Mineral deposit models: U.S. Geological Survey Bulletin 1693, 1986, 175 p.

100. Berger, B.R.; Bagby, W.C. The geology and origin of Carlin-type gold deposits. In *Gold Metallogeny and Exploration*, Foster, R.P., Ed.; Blackie and Son Ltd: Glasgow, Scotland, 1990, pp. 210-248.

101. Trexler, J.H., Jr.; Cashman, P.H.; Cole, J.C.; Snyder, W.S.; Tosdal, R.M.; V.I. Davydov Widespread effects of middle Mississippian deformation in the Great Basin of western North America. *Geol. Soc. Am. Bull.* **2003**, 115, 1278-1288.

102. Kluth, C.F.; Coney, P.J. Plate tectonics of the Ancestral Rocky Mountains. *Geology* **1981**, 9, 10-15.

103. Speed, R.C. Collided Paleozoic microplate in the western United States. *J Geol* **1979**, 89, 279-292.

104. Heller, P.L.; Bowdler, S.S.; Chambers, H.P.; Coogan, J.C.; Hagen, E.S.; Shuster, M.W.; Winslow, N.S. Time of initial thrusting in the Sevier orogenic belt, Idaho-Wyoming and Utah. *Geology*, **1986**, 14, 388-391.

105. Blackstone, D.L. Jr.; P.W. Huntoon Tectonic structures responsible for anisotropic transmissivities in the Paleozoic aquifers of the southern Bighorn Basin: Wyoming:

U.S. Geological Survey Research Project Technical Completion Report G-879, 1984, no. 2, pp. 1-74.

106. Lanphere, M.A.; Champion, D.E.; Christiansen, R.L.; Izett, G.A.; Obradovich, J.D. Revised ages for tuffs of the Yellowstone Plateau volcanic field: Assignment of the Huckleberry Ridge Tuff to a new geomagnetic polarity event. *Geol. Soc. Am. Bull.* **2002**, 114, 5, 559-568.

107. Tilling, R.I.; Klepper, M.R.; Obradovich, J.D. K-Ar ages and time span of emplacement of the Boulder Batholith, Montana *Amer J Sci* **1968**, 266, 8, 671-689.

108. Hiza, M. The Geologic History of the Absaroka Volcanic Province, *Yellowstone Science*. **1998**, 6, 2, 2-7. Available online: https://www.nps.gov/yell/learn/upload/YS_6_2_sm.pdf (Accessed 7, December 2016).

109. Smedes, H.W.; Thomas, H.H. Reassignment of the Lowland Creek Volcanics to Eocene Age. *J Geol* **1965**, 73, 3, 508-510.

110. Skipp, B.; McGrew, L.W. The Maudlow and Sedan Formations of the Upper Cretaceous Livingston Group on the west edge of the Crazy Mountains Basin, Montana. (Contributions to stratigraphy), Geological Survey Bulletin 1422-B, 1977.

111. Sadeghi, S.; Sheikhzadeh, E. Solid phase extraction using silica gel modified with murexide for preconcentration of uranium (VI) ions from water samples. *J. Hazard Mater.* **2009**, 163, 2, 861-868.

112. Allen, J.; Berlin, M.; Hughes, M.; Johnston, E.; Kailasam, V.; Rosenberg, E.; Sardot, T.; Wood, J.; Hart, C. Structural design at the polymer surface interface in nanoporous silica polyamine composites. *Mater. Chem. Phys.* **2011**, 126, 973-982.

113. Rosenberg, E.; Pang, D. Inventors 1999.

114. Rosenberg E, Pang D. Inventors 1997.

115. Allen, J.J.; Rosenberg. E.; Johnston, E.; Hart, C. Sol-gel synthesis and characterization of silica polyamine composites: Applications to metal ion capture. *ACS Appl. Mater. Interfaces* **2012**, 4, 3-1573.

116. Hughes, M.A.; Nielsen, D.; Rosenberg, E.; Gobetto, R.; Viale, A.; Burton, S.D.; Ferel, J. Structural investigations of silica polyamine composites: Surface coverage, metal ion coordination, and ligand modification. *Ind. Eng. Chem. Res.* **2006**, 45, 19 6538-6547.

117. Kailasam, V.; Rosenberg, E.; Nielsen, D. Characterization of surface-bound Zr(IV) and its application to removal of As(V) and As(III) from aqueous systems using phosphonic acid modified nanoporous silica polyamine composites. *Ind. Eng. Chem. Res.* **2009**, 48, 8, 3991-4001.

118. Hughes, M.A.; Rosenberg, E. Characterization and applications of poly-acetate modified silica polyamine composites. *Sep. Sci. Technol.* **2007**, 42, 2, 261-283.

119. Kailasam, V. The removal and recovery of oxo-anions from aqueous systems using nano-porous silica polyamine composites, PhD Dissertation, University of Montana, Missoula, MT, 2009.

120. Hughes, M.; Miranda, P.; Nielsen, D.; Edward Rosenberg, E.; Gobetto, R.; Alessandra Viale, A.; Burton, S. Silica polyamine composites: New supramolecular materials for cation and anion recovery and remediation. *Macromol. Symp*. **2006**, 235, 1, 161–178.

121. Taylor, S.R.; McLennan, S.M.; The Continental Crust: its Composition and Evolution. Blackwell Scientific Publishing: Oxford, UK, 1985, pp. 312.

122. Mulkey J.P.; Oehme, F.W. A review of thallium toxicity. *Vet Hum Toxicol* **1993**, 35, 445–53.

123. Thallium element information. Available on line: http://www.rsc.org/periodic-table/element/81/thallium (Accessed: 17 February 2016).

124. Xiao, T.; Yang, F.; Li, S.; Zheng, B.; Ning, Z. Thallium pollution in China: A geo-environmental perspective. *Sci Total Environ* **2012**, 421-422, 51–58.

125. Haynes, W.M.; Ed., CRC Handbook of Chemistry and Physics. CRC Press/Taylor and Francis: Boca Raton, FL, USA, 95th Edition, 2012, 2664 p.

126. Eggers, M. Results of Tl MS-ICP analyses of drinking water well samples from the Crow Reservation performed at University of New Mexico, Albuquerque, NM. Personal communication via e-mail, 2 May 2016

CHAPTER 6

SUMMARY

The goal of this research project was to investigate the geology of the portions of the Pryor Mountains, Montana and northern Bighorn Mountains, Wyoming that host two abandoned uranium and vanadium mining districts. Originally the study was implemented to see if these areas may provide a geological source for the contaminants lead (Pb) and mercury (Hg) in the Bighorn River. As the study progressed, literature and data research showed elevated uranium in home water wells was also an issue on the Crow Reservation. I learned a lot about how widespread uranium in water is on many Indian Reservations during the course of this study. Of course, the uranium contamination is also of concern to the health of the general public that do not live on Indian Reservations. The difference, though, is that there are many factors and health disparities related to the life on the reservation; issues such as water quality that might not be recognized by the greater U.S. population and regulating authorities addressing different aspects of the issues involved. Often there are not academic partners and little funding available for research in these areas. If uranium or other contaminants were found in a community that had more financial capabilities, many of these issues would be addressed in a timelier manner.

In Chapter 2 of this dissertation, though not directly a result of the uranium mining in the PMD and the LMD, I present some of the impacts uranium mining has had on many reservations. The mobility of uranium in especially oxidized fluids is of concern

in many areas that have either naturally occurring uranium or uranium that was introduced to the area from an outside source such as the processing mill near the Wind River Indian Reservation where ore from this study was processed. The health of people everywhere that have been or are still being exposed to uranium contamination is of concern. The chapter focuses on uranium but other contaminants have impacted the health of Native American people living on or near reservations where natural resources occur and or have been developed.

Chapter 3 examines the health risks from uranium contaminated drinking water. Though the source of the uranium is not known the risks are still real. A community based participatory research project started with the need for better water quality on the reservation. This will be an ongoing future project that I will likely be involved in in some capacity. This chapter shows how community involved research can bring about changes from cooperative research. Often research conducted on Indian Reservations was not communicated back with the people. This resulted in research not always being welcomed on reservations and viewed as invasive or simple inconsequential. With community based participatory research projects such as this one and more Native American students being a part of projects such as this, there may be hope for raising awareness and addressing issues that have long been a part of life on the reservation. Health issues that are sometimes unique to people living on the reservation may be better understood and possibly solutions will be found to improve the quality of life for the people on the reservation.

In Chapter 4, I use geochemistry to characterize the cements of breccias and minerals to establish the origin of fluids that migrated into the deposits. I learned a lot about the process of tectonic brecciation during the course of my studies at MSU. I present stable C, O, and radiogenic Sr isotope data to support the episodic hydrothermal nature of tectonic brecciation that is present in both mining districts of this study. I did a computer aided lineament analysis of the study area and then a field based fracture analysis to investigate the nature of the breccias present in the districts. I examined fracture analysis data from siliceous tectonic breccias only present in the Pryor Mountain Mining District as well as other fracture data associated with the host rocks to evaluate whether there was a structural control of mineralized versus unmineralized breccias. I presented just the breccia data as that seemed most relevant to this study. I determined that the main structural control of the mineralization is due to the proximity of the breccias to the ruptured Crooked Creek fault. The folding that produced the Pryor Mountains introduced fractures and also enhanced collapse brecciation in paleokarst. Ultimately the fractures provided pathways for migrating fluids.

The last Chapter 5, extends the previous chapter by examining the mineralization of the uranium and vanadium deposits and concludes that the source of the metals in the deposits was oil derived from the Bighorn Basin. The chapter concludes with a section on the development of silica polyamine composites (SPC's) to aid in removal of U and other toxic metals from contaminated drinking water to tie in with Chapter 3 of U in home well water. The research is also a collaborative effort between tribal participants and academic partners which will likely evolve into future projects.

In summary I feel that the exact source for contaminants in the Bighorn River and the uranium in home wells has not been specifically identified with this research. Hg and Pb was shown to be elevated in the two mining districts in this study. This supports the elevated concentrations in NURE stream sediment data in the PMD. This research, however, has been important because it has made people aware of uranium in their drinking water on the Crow Reservation. Cooperative research between other reservations and academic partners involving Native American students is also a contribution of this research. This dissertation will also add to the data base of Sr, C and O isotope and REE data for the Bighorn Basin and to the tectonic hydrothermal breccias present in this part of the basin.

The research may increase our understanding of how much we really do not know about all the processes involved as metals in fluids migrate through the environment. Microbial influences are becoming more understood in all aspects of science. Though this topic was lightly addressed as it was beyond the scope of this dissertation, it is an area that is of importance in understanding how elements move through the environment. The Pb, Hg, and other metals may have been mobilized by microbial processes. Thus, understanding the complex ways that microbes use energy sources such as the light hydrocarbon fractions of oil and the byproducts of these metabolic processes may aid in understanding how some metals are mobilized and others are “demobilized” in contaminated reservoirs. Microbes have been used for bioremediation. Those that are present in radioactive environments may aid in cleaning up nuclear waste and naturally occurring U and its byproducts.

CUMULATIVE REFERENCES

1. Abandoned Mine Lands Portal. Available online: http://www.abandonedmines.gov/wbd_um.html (accessed on 20 December 2014).

2. Agencies Cite Progress, Work Still Remaining on Navajo Uranium Cleanup. Chronkite News, 24 January 2013. Available online: http://cronkitenewsonline.com/2013/01/agencies-cite-progress-work-still-remaining-on-navajo-uranium-cleanup/ (accessed on 8 December 2014).

3. Agency for Toxic Substances and Disease Registry, U.S. Department of Health and Human Services. Toxicological Profile for Uranium; ATSDR: Atlanta, GA, USA, 2013.

4. Agency for Toxic Substances and Disease Registry, U.S. Department of Health and Human Services. Toxicological Profile for Uranium; ATSDR: Atlanta, GA, USA, 2013.

5. Ali, S.H. Mining, the Environment, and Indigenous Development Conflicts; The University of Arizona Press: Tucson, AZ, USA, 2003; p. 254.

6. Allan, J. R.; Wiggins, W.D. Dolomite reservoirs, geochemical techniques for evaluating origin and distribution: *AAPG* Continuing Education Course Note Series 1993, 36, 129 p.

7. Allen, J.; Berlin, M.; Hughes, M.; Johnston, E.; Kailasam, V.; Rosenberg, E.; Sardot, T.; Wood, J.; Hart, C. Structural design at the polymer surface interface in nanoporous silica polyamine composites. *Mater. Chem. Phys*. **2011**, 126, 973-982.

8. Allen, J.J.; Rosenberg. E.; Johnston, E.; Hart, C. Sol-gel synthesis and characterization of silica polyamine composites: Applications to metal ion capture. *ACS Appl. Mater. Interfaces* **2012**, 4, 3-1573.

9. Arnold, C. Once upon a mine: The legacy of uranium on the Navajo Nation. *Environ. Health Perspect*. **2014**, 122, A44–A49.

10. Arthur, M.A.; Anderson, T.F.; Kaplan, I.R.; Veizer, J.; Land, L.S. Stable isotopes in sedimentary geology: *SEPM* Short Course, **1983**, 10, 5–54.

11. Arzuaga, X.; Rieth, S.H.; Bathija, A.; Cooper, G.S. Renal effects of exposure to natural and depleted uranium: A review of the epidemiologic and experimental data. *J. Toxicol. Environ. Health B Crit. Rev.* **2010**, 13, 527–545.

12. Balazs, C.L.; Ray, I. The drinking water disparities framework: On the origins and persistence of inequities in exposure. *Am. J. Public Health* **2014**, 104, 603–611.

13. Barnhart, E. Differentiating natural vs. anthropogenic mercury inputs and subsequent Se/Hg interactions and biogeochemical cycling in Bighorn Lake, Bighorn Canyon National Recreation Area, Montana and Wyoming. NOROCK EcoLunch and webinar, 24 March 2016; Montana State University, Bozeman, MT, USA

14. Barrington, J.; Kerr, P.F. Collapse Features and Silica Plugs near Cameron, Arizona: *Geol. Soc. Am. Bull.* **1963,** 74, 1237-1258.

15. Beaudoin, N.; Bellahsen, N.;Lacombe, O.; Emmanuel, L. Fracture-controlled paleohydrogeology in a basement-cored, fault-related fold: Sheep Mountain Anticline, Wyoming, United States. *Geochem. Geophys. Geosyst*. **2011**, 12, 6, 1-15.

16. Bends, A.L. Health Disparities on the Crow Reservation; Center for Native Health Partnerships, Montana State University: Bozeman, MT, USA, 2010, unpublished data.

17. Berger, B.R. Descriptive model of carbonate-hosted Au-Ag. In Cox, D.P.; Singer, D.A., Eds.; Mineral deposit models: U.S. Geological Survey Bulletin 1693, 1986, 175 p.

18. Berger, B.R.; Bagby, W.C. The geology and origin of Carlin-type gold deposits. In Foster, R.P., Ed.; Gold Metallogeny and Exploration. Blackie and Son Ltd: Glasgow, Scotland, 1990, p. 210-248.

19. Bird, P. Stress direction history of the western United States and Mexico since 85 Ma. *Tectonics* **2002**, 21, 3, 1-12.

20. Blackstone, D. L., Jr. Structure of the Pryor Mountains, Montana: *J Geol* **1940**, 48, 6, 590-618.

21. Blackstone, D.L., Jr. Preliminary geologic map of the Red Pryor Mountain 7.5' quadrangle, Carbon County, Montana: Montana Bureau of Mines and Geology Open File Report 68, 1:24,000, 1974a.

22. Blackstone, D.L., Jr. Preliminary geologic map of the Section House Draw 7.5' quadrangle, Big Horn and Carbon County, Montana: Montana Bureau of Mines and Geology Open File Report 69, 1:24,000, 1974b.

23. Blackstone, D.L., Jr. Preliminary geologic map of the Mystery Cave 7.5' quadrangle, Big Horn and Carbon County, Montana: Montana Bureau of Mines and Geology Open File Report 70, 1:24,000, 1974c.

24. Blackstone, D.L., Jr. Foreland deformation, compression as a cause. *Rocky Mountain Geology* **1980**, 18, 2, 83-100.

25. Blackstone, D.L., Jr. Structural geology, northwest margin, Bighorn Basin, Park County, Wyoming and Carbon County, Montana. In Geology of the Beartooth uplift and adjacent basins; Montana Geological Society and Yellowstone Bighorn Research Association, joint Field conference and Symposium; Montana Geological Society: Billings, MT, USA, 1986, pp. 125-135.

26. Blackstone, D.L. Jr.; P.W. Huntoon Tectonic structures responsible for anisotropic transmissivities in the Paleozoic aquifers of the southern Bighorn Basin: Wyoming: U.S. Geological Survey Research Project Technical Completion Report G-879, 1984, 2, 1-74.

27. Broadhead and Robertson, 1993, Introduction to the atlas, in Robertson, J.M., and Broadhead, R.F., eds., Atlas of major Rocky Mountain gas reservoirs: New Mexico Bureau of Mines and Mineral Resources, 206 p.

28. Brown, W. G., 1993, Structural style of Laramide basement-cored uplifts and associated folds, in Snoke, A. W., Steidtmann, J. R., and Roberts, S. M., eds., Geology of Wyoming: Geological Survey of Wyoming Memoir, no. 5, p. 312-371.

29. Brozdowski, R.A. Geologic setting and xenoliths of the Lodgepole intrusive area - Implications for the northern extent of the Stillwater Complex, Montana: Philadelphia, Pa., Temple University, unpublished Ph.D. dissertation, 1983, 322 p.

30. Brugge, D.; Benally, T.; Harrison, P.; Austin-Garrison, M.; Begay, L.F. Memories come to US in the rain and the wind: Oral histories and photographs of Navajo Uranium miners and their families. In *The Navajo Uranium Miner Oral History and Photography Project*; Tufts School of Medicine: Boston, MA, USA, 1997; pp. 1-63.

31. Brugge, D.; Benally, T. Navajo Indian voices and faces testify to the legacy of uranium mining. *Cult. Surviv. Q.* **1998**, 22, 16–19.

32. Brugge, D.; Benally, T.; Harrison, P.; Austin-Garrison, M.; Stilwell, C.; Elsner, M.; Bomboy, K.; Johnson, H.; Fasthorse-Begay, L. The Navajo Uranium miner oral history and photography project. In Dine Baa Hane Bi Naaltsoos: Collected Papers from the Seventh through the Tenth Navajo Studies Conferences; Piper, J., Ed.; Navajo Nation Historic Preservation Department: Window Rock, AZ, USA, 1999; pp. 85–96.

33. Brugge, D.; Goble, R. The history of Uranium mining and the Navajo people. *Am. J. Public Health* **2002**, 92, 1410–1419.

34. Brugge, D.; Goble, R. A documentary history of Uranium mining and the Navajo people. In The Navajo People and Uranium Mining; Brugge, D., Benally, T., Yazzie-Lewis, E., Eds.; UNM Press: Albuquerque, NM, USA, 2007; pp. 25–47.

35. Brugge, D.; de Lemos, J.L.; Oldmixon, B. Exposure pathways and health effects associated with chemical and radiological toxicity of natural uranium: A review. *Rev. Environ. Health* **2005**, 20, 177–193.

36. Brugge, D.; de Lemos, J.L. The Sequoyah Corporation fuels release and the church rock spill: Unpublicized nuclear releases in American Indian communities. *Am. J. Public Health* **2007**, 97, 1595–1600.

37. Brugge, D.; Buchner, V. Health effects of uranium: New research findings. *Rev. Environ. Health* **2011**, 26, 231–249.

38. BLM. Crow Natural, Socio-Economic and Cultural Resources Assessment and Conditions Report, Hydrology; BLM: Billings, MT, USA, 2002; pp. 74–84. Available online: http://www.blm.gov/style/medialib/blm/mt/field_offices/miles_city/og_eis/ crow.Par.48024.File.dat/hydrology.pdf (accessed on 10 December 2014).

39. Bureau of Land Management Montana State Office. Crow Indian Tribe: Geology and Minerals Resources Report; BLM: Billings, MT, USA, 2002; pp. 67–73. Available online: http://www.blm.gov/style/medialib/blm/mt/field_offices/miles_city/og_eis/crow.Par.79832.File.dat/minerals.pdf (accessed on 10 December 2014).

40. Burns, P.C.; Finch, R., Eds. Reviews in Mineralogy, Uranium: Mineralogy, Geochemistry and the Environment. Mineralogical Society of America: Washington, D.C., USA, 1999, vol. 38, 680 p.

41. Butterfield, P.G.; Hill, W.; Postma, J.; Butterfield, P.W.; Odom-Maryon, T. Effectiveness of a household environmental health intervention delivered by rural public health nurses. *Am. J. Public Health* **2011**, 101, S262–S270.

42. Caldwell, R. Technical Announcement. USGS Samples for Radioactive Constituents in Groundwater of Southwestern Montana. Available online: http://mt.water.usgs.gov/ (accessed on 7 August 2013).

43. Collman, G.W. Community-based approaches to environmental health research around the globe. *Rev. Environ. Health* **2014**, 29, 125–128.

44. Caldwell, R. Uranium and Other Radioactive Elements in Jefferson County Ground Water; U.S. Geological Survey: Helena, MT, USA, 2008.

45. Carnes, J.D. Phosphate rock in Wyoming: Wyoming State Geological Survey Report of Investigations No. 68, 2015, 34 p.

46. Carnotite Group. Available online: http://www.mindat.org/min-32551.html (Accessed: 21 December 2015).

47. CDC Navajo Uranium Impact Studies: Dr. Johnnye Lewis. Available online: https://lajicarita.wordpress.com/2012/08/31/cdc-navajo-uranium-impact-studies-dr-johnnye-lewis/ (accessed on 7 December 2014).

48. Centers for Disease Control and Prevention, HTDS Guide—How the Study Was Conducted. Available online: http://www.cdc.gov/nceh/radiation/hanford/htdsweb/guide/conduct.htm (accessed on 16 January 2015).

49. Census 2010 Brief: The American Indian and Alaska Native population: 2010. Available online: http://www.census.gov/prod/cen2010/briefs/c2010br-10.pdf (accessed on 11 March 2013).

50. Cherniak, D.J.; Zhang, X.Y.; Wayne, N.K.; Watson, E.B. Sr, Y, and REE diffusion in fluorite. *Chem. Geol*. **2001**, 181, 99-111.

51. Churchhill, W. A breach of trust. In *Acts of Rebellion: The Ward Churchill Reader; Routledge*: London, UK, 2002; pp. 103–130.

52. Cleanup of Midnite Mine on Reservation to Begin by 2015. The Spokesman-Review. Available online: http://www.spokesman.com/stories/2013/nov/21/cleanup-of-midnite-mine-on-reservation-to-begin/ (accessed on 8 December 2014).

53. Creed, J.T.; Brockhoff, C.A.; Martin, T.D. Method 200.8. Determination of Trace Elements in Waters and Wastes by Inductively Coupled Plasma-Mass Spectrometry, Revision 5.4., EMCC Version; U.S. Environmental Protection Agency: Cincinnati, OH, USA. Available online: http://water.epa.gov/scitech/methods/cwa/bioindicators/upload/2007_07_10_methods_method_200_8.pdf (accessed on 5 March 2015).

54. Cummins, C., Eggers, M., Hamner, S., Camper, A., Ford, T.E. Mercury levels detected in fish from rivers of the Crow Reservation, Montana. Poster presented at: 2009 SCREES National Water Conference; February 8-11, 2009; St. Louis, MO.

55. Cummins, C.; Doyle, J.; Kindness, L.; Young, S.; Ford, T.; Eggers, M. Community Based Risk Assessment of Exposure to Contaminants via Water Sources on the

Crow Reservation in Montana. In *Proceedings of the EPA National Tribal Science Forum*, Traverse City, MI, USA, 6-10 June 2010.

56. Cummins, C.; Doyle, J., Kindness, L.; Lefthand, M.J.; Bear Don't Walk, U.J.; Bends, A.L., Broadway; S.C., Camper, A.K.; Fitch, R.; Ford, T.E.; et al. Community-based participatory research in Indian country: Improving health through water quality research and awareness, *Fam Comm Health*, **2010**, 33, 166–174.

57. Davies, G.R.; Smith, L.B. Structurally controlled hydrothermal dolomite reservoir facies: An overview: *AAPG Bull.* **2006**, 90, 11, 1641–1690.

58. Dawson, S.E.; Madsen, G.E. Uranium Mine Workers, Atomic Downwinders, and the Radiation Exposure Compensation Act (RECA). In *Half-Lives & Half-Truths, Confronting the Radioactive Legacies of the Cold War*; Johnston, B.R., Ed.; School for Advanced Research Press: Sante Fe, NM, USA, 2007; pp. 117–143.

59. Day, G.E.; Lanier, A.P. Alaska native mortality, 1979–1998. *Public Health Rep*. **2003**, 118, 518–530.

60. De Albuquerque, C.A.R.; Shaw, D.M. Thallium. In *Handbook of geochemistry*, Wedepohl, K.H., Ed.; Berlin: Springer-Verlag, 1972, 81-D-1–81-D-18.

61. De Lemos, J.L.; Bostick, B.C.; Quicksall, A.N.; Landis, J.D.; George, C.C.; Slagowski, N.L.; Rock, T.; Brugge, D.; Lewis, J.; Durant, J.L.; Rapid dissolution of soluble Uranyl phases in arid, mine-impacted catchments near Church Rock, NM. *Environ. Sci. Technol.* **2008**, 42, 3951–3957.

62. De Lemos, J.L.; Burgge, D.; Cajero, M.; Downs, M.; Durant, J.L.; George, C.M.; Henio-Adeky, S.; Nez, T.; Manning, T.; Rock, T.; Seschillie, B.; Shuey, C.; Lewis, J. Development of risk maps to minimize uranium exposures in the Native Churchrock Mining District. *Environ. Health* **2009**, 8, 29, doi:10.1186/1476-069X-8-29.

63. Department of Energy Hanford. Hanford Overview and History. Available online: http://www.hanford.gov/page.cfm/HanfordOverviewandHistory (accessed on 28 December 2014).

64. DeSimone, L.A. Quality of Water from Domestic Wells in Principal Aquifers of the United States, 1991–2004; U.S. Geological Survey Scientific Investigations Report 2008-5227; U.S. Geological Survey: Reston, VA, USA, 2009.

65. Dicken, A.P., 2005, Radiogenic Isotope Geology, Second Edition, Cambridge University Press, New York, 492 p.

66. Dickinson, W. R.; Klute, M. A.; Hayes, M. J.; Janacek, S. U.; Lundin, E. R.; McKittrick, M. A.; Olivares, M. D. Paleogeographic and paleotectonic setting of Laramide sedimentary basins in the Rocky Mountain region: *Geol. Soc. Am. Bull.* **1988**, 100, 1023–1039.

67. Dickson, J.A.D. A modified technique for carbonates in thin section, *Nature*, **1965**, 205, 587-587.

68. Dixon, M.; Roubideaux, Y. Promises to Keep: Public Health Policy for American Indians and Alaska Natives in the 21st Century; American Public Health Association: Washington, DC, USA, 2001, 311 p.

69. Doyle, J.T.; Kindness, L.; Bear Don't Walk, U.J.; Realbird, J.; Eggers, M.J.; Bends, A.L.; Crow Environmental Health Steering Committee; Camper, A.K. For as Long as the Grass Shall Grow and the Rivers Shall Flow: Making Clean Water a Sovereign Responsibility. Plenary Talk. In *Proceedings of the National Congress of American Indians Tribal Leader/Scholar Forum*, Lincoln, NE, USA, 2012.

70. Doyle, J.T.; Kindness, L.; Bends, A.L.; Eggers, M.J.; Coyote, T.J.O.; Crow Environmental Health Steering Committee; Camper, A.K. For as Long as the Grass Shall Grow and the Rivers Shall Flow: Clean Water, a Sovereign Responsibility. In *Proceedings of National Congress of American Indians Tribal Leader/Scholar Forum*, Lincoln, NE, USA, 2012.

71. Doyle, J.T.; Redsteer, M.H.; Eggers, M.J. Exploring effects of climate change on Northern Plains American Indian health. *Clim. Chang.* **2013**, 120, 643–655.

72. Du Bray, E.A.; Harlan, S.S. Geology and tectonic setting of the Cretaceous Sliderock Mountain volcano, Montana. U.S. Geological Survey professional paper 1602, 1998, 19 p. Available online: http://pubs.er.usgs.gov/publication/pp1602 (Accessed: 10 December 2015).

73. Dufault, R., 2005, In another country: Indian Country Environmental Hazard Assessment Training Project seeks IH instructors and mentors. Synergist. Available online: http://www.epa.gov/air//tribal/pdfs/synergistarticle.pdf (Accessed: 10 December 2015).

74. Egemeier, S. J., 1973, Cave development by thermal waters with a possible bearing on ore deposition, Ph.D. dissertation: Stanford University, CA, USA, 88 p.

75. Egemeier, S. J. Cave development by thermal waters, *NSS* **1981**, 43, 2, 31-51.

76. Eggers, M. Results of Tl MS-ICP analyses of drinking water well samples from the Crow Reservation performed at University of New Mexico, Albuquerque, NM. Personal communication via e-mail, 2 May 2016

77. Eggers, M.J.; Cummins, C.; Crow Environmental Health Steering Committee; et al. Community based risk assessment on the Crow Reservation. Poster presented at: NIH Summit: The Science of Eliminating Health Disparities; December 16-18, 2008; National Harbor, MD. (Abstract published.)

78. Eggers, M.J. Community based risk assessment of exposure to waterborne contaminants on the Crow Reservation, Montana, Ph.D. Dissertation: Montana State University, Bozeman, MT, USA, 2014, 217 p.

79. Eggers, M.J.; Lefthand, M.J.; Young, S.L.; Doyle, J.T.; Plenty Hoops, A. When It Comes to Water, We Are All Close Neighbors. EPA Blog It All Starts With Science. Available online: http://blog.epa.gov/science/2013/06/when-it-comes-to-water-we-are-all-close-neighbors/ (accessed on 30 June 2013).

80. Eggers, M.J.; Moore-Nall, A.L.; Doyle, J.T.; Lefthand, M.J.; Young, S.L., Bends, A.L.; Committee; C.E.H.S.; Camper, A.K. Potential Health Risks from Uranium in Home Well Water: An Investigation by the Apsaalooke (Crow) Tribal Research Group. *Geosciences* **2015**, no. 5, p. 67-94.

81. Eichstaedst, P. If You Poison Us: Uranium and Native Americans; Red Crane Books: Santa Fe, NM, USA, 1994; p. 194.

82. Elderfield, H.; Greaves, M. The rare earth elements in seawater. *Nature* **1982**, 296, 214–219.

83. Eldam, N.S., 2012, Structural Controls on Evaporite Paleokarst Development: Mississippian Madison Formation, Bighorn Canyon Recreation Area, Wyoming and Montana, Master's thesis: University of Texas at Austin, Austin, TX, USA, 170 p.

84. Emsbo, P.; McLaughlin, P.I.; Breit, G.N.; du Bray, E.A.; Koenig, A.E. Rare earth elements in sedimentary phosphate deposits: Solution to the global REE crisis? *Gondwana Res* **2015**, 27, 776–785. Available online: http://www.sciencedirect.com/science/article/pii/S1342937X14003128 (Accessed: 27 March 2016).

85. Energy Laboratories. Certifications/quality control. Available online: http://www.energylab.com/why-us/certifications-quality-control/ (accessed March 5, 2015).

86. Engel, A.S.; Stern, L.A.; Bennett, P.C. Microbial contributions to cave formation: new insight into sulfuric acid speleogenesis. *Geology*, **2004**, 32, 369-372.

87. Engel, A.S.; Engel, S.A.; Moore, P.J.; DuChene, H., Eds.; Carbonate Geochemistry: Reactions and Processes in Aquifers and Reservoirs, Selected papers and abstracts of the symposium held in Billings, Montana, August 6-9, 2011, Karst Waters Institute Special Publication 16: Leesburg, Virginia, Karst Waters Institute, 84 p.

88. EPA, U.S. Environmental Protection Agency, Summary of the Clean Water Act. Available online: http://www.epa.gov/laws-regulations/summary-clean-water-act (accessed November 14, 2015).

89. EPA Pacific Southwest Region 9. Addressing Uranium Contamination on the Navajo Nation. Contaminated Water Sources. Available online: http://www.epa.gov/region9/superfund/navajo-nation/contaminated-water.html (accessed on 8 December 2014).

90. EPA Pacific Southwest Region 9. Addressing Uranium Contamination on the Navajo Nation. Cleanup of Abandoned Mines. Available online: http://www.epa.gov/region9/superfund/navajo-nation/abandoned-uranium.html (accessed on 8 December 2014).

91. Epstein, S.; Mayeda, T. Variation of O18 content of waters from natural sources. *Geochim Cosmochim Acta* **1953**, 4, 213– 224.

92. Epstein, S.; Buchsbaum, R.; Lowenstam, H.A.; Urey, H.C. Revised carbonate-water isotopic temperature scale. *Geol Soc Amer Bull* 1953, 64, 1315-1326.

93. Erslev, E.A. Thrusts, back-thrusts, and detachment of Rocky Mountain foreland arches, in C.J. Schmidt, R.B. Chase, and E.A. Erslev, eds., Laramide basement deformation in the Rocky Mountain foreland of the western United States: *Geol. Soc. Amer. Special Paper* **1993**, 280, 339-358.

94. Farrell, J.; Bostick, W.D.; Jarabek, R.J.; Fiedor, J.N. Uranium removal from ground water using zero valent iron media. *Groundwater* **1999**, 37, 618–624.

95. Faure, G. Principles and Applications of Geochemistry: Prentice Hall, ed. 2, 1998, 544 p.

96. Finch, R.; Murakami, T. Systematics and Paragenesis of Uranium Minerals. In *Reviews in Mineralogy, Uranium: Mineralogy, Geochemistry and the Environment*, Burns, P.C.; Finch, R., Eds.; Mineralogical Society of America: Washington, D.C., USA, 1999, vol. 38, pp. 91-179.

97. Florentine, C.; Krause, T.; Eggers, M.J. Biogeochemical Cycling of Uranium. Presented at Montana State University, Bozeman, MT, USA, April 2013.

98. Foose, R.M.; Wise, D.U.; Garbarini, G. S. Structural geology of the Beartooth mountains, Montana and Wyoming, *Geol. Soc. Amer. Bull.* **1961**, 72, 1143-1172.

99. Ford, T.E.; Eggers, M.J.; Old Coyote, T.J.; Good Luck, B.; Felicia, D.L. Additional contributors: Doyle JT; Kindness L.; Leider A.; Moore-Nall A.; Dietrich E.; Camper, A.K. Comprehensive community-based risk assessment of exposure to water-borne contaminants on the Crow Reservation. EPA Tribal Environmental Health Research Program Webinar presented October 17, 2012.

100. Francevillite. Available online: http://www.handbookofmineralogy.org/pdfs/francevillite.pdf (Accessed: 21 December 2015).

101. Frost, C.L.; Toner, R.N. 2004, Strontium Isotopic Identification of Water-Rock Interaction and Ground Water Mixing. *Groundwater* **2004**, 42, 418-432.

102. Frost, C.D.; Frost, B.R.; Kirkwood, R.; Chamberlain, K.R. The tonalite-trondhjemite granodiorite (TTG) to granodiorite-granite (GG) transition in the Late Archean plutonic rocks of the central Wyoming province. *Can. J Earth Sci.* **2006**, 43, 1419-1444.

103. Garrels, R.M.; Christ, C.L. Behavior of uranium minerals during oxidation. In *Geochemistry and Mineralogy of the Colorado Plateau Uranium Ores*, Garrels, R.M.; Larsen, E.S., Eds.; USGS Prof. Paper 320: Washington, D.C., USA, 1959, pp. 81-90.

104. Georgia Department of Human Resources. Radium and Uranium in Public Drinking Water Systems. Available online: http://www.gaepd.org/Documents/radwater.html (accessed on 2 August 2013).

105. Goldberg, E.D. Chemistry in the Oceans. In *Oceanography*, Sears, M., Ed.; *Am. Assoc. Advance. Sci. Publ.* **1961**, 67, 583-597.

106. Gulbrandsen, R.A.; Reeser, D.W. An occurrence of Permian manganese nodules near Dillon, Montana. U.S. Geological Survey Professional Paper 650-C, 1969, pp. C49-C57.

107. Gulbrandsen, R.A. Analytical data on the Phosphoria Formation Western United States. U.S. Geological Survey Open-file report 75-554: US Gov. Printing office, Washington, D.C., USA, 1975, 45 p. Available online: http://pubs.usgs.gov/of/1975/0554/report.pdf (Accessed: 17 February 2016).

108. Habermann, D.; Neuser, R.D.; Richter, D.K. REE-activated cathodoluminescence of calcite and dolomite: high-resolution spectrometric analysis of CL emission (HRS-CL), *Sed. Geol.* **1996**, 101, 1-7.

109. Halloysite. Available online: http://www.mindat.org/min-1808.html (Accessed: 17 February 2016).

110. Hamner, S.; Broadaway, S.C.; Berg, E.; Stettner, S.; Pyle, B.H.; Big Man, N.; Old Elk, J.; Eggers, M.J.; Doyle, J.; Kindness, L.; et al. Detection and source tracking of Escherichia coli, harboring intimin and Shiga toxin genes, isolated from the Little Bighorn River, Montana. *Int. J. Environ. Health Res.* **2014**, 24, 341–362.

111. Hardie, L.A. Dolomitization: A critical view of some current views. *J Sed. Petrol.* **1987**, 57, 166-183.

112. Harris, R.E. Uranium and thorium in the Bighorn Basin. In *Geology of the Bighorn Basin*, Wyoming Geological Association, 34th annual field conference; Boberg, W.W., Ed., Guidebook; Wyoming Geological Association: Casper, WY, USA, 1983; pp. 171-177.

113. Hart, O.M. Uranium deposits in the Pryor-Bighorn Mountains, Carbon County, Montana, and Big Horn County, Wyoming: United Nations 2nd International Conference on Peaceful Uses of Atomic Energy, Proceedings, 1958, vol. 2, pp. 523-526.

114. Hauptman, C.M. Uranium in the Pryor Mountain area of southern Montana and northern Wyoming, *Uranium Magazine* **1956**, 3,11, 14-21.

115. Haynes, W.M.; Ed., CRC Handbook of Chemistry and Physics. CRC Press/Taylor and Francis: Boca Raton, FL, USA, 95th Edition, 2012, 2664 p.

116. Health Canada. Water talk-Uranium in drinking water. Available online: http://www.hc-sc.gc.ca/ewh-semt/pubs/water-eau/uranium-eng.php/ (accessed on 25 September 2012).

117. Hein, J.R.; McIntyre, B.; Perkins; R.B.; Piper, D.Z.; Evans, J. Composition of the Rex Chert and associated rocks of the Permian Phosphoria Formation: Soda Springs area, SE Idaho, U.S. Geological Survey Open File Report 02-345, 2002, 30 p.

118. Heller, P.L.; Bowdler, S.S.; Chambers, H.P.; Coogan, J.C.; Hagen, E.S.; Shuster, M.W.; Winslow, N.S. Time of initial thrusting in the Sevier orogenic belt, Idaho-Wyoming and Utah. *Geology*, **1986**, 14, 388-391.

119. Hiza, M. The Geologic History of the Absaroka Volcanic Province, *Yellowstone Science*. **1998**, 6, 2, 2-7. Available online: https://www.nps.gov/yell/learn/upload/YS_6_2_sm.pdf (Accessed 7, December 2016).

120. Hoefs, J., 2009, Stable Isotope Geochemistry 6th ed., Berlin, Springer, 285 p.

121. Hollerbach, A. Influence of Biodegradation on the Chemical Composition of Heavy Oil and Bitumen: Characterization, Maturation, and Degradation. In Section II Exploration for Heavy Crude Oil and Natural Bitumen, Meyer, R.F., Ed.; AAPG, Studies in Geology: Tulsa, OK, USA, 1997, pp. 243-247.

122. Hoover, E.; Cook, K.; Plain, R.; Sanchez, K.; Waghiyi, V.; Miller, P.; Dufault, R.; Sislin, C.; Carpenter, D.O. Indigenous peoples of North America: Environmental exposures and reproductive justice. *Environ. Health Perspect*. **2012**, 120, 1645–1649.

123. Hughes, M.A.; Nielsen, D.; Rosenberg, E.; Gobetto, R.; Viale, A.; Burton, S.D.; Ferel, J. Structural investigations of silica polyamine composites: Surface coverage, metal ion coordination, and ligand modification. *Ind. Eng. Chem. Res*. **2006**, 45, 19 6538-6547.

124. Hughes, M.A.; Rosenberg, E. Characterization and applications of poly-acetate modified silica polyamine composites. *Sep. Sci. Technol*. **2007**, 42, 2, 261-283.

125. Hughes, M.; Miranda, P.; Nielsen, D.; Edward Rosenberg, E.; Gobetto, R.; Alessandra Viale, A.; Burton, S. Silica polyamine composites: New supramolecular materials for cation and anion recovery and remediation. *Macromol. Symp*. **2006**, 235, 1, 161–178.

126. Huntoon, P.W. The influence of Laramide foreland structures on modern ground-water circulation in Wyoming artesian basins. In *Geology of Wyoming*; Snoke, A.W., Steidtmann, J.R., Roberts, S.M., Eds; Geological Survey of Wyoming Memoir, 1993, no. 5, pp. 756-789.

127. Hurley, G. Geology and Mineralogy of the Devil Canyon/Little Mountain Area, Northern Big Horn Mountains, Wyoming. In *Resources of the Bighorn Basin*; 47th Annual Field Conference Guidebook; Wyoming Geological Association: Casper, WY, USA, 1996, pp. 281-295.

128. Ikramuddin, M.; Asmeron, Y.; Nordstrom, P.M.; Kinart, K.P.; Martin, W.M.; Digby, S.J.M.; Elder, D.D.; Nijak, W.F.; Afemari, A.A. Thallium: a potential guide to mineral deposits. *J. Geochem. Explor*. **1983**, 19, 465--490.

129. Indian Health Service (IHS) Website. Available online: http://www.ihs.gov/index.cfm?module=ihsIntro (accessed on 11 March 2013).

130. Indian Health Service (IHS) Environmental Health Services Fact Sheet. Available online: http://www.ihs.gov/factsheets (accessed on 11 March 2013).

131. Jackpile Mine (Jackpile-Paguate), Laguna District, Cibola Co., New Mexico, USA. Available online: http://www.mindat.org/loc-33622.html (accessed on 28 December 2014).

132. Jasinski, S.M. Phosphate rock. U.S. Geological Survey Mineral Commodity Summaries, 2011, pp. 118–119.

133. Johnston, B.R.; Dawson, S.E.; Madsen, G.E. Uranium mining and milling, Navajo experiences in the American southwest. In *Half-Lives & Half-Truths, Confronting the Radioactive Legacies of the Cold War*; Johnston, B.R., Ed.; School for Advanced Research Press: Santa Fe, NM, USA, 2007, pp. 97–117.

134. Kailasam, V.; Rosenberg, E.; Nielsen, D. Characterization of surface-bound Zr(IV) and its application to removal of As(V) and As(III) from aqueous systems using phosphonic acid modified nanoporous silica polyamine composites. *Ind. Eng. Chem. Res*. **2009**, 48, 8, 3991-4001.

135. Kailasam, V. The removal and recovery of oxo-anions from aqueous systems using nano-porous silica polyamine composites, PhD Dissertation, University of Montana, Missoula, MT, USA, 2009.

136. Katz, D.A., Eberli, G.P., Swart, P.K., and Smith, L.B., 2006, Tectonic-hydrothermal brecciation associated with calcite precipitation and permeability destruction in Mississippian carbonate reservoirs, Montana and Wyoming: *AAPG Bull*. **2006**, 90, 1803–1841.

137. Kislak, J.; Smith, L.; Peacock, D.; Eberli, G.; Swart, P. Classification, distribution, and origin of hydrothermal breccia, Madison Formation, Wyoming (abs.): AAPG Annual Meeting Program, 2001, v. 10, p. A105.

138. Klauk, E. Impacts of Resource Development on Native American Lands. Available online: http://serc.carleton.edu/research_education/nativelands/navajo/humanhealth.html (accessed on 10 December 2014).

139. Kluth, C.F.; Coney, P.J. Plate tectonics of the Ancestral Rocky Mountains. *Geology* **1981**, 9, 10-15.

140. Kunitz, S.J. Changing patterns of mortality among American Indians. *Am. J. Public Health* **2008**, 98, 404–412.

141. Kurttio, P.; Auvinen, A.; Salonen, L.; Saha, H.; Pekkanen, J.; Makelainen, I.; Vaisanen, S.B.; Penttila, I.M.; Komulainen, H. Renal Effects of Uranium in Drinking Water. *Environ. Health Perspect*. **2002**, 110, 337–342.

142. Lageson, D.R.; Larsen, M.C.; Lynn, H.B.; Treadway, W.A. Applications of Google Earth Pro to fracture and fault studies of Laramide anticlines in the Rocky Mountain foreland, In *Google Earth and Virtual Visualizations in Geoscience Education and Research*; Whitmeyer, S.J., Bailey, J.E., De Paor, D.G., Ornduff, T., Eds.; *Geol. Soc. Am. Special Paper* **2012**, 492, p. 1–12.

143. Lanphere, M.A.; Champion, D.E.; Christiansen, R.L.; Izett, G.A.; Obradovich, J.D. Revised ages for tuffs of the Yellowstone Plateau volcanic field: Assignment of the Huckleberry Ridge Tuff to a new geomagnetic polarity event. *Geol. Soc. Am. Bull.* **2002**, 114, 5, 559-568.

144. Langmuir, D. Uranium solution-mineral equilibria at low temperatures with applications to sedimentary ore deposits: *Geochim. Cosmochim. Acta* **1978**, 42, 547-569.

145. Laznicka, P. Breccias and coarse fragmentites; petrology, environments, associations, ores: Developments in Economic Geology. Elsevier Science & Technology Books: University of California, USA, 1988, v. 25, 832 p.

146. Lefthand, M.J.; Eggers, M.J.; Old Coyote, T.J.; Doyle, J.T.; Kindness, L.; Bear Don't Walk, U.J.; Young, S.L.; Bends, A.L.; Good Luck, B.; Stewart, R.; et al. Holistic community based risk assessment of exposure to contaminants via water sources. In *Proceedings of the American Public Health Association Conference*, San Francisco, CA, USA, 10 October 2012.

147. Lefthand, M.J.; Eggers, M.J.; Crow Environmental Health Steering Committee; Camper, A.K. Community-Based Cumulative Risk Assessment of Well Water Contamination: A Tribal Environmental Health Disparity. Presented at the NIH Native American Research Centers for Health's Tribal Environmental Health Summit, Pablo, MT, USA, 24 June 2014.

148. Liebow, E. Hanford, tribal risks, and public health in an era of forced federalism. In *Half-Lives & Half-Truths, Confronting the Radioactive Legacies of the Cold War*; Johnston, B.R., Ed.; School for Advanced Research Press: Santa Fe, NM, USA, 2007; pp. 145–165.

149. Lillie-Blanton, M.; Roubideaux, Y. Understanding and addressing the health care needs of American Indians and Alaska natives. *Am. J. Public Health* **2005**, 95, 759–761.

150. Lillis, P.G.; Selby, D. Evaluation of the rhenium–osmium geochronometer in the Phosphoria petroleum system, Bighorn Basin of Wyoming and Montana, USA. *Geochim. Cosmochim. Acta* **2013**, 118, 312–330.

151. Little Big Horn College Library. Map of the Crow Reservation. Available online: http://lib.lbhc.edu (accessed on 2 August 2013)

152. Lopez, D.A. Field guide to the northern Pryor Bighorn structural block, south central Montana. Open-File Report 330. Montana Bureau of Mines and Geology, Butte, Montana, USA, 1995, 26 p.

153. Lopez, D.A., 2000, Geologic Map of the Bridger 30' × 60' Quadrangle, Montana: Montana Bureau of Mines and Geology Geologic Map Series No. 58.

154. Los Alamos National Laboratory. Our History. Available online: http://www.lanl.gov/about/history-innovation/index.php (accessed on 28 December 2014).

155. Love, J.D. Vanadium and associated elements in the Phosphoria Formation in the Afton area, western Wyoming: U.S. Geological Survey Professional Paper 424C, 1961, pp. C279-C282.

156. Love, J.D. Vanadium deposits in the Lower Permian Phosphoria Formation, Afton area, Lincoln County, western Wyoming: U.S. Geological Survey Professional Paper 1637, 2003, 28 p.

157. Love, J.D. Uraniferous phosphatic lake beds of Eocene age in intermontane basins of Wyoming and Utah: U.S. Geological Survey Professional Paper 474- E, 1964, 66 p.

158. Manhattan Project. Energy.gov Office of Management. Available online: http://energy.gov/management/officemanagement/operationalmanagement/history/manhattan-project (accessed on 28 December 2014).

159. Mark, D.; Byron, R. Bighorn Valley Health Center Program Narrative; Bighorn Valley Health Center (BVHC): Hardin, MT, USA, 2010, unpublished.

160. Mao, Y.; Desmeules, M.; Schaubel, D.; Berube, D.; Dyck, R.; Brule, D.; Thomas, B. Inorganic components of drinking water and microalbuminuria. *Environ. Res.* **1995**, 71, 135–140.

161. Mapel, W.J.; Roby, R.N.; Sarnecki, J.C.; Sokaski, M.; Bohor, B.F.; McIntyre, G. Status of Mineral Resource Information for the Crow Indian Reservation, Montana. Available online: https://www1.eere.energy.gov/tribalenergy/guide/pdfs/crow_7.pdf (accessed on 10 December 2014).

162. Mariano, A.N. Some further geological applications of cathodoluminescence. In *Cathodoluminescence of Geological Materials*, Marshall, D. J., Ed.; Boston, Unwin Hyman, 1988, 146 p.

163. Marshall, D. J. *Cathodoluminescence of Geological Materials*. Boston, Unwin Hyman, 1988, 146 p.

164. Marshak, S.; Mitra, G. Basic Methods of Structural Geology: Prentice Hall, Englewood Cliffs, NJ, USA, 1988, 446 p.

165. Marshall, D. J. *Cathodoluminescence of Geological Materials*. Boston, Unwin Hyman, 1988, 146 p.

166. Maughan, E.K. Tectonic setting of the Rocky Mountain region during the late Paleozoic and early Mesozoic. In *Proceedings of the Symposium on the Genesis of Rocky Mountain Ore Deposits, Changes with Time and Tectonics*; J.W. Babcock, Ed.; Regional Exploration Geologists Society, Denver, CO. 1983, pp. 39-50.

167. McEldowney, R.C.; Abshier, J.F.; Lootens, D.J. Geology of uranium deposits in the Madison Limestone, Little Mountain area, Big Horn County, Wyoming. In *Exploration frontiers of the Central and Southern Rockies*; Veal, H.K., Ed.; Rocky Mountain Association of Geologists, 1977, pp. 321-336.

168. McKelvey, V.E; Strobell, J.D., Jr.; Slaughter, A.L. The vanadiferous zone of the Phosphoria Formation in western Wyoming and southeastern Idaho: U.S. Geological Survey, Professional Paper 1465, 1986, 27p.

169. McOliver, C.A.; Camper, A.K.; Doyle, J.T.;Eggers, M.J.; Ford, T.E.;Lila, M.A.; Berner, J.; Campbell, L.; Donatuto, J. Community-Based Research as a Mechanism to Reduce Environmental Health Disparities in American Indian and Alaska Native Communities, *Int J Environ Health Res* **2015**, 12, 4, 4076-4100.

170. Medrano, M. D.; D. Z. Piper Partition of minor elements and major-element oxides between rock components and calculation of the marine-derived fraction of the minor elements in rocks of the Phosphoria Formation, Idaho and Wyoming: U.S. Geological Survey Open-File Report 95-270, 1995, 79 p.

171. Meyer, R.F.; Attanasi, E.D.; Freeman, P.A. Heavy oil and natural bitumen resources in geological basins of the world: U.S. Geological Survey Open-File

Report 2007-1084, 2007, Available online: http://pubs.usgs.gov/of/2007/1084/ (Accessed October, 2016).

172. Minkler, M.; Wallerstein, N. Community-Based Participatory Research for Health; Jossey-Bass: San Francisco, CA, USA, 2008.

173. Montana Bureau of Mines and Geology Ground Water Information Center. Available online: http://mbmggwic.mtech.edu/ (accessed February, 2011).

174. Montana Department of Environmental Quality Big Horn County Radon Information. Available online: http://county-radon.info/MT/Big_Horn.html (accessed on 6 August 2013).

175. Montana Department of Environmental Quality Montana's Clean Water Act Information Center (MCWAIC). Available online: http://deq.mt.gov/wqinfo/cwaic/reports.mcpx (accessed July, 2016).

176. Montana Department of Environmental Quality (MTDEQ). Uranium in Drinking Water. Available online: http://deq.mt.gov/wqinfo/swp/Guidance.mcpx (accessed on 6 August 2013).

177. Montana Department of Public Health and Human Services. 2004-2008 Statistics.

178. Montana Department of Public Health and Human Services. Big Horn County Health Profile. Available online: http://www.docstoc.com/docs/86526062/2006-Montana-County-Health-Profiles-Department-of-Public-Health (accessed on 3 December 2014).

179. Montana Department of Revenue. 2013 Agricultural Land Classification and fallow adjustment zones. Available online: https://revenue.mt.gov/Portals/9/committees/Ag_LandValuation/map_summer_fallow_adj_zones.jpg (accessed on 6 March 2015).

180. Montana Hospital Association. Age-adjusted rates calculated based on the primary diagnosis by the Montana Hospital Discharge Data System, based on data provided by the Montana Hospital Association, Population denominators: NCHS bridged race estimates of the resident population of Montana for 1 July 2000–1 July 2008 (Vintage 2008).

181. Montana Natural Resources Information System. Available online: http://nris.mt.gov (accessed February 2011).

182. Montana State University Well Educated Program. Well Educated Parameter List. Available online:

http://waterquality.montana.edu/docs/WELL_EDUCATED/ParameterPackageList2014.pdf (accessed on 23 December 2014).

183. Moore-Nall, A.L.; Lageson, D.R.; Herkimer diamonds in the Pennsylvanian Tensleep Formation may indicate hydrothermal influences for mineralization of the Red Pryor Mountain uranium/vanadium deposits. Presented at the GSA Annual Meeting, Minneapolis, Minnesota, USA, 9-12 October 2011. Available online: https://gsa.confex.com/gsa/2011AM/finalprogram/abstract_198138.htm (Accessed 10 December 2015).

184. Moore-Nall, A.L.; Lageson, D.R.; Uranium Vanadium Mineralization in Mississippian Aged Paleokarst, Northern Bighorn Basin, Montana and Wyoming, Indicates a Hydrothermal Permian Phosphoria Formation Source of Metals Including REE and Tl. Presented at the GSA Annual Meeting, Denver, Colorado, USA, 9-12 October 2011. Available online: https://gsa.confex.com/gsa/2016AM/webprogram/Paper287959.html (Accessed 13 October 2016).

185. Moore-Nall, A.L.; Lageson, D.R. Lower health status on Indian Reservations a geologic or geographic correlation associated with natural resources? In *Proceedings of the 5th International Conference on Medical Geology*, Arlington, VA, USA, 25–29 August 2013.

186. Moore-Nall, A.L.; Lageson, D.R. Francevillite [(Ba,Pb)(UO2)2(V2O8)•5H2O] identified in the Uranium Vanadium deposits in the Pryor Mountain Mining District, Montana and the Little Mountain Mining District, Wyoming may provide a link to the elevated lead in the Bighorn River and be related to fluid migration of the Lower Kane Cave, Wyoming. Presented at the GSA Annual Meeting, Denver, CO, USA, 27-30 October 2013. Available online: http://www.geosociety.org/meetings/2013/documents/13AM-progALL.pdf (Accessed 10 December, 2015).

187. Moore-Nall, A. The legacy of uranium development on or near Indian reservations and health implications rekindling public awareness. *Geosciences* **2015**, 5, 15–29.

188. Moore-Nall, A.; Eggers, M.J.; Camper, A.K; Lageson, D. Elevated Uranium and Lead in Wells on the Crow Reservation, Big Horn County-A Potential Problem. Presented at the Earth Science Colloquium, Bozeman, MT, USA, 12–13 April 2013.

189. Moyle, P.R.; Causey, D.J. Chemical Composition of Samples Collected from Waste Rock Dumps and Other Mining-Related Features at Selected Phosphate Mines in Southeastern Idaho, Western Wyoming, and Northern Utah. U.S. Geological Survey Open-File Report 01-411, 2001, 46p.

190. Thallium element information. Available on line: http://www.rsc.org/periodic-table/element/81/thallium (Accessed: 17 February 2016).

191. National Uranium Resource Evaluation (NURE) Hydrogeochemical and Stream Sediment Reconnaissance (HSSR) Program's database for Montana and Wyoming. Available online: http://tin.er.usgs.gov/nure/water/ (accessed February 2011).

192. National Vital Statistics System, Center for Disease Control and Prevention, U.S.: Death certificate Montana resident data from 2004-2008.

193. Native American Health Care Disparities Briefing Executive Summary; Office of the General Counsel U.S. Commission on Civil Rights: 2004; 52 p. Available online: http://www.law.umaryland.edu/marshall/usccr/documents/nativeamerianhealthcaredi.pdf (accessed on 11 March 2013).

194. Native Sun News: Laguna Pueblo Still Affected by Uranium Mine. Available online: http://www.indianz.com/News/2014/014847.asp (accessed on 28 December 2014).

195. Natural Resource Conservation Service's Data Gateway. Available online: http://datagateway.nrcs.usda.gov/ (accessed on 4 February 2013).

196. Navajo Health Research: Dr. Johnnye Lewis Continues. Available online: http://lajicarita.wordpress.com/2012/09/21/navajo-health-research-dr-johnnye-lewis-continues/ (accessed on 7 December 2014).

197. Neely, T.G.; Erslev, E.A. The interplay of fold mechanisms and basement weaknesses at the transition between Laramide basement-involved arches, northcentral Wyoming, U.S.A: *J Struct. Geol.* **2009**, 31, 1012–1027.

198. Nuclear War: Uranium Mining and Nuclear Tests on Indigenous Lands. Available online: http://www.culturalsurvival.org/publications/cultural-survival-quarterly/united -states/nuclear-war-uranium-mining-and-nuclear-tests- (accessed on 8 December 2014).

199. Orem, W.; Tatu, C.; Pavlovic, N.; Bunnell, J.; Kolker, A.; Engle, M.; Stout, B. Health Effects of Energy Resources. U.S. Department of the Interior, U.S. Geological Survey, FS 2009-3096. Available online: http://pubs.usgs.gov/fs/2009/3096/ (accessed on 30 December 2014).

200. Orloff, K.G.; Mistry, K.; Charp, P.; Metcalf, S.; Marino, R.; Shelly, T.; Melaro, E.; Donohoe, A.M.; Jones, R.L. Human exposure to uranium in groundwater. *Environ. Res.* **2004**, 94, 319–326.

201. Pasternak, J. Yellow Dirt: A Poisoned Land and a People Betrayed; Free Press: New York, NY, USA, 2010; p. 149.

202. Patterson, C.G., Toth, M.I., and Kulik, D.M., 1988, Mineral resources of the Pryor Mountain, Burnt Timber Canyon, and Big Horn Tack-On Wilderness Study Areas, Carbon County, Montana and Big Horn County, Wyoming: U.S. Geological Survey Bulletin 1723, 15 p.

203. Pelizza, M. Uranium and uranium progeny in groundwater associated with uranium ore bearing formations. In *Proceedings of the 5th International Conference on Medical Geology*, Arlington, VA, USA, 27 August 2013.

204. Perkins, R.B.; McIntyre, B.; Hein, J.R.; Piper, D.Z. Geochemistry of Permian rocks from the margins of the Phosphoria Basin: Lakeridge core, Western Wyoming, U.S. Geological Survey Open File Report 03-21, 2003, 60 p.

205. Perry, E.S. Montana in the Geological Past. Montana Bulletin 26; Montana Bureau of Mines and Geology: Montana Tech of the University of Montana, Butte, MT, USA, 1962.

206. Peterson, D.A.; Boughton, G.K. Organic compounds and trace elements in fish tissue and bed sediment from streams in the Yellowstone River Basin, Montana and Wyoming, U.S. Geologic Survey Water-Resources Investigations Report 00-4190, 1998, 46 p.

207. Peterson, D.A.; Zelt, R.B. Element concentrations in bed sediment of the Yellowstone River Basin, Montana, North Dakota, and Wyoming - A retrospective analysis, U.S. Geologic Survey Water-Resources Investigations Report99-4185, 1999, 30 p.

208. Phillips, W.J. Hydraulic fracturing and mineralization: *J Geol. Soc.* **1972**, 128, 337–359.

209. Piper, D.Z. Trace elements and major-element oxides in the Phosphoria Formation at Enoch Valley, Idaho; Permian sources and current reactivities: U.S. Geological Survey Open File Report 99-0163, 1999, 66 p.

210. Piper, D.Z., Perkins, R.B., and Rowe, H.D., 2007, Rare-earth elements in the Permian Phosphoria Formation: Paleo proxies of ocean geochemistry. *Deep-Sea Res. II* **2007**, 54, 1396-1413.

211. Piper, D.Z.; Skorupa, J.P.; Presser, T.S.; Hardy, M.A.; Hamilton, S.J.; Huebner, M.; Gulbrandsen, R.A. The Phosphoria Formation at the Hot Springs mine in Southeast Idaho: a source of selenium and other trace elements to surface water, ground water, vegetation, and biota. U.S. Geological Survey Open-File Report 00-050, 2000, 73 p.

212. Prados, J. Presidents' Secret Wars: CIA and Pentagon Secret Operations since World War II; William Morrow & Co.: New York, NY, USA, 1986; pp. 255–256.

213. Ramsay, J. G.; Huber, R. M. The techniques of modern structural geology, vol. 2: folds and fractures, Elsevier Science, 1987, 697 p.

214. RECA Radiation Exposure Compensation Act: Radiation Exposure Compensation Program-About the Program United States Department of Justice. Available online: http://usdoj.gov/civil/torts/const/reca/about.htm (accessed on 30 December 2012).

215. Reynolds, T. Final Report of Hanford Thyroid Disease Study Released. *J. Natl. Cancer Inst.* **2002**, 94, 1046–1048.

216. Reynolds, J.A. In *Description of fluid inclusion work done on Pryor Mountain samples at Fluid Inc*., submitted for the author by Lori Summa, Senior Technical Consultant, ExxonMobil Upstream Research Company for the authors. Personal communication via e-mail, 2 December 2011.

217. Richards, C.; Broadaway, S.; Eggers, M.J.; Doyle, J.T.; Pyle, B.H.; Camper, A.K.; Ford, T.E. Detection of Pathogenic and Non-pathogenic Bacteria in Drinking Water and Associated Biofilms on the Crow Reservation, Montana, USA. Microb. Ecol. **2015**, accepted for publication.

218. Richards, P.W. Geology of the Bighorn Canyon-Hardin area, Montana and Wyoming: U.S. Geological Survey Bulletin 1026, 1955, 93 p.

219. Riederer, A.M.; Thompson, K.M.; Fuentes, J.M.; Ford, T.E. Body weight and water ingestion estimates for women in two communities in the Philippines: The importance of collecting site-specific data. Int. J. Hyg. *Environ. Health* **2006**, 209, 69–80.

220. Rogers, D.; Petereit, D. Cancer disparities research partnerships in Lakota Country: Clinical trials, patient services, and community education for the Oglala, Rosebud, and Cheyenne River Sioux Tribes. *Am. J. Public Health* **2005**, 95, 2129–2132.

221. Rosenberg, E.; Pang, D. Inventors 1999.

222. Rosenberg E, Pang D. Inventors 1997.

223. Rubey, W. W., 1943, Vanadiferous shale in the Phosphoria Formation, Wyoming and Idaho [abs.]: Economic Geology, v. 38, no. 1, p. 87.

224. Sadeghi, S.; Sheikhzadeh, E. Solid phase extraction using silica gel modified with murexide for preconcentration of uranium (VI) ions from water samples. *J. Hazard Mater*. **2009**, 163, 2, 861-868.

225. Sahinen, U.M. Fluorspar deposits in Montana. *MBMG Bull*. **1962**, 28, 34-35.

226. Sando, W.J. Ancient solution phenomena in the Madison Limestone (Mississippian) of north-central Wyoming. *USGS J. Res.* **1974**, 2, 133-141.

227. Sando, W.J.; Mamet, B.L. New evidence on the age of the top of the Madison Limestone (Mississippian), Big Horn Mountains, Wyoming and Montana. *USGS J Res.* **1974**, 2, 5, 619-624.

228. Sando, W.J.; Gordon Jr., M.; Dutro Jr., J.T. Stratigraphy and geologic history of the Amsden Formation (Mississippian and Pennsylvanian) of Wyoming: U.S. Geological Survey Professional Paper 858-A, 1975, 78 p.

229. Sando, W. J. Mississippian history of the northern Rocky Mountains region: *USGS J Res.* **1976**, 4, 317-338.

230. Sando, W. J. Madison Limestone (Mississippian) paleokarst: a geologic synthesis. In *Paleokarst*; James, N. P., Choquette, P.W., Eds.; Springer-Verlag, New York, 1988, pp. 256-277.

231. Scher, H. D.; Griffith, E. M.; Buckley, W. P. Accuracy and precision of 88Sr/86Sr and 87Sr/86Sr measurements by MC-ICPMS compromised by high barium concentrations, *Geochem, Geophy, Geosys*, **2014**, 15, 499-508.

232. Schiller, R. Radon Program Contact, U.S. Environmental Protection Agency, Region 8, Denver, CO, USA. Personal communication, 2013.

233. Schilmoeller, J. Decades of Environmental Injustice: Wyoming Indian Reservation Faces High Cancer Rates. In *Mint Press News*, 2012. Available online: http://www.mintpress.net/decades-of-environmental-injustice-wyoming-indian-reservation-faces-deteramental-rates-of-cancer/ (accessed on 13 December 2012).

234. Schnug, E.; Lottermoser, B.G. Fertilizer-deirved uranium and its threat to human health. *Environ. Sci. Technol*. **2013**, 47, 2433–2434.

235. Schnug, E. Uran in Phosphor-Dungemitteln und dessen Verbleib in der Umwelt. *Strahlentelex* **2012**, 26, 3-10. (In German)

236. Schultz, R.L., Caves of the Bighorn-Pryor Mountains of Montana and Wyoming. *NSS* **1969**, 10, 1-28.

237. Serc.carleton website http://serc.carleton.edu/research_education/geochemsheets/index.html (accessed: October 29, 2014).

238. Selden, A.I.; Lundhom, C.; Edlund, B.; Hogdaul, C.; Ek, B-M.; Bergstrom, B.E.; Ohlson, C.-G. Nephrotoxicity of uranium in drinking water from private drilled wells. *Environ. Res*. **2009**, 109, 486–494.

239. Sexton, K.; Hattis, D. Assessing cumulative health risks from exposure to environmental mixtures-Three fundamental questions. *Environ. Health Perspect*. **2007**, 115, 825–832.

240. Sheldon, R.P. Physical Stratigraphy and Mineral Resources of Permian Rocks in Western Wyoming: U.S. Geological Survey, Professional Paper 313-B, 1963, 273 p.

241. Sheldon, R.P. Long distance migration of oil in Wyoming: *The Mountain Geologist*, **1967**, 4, 53-65.

242. Sholkovitz, E.R. Ocean particle chemistry: the fractionation of rare earth elements between suspended particles and seawater. *Geochim Cosmochim Acta* **1994**, 58, 1567–1579.

243. Sibson, R.H.; Moore, J. McM.; Rankin, A.H. Seismic pumping - a hydrothermal fluid transport mechanism. *J Geol Soc London* **1975**, 131, 6, 653-659.

244. Sibson, R.H. Brecciation processes in fault zones – Inferences from earthquake rupturing. *Pure Applied Geophy* **1986**, 124, 159–175.

245. Skipp, B.; McGrew, L.W. The Maudlow and Sedan Formations of the Upper Cretaceous Livingston Group on the west edge of the Crazy Mountains Basin, Montana. (Contributions to stratigraphy), Geological Survey Bulletin 1422-B, 1977.

246. Smedes, H.W.; Thomas, H.H. Reassignment of the Lowland Creek Volcanics to Eocene Age. *J Geol* **1965**, 73, 3, 508-510.

247. Smith, S. M., 1997, National Geochemical Database: Reformatted Data from the National Uranium Resource Evaluation (NURE) Hydrogeochemical and Stream Sediment Reconnaissance (HSSR) Program: U.S. Geological Survey Open-File Report 97-492.

248. Smith, S.M., 2011; 2016, Geologist, U.S. Geological Survey, Denver Federal Center, Denver, CO, personal communication via e-mail.

249. Smith, L.B.; Davies, G.R. Structurally controlled hydrothermal alteration of carbonate reservoirs: Introduction: *AAPG Bull.* **2006**, 90, 1635-1640.

250. Smith, L. B. Jr.; Eberli, G.P.; Sonnenfeld, M.D. Sequence stratigraphic and paleogeographic distribution of reservoir quality dolomite, Madison Formation, Wyoming and Montana. In *Integration of outcrop and modern analogues in reservoir modeling*, Grammer, G.M., Eberli, G.P., Harris, P.M., Eds.; *AAPG Memoir* **2004**, 80, 94-118.

251. Sonnenfeld, M. D. Sequence evolution and hierarchy within the lower Mississippian Madison Limestone of Wyoming. *In Paleozoic systems of the Rocky Mountain region*; Longman, M.W., Sonnenfeld, M.D., Eds.; Rocky Mountain Section, *SEPM*, **1996**, 165-192.

252. Southwest Research and Information Center. Available online: http://www.sric.org/nbcs/index.php (accessed on 7 December 2014).

253. Speed, R.C. Collided Paleozoic microplate in the western United States. *J Geol* **1979**, 89, 279-292.

254. Spokane Tribe Members Worked Gladly in Uranium Mines. In *The Spokesman-Review.* Available online: http://www.spokesman.com/stories/2011/jun/05/i-watch-them-die-young-and-old/ (accessed on 8 December 2014).

255. Spötl, C.; J. K. Pitman Saddle (Baroque) Dolomite in Carbonates and Sandstones: A Reappraisal of a Burial-Diagenetic Concept. In *Carbonate Cementation in Sandstones: Distribution Patterns and Geochemical Evolution*, Morad, S., Ed.; Blackwell Publishing Ltd.: Oxford, UK, 1998, ch 19, pp. 437-460.

256. Stewart, J.C. Geology of the Dryhead-Garvin Basin, Bighorn and Carbon Counties, Montana: Map G-2; Montana Bureau of Mines and Geology Special Publication 17; Montana Bureau of Mines and Geology: Montana Tech of the University of Montana, Butte, MT, USA, 1958.

257. Stock, G.M.; Riihimaki, C.A.; Anderson, R.S. Age constraints on cave development and landscape evolution in the Bighorn basin of Wyoming, USA: *J Karst Stud* **2006**, 68, 2, 76-84.

258. Stone, D.S. Theory of Paleozoic oil and gas accumulation in Bighorn Basin, Wyoming. *AAPG Bull*. **1967**, 51, 10, 2056-2114.

259. Stricker, G.D.; Ellis, M.S. Coal Quality and Geochemistry, Powder River Basin, Wyoming and Montana. In *1999 Resource assessment of selected Tertiary coal beds and zones in the northern Rocky Mountains and Great Plains region*, U.S. Geological Survey Professional Paper 1625-A, 1999.

260. Sullivan, P.W.; Wyatt, H.R.; Morrato, E.H.; Hill, J.O.; Ghushchyan, V. Obesity, inactivity, and the prevalence of diabetes and diabetes-related cardiovascular comorbidities in the U.S., 2000–2002. *Diabetes Care*. **2005**, 8, 1599–1603.

261. Summa, L. Results of fluid inclusion work from Pryor Mountains performed at Fluid Inc., Denver, CO. Personal communication via e-mail, 6 December 2011.

262. Szabo, Z. Geochemistry as a critical factor in defining radionuclide occurrence in water from principal drinking-water aquifers of the United States. In *Proceedings of the 5th International Conference on Medical Geology*, Arlington, VA, USA, 27 August 2013.

263. Taylor, S.R.; McLennan, S.M. The Continental Crust: its Composition and Evolution. Blackwell Scientific Publishing: Oxford, UK, 1985, 312 p.

264. Tilling, R.I.; Klepper, M.R.; Obradovich, J.D. K-Ar ages and time span of emplacement of the Boulder Batholith, Montana *Amer J Sci* **1968**, 266, 8, 671-689.

265. Trexler, J.H., Jr.; Cashman, P.H.; Cole, J.C.; Snyder, W.S.; Tosdal, R.M.; V.I. Davydov Widespread effects of middle Mississippian deformation in the Great Basin of western North America. *Geol. Soc. Am. Bull.* **2003**, 115, 1278-1288.

266. Mulkey J.P.; Oehme, F.W. A review of thallium toxicity. *Vet Hum Toxicol* **1993**, 35, 445–53.

267. Taylor, S.R.; McLennan, S.M.; Rare Earth Elements in Sedimentary Rocks: Influence of Provenance and Sedimentary Processes. In *Geochemistry and Mineralogy of Rare Earth Elements*, Lipin, R.R.; McKay, G.A., Eds.; Mineralogical Society of America: Washington D.C., USA, 1989; Volume 21, pp. 169-200.

268. Thallian carnotite. Available online: http://www.mindat.org/min-32379.html (Accessed: 21 December 2015).

269. Technical Report on Technologically Enhanced Naturally Occurring Radioactive Materials from Uranium Mining Volume 2: Investigation of Potential Health, Geographic, and Environmental Issues of Abandoned Uranium Mines, EPA 402-R-08-005, April 2008. Available online: http://www.epa.gov/radiation/docs/tenorm/402-r-08–005-volii/402-r-08-005-v2.pdf (accessed on 20 December 2014).

270. The Centers for Disease Control and Prevention (CDC), National Center for Health Statistics, Division of Vital Statistics, National Vital Statistics Report Volume 58, Number 19, May 2010, Table 29. Available online: http://www.cdc.gov/nchs/data/nvsr/nvsr58/nvsr58_19.pdf (accessed on 7 June 2010).

271. Tsaih, S.-W.; Korrick, S.; Schwartz, J.; Amarasiriwardena, C.; Aro, A.; Sparrow, D.; Hu, H. Lead, Diabetes, Hypertension, and Renal Function: The Normative Aging Study. *Environ. Health Perspect.* **2004**, 112, 1178–1182.

272. Tuck, L. Ground-Water Resources along the Little Bighorn River, Crow Indian Reservation, Montana; Water-Resources Investigations Report 03-4052; U.S. Department of the Interior and the U.S. Geological Survey: Helena, MT, USA, 2003.

273. Tucker, M. E., and Wright, V. P., 1990, Radiogenic isotopes, in Tucker, M. E., Wright, P. V., and Dickson, J. A. D., eds., Carbonate sedimentology: Oxford, United Kingdom, Blackwell Science Publishing (GBR), 312 p.

274. Tucker, M. Techniques in Sedimentology, Blackwell Scientific Publications, Oxford, England, 1988, 408 p.

275. United States Census. 2000. Available online: http://www.census.gov/main/www/cen2000.html (accessed on 11 January 2010).

276. U.S. Census Bureau. DP-1-Geography-Big Horn County, Montana: Profile of General Population and Housing Characteristics: 2010. Available online: http://factfinder2.census.gov/ (accessed on 25 November 2013).

277. U.S. Census Bureau. Montana locations by per capita income. Available online: http://en.wikipedia.org/wiki/Montana_locations_by_per_capita_income (accessed on 2 April 2014).

278. US Department of Energy, Billings quadrangle-Residual intensity magnetic anomaly contour map: US Department of Energy, GJM-096, pl.4, 1982.

279. USGS Water Quality Data for Wyoming. Available online: http://waterdata.usgs.gov/wy/nwis/qw (accessed on 4 February 2013).

280. University of Wyoming's Water Resources Data System. Available online: http://www.wrds.uwyo.edu/ (accessed on 4 February 2013).

281. Uranium Mining Wastes. What is the History of Uranium Mining in the U.S.? Available online: http://www.epa.gov/radiation/tenorm/uranium.html#history (accessed on 20 December 2014).

282. U.S. Census Bureau. DP-1-Geography-Big Horn County, Montana: Profile of General Population and Housing Characteristics: 2010. Available online: http://factfinder2.census.gov/ (accessed on 25 November 2013).

283. U.S. Census Bureau. Montana locations by per capita income. Available online: http://en.wikipedia.org/wiki/Montana_locations_by_per_capita_income (accessed on 2 April 2014).

284. U.S. Department of Energy Billings quadrangle-Residual intensity magnetic anomaly contour map: US Department of Energy, GJM-096, 1982, pl.4.

285. U.S. Environmental Protection Agency. A Decade of Tribal Environmental Research: Results and Impacts from EPA's Extramural Grants and Fellowship Programs. In *Tribal Environmental Health Research Program*; NCER, ORD, EPA: Washington, DC, USA, 2014. Available online: http://epa.gov/ncer/tribalresearch/news/results-impacts-010714.pdf (accessed on 12 February 2014).

286. U.S. Environmental Protection Agency. Montana—EPA Map of Radon Zones. Available online: http://www.epa.gov/radon/pdfs/statemaps/montana.pdf (accessed on 6 August 2013).

287. U.S. Environmental Protection Agency. Radiation Protection: Decay Chains: Uranium-238 Decay Chain. Available online: http://www.epa.gov/radiation/understand/chain.html#u_decay (accessed on 3 August 2013).

288. U.S. Environmental Protection Agency. Uranium. Available online: http://www.epa.gov/radiation/radionauclides/uranium.html (accessed on 25 September 2012).

289. Van Gosen, B.S.; Wilson, A.B.; Hammarstrom J.M. Mineral Resource Assessment of the Custer National Forest in the Pryor Mountains, Carbon County, South-Central Montana, U.S. Geologic Survey Open-File Report 96-256, 1996, 69 p.

290. Veizer, J.; Compston, W. 87Sr/86Sr composition of seawater during the Phanerozoic, *Geochim. Cosmochim. Acta* **2004**, 38, 1461-1484.

291. Vermont Department of Health. Uranium. Available online: http://healthvermont.gov/enviro/rad/Uranium.aspx (accessed on 10 December 2014).

292. Warchola, R.J.; Stockton, T.J. National Uranium Resource Evaluation, Billings quadrangle, Montana: U.S. Department of Energy publication No. PGJ/F-015(82), prepared for U.S. Department of Energy, Grand Junction Colo., by Bendix Field Engineering Corp., Grand Junction Operations, 1982, 33 p.

293. Westphal, H.; Eberli, G.P.; Smith, L.B.; Grammer, G.M.; Kislak, J. Reservoir characterization of the Mississippian Madison Formation, Wind River Basin, Wyoming. *AAPG Bull* **2004**, 88, 4, 405-432.

294. Witherite. Available online: http://www.mindat.org/min-4299.html (Accessed: 17 February 2016).

295. Wilson, C.W. Geology of the Nye-Bowler lineament, Stillwater and Carbon Counties, Montana: *AAPG Bull* **1936**, 20, 9, 1161-1188.

296. Wilson, W.H. Radioactive Mineral Deposits of Wyoming Geological Survey of Wyoming; Report of Investigations; Wyoming Geologic Survey: Laramie, WY, USA, 1960, 7, 41 p.

297. Wingate, L. C and O isotope protocol, personal communication, 2013.

298. Woessner, B. Professor at University of Montana, Missoula, MT, did work with the NURE sampling program on the Northern Cheyenne Reservation, personal communication, 2012; 2016.

299. Wooden, J.L.; Mueller, P.A. Pb, Sr, and Nd isotopic compositions of a suite of Late Archean, igneous rocks, eastern Beartooth Mountains: implications for crust-mantle evolution. *Earth Planet. Sci. Lett* **1988**, 87, 59-72.

300. World Health Organization. Uranium in drinking water: Background document for development of WHO Guidelines for drinking-water quality. Available online: http://www.who.int/water_sanitation_health/dwq/chemicals/en/uranium.pdf (accessed on 25 September 2012).

301. Wrenn, M.E.; Durbin, P.W.; Lipsztein, H.B.; Rundo, J.; Still, E.T.; Willis, D.L. Metabolism of ingested U and Ra. *Health Phys.* **1985**, 48, 601–633.

302. Wright, Q. The law of the Nuremberg trial. *Am J Int Law.* **1942**, 41, 38-42.

303. Wyoming Geographic Information Center. Available online: National Uranium Resource Evaluation (NURE) Hydrogeochemical and Stream Sediment Reconnaissance (HSSR) Program's data base for Montana and Wyoming. Available online: http://tin.er.usgs.gov/nure/water/ (accessed on 18 February 2013).

304. Wyoming State Geological Survey website. Oil and Gas map. Available online: http://www.wsgs.wyo.gov/products/wsgs-2016-ms-103.pdf (Accessed: 8 October, 2016).

305. Xiao, T.; Yang, F.; Li, S.; Zheng, B.; Ning, Z. Thallium pollution in China: A geo-environmental perspective. *Sci Total Environ* **2012**, 421-422, 51–58.

306. Yazzie-Lewis, E.; Zion, J. Leetso, the powerful yellow monster a Navajo cultural interpretation of Uranium mining. In The Navajo People and Uranium Mining; Brugge, D., Benally, T., Yazzie-Lewis, E., Eds.; UNM Press: Albuquerque, NM, USA, 2007; pp. 1–10.

307. Young, T.K. Diabetes mellitus among Native Americans in Canada and the United States: An epidemiological review. *Am. J. Hum. Biol*. **1993**, 5, 399–413.

308. Zamora, M.L.; Tracy, B.L.; Zielinski, J.M.; Meyerhof, D.P.; Moss, M.A. Chronic Ingestion of Uranium in Drinking Water: A Study of Kidney Bioeffects in Humans. *Toxicol. Sci.* **1998**, 43, 68–77.

APPENDICES

APPENDIX A

SUPPORTING INFORMATION FOR CHAPTER 1

NURE Program - Data and Analyses

In 1973 the National Uranium Resource Evaluation (NURE) program was initiated to evaluate the uranium resources in the United States. The Department of Energy (DOE) administered the NURE program from 1977 until 1984 when funding disappeared and the program effectively ended. The Hydrogeochemical and Stream Sediment Reconnaissance (HSSR) program (initiated in 1975) was one of nine components of the NURE program. Four DOE labs developed their own sample collection, analytical, and data management methodologies and hired contractors to do much of the actual work for the program. The labs were the Lawrence Livermore Laboratory (LLL), Los Alamos Scientific Laboratory (LASL), Oak Ridge Gaseous Diffusion Plant (ORGDP), and Savannah River Laboratory (SRL). Los Alamos Scientific Laboratory (LASL), New Mexico, was assigned Alaska and the Rocky Mountain States. These included Colorado, Montana, New Mexico, Wyoming, and parts of Arizona, Idaho, Texas, and Utah. In 1977, the entire NURE program changed from a study area basis (state, county, or geomorphic provinces) to a 1° x 2° quadrangle basis. Many of the early study areas were not coincident with quadrangle boundaries and so additional sampling was done later to complete the quadrangle studies. Some quadrangles were never completed. Originally, all samples were only analyzed for uranium. Analyses for additional elements other than uranium, up to 45 in some cases, were authorized in 1977. Many early samples were reanalyzed. Out of a total of 625 quadrangles that cover the entire lower 48 States and Alaska, only 307 quadrangles were completely sampled and another 86 quadrangles were partially sampled. In Montana only three quadrangles,

(Butte, Dillon and Billings) were sampled for elements additional to U. The sample archive, including original maps, field notes and data tapes was transferred to the United States Geological Survey (USGS) in 1985. The USGS compiled and reformatted the databases from all the DOE laboratories, and reports from contractors to enhance the usefulness of the database. This data is publically available on-line and in CD-Rom format (Smith, 1997).

In the early phases of this study the NURE uranium, mercury, and lead data for stream sediment and water samples in watershed basins of the Big Horn River in Montana and Wyoming that contribute to the greater hydrologic basin of the Big Horn River were examined. Using GIS methods the available data was intersected with the greater hydrologic basin for the Bighorn River, a total of 416 samples were part of the resulting intersection (Figure A1). Smaller hydrologic units are displayed in the figures as the grey polygons that make up the larger polygons. The data was analyzed using the hydrologic units 8 (HUC_8) which were composed of smaller hydrologic units (HUC_10 and HUC_12). The smaller units are included in the tables of some of the figures for reference to further delineate the analyses locations. This data analysis set included eight hydrologic units: 1008007, 1008008, 1008009, 1008010, 1008011, 1008014, 1008015, and 1008016. These are displayed as shaded polygons in Figures A1-A6.

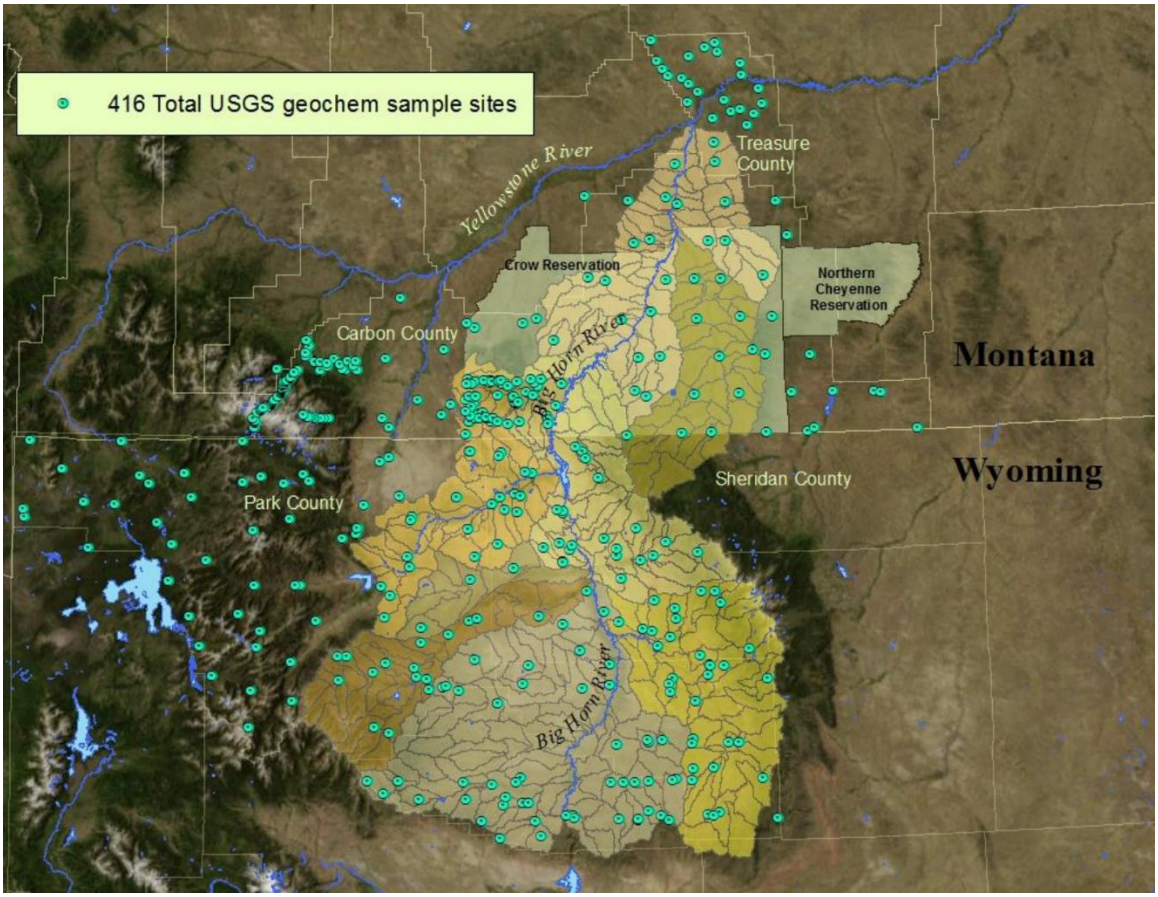


Figure A1. Total sediment samples analyzed in the Bighorn River hydrologic basin after intersecting available data from NURE database. The grid pattern is obvious where resampling was followed up in the different quadrangles. This may contribute to some sample bias in the dataset. The Crow and Northern Cheyenne Reservations are shown as shaded polygons in this and following figures. No samples are recorded in the data base for the Northern Cheyenne Reservation, though the author learned that the area was sampled during a field program that was completed and sent in (between 1975 and 1979) (Bill Woessner, pers. com., 2012; 2016). "In 1984, the Department of Energy (DOE) and their sub-contractors officially ended their part in the NURE program and all of the available digital NURE data, reports, field sheets, field maps, and archived sediment sample splits were given to the USGS. Although people continued to work with those resources at the USGS, no new samples, data, or information about samples appeared from the DOE or their sub-contractors since 1984. Because the NURE program was shut down so quickly when Congress refused to fully fund the completion of the project, some samples or data may have been lost in the shuffle," (Steven Smith, pers. com, 2016).

The sediment data was reviewed for lead (Pb), mercury (Hg), and uranium (U) concentrations. The Hg data showed the sample analyzed with the highest Hg concentration was from the Pryor Mountain Mining District (Figure A2).

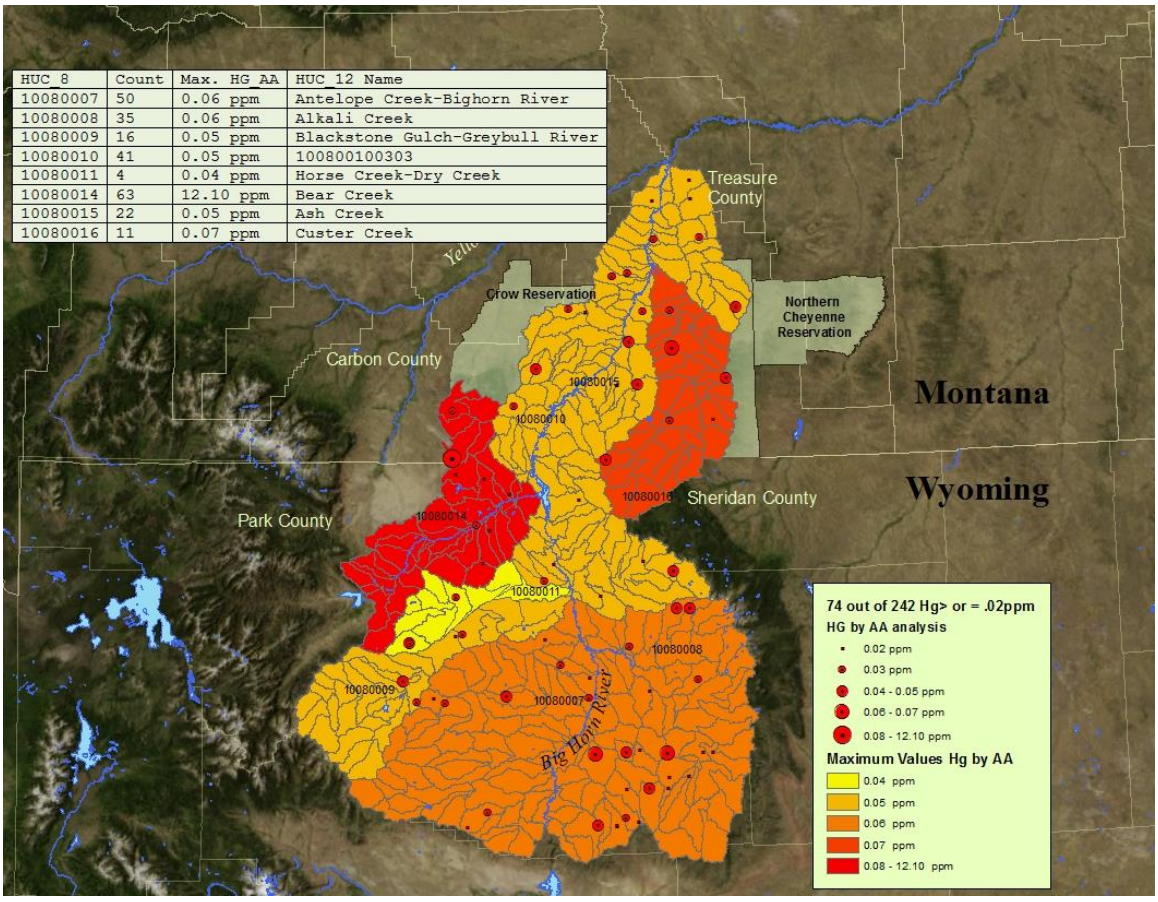


Figure A2. A total of 74 sediment samples had 0.02ppm or greater Hg in the Bighorn River hydrologic basin. The highest Hg concentration was from a sample in the Pryor Mountain Mining District. Table in the figure displays the number of samples in each hydrologic unit that Hg was detected and the maximum value in that unit. Hg was analyzed by AA.

The Pb data showed the samples analyzed with the highest Pb concentrations were from the Pryor Mountain Mining District (Figure A3).

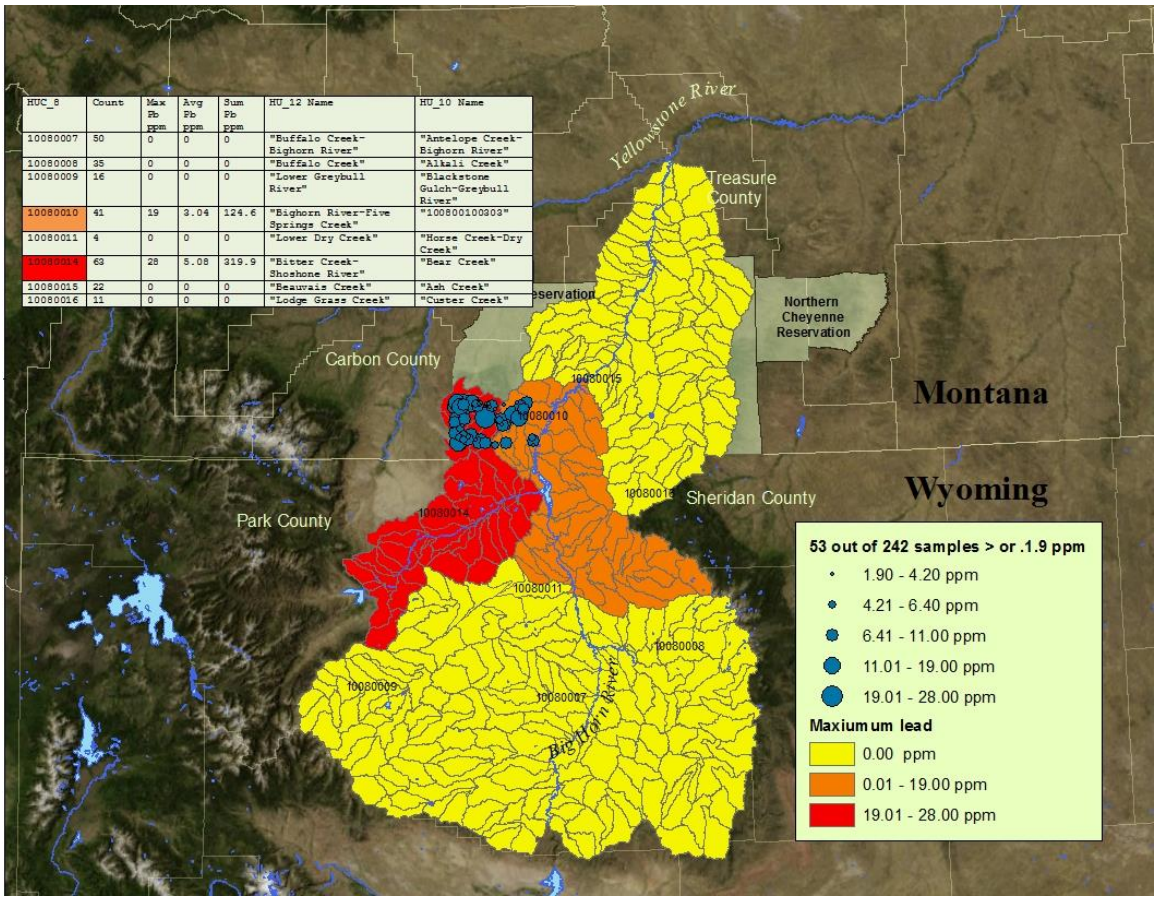


Figure A3. From the 242 sediment samples analyzed for Pb in the Bighorn River hydrologic from NURE database, 53 samples had Pb greater than 1.9 ppm. The highest Pb concentrations were from samples in the Pryor Mountain Mining District.

The U stream sediment data showed that samples analyzed in both of the mining districts and the Crow Reservation did not have elevated U concentrations when compared to the average crustal abundance for U (Taylor and McLennan, 1995). The highest values were in the hydrologic basins in HUC-8 (dark blue unit) in the southeast portion of the greater Bighorn River hydrologic basin (Figure A5).

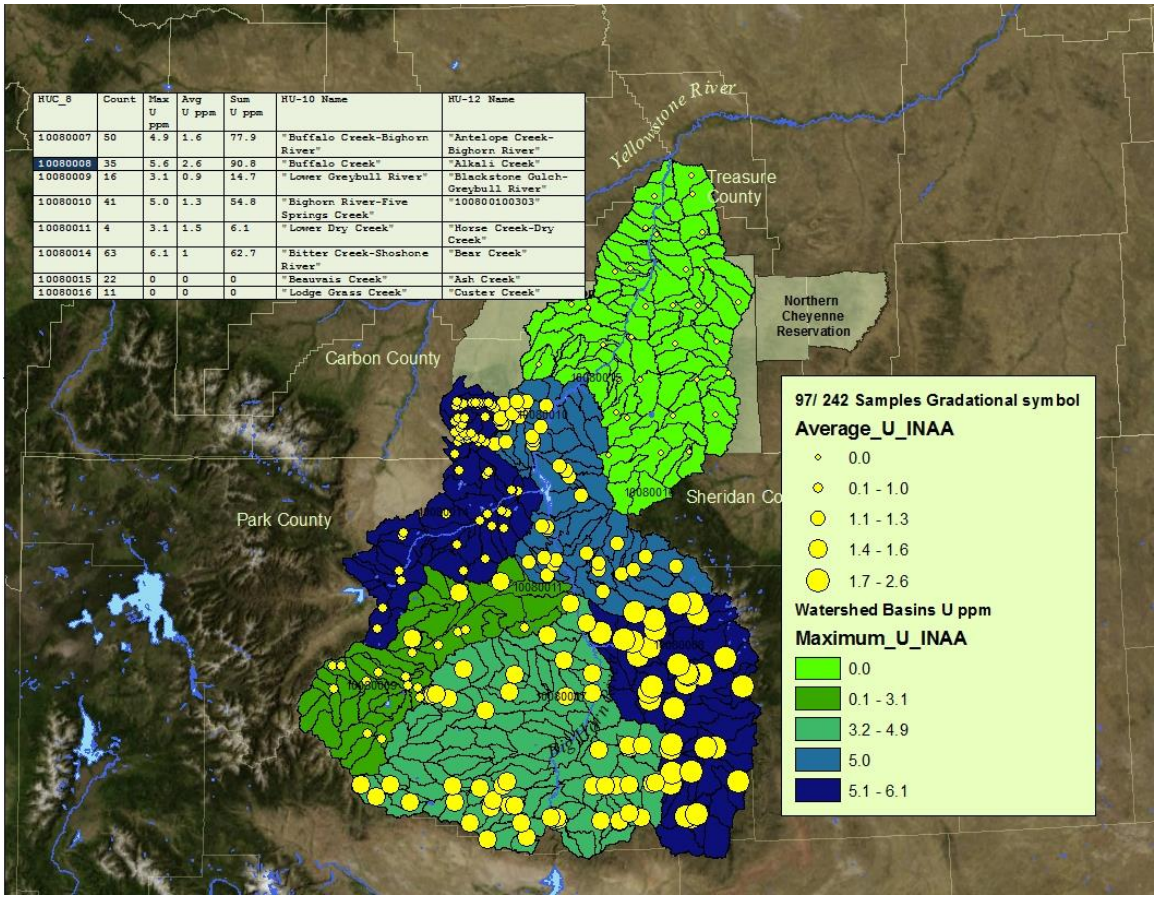


Figure A4. The highest U concentrations were from samples in the southeast portion of the Bighorn hydrologic basin. The map shows gradational symbols with the average concentrations of the U samples plotted as yellow filled symbols. The PMD and the LMD do show higher values than the Crow Reservation sediment samples though all are within normal crustal abundance for U.

The water analyses from the NURE database included 1403 samples that were included in the Bighorn hydrologic basin data. The data showed that samples analyzed in the PMD had the highest concentration of Pb in water samples analyzed (Figure A5).

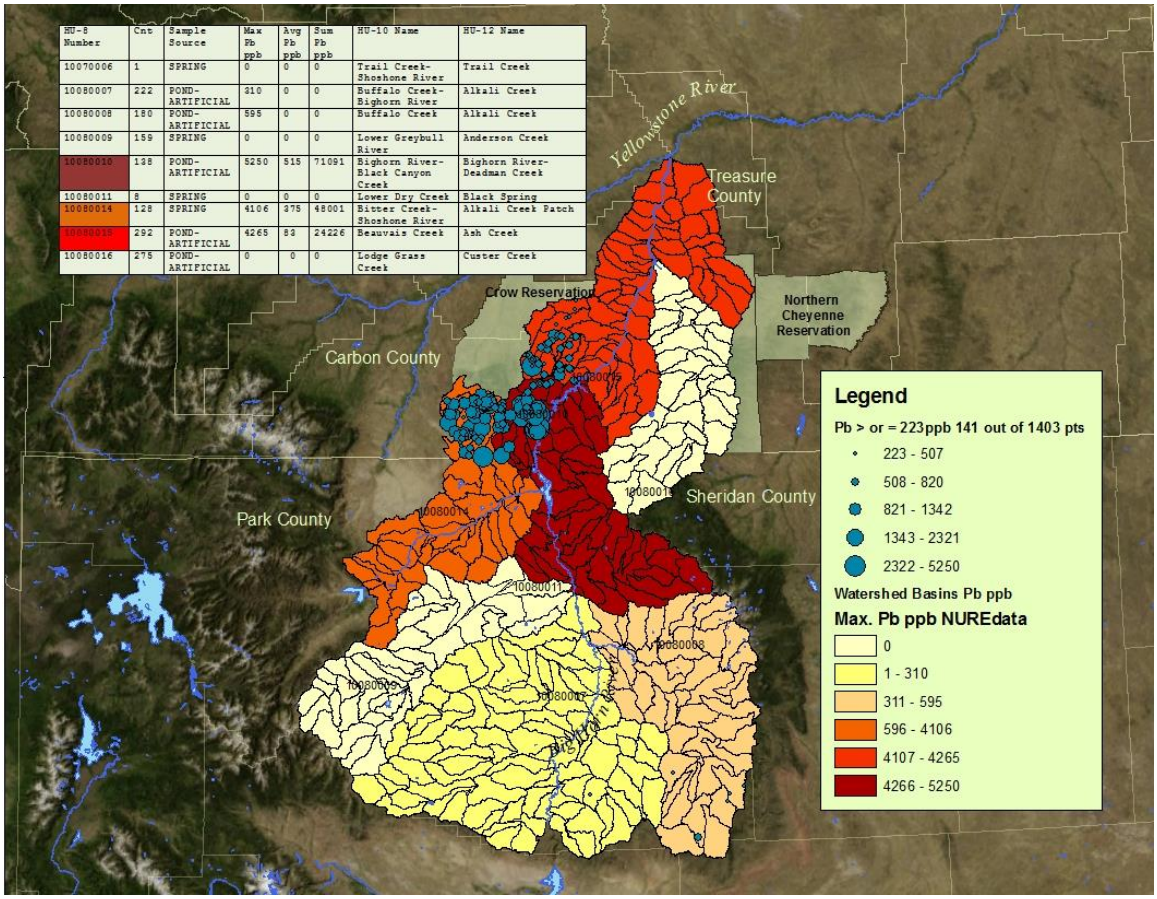


Figure A5. The highest Pb concentrations in water samples in the NURE database were from samples in the PMD and a few samples in the LMD. The sample with the highest Pb concentration was from a sample that was at the confluence of the Bighorn River and the Black Canyon in the Bighorn River reservoir, an "artificial pond", with 5350 ppb Pb. Some of these sites were later resampled by the author and submitted for analysis of Pb to Energy laboratories, an accredited EPA laboratory (Energy Labs, 2011). None of the resampled water samples had detectable Pb.

The data showed that samples analyzed in the hydrologic basin units (dark blue) that contributed to the Little Bighorn River had the highest concentration of U in NURE water samples analyzed (Figure A6). The mining districts did not show elevated U in water samples.

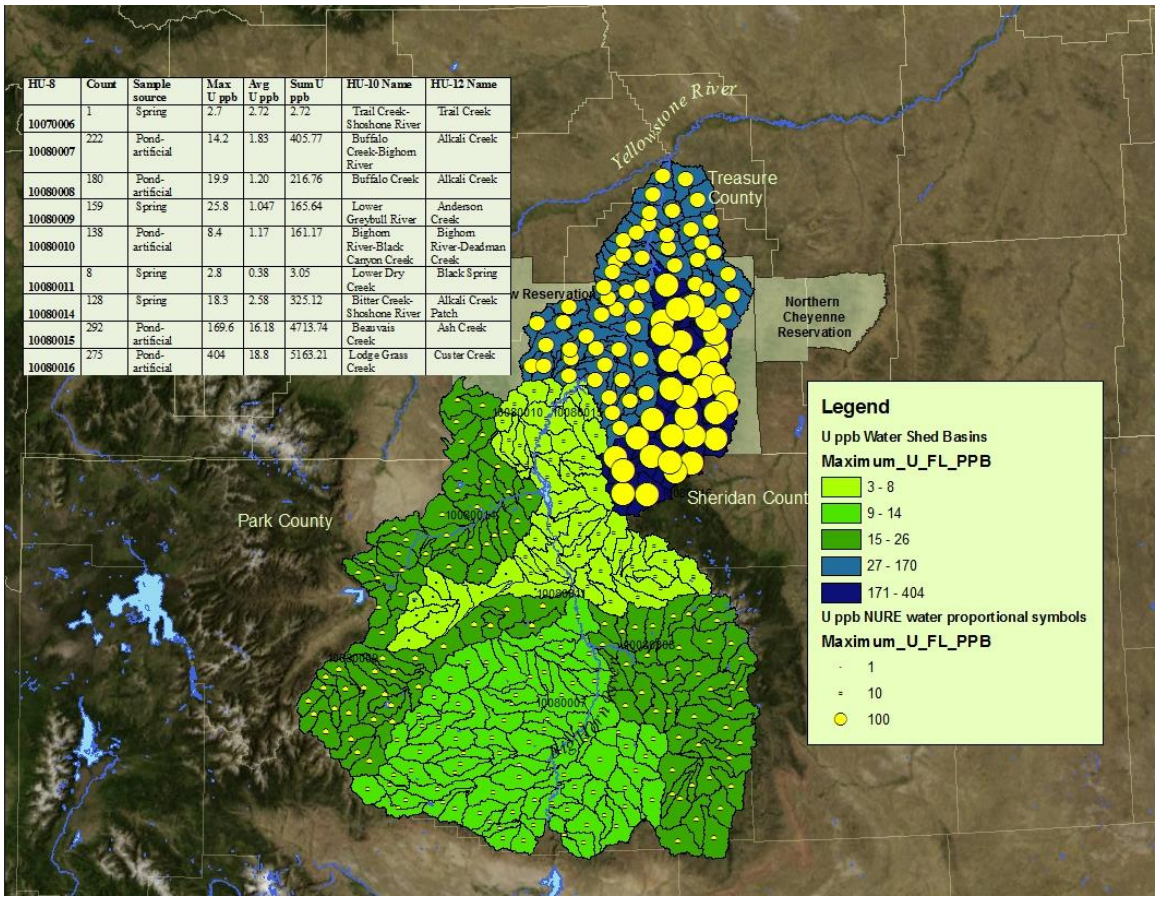


Figure A6. The highest U concentrations in water samples in the NURE database were from samples in the unit 10080016 of the HUC_8 unit. These were drainages that contributed to the Little Bighorn River and then contributed to the Bighorn River drainage basin. The analysis for U in water was by fluorometric methods.

APPENDIX B

SUPPORTING INFORMATION FOR CHAPTER 4

Stable C and O isotope analyses and methodology

Lora Wingate at the University of Michigan, Ann Arbor, MI, performed isotopic analysis of 53 carbonate samples used in this study (Wingate, pers. com.). The following is a description of the methodology.

A minimum of ten micrograms of powdered sample was placed in a stainless steel boat with four drops of anhydrous phosphoric acid for a minimum of eight minutes and a maximum of twelve minutes (for predominantly dolomitic samples) in a borosilicate reaction vessel at 77 ± 1°C. The reaction vessels were then placed in a Finnigan MAT Kiel IV preparation device coupled with a Finnigan MAT 253 triple collector isotope mass spectrometer. O^{17} data was corrected for acid fractionation and source mixing by correcting to a best fit regression line defined by the standard NBS-19. Machine precision is accurate to within 0.1‰ (Wingate, pers. com.). The results were provided in spreadsheet format with an identification number based on sample material submitted.

Stable isotope results are reported in comparison to the reference standard Vienna Pee Dee Belemnite (VPDB), which is calibrated by the U.S. Natural Bureau of Standards (NBS) through the analysis of an international reference laboratory standard (Arthur, 1983). NBS-19 is a standard derived from a homogenized white marble of unknown origin. The Standard Mean Ocean Water (SMOW) is a hypothetical standard in which hydrogen and oxygen ratios are similar to that of average ocean water. The SMOW is compared to VPDB by equation 1.

$$\delta^{18}O_{SMOW} = 1.03086\ \delta^{18}O_{VPDB} + 30.86 \quad (1)$$

(Faure, 1998). Results are reported in delta (δ) notation, which is a ratio of stable isotopes given by equation 2.

$$\boldsymbol{\delta = \frac{R_{sample} - R_{standard}}{R_{standard}} \times 1000} \quad (2)$$

where R is the ratio between either $^{13}C/^{12}C$ or $^{18}O/^{16}O$, the standard is either SMOW or VPDB, and units are per mil (‰)(Faure, 1998). Data in this paper given relative to the standard VPBD.

The NBS 19 standard was analyzed with samples in this study with published values +1.95/-2.2 and the analytical error better than +/-0.1 per mil for both C and O. Analyses are a compilation of four sets of samples submitted during the course of the study. Standards run with the samples (n=21) averaged +1.93/-2.21 and the average standard deviation was +0.04/+0.06. One or two splits (duplicates) were run with each sample set to assure accuracy. Results of $\delta^{13}C$ and $\delta^{18}O$ compositions measured for samples in this study are in Table B1. Samples are color coded for reference for Figures 4.5 and 4.7 in the main text.

Sample ID	Sample Description	$\delta^{13}C$ VPBD	$\delta^{18}O$ VPBD
	Little Mountain		
LeoInclineA	Calcite vein material; green calcite	-6.20	-19.18
LeoInclineB	Green calcite fracture fill vein material	-6.13	-21.08
LMLeoB	Calcite fill in breccia below - white calcite	-5.45	-23.48
*LMLisbon	Green calcite fracture fill vein material	-5.29	-19.89
LMLeoIncline	Limestone breccia; mineralization in fracture	-4.43	-16.79

	Pryor Mountains		
Sandra002	Sandra mine; fossiliferous tan limestone	-0.28	-7.92
Sandra713B	Sandra mine area; minor UV mineral; limestone	6.00	-10.66
MM1021B	Limestone tan micritic with brachiopods; Marie mine	-0.41	-18.23
DH22	Host rock; Dandy mine adit; limestone	-1.02	-6.74
PSE001A	Prospect west of Old Glory mine; grey recrystallized LS	-1.76	-18.33
PSE001BH	Prospect west of Old Glory mine; bleached limestone host	1.47	-7.13
PSE001GH	Prospect west of Old Glory mine; LS host of green calcite	-1.82	-18.04
EP001H	Limestone host; East Pryor mine area	-2.35	-19.07
SBB01	Bleached limestone; near mineralized breccia Sandra mine	-0.09	-6.81
SBM01	Bleached limestone; near mineralized breccia Sandra mine	-0.15	-6.73
SUBH01	Limestone; near unmineralized breccia SE of Sandra mine	0.69	-3.22
UMB9	LS host of unmineralized breccia UMB9 site; barite present	-0.66	-5.16
D2001C	LS w/calcite vein; waste pile 2nd below Dandy mine	-4.55	-23.60
DandySPMH	Stockpile area of Dandy mine; mineralized limestone host	-2.28	-21.04
UMBH17	Unmineralized breccia host; bleached sugary dolomite	1.39	-9.84
SWMP_BH	Swamp Frog mine bleached dolomite host rock	-0.83	-7.90
DRPG	Dolomite gouge from Red Pryor Mountain.	4.54	0.68
MHA01	Marie mine area; tan bleached dolomite	-1.91	-11.14
MH01	Marie mine adit host rock; tan dolomite	-2.04	-5.34
RLS1021A	Top pitted grey dolomite in Amsden Formation	-1.66	-3.43
RLS1021B	Dolomite overlying buff shales Amsden Formation	-1.88	-0.03
1028_LSH	Dolomite host of UMB with barite and fluorite	2.61	-1.00
PSE001H	Prospect; dolomite host rock; slightly silicified; calcite vugs	2.38	-5.26
PSE006	Bleached wall rock of prospect - dolomite	0.32	-6.91
PSE005	Prospect host rock of white calcite vug; dolomite	0.55	-4.07
PSE003	Prospect host rock near green calcite - dolomite	1.14	-3.75
Lisbon001A	Ferroan dolomite chaotic breccia (stained sample)	0.20	0.15
MM1021A	Madison Group dolomite host solution breccia	2.04	-2.87
EP002B	Breccia intruded by EP002DB; dolomite	-0.81	-16.47
UMBH18	Dolomite host rock of unmineralized breccia	2.12	-10.08

	UMB018 with quartz veining.		
EP002DB	Dark grey matrix silicified dolomite breccia with sulfides	-1.94	-19.22
UMB018	Clast in unmineralized silicified breccia	-1.59	-19.06
EP003	Calcite covered limestone breccia; East Pryor mine area	0.04	-17.06
Sandra001	Limestone from mine sample; mosaic breccia	-3.27	-15.34
SWMP01V	Dolomite vein; ore/waste pile near Swamp Frog mine	-0.79	-15.28
Lisbon001C	Ferroan calcite from vug of Lisbon001A (stained sample in figure 4.5 main text)	-0.59	-15.99
*SBC	Speleothem Big Pryor Mountain	0.32	-16.44
*BPM_BC	Speleothem Big Pryor Mountain	0.24	-16.55
Lisbon001B	Calcite vug of Lisbon001A, Lisbon mine (stained sample)	-0.40	-11.99
EP001	East Pryor mine area calcite vein material, 1-2" crystals	-6.02	-23.34
EP002	E. Pryor area calcite with very fine inclusions of marcasite or pyrite	-2.09	-18.55
EP003	Sample from fracture fill vein material; calcite	-3.29	-20.53
PSE004	Prospect 004 W of Old Glory mine, white calcite vug	-2.30	-18.49
PSE001RC	Prospect 001 west of Old Glory mine vug filling calcite	-1.59	-17.18
PSE002	Prospect 002 west of Old Glory mine green calcite	-3.28	-19.01
2PSE001GC	2nd prospect west of Old Glory mine green calcite	-4.35	-19.57
DandySPGC	From stockpile area near Dandy mine; green calcite	-3.93	-20.90
DandySPMV	Dandy mine stockpile; vein in mineralized host	-2.33	-24.80
SBRX	Dandy mine recrystallized calcite on fracture surface	-2.07	-21.87
DH22V	Calcite vein in host rock at Dandy mine adit	-0.03	-17.91
OGM715GC	Green calcite from Old Glory mine area	-5.60	-19.49
FS139	Big Pryor Mountain colorful 2" vein fill material unmineralized	-1.86	-17.36

Table B1. Stable C and O isotope data of representative samples from the mining districts. Abbreviations in the sample description: LS, limestone and UMB, unmineralized breccia. Two speleothem calcite and one calcite from the Little Mountain area were measured at the University of Wyoming Stable Isotope facility, these are denoted with an * in front of the Sample ID. All other carbonate samples were measured at the University of Michigan Stable Isotope Laboratory.

Radiogenic Sr isotope methodology

Sr was separated from barite and $^{87}Sr/^{86}Sr$ was measured on a NEPTUNE MC-ICPMS at the institute of Marine Sciences, University of California, Santa Cruz, California, using the methods described by Scher et al., 2013 (Paytan, per. com.). Sr was separated from carbonates, fluorite and breccia material at the University of Wyoming. The following is a detailed summary of the Sr separation procedure as outlined by Ken Sims, and edited by Erin H.W. Phillips. Separation and analysis of Sr was performed by the Anita Moore-Nall under the guidance of Erin H.W. Phillips and Sean Scott at the University of Wyoming.

Powdered samples were prepared as described for XRD portion above at MSU. Sr was separated from powdered samples in the clean labs at the University of Wyoming Geology and Geophysics Department. Approximately 100 mg of each of the powdered samples was weighed and put into Teflon beakers. Calcite, limestone and dolomite were dissolved in 3 ml 1N hydrochloric acid (HCl) for 24-48 hours at room temperature. Fluorite was dissolved in 1ml concentrated nitric acid (HNO_3) and 3 ml perchloric acid ($HClO_4$); the samples were heated gradually over 10 hours to 180°C in an Analab Eurotherm 2132 model gas collector to dissolve. This procedure was repeated three times. Breccia samples were dissolved with 3 ml concentrated HNO_3 + 1ml $HClO_4$ + 2ml concentrated hydrofluoric acid (HF) and placed on a hot plate at 130°C to dissolve for 48 hours and then dried down in the Analab Eurotherm.

After calcite, limestone and dolomite dissolution, each sample was centrifuged at 3000 rpm for 2 minutes. The supernatant was retained and subsequently dried down on a

hot plate at 130°C. When dry, 8-10 ml 7N HNO_3 was added to each sample to convert to nitrate form prior to loading onto columns. The samples were capped and placed on a hot plate at 130°C for at least 8 hours and then dried down.

Sr was purified using Sr Resin microcolumns, which consist of snipped-off HDPE transfer pipettes fitted with polyethylene frits and have a reservoir capacity of ~4 ml. Approximately 500 µl of Eichrom 50-100 µm Sr Resin was added to each column. Resin was prepared by making a slurry in ultrapure H_2O the night before use and pipetting off floating surface material with transfer pipette prior to adding to columns.

Sr Resin microcolumns were cleaned with successive reservoirs of ultrapure H_2O, 6N HCl, ultrapure H_2O, 0.5N HCl, and ultrapure H_2O. After cleaning, columns were wrapped in parafilm and stored overnight in ultrapure H_2O.

Columns were conditioned with 1 reservoir 3N HNO_3. Samples were dissolved in 6 ml 3N HNO_3 on hot plate for ~30 minutes. After centrifugation, 1.5 to 3 ml of each sample was loaded onto columns, avoiding any precipitate. Columns were rinsed with 1 ml 3N HNO_3. Matrix was eluted with 4 ml 3N HNO_3. Sr was collected by 2 successive additions of 3 ml H_2O to each column. Collection beakers were placed on hot plate at 90°C to dry overnight.

To reduce organics prior to mass spectrometric analysis, 3 drops concentrated HNO_3 and 1 drop H_2O_2 were added to each sample and immediately dried down. Isotopic analysis was performed at the Wyoming High-Precision Isotope Laboratory at the University of Wyoming on the NEPTUNE Plus, a next-generation Multicollector-Inductively Coupled Plasma Mass Spectrometer (MC-ICPMS). Samples were dissolved

in 1 ml 1N HNO_3 for analysis and then diluted appropriately. A procedural blank was run with each set of 8-9 samples and NBS987 standard was run 6-8 times with each sample set. BCR-2 (Columbia River basalt) and SRM915b (a $CaCO_3$ standard) were also analyzed multiple times with each sample set. $^{87}Sr/^{86}Sr$ is reported relative to NBS987 = 0.710240 and each day all data was normalized to the NBS987 average for that day.

Results of $^{87}Sr/^{86}Sr$ composition measured for samples in this study follow in Table B2 below. Samples are color coded for reference for Figures 4.10, 4.11, and 4.12 in the main text.

#	Sample ID	Composition	$\delta^{18}O$	$^{87}Sr/^{86}Sr$
1	OGMF	Dark purple fluorite, Old Glory mine, PMD	na	0.709974
2	DandyF	Purple fluorite, Dandy mine, PMD	na	0.709933
3	MBEPryor02	Purple fluorite, East Pryor mine, PMD	na	0.709458
4	OGM B	Barite, Old Glory mine, PMD	na	0.709509
5	SWMP B	Barite, Swamp Frog mine, PMD	na	0.709907
6	D2001C	Limestone with calcite & UV minerals, Dandy mine, PMD	-23.60	0.709090
7	PSE002A	Mineralized, recrystallized limestone from UV prospect	-18.33	0.710048
8	DH22	Limestone host, Dandy mine	-6.74	0.708340
9	Mm	Madison limestone, ~ 20 km from mineralized zone	-6.93	0.707913
10	PSE003	Dolomite host rock near a prospect	-3.75	0.708754

11	1028LSH	Pennsylvanian age dolomite, Ranchester Limestone member	-1.00	0.709207
12	SWMP01V	Dolomite vein Swamp Frog mine	-15.28	0.709676
13	LeoInclineA	Calcite Leo Incline area, LMD	-19.18	0.708316
14	LMLisbon	Calcite Lisbon mine, LMD	na	0.708845
15	DandySPMV	Stock Pile ~ calcite vein with U-V mineralization, Dandy mine, PMD	-24.80	0.709220
16	SBRX	Calcite & U-V vein	-21.87	0.709591
17	FS139	Calcite vein from top of Big Pryor Mtn. away from mineralized zone	-17.36	0.709342
18	OGM715GC	Green calcite Old Glory mine, PMD	-19.49	0.708718
19	2PSE001GC	Green calcite from U-V prospect, Red Pryor Mountain, PMD	-19.57	0.709294
20	PSE002	Calcite from U-V prospect Red Pryor Mountain, PMD	-19.01	0.709375
21	Lisbon001C	Unmineralized ferroan calcite that healed sample Lisbon001A	-15.99	0.709781
22	Lisbon001A	Unmineralized ferroan dolomite chaotic floating clast breccia, Lisbon mine area, PMD	0.15	0.714931
23	Mm1021A	Madison Group solution breccia dolomite host	-2.87	0.708116
24	EP002B	Dolomite breccia that was intruded by EP002DB, East Pryor mine area	-16.47	0.709589
25	EP002DB	Dark silicified limestone breccia with sulfides, East Pryor mine area	-19.22	0.710132
26	MB15UV	Mineralized silicified limestone breccia, PMD	na	0.709874
27	UMB018	Unmineralized silicified limestone breccia, PMD	-19.06	0.709855
28	OGM04	Silicified limestone breccia	na	0.709544

29	LMLeoIncline	Mineralized limestone breccia, Leo Incline area, LMD	-16.79	0.708726
30	BCR-2 (mean n = 5)	Columbia River Basalt	na	0.705008
31	NBS987 (mean n= 21)	Reference standard - $SrCO_3$	na	0.710265
32	SRM915b (mean n=9)	Reference standard – $CaCO_3$	na	0.707990

Table B2. $^{87}Sr/^{86}Sr$ composition of samples from the two mining districts. Shaded colors in the Sample ID column correspond to sample types cross-plotted with $^{87}Sr/^{86}Sr$ compositions in Figure 4.10. The sample number also corresponds to the x-axis for the cross-plot of Figure 4.11. $\delta^{18}O$ composition included for those samples which were analyzed for stable C and O isotopes, used in Table A1. Not analyzed (na).

Google Earth Pro lineament data

Google Earth Pro (GEP) version 7.2.1 was used to identify dominant lineament orientations at the macroscale on Big Pryor Mountain, the southwestern block of the Pryor Mountains. Lineaments were extracted from GEP and imported in ESRI ArcGIS as a KML file and converted to a polyline feature shapefile. The lineaments were divided into six classes (1-6) based on their orientation (Table B3). The actual dip of the lineations is not known. A dip of 90° was added to be able to use the Rockware StereoStat version 1.6.1 to plot and compare the lineament and field data orientation data on rose diagrams. Table B3 is shown in two columns.

Group	Length (m)	Orientation	Dip
1	126	298	90
1	84	297	90
1	160	293	90
1	101	293	90
1	71	293	90
1	300	290	90
1	262	290	90
1	367	288	90
1	143	288	90
1	75	288	90
1	48	288	90
1	1022	287	90
1	139	287	90
1	38	287	90
1	335	286	90
1	142	286	90
1	111	286	90
1	74	286	90
1	62	286	90
1	41	286	90
1	104	285	90
1	79	285	90
1	69	285	90
1	219	284	90
1	129	284	90
1	110	284	90
1	80	284	90
1	78	284	90
1	147	283	90
1	109	283	90
1	99	283	90
1	77	283	90
1	60	283	90
1	175	282	90
1	158	282	90
1	86	282	90
1	57	282	90
1	219	281	90
1	215	281	90
1	165	281	90
1	103	281	90
1	98	281	90
1	39	281	90
1	34	281	90
1	460	280	90
1	338	280	90
1	277	280	90
1	256	280	90
1	253	280	90
1	192	280	90
1	141	280	90
1	114	280	90
1	89	280	90
1	88	280	90
1	72	280	90
1	57	280	90
1	310	279	90
1	305	279	90
1	93	279	90
1	70	279	90
1	1551	278	90
1	637	278	90
1	480	278	90
1	402	278	90
1	390	278	90
1	230	278	90
1	219	278	90
1	176	278	90
1	174	278	90
1	169	278	90
1	164	278	90
1	123	278	90
1	112	278	90
1	106	278	90
1	104	278	90
1	84	278	90

1	62	278	90
1	58	278	90
1	679	277	90
1	455	277	90
1	418	277	90
1	378	277	90
1	311	277	90
1	299	277	90
1	246	277	90
1	230	277	90
1	226	277	90
1	160	277	90
1	132	277	90
1	110	277	90
1	101	277	90
1	97	277	90
1	95	277	90
1	70	277	90
1	65	277	90
1	49	277	90
1	1546	276	90
1	561	276	90
1	402	276	90
1	358	276	90
1	291	276	90
1	252	276	90
1	251	276	90
1	242	276	90
1	235	276	90
1	218	276	90
1	217	276	90
1	212	276	90
1	133	276	90
1	131	276	90
1	120	276	90
1	103	276	90
1	102	276	90
1	91	276	90
1	88	276	90
1	78	276	90

1	65	276	90
1	64	276	90
1	53	276	90
1	51	276	90
1	44	276	90
1	42	276	90
1	42	276	90
1	38	276	90
1	836	275	90
1	491	275	90
1	460	275	90
1	399	275	90
1	380	275	90
1	330	275	90
1	290	275	90
1	238	275	90
1	203	275	90
1	200	275	90
1	185	275	90
1	181	275	90
1	153	275	90
1	150	275	90
1	143	275	90
1	140	275	90
1	134	275	90
1	101	275	90
1	93	275	90
1	88	275	90
1	86	275	90
1	80	275	90
1	72	275	90
1	58	275	90
1	48	275	90
1	43	275	90
1	39	275	90
1	30	275	90
1	7	275	90
1	953	274	90
1	953	274	90
1	870	274	90

1	729	274	90
1	439	274	90
1	390	274	90
1	307	274	90
1	296	274	90
1	261	274	90
1	254	274	90
1	225	274	90
1	193	274	90
1	189	274	90
1	184	274	90
1	173	274	90
1	170	274	90
1	158	274	90
1	152	274	90
1	140	274	90
1	137	274	90
1	125	274	90
1	104	274	90
1	100	274	90
1	96	274	90
1	90	274	90
1	79	274	90
1	73	274	90
1	65	274	90
1	65	274	90
1	61	274	90
1	60	274	90
1	56	274	90
1	53	274	90
1	50	274	90
1	49	274	90
1	42	274	90
1	25	274	90
1	22	274	90
1	14	274	90
1	1405	273	90
1	1058	273	90
1	728	273	90
1	560	273	90
1	545	273	90
1	418	273	90
1	404	273	90
1	392	273	90
1	362	273	90
1	357	273	90
1	307	273	90
1	282	273	90
1	256	273	90
1	232	273	90
1	194	273	90
1	186	273	90
1	170	273	90
1	166	273	90
1	160	273	90
1	149	273	90
1	144	273	90
1	138	273	90
1	129	273	90
1	120	273	90
1	103	273	90
1	100	273	90
1	87	273	90
1	67	273	90
1	62	273	90
1	61	273	90
1	55	273	90
1	54	273	90
1	53	273	90
1	53	273	90
1	49	273	90
1	42	273	90
1	28	273	90
1	16	273	90
1	1779	272	90
1	802	272	90
1	776	272	90
1	734	272	90
1	730	272	90
1	559	272	90

1	504	272	90
1	501	272	90
1	495	272	90
1	393	272	90
1	374	272	90
1	366	272	90
1	339	272	90
1	336	272	90
1	328	272	90
1	262	272	90
1	227	272	90
1	225	272	90
1	216	272	90
1	204	272	90
1	194	272	90
1	181	272	90
1	178	272	90
1	171	272	90
1	163	272	90
1	147	272	90
1	140	272	90
1	139	272	90
1	130	272	90
1	110	272	90
1	104	272	90
1	99	272	90
1	98	272	90
1	95	272	90
1	76	272	90
1	71	272	90
1	63	272	90
1	61	272	90
1	58	272	90
1	50	272	90
1	50	272	90
1	47	272	90
1	42	272	90
1	27	272	90
1	24	272	90
1	24	272	90

1	21	272	90
1	12	272	90
1	1033	271	90
1	977	271	90
1	965	271	90
1	942	271	90
1	832	271	90
1	760	271	90
1	674	271	90
1	632	271	90
1	544	271	90
1	502	271	90
1	486	271	90
1	389	271	90
1	351	271	90
1	314	271	90
1	312	271	90
1	291	271	90
1	253	271	90
1	243	271	90
1	228	271	90
1	208	271	90
1	199	271	90
1	191	271	90
1	189	271	90
1	188	271	90
1	183	271	90
1	177	271	90
1	144	271	90
1	143	271	90
1	143	271	90
1	131	271	90
1	128	271	90
1	125	271	90
1	123	271	90
1	122	271	90
1	119	271	90
1	106	271	90
1	102	271	90
1	85	271	90

1	83	271	90
1	82	271	90
1	80	271	90
1	77	271	90
1	75	271	90
1	66	271	90
1	60	271	90
1	58	271	90
1	56	271	90
1	50	271	90
1	49	271	90
1	41	271	90
1	39	271	90
1	36	271	90
1	33	271	90
1	31	271	90
1	28	271	90
1	24	271	90
1	23	271	90
1	9	271	90
1	9	271	90
1	7	271	90
1	6	271	90
1	1568	270	90
1	1176	270	90
1	1147	270	90
1	877	270	90
1	797	270	90
1	766	270	90
1	720	270	90
1	717	270	90
1	684	270	90
1	637	270	90
1	637	270	90
1	597	270	90
1	587	270	90
1	554	270	90
1	505	270	90
1	443	270	90
1	425	270	90
1	419	270	90
1	342	270	90
1	329	270	90
1	309	270	90
1	295	270	90
1	285	270	90
1	265	270	90
1	224	270	90
1	221	270	90
1	206	270	90
1	202	270	90
1	196	270	90
1	191	270	90
1	184	270	90
1	183	270	90
1	176	270	90
1	154	270	90
1	149	270	90
1	148	270	90
1	138	270	90
1	131	270	90
1	119	270	90
1	108	270	90
1	105	270	90
1	104	270	90
1	95	270	90
1	93	270	90
1	86	270	90
1	78	270	90
1	63	270	90
1	58	270	90
1	55	270	90
1	52	270	90
1	50	270	90
1	49	270	90
1	49	270	90
1	47	270	90
1	42	270	90
1	32	270	90
1	29	270	90

1	23	270	90
1	21	270	90
1	18	270	90
1	17	270	90
1	10	270	90
1	9	270	90
1	8	270	90
1	6	270	90
1	5820	269	90
1	914	269	90
1	878	269	90
1	867	269	90
1	527	269	90
1	461	269	90
1	434	269	90
1	423	269	90
1	367	269	90
1	363	269	90
1	333	269	90
1	327	269	90
1	306	269	90
1	293	269	90
1	280	269	90
1	246	269	90
1	240	269	90
1	236	269	90
1	207	269	90
1	197	269	90
1	191	269	90
1	172	269	90
1	169	269	90
1	158	269	90
1	155	269	90
1	109	269	90
1	103	269	90
1	102	269	90
1	100	269	90
1	89	269	90
1	86	269	90
1	82	269	90

1	75	269	90
1	73	269	90
1	70	269	90
1	69	269	90
1	68	269	90
1	66	269	90
1	60	269	90
1	56	269	90
1	53	269	90
1	50	269	90
1	46	269	90
1	44	269	90
1	35	269	90
1	31	269	90
1	30	269	90
1	28	269	90
1	26	269	90
1	22	269	90
1	16	269	90
1	13	269	90
1	5	269	90
1	2473	268	90
1	1759	268	90
1	1407	268	90
1	904	268	90
1	669	268	90
1	657	268	90
1	617	268	90
1	446	268	90
1	441	268	90
1	411	268	90
1	372	268	90
1	336	268	90
1	308	268	90
1	262	268	90
1	255	268	90
1	242	268	90
1	239	268	90
1	157	268	90
1	144	268	90

1	99	268	90
1	89	268	90
1	81	268	90
1	80	268	90
1	76	268	90
1	66	268	90
1	58	268	90
1	52	268	90
1	48	268	90
1	12	268	90
1	920	267	90
1	754	267	90
1	656	267	90
1	590	267	90
1	586	267	90
1	320	267	90
1	289	267	90
1	273	267	90
1	268	267	90
1	252	267	90
1	196	267	90
1	178	267	90
1	176	267	90
1	172	267	90
1	157	267	90
1	142	267	90
1	129	267	90
1	110	267	90
1	93	267	90
1	92	267	90
1	83	267	90
1	82	267	90
1	69	267	90
1	60	267	90
1	51	267	90
1	40	267	90
1	38	267	90
1	26	267	90
1	19	267	90
1	10	267	90

1	8	267	90
1	732	266	90
1	711	266	90
1	413	266	90
1	407	266	90
1	406	266	90
1	392	266	90
1	357	266	90
1	329	266	90
1	249	266	90
1	247	266	90
1	234	266	90
1	212	266	90
1	194	266	90
1	187	266	90
1	165	266	90
1	163	266	90
1	163	266	90
1	92	266	90
1	73	266	90
1	66	266	90
1	61	266	90
1	47	266	90
1	42	266	90
1	38	266	90
1	28	266	90
1	24	266	90
1	19	266	90
1	18	266	90
1	16	266	90
1	12	266	90
1	922	265	90
1	846	265	90
1	248	265	90
1	239	265	90
1	221	265	90
1	216	265	90
1	126	265	90
1	109	265	90
1	98	265	90

1	74	265	90
1	69	265	90
1	62	265	90
1	61	265	90
1	58	265	90
1	52	265	90
1	31	265	90
1	20	265	90
1	13	265	90
1	11	265	90
1	520	264	90
1	348	264	90
1	228	264	90
1	222	264	90
1	218	264	90
1	217	264	90
1	193	264	90
1	132	264	90
1	87	264	90
1	70	264	90
1	50	264	90
1	42	264	90
1	31	264	90
1	21	264	90
1	679	263	90
1	32	263	90
1	392	262	90
1	292	262	90
1	220	262	90
1	159	262	90
1	126	262	90
1	50	262	90
1	20	262	90
1	204	261	90
1	203	261	90
1	174	261	90
1	64	261	90
1	45	261	90
1	41	261	90
1	1002	260	90

1	340	260	90
1	169	260	90
1	132	260	90
1	119	260	90
1	35	260	90
1	11	260	90
1	210	259	90
1	183	259	90
1	73	259	90
1	57	259	90
1	30	259	90
1	307	258	90
1	283	258	90
1	167	258	90
1	83	258	90
1	27	258	90
1	11	258	90
1	524	257	90
1	81	257	90
1	44	257	90
1	782	256	90
1	415	255	90
1	56	255	90
1	517	253	90
1	355	253	90
1	340	251	90
1	320	251	90
1	89	250	90
1	81	244	90
1	86	239	90
1	378	94	90
1	248	92	90
1	117	92	90
1	821	91	90
1	259	91	90
1	92	91	90
1	92	90	90
1	92	90	90
1	362	85	90
1	62	83	90

1	478	74	90
1	145	71	90
2	88	277	90
2	229	270	90
2	533	269	90
2	193	268	90
2	127	268	90
2	369	267	90
2	331	266	90
2	266	266	90
2	769	265	90
2	630	265	90
2	232	265	90
2	169	265	90
2	73	265	90
2	1488	264	90
2	547	264	90
2	488	264	90
2	282	264	90
2	89	264	90
2	53	264	90
2	45	264	90
2	373	263	90
2	307	263	90
2	266	263	90
2	196	263	90
2	103	263	90
2	77	263	90
2	45	263	90
2	154	262	90
2	88	262	90
2	67	262	90
2	41	262	90
2	945	261	90
2	588	261	90
2	494	261	90
2	389	261	90
2	100	261	90
2	455	260	90
2	391	260	90

2	272	260	90
2	228	260	90
2	173	260	90
2	96	260	90
2	80	260	90
2	71	260	90
2	1065	259	90
2	935	259	90
2	774	259	90
2	669	259	90
2	353	259	90
2	293	259	90
2	229	259	90
2	202	259	90
2	165	259	90
2	161	259	90
2	1314	258	90
2	1050	258	90
2	940	258	90
2	581	258	90
2	531	258	90
2	248	258	90
2	90	258	90
2	87	258	90
2	33	258	90
2	1161	257	90
2	498	257	90
2	433	257	90
2	382	257	90
2	170	257	90
2	157	257	90
2	145	257	90
2	1070	256	90
2	638	256	90
2	569	256	90
2	527	256	90
2	163	256	90
2	125	256	90
2	98	256	90
2	81	256	90

2	62	256	90
2	1652	255	90
2	420	255	90
2	416	255	90
2	365	255	90
2	156	255	90
2	127	255	90
2	100	255	90
2	78	255	90
2	2677	254	90
2	549	254	90
2	320	254	90
2	312	254	90
2	285	254	90
2	225	254	90
2	216	254	90
2	165	254	90
2	135	254	90
2	108	254	90
2	38	254	90
2	2039	253	90
2	1937	253	90
2	1571	253	90
2	954	253	90
2	476	253	90
2	443	253	90
2	428	253	90
2	418	253	90
2	334	253	90
2	322	253	90
2	311	253	90
2	277	253	90
2	240	253	90
2	222	253	90
2	196	253	90
2	97	253	90
2	90	253	90
2	29	253	90
2	994	252	90
2	563	252	90
2	552	252	90
2	211	252	90
2	46	252	90
2	235	251	90
2	183	251	90
2	183	251	90
2	1122	250	90
2	788	250	90
2	665	250	90
2	376	250	90
2	369	250	90
2	353	250	90
2	338	250	90
2	185	250	90
2	119	250	90
2	105	250	90
2	69	250	90
2	52	250	90
2	36	250	90
2	751	249	90
2	732	249	90
2	732	249	90
2	626	249	90
2	560	249	90
2	356	249	90
2	191	249	90
2	190	249	90
2	146	249	90
2	124	249	90
2	113	249	90
2	71	249	90
2	62	249	90
2	11	249	90
2	8	249	90
2	1345	248	90
2	1060	248	90
2	811	248	90
2	359	248	90
2	265	248	90
2	225	248	90

2	177	248	90
2	128	248	90
2	127	248	90
2	72	248	90
2	1849	247	90
2	553	247	90
2	483	247	90
2	435	247	90
2	426	247	90
2	339	247	90
2	330	247	90
2	245	247	90
2	210	247	90
2	179	247	90
2	173	247	90
2	139	247	90
2	104	247	90
2	82	247	90
2	886	246	90
2	403	246	90
2	313	246	90
2	287	246	90
2	263	246	90
2	252	246	90
2	218	246	90
2	116	246	90
2	63	246	90
2	35	246	90
2	12	246	90
2	1000	245	90
2	459	245	90
2	310	245	90
2	237	245	90
2	173	245	90
2	143	245	90
2	1067	244	90
2	891	244	90
2	619	244	90
2	459	244	90
2	395	244	90

2	213	244	90
2	203	244	90
2	187	244	90
2	174	244	90
2	49	244	90
2	1384	243	90
2	860	243	90
2	524	243	90
2	476	243	90
2	456	243	90
2	198	243	90
2	176	243	90
2	112	243	90
2	104	243	90
2	70	243	90
2	7	243	90
2	1900	242	90
2	1292	242	90
2	788	242	90
2	785	242	90
2	552	242	90
2	519	242	90
2	461	242	90
2	354	242	90
2	254	242	90
2	163	242	90
2	148	242	90
2	129	242	90
2	105	242	90
2	50	242	90
2	608	241	90
2	606	241	90
2	437	241	90
2	282	241	90
2	184	241	90
2	143	241	90
2	138	241	90
2	76	241	90
2	32	241	90
2	12	241	90

2	510	240	90
2	436	240	90
2	279	240	90
2	269	240	90
2	171	240	90
2	148	240	90
2	95	240	90
2	679	239	90
2	502	239	90
2	456	239	90
2	391	239	90
2	84	239	90
2	52	239	90
2	950	238	90
2	695	238	90
2	254	238	90
2	251	238	90
2	148	238	90
2	130	238	90
2	98	238	90
2	93	238	90
2	555	237	90
2	280	237	90
2	224	237	90
2	143	237	90
2	98	237	90
2	93	237	90
2	639	236	90
2	589	236	90
2	456	236	90
2	191	236	90
2	115	236	90
2	99	236	90
2	82	236	90
2	22	236	90
2	441	235	90
2	247	235	90
2	165	235	90
2	152	235	90
2	131	235	90

2	78	234	90
2	1688	233	90
2	1456	233	90
2	357	233	90
2	167	233	90
2	138	233	90
2	121	233	90
2	999	232	90
2	585	232	90
2	361	232	90
2	242	232	90
2	206	232	90
2	173	232	90
2	83	232	90
2	264	231	90
2	257	231	90
2	914	230	90
2	193	230	90
2	1421	229	90
2	1291	229	90
2	55	229	90
2	1333	228	90
2	508	228	90
2	212	228	90
2	66	227	90
2	282	226	90
2	212	226	90
2	269	225	90
2	86	225	90
2	963	224	90
2	80	224	90
2	177	222	90
2	243	221	90
2	118	221	90
2	155	220	90
2	85	219	90
2	164	216	90
2	191	215	90
2	84	213	90
2	64	84	90

2	109	83	90
2	114	74	90
2	239	64	90
2	832	59	90
2	151	52	90
3	95	314	90
3	49	309	90
3	232	308	90
3	1076	305	90
3	848	305	90
3	708	305	90
3	111	304	90
3	49	304	90
3	900	303	90
3	856	303	90
3	98	303	90
3	18	303	90
3	807	302	90
3	269	302	90
3	90	300	90
3	469	299	90
3	170	299	90
3	241	298	90
3	1449	296	90
3	319	296	90
3	199	295	90
3	91	295	90
3	134	293	90
3	432	292	90
3	308	292	90
3	279	292	90
3	1013	291	90
3	399	291	90
3	242	291	90
3	158	291	90
3	408	290	90
3	406	290	90
3	347	290	90
3	235	290	90
3	189	290	90

3	727	289	90
3	141	289	90
3	32	289	90
3	15	289	90
3	64	287	90
3	8	287	90
3	759	286	90
3	625	286	90
3	149	286	90
3	38	286	90
3	25	286	90
3	374	285	90
3	258	285	90
3	181	285	90
3	138	285	90
3	173	284	90
3	30	284	90
3	131	283	90
3	1145	282	90
3	843	282	90
3	382	282	90
3	266	281	90
3	252	281	90
3	49	281	90
3	855	280	90
3	404	279	90
3	126	277	90
3	98	275	90
3	286	271	90
3	184	142	90
3	282	135	90
3	214	135	90
3	325	132	90
3	494	131	90
3	365	130	90
3	145	127	90
3	135	127	90
3	814	126	90
3	710	126	90
3	890	125	90

3	1265	123	90
3	894	123	90
3	261	122	90
3	99	122	90
3	947	121	90
3	523	121	90
3	266	121	90
3	186	121	90
3	1785	120	90
3	461	120	90
3	243	119	90
3	103	119	90
3	16	119	90
3	155	117	90
3	30	117	90
3	23	117	90
3	331	116	90
3	16	116	90
3	522	115	90
3	13	115	90
3	259	114	90
3	106	114	90
3	45	114	90
3	232	113	90
3	40	112	90
3	771	111	90
3	93	111	90
3	783	110	90
3	87	110	90
3	125	109	90
3	953	108	90
3	615	108	90
3	51	108	90
3	21	108	90
3	171	107	90
3	66	106	90
3	349	105	90
3	1228	104	90
3	567	104	90
3	438	103	90

3	266	102	90
3	66	102	90
3	254	101	90
3	41	101	90
3	76	97	90
3	5	92	90
3	210	90	90
4	253	348	90
4	3417	347	90
4	20	342	90
4	178	341	90
4	134	340	90
4	111	333	90
4	63	331	90
4	287	328	90
4	167	328	90
4	286	327	90
4	102	327	90
4	112	323	90
4	147	321	90
4	1009	307	90
4	214	306	90
4	80	304	90
4	358	302	90
4	200	302	90
4	1096	297	90
4	198	297	90
4	348	294	90
4	166	293	90
4	126	288	90
4	129	287	90
4	232	185	90
4	303	182	90
4	266	179	90
4	680	176	90
4	194	174	90
4	84	174	90
4	158	173	90
4	399	172	90
4	116	172	90

4	46	172	90
4	420	171	90
4	313	171	90
4	143	171	90
4	1094	170	90
4	661	170	90
4	463	170	90
4	208	169	90
4	796	168	90
4	348	168	90
4	232	168	90
4	178	168	90
4	154	168	90
4	472	167	90
4	151	167	90
4	147	167	90
4	195	166	90
4	73	166	90
4	691	165	90
4	405	165	90
4	311	165	90
4	215	165	90
4	349	164	90
4	345	164	90
4	132	164	90
4	111	164	90
4	101	164	90
4	1134	163	90
4	185	163	90
4	1697	162	90
4	188	162	90
4	82	162	90
4	3292	161	90
4	424	161	90
4	257	161	90
4	76	161	90
4	408	160	90
4	227	160	90
4	190	160	90
4	493	159	90

4	323	159	90
4	141	159	90
4	126	159	90
4	103	159	90
4	14	159	90
4	939	158	90
4	606	158	90
4	362	158	90
4	269	158	90
4	255	158	90
4	180	158	90
4	71	158	90
4	69	158	90
4	187	157	90
4	136	157	90
4	73	157	90
4	585	156	90
4	229	156	90
4	147	156	90
4	88	156	90
4	785	155	90
4	567	155	90
4	98	155	90
4	83	155	90
4	64	155	90
4	101	154	90
4	34	154	90
4	26	154	90
4	1344	153	90
4	369	153	90
4	135	153	90
4	36	153	90
4	21	153	90
4	13	153	90
4	699	152	90
4	445	152	90
4	232	152	90
4	162	152	90
4	115	152	90
4	71	152	90

4	63	152	90
4	633	151	90
4	246	151	90
4	162	151	90
4	159	151	90
4	153	151	90
4	79	151	90
4	936	150	90
4	339	150	90
4	281	150	90
4	272	150	90
4	221	150	90
4	107	150	90
4	95	150	90
4	67	150	90
4	2043	149	90
4	581	149	90
4	353	149	90
4	345	149	90
4	306	149	90
4	225	149	90
4	136	149	90
4	99	149	90
4	28	148	90
4	1080	147	90
4	387	147	90
4	232	147	90
4	172	147	90
4	131	147	90
4	8	147	90
4	541	146	90
4	360	146	90
4	337	146	90
4	245	146	90
4	209	146	90
4	111	146	90
4	15	146	90
4	370	145	90
4	289	145	90
4	115	145	90

4	36	145	90
4	35	145	90
4	19	145	90
4	807	144	90
4	545	144	90
4	497	144	90
4	368	144	90
4	91	144	90
4	803	143	90
4	666	143	90
4	239	143	90
4	137	143	90
4	126	143	90
4	112	143	90
4	730	142	90
4	344	142	90
4	185	142	90
4	96	142	90
4	61	142	90
4	441	141	90
4	437	141	90
4	178	141	90
4	65	141	90
4	26	141	90
4	1140	140	90
4	216	140	90
4	192	140	90
4	160	140	90
4	993	139	90
4	925	139	90
4	329	139	90
4	234	139	90
4	73	139	90
4	30	139	90
4	862	138	90
4	505	137	90
4	244	137	90
4	236	137	90
4	129	137	90
4	95	137	90

4	84	137	90
4	82	137	90
4	584	136	90
4	286	136	90
4	270	136	90
4	70	136	90
4	45	136	90
4	16	136	90
4	285	135	90
4	144	135	90
4	124	135	90
4	115	135	90
4	96	135	90
4	69	135	90
4	50	135	90
4	108	134	90
4	78	134	90
4	67	134	90
4	633	133	90
4	456	133	90
4	223	133	90
4	83	133	90
4	14	133	90
4	419	132	90
4	326	132	90
4	140	132	90
4	451	131	90
4	412	131	90
4	266	131	90
4	120	131	90
4	91	131	90
4	218	130	90
4	121	130	90
4	116	130	90
4	185	129	90
4	165	129	90
4	107	129	90
4	41	129	90
4	182	128	90
4	108	128	90
4	62	128	90
4	11	128	90
4	101	127	90
4	63	127	90
4	39	127	90
4	9	127	90
4	245	126	90
4	203	126	90
4	192	126	90
4	153	126	90
4	91	126	90
4	78	126	90
4	257	125	90
4	42	125	90
4	13	125	90
4	42	124	90
4	317	123	90
4	170	123	90
4	156	121	90
4	86	121	90
4	44	121	90
4	36	121	90
4	51	120	90
4	282	119	90
4	92	119	90
4	43	119	90
4	2	119	90
4	295	118	90
4	79	118	90
4	138	117	90
4	124	117	90
4	562	116	90
4	92	116	90
4	77	116	90
4	67	116	90
4	21	116	90
4	340	113	90
4	754	112	90
4	51	111	90
4	168	105	90

4	23	105	90
4	2	104	90
4	160	101	90
4	224	97	90
5	1012	360	90
5	42	356	90
5	37	355	90
5	688	353	90
5	149	353	90
5	50	349	90
5	125	346	90
5	391	241	90
5	1739	236	90
5	141	226	90
5	278	222	90
5	76	222	90
5	670	218	90
5	231	218	90
5	46	216	90
5	173	214	90
5	174	213	90
5	266	212	90
5	186	212	90
5	88	212	90
5	225	211	90
5	541	209	90
5	80	209	90
5	77	209	90
5	160	208	90
5	336	207	90
5	178	207	90
5	77	207	90
5	196	206	90
5	152	206	90
5	102	206	90
5	68	206	90
5	54	206	90
5	630	205	90
5	241	205	90
5	168	205	90
5	108	205	90
5	107	205	90
5	96	205	90
5	657	204	90
5	574	204	90
5	389	204	90
5	98	204	90
5	96	203	90
5	765	202	90
5	454	202	90
5	319	202	90
5	280	202	90
5	162	202	90
5	105	202	90
5	80	202	90
5	44	202	90
5	146	201	90
5	192	200	90
5	83	200	90
5	37	200	90
5	204	199	90
5	144	199	90
5	143	199	90
5	133	199	90
5	117	199	90
5	64	199	90
5	59	199	90
5	184	198	90
5	129	198	90
5	126	198	90
5	124	198	90
5	88	198	90
5	831	197	90
5	677	197	90
5	567	197	90
5	266	197	90
5	132	197	90
5	81	197	90
5	80	197	90
5	310	196	90

5	249	196	90
5	203	196	90
5	177	196	90
5	89	196	90
5	81	196	90
5	51	196	90
5	422	195	90
5	373	195	90
5	333	195	90
5	326	195	90
5	319	195	90
5	132	195	90
5	129	195	90
5	107	195	90
5	81	195	90
5	74	195	90
5	1467	194	90
5	290	194	90
5	259	194	90
5	207	194	90
5	88	194	90
5	53	194	90
5	472	193	90
5	422	193	90
5	254	193	90
5	170	193	90
5	153	193	90
5	148	193	90
5	146	193	90
5	68	193	90
5	63	193	90
5	62	193	90
5	59	193	90
5	56	193	90
5	32	193	90
5	671	192	90
5	609	192	90
5	227	192	90
5	225	192	90
5	197	192	90
5	147	192	90
5	103	192	90
5	83	192	90
5	47	192	90
5	726	191	90
5	402	191	90
5	348	191	90
5	302	191	90
5	198	191	90
5	192	191	90
5	112	191	90
5	81	191	90
5	66	191	90
5	922	190	90
5	397	190	90
5	306	190	90
5	241	190	90
5	116	190	90
5	110	190	90
5	55	190	90
5	46	190	90
5	938	189	90
5	433	189	90
5	351	189	90
5	315	189	90
5	291	189	90
5	265	189	90
5	234	189	90
5	163	189	90
5	144	189	90
5	103	189	90
5	91	189	90
5	88	189	90
5	77	189	90
5	42	189	90
5	42	189	90
5	39	189	90
5	33	189	90
5	25	189	90
5	1680	188	90

5	449	188	90
5	406	188	90
5	380	188	90
5	343	188	90
5	308	188	90
5	300	188	90
5	212	188	90
5	194	188	90
5	151	188	90
5	98	188	90
5	72	188	90
5	61	188	90
5	53	188	90
5	30	188	90
5	586	187	90
5	452	187	90
5	340	187	90
5	170	187	90
5	152	187	90
5	147	187	90
5	114	187	90
5	106	187	90
5	97	187	90
5	82	187	90
5	71	187	90
5	59	187	90
5	40	187	90
5	36	187	90
5	1474	186	90
5	1118	186	90
5	791	186	90
5	643	186	90
5	578	186	90
5	416	186	90
5	204	186	90
5	193	186	90
5	90	186	90
5	82	186	90
5	66	186	90
5	35	186	90

5	789	185	90
5	669	185	90
5	450	185	90
5	426	185	90
5	405	185	90
5	354	185	90
5	230	185	90
5	228	185	90
5	164	185	90
5	163	185	90
5	149	185	90
5	129	185	90
5	120	185	90
5	95	185	90
5	77	185	90
5	67	185	90
5	60	185	90
5	47	185	90
5	31	185	90
5	19	185	90
5	14	185	90
5	1008	184	90
5	861	184	90
5	834	184	90
5	779	184	90
5	683	184	90
5	414	184	90
5	411	184	90
5	360	184	90
5	295	184	90
5	276	184	90
5	271	184	90
5	254	184	90
5	251	184	90
5	209	184	90
5	199	184	90
5	177	184	90
5	171	184	90
5	156	184	90
5	152	184	90

5	135	184	90
5	115	184	90
5	98	184	90
5	85	184	90
5	49	184	90
5	46	184	90
5	43	184	90
5	23	184	90
5	494	183	90
5	491	183	90
5	485	183	90
5	407	183	90
5	380	183	90
5	347	183	90
5	304	183	90
5	255	183	90
5	226	183	90
5	215	183	90
5	201	183	90
5	166	183	90
5	162	183	90
5	156	183	90
5	142	183	90
5	120	183	90
5	115	183	90
5	98	183	90
5	88	183	90
5	68	183	90
5	59	183	90
5	54	183	90
5	51	183	90
5	996	182	90
5	567	182	90
5	542	182	90
5	435	182	90
5	420	182	90
5	360	182	90
5	316	182	90
5	298	182	90
5	269	182	90
5	268	182	90
5	243	182	90
5	224	182	90
5	140	182	90
5	101	182	90
5	88	182	90
5	58	182	90
5	37	182	90
5	35	182	90
5	660	181	90
5	646	181	90
5	349	181	90
5	309	181	90
5	261	181	90
5	218	181	90
5	211	181	90
5	169	181	90
5	136	181	90
5	125	181	90
5	98	181	90
5	80	181	90
5	74	181	90
5	69	181	90
5	63	181	90
5	60	181	90
5	56	181	90
5	26	181	90
5	8	181	90
5	939	180	90
5	661	180	90
5	465	180	90
5	426	180	90
5	362	180	90
5	338	180	90
5	287	180	90
5	259	180	90
5	226	180	90
5	200	180	90
5	183	180	90
5	170	180	90

5	158	180	90
5	150	180	90
5	149	180	90
5	131	180	90
5	119	180	90
5	100	180	90
5	84	180	90
5	69	180	90
5	64	180	90
5	52	180	90
5	641	179	90
5	517	179	90
5	407	179	90
5	384	179	90
5	371	179	90
5	310	179	90
5	238	179	90
5	221	179	90
5	213	179	90
5	211	179	90
5	192	179	90
5	165	179	90
5	163	179	90
5	157	179	90
5	117	179	90
5	115	179	90
5	102	179	90
5	77	179	90
5	63	179	90
5	55	179	90
5	53	179	90
5	28	179	90
5	20	179	90
5	6	179	90
5	1322	178	90
5	820	178	90
5	576	178	90
5	511	178	90
5	456	178	90
5	377	178	90

5	321	178	90
5	253	178	90
5	247	178	90
5	233	178	90
5	231	178	90
5	209	178	90
5	194	178	90
5	126	178	90
5	125	178	90
5	122	178	90
5	117	178	90
5	102	178	90
5	88	178	90
5	87	178	90
5	68	178	90
5	65	178	90
5	59	178	90
5	52	178	90
5	50	178	90
5	621	177	90
5	565	177	90
5	560	177	90
5	516	177	90
5	471	177	90
5	376	177	90
5	344	177	90
5	318	177	90
5	257	177	90
5	171	177	90
5	159	177	90
5	146	177	90
5	133	177	90
5	116	177	90
5	110	177	90
5	104	177	90
5	93	177	90
5	82	177	90
5	39	177	90
5	16	177	90
5	12	177	90

5	10	177	90
5	938	176	90
5	914	176	90
5	828	176	90
5	304	176	90
5	258	176	90
5	212	176	90
5	211	176	90
5	208	176	90
5	169	176	90
5	134	176	90
5	107	176	90
5	65	176	90
5	57	176	90
5	55	176	90
5	48	176	90
5	40	176	90
5	24	176	90
5	1030	175	90
5	836	175	90
5	551	175	90
5	527	175	90
5	415	175	90
5	273	175	90
5	222	175	90
5	217	175	90
5	200	175	90
5	186	175	90
5	119	175	90
5	96	175	90
5	89	175	90
5	61	175	90
5	54	175	90
5	50	175	90
5	29	175	90
5	22	175	90
5	16	175	90
5	607	174	90
5	333	174	90
5	281	174	90
5	279	174	90
5	216	174	90
5	201	174	90
5	172	174	90
5	164	174	90
5	79	174	90
5	56	174	90
5	34	174	90
5	887	173	90
5	853	173	90
5	801	173	90
5	587	173	90
5	557	173	90
5	346	173	90
5	317	173	90
5	314	173	90
5	308	173	90
5	293	173	90
5	291	173	90
5	275	173	90
5	266	173	90
5	240	173	90
5	225	173	90
5	221	173	90
5	194	173	90
5	134	173	90
5	111	173	90
5	107	173	90
5	106	173	90
5	84	173	90
5	64	173	90
5	45	173	90
5	44	173	90
5	43	173	90
5	686	172	90
5	543	172	90
5	513	172	90
5	348	172	90
5	236	172	90
5	228	172	90

5	195	172	90
5	150	172	90
5	84	172	90
5	77	172	90
5	68	172	90
5	52	172	90
5	630	171	90
5	469	171	90
5	401	171	90
5	324	171	90
5	316	171	90
5	207	171	90
5	150	171	90
5	141	171	90
5	123	171	90
5	102	171	90
5	101	171	90
5	96	171	90
5	62	171	90
5	1094	170	90
5	311	170	90
5	183	170	90
5	126	170	90
5	125	170	90
5	85	170	90
5	2172	169	90
5	1397	169	90
5	545	169	90
5	525	169	90
5	270	169	90
5	239	169	90
5	25	169	90
5	532	168	90
5	343	168	90
5	284	168	90
5	282	168	90
5	274	168	90
5	218	168	90
5	210	168	90
5	162	168	90

5	48	168	90
5	15	168	90
5	495	167	90
5	472	167	90
5	77	167	90
5	48	167	90
5	746	166	90
5	605	166	90
5	586	166	90
5	560	166	90
5	146	166	90
5	127	166	90
5	121	166	90
5	56	166	90
5	39	166	90
5	787	165	90
5	336	165	90
5	264	165	90
5	172	165	90
5	171	165	90
5	71	165	90
5	70	165	90
5	588	164	90
5	470	164	90
5	451	164	90
5	180	164	90
5	165	164	90
5	143	164	90
5	131	164	90
5	107	164	90
5	85	164	90
5	31	164	90
5	343	163	90
5	203	163	90
5	150	163	90
5	81	163	90
5	949	162	90
5	682	162	90
5	289	162	90
5	210	162	90

5	176	162	90
5	163	162	90
5	80	162	90
5	51	162	90
5	26	160	90
5	45	159	90
5	165	158	90
5	80	158	90
5	73	158	90
5	339	156	90
5	97	156	90
5	40	155	90
5	69	153	90
5	327	152	90
5	190	149	90
5	162	149	90
5	403	148	90
5	654	26	90
5	81	25	90
5	61	18	90
5	740	17	90
5	264	16	90
5	78	15	90
5	104	14	90
5	45	13	90
5	36	12	90
5	23	12	90
5	169	10	90
5	118	9	90
5	368	8	90
5	62	3	90
5	106	2	90
5	73	2	90
5	155	1	90
5	66	1	90
5	77	0	90
6	273	254	90
6	102	252	90
6	72	251	90
6	759	250	90
6	57	250	90
6	545	249	90
6	512	249	90
6	482	249	90
6	423	249	90
6	261	249	90
6	146	249	90
6	115	249	90
6	485	248	90
6	34	248	90
6	21	248	90
6	380	247	90
6	238	247	90
6	130	247	90
6	114	246	90
6	112	246	90
6	105	246	90
6	50	246	90
6	416	245	90
6	305	245	90
6	137	245	90
6	370	244	90
6	139	244	90
6	248	243	90
6	236	243	90
6	230	243	90
6	998	242	90
6	190	242	90
6	144	242	90
6	102	242	90
6	71	242	90
6	1219	241	90
6	674	241	90
6	610	241	90
6	518	241	90
6	451	241	90
6	181	241	90
6	139	241	90
6	70	241	90
6	52	241	90

6	28	241	90
6	10	241	90
6	1326	240	90
6	47	240	90
6	21	240	90
6	1617	239	90
6	1355	239	90
6	761	239	90
6	697	239	90
6	622	239	90
6	607	239	90
6	575	239	90
6	512	239	90
6	454	239	90
6	330	239	90
6	241	239	90
6	227	239	90
6	194	239	90
6	694	238	90
6	465	238	90
6	302	238	90
6	277	238	90
6	198	238	90
6	104	238	90
6	93	238	90
6	60	238	90
6	56	238	90
6	9	238	90
6	739	237	90
6	667	237	90
6	461	237	90
6	310	237	90
6	255	237	90
6	221	237	90
6	184	237	90
6	172	237	90
6	74	237	90
6	28	237	90
6	513	236	90
6	455	236	90
6	453	236	90
6	176	236	90
6	165	236	90
6	161	236	90
6	36	236	90
6	12	236	90
6	11	236	90
6	3645	235	90
6	2342	235	90
6	991	235	90
6	417	235	90
6	321	235	90
6	292	235	90
6	175	235	90
6	145	235	90
6	18	235	90
6	1269	234	90
6	1102	234	90
6	466	234	90
6	120	234	90
6	106	234	90
6	92	234	90
6	87	234	90
6	68	234	90
6	41	234	90
6	2334	233	90
6	1009	233	90
6	1006	233	90
6	275	233	90
6	273	233	90
6	75	233	90
6	50	233	90
6	28	233	90
6	12	233	90
6	934	232	90
6	665	232	90
6	444	232	90
6	355	232	90
6	187	232	90
6	181	232	90

6	177	232	90
6	166	232	90
6	93	232	90
6	93	232	90
6	91	232	90
6	33	232	90
6	19	232	90
6	2109	231	90
6	717	231	90
6	571	231	90
6	429	231	90
6	238	231	90
6	216	231	90
6	215	231	90
6	136	231	90
6	64	231	90
6	817	230	90
6	561	230	90
6	432	230	90
6	325	230	90
6	251	230	90
6	127	230	90
6	125	230	90
6	56	230	90
6	32	230	90
6	29	230	90
6	861	229	90
6	854	229	90
6	730	229	90
6	724	229	90
6	444	229	90
6	424	229	90
6	319	229	90
6	298	229	90
6	240	229	90
6	162	229	90
6	157	229	90
6	118	229	90
6	111	229	90
6	94	229	90
6	85	229	90
6	75	229	90
6	31	229	90
6	705	228	90
6	382	228	90
6	380	228	90
6	293	228	90
6	291	228	90
6	231	228	90
6	221	228	90
6	212	228	90
6	128	228	90
6	46	228	90
6	1738	227	90
6	1429	227	90
6	1013	227	90
6	889	227	90
6	498	227	90
6	400	227	90
6	360	227	90
6	243	227	90
6	183	227	90
6	169	227	90
6	157	227	90
6	135	227	90
6	129	227	90
6	111	227	90
6	78	227	90
6	2021	226	90
6	264	226	90
6	260	226	90
6	193	226	90
6	174	226	90
6	160	226	90
6	75	226	90
6	68	226	90
6	41	226	90
6	33	226	90
6	1195	225	90
6	1144	225	90

6	428	225	90
6	203	225	90
6	201	225	90
6	149	225	90
6	145	225	90
6	137	225	90
6	107	225	90
6	75	225	90
6	66	225	90
6	45	225	90
6	1520	224	90
6	1520	224	90
6	1033	224	90
6	932	224	90
6	932	224	90
6	743	224	90
6	441	224	90
6	313	224	90
6	274	224	90
6	212	224	90
6	77	224	90
6	49	224	90
6	43	224	90
6	37	224	90
6	33	224	90
6	1077	223	90
6	634	223	90
6	612	223	90
6	486	223	90
6	439	223	90
6	399	223	90
6	332	223	90
6	303	223	90
6	275	223	90
6	222	223	90
6	141	223	90
6	140	223	90
6	133	223	90
6	92	223	90
6	82	223	90

6	41	223	90
6	35	223	90
6	17	223	90
6	1813	222	90
6	1089	222	90
6	910	222	90
6	694	222	90
6	644	222	90
6	613	222	90
6	611	222	90
6	538	222	90
6	304	222	90
6	196	222	90
6	160	222	90
6	94	222	90
6	1799	221	90
6	474	221	90
6	346	221	90
6	259	221	90
6	256	221	90
6	253	221	90
6	214	221	90
6	157	221	90
6	152	221	90
6	73	221	90
6	71	221	90
6	68	221	90
6	57	221	90
6	53	221	90
6	38	221	90
6	17	221	90
6	532	220	90
6	508	220	90
6	335	220	90
6	316	220	90
6	304	220	90
6	219	220	90
6	104	220	90
6	99	220	90
6	22	220	90

6	1062	219	90
6	1028	219	90
6	689	219	90
6	673	219	90
6	469	219	90
6	355	219	90
6	331	219	90
6	305	219	90
6	285	219	90
6	194	219	90
6	183	219	90
6	106	219	90
6	90	219	90
6	54	219	90
6	750	218	90
6	635	218	90
6	372	218	90
6	350	218	90
6	185	218	90
6	122	218	90
6	84	218	90
6	28	218	90
6	916	217	90
6	736	217	90
6	707	217	90
6	665	217	90
6	469	217	90
6	366	217	90
6	237	217	90
6	196	217	90
6	177	217	90
6	140	217	90
6	108	217	90
6	27	217	90
6	921	216	90
6	559	216	90
6	531	216	90
6	167	216	90
6	87	216	90
6	1086	215	90

6	528	215	90
6	504	215	90
6	398	215	90
6	366	215	90
6	346	215	90
6	320	215	90
6	260	215	90
6	207	215	90
6	181	215	90
6	86	215	90
6	68	215	90
6	56	215	90
6	48	215	90
6	26	215	90
6	2436	214	90
6	836	214	90
6	526	214	90
6	447	214	90
6	352	214	90
6	240	214	90
6	204	214	90
6	170	214	90
6	128	214	90
6	93	214	90
6	86	214	90
6	85	214	90
6	52	214	90
6	46	214	90
6	739	213	90
6	431	213	90
6	389	213	90
6	343	213	90
6	287	213	90
6	20	213	90
6	7	213	90
6	344	212	90
6	230	212	90
6	219	212	90
6	157	212	90
6	146	212	90

6	131	212	90
6	76	212	90
6	13	212	90
6	1270	211	90
6	1027	211	90
6	431	211	90
6	313	211	90
6	253	211	90
6	249	211	90
6	230	211	90
6	150	211	90
6	118	211	90
6	102	211	90
6	14	211	90
6	5	211	90
6	1491	210	90
6	691	210	90
6	628	210	90
6	360	210	90
6	337	210	90
6	170	210	90
6	141	210	90
6	1777	209	90
6	1711	209	90
6	794	209	90
6	744	209	90
6	229	209	90
6	186	209	90
6	143	209	90
6	79	209	90
6	49	209	90
6	26	209	90
6	14	209	90
6	13	209	90
6	11	209	90
6	697	208	90
6	407	208	90
6	115	208	90
6	31	208	90
6	22	208	90
6	8	208	90
6	1171	207	90
6	1074	207	90
6	500	207	90
6	262	207	90
6	155	207	90
6	133	207	90
6	131	207	90
6	114	207	90
6	75	207	90
6	8	207	90
6	470	206	90
6	211	206	90
6	32	206	90
6	21	206	90
6	669	205	90
6	654	205	90
6	548	205	90
6	244	205	90
6	242	205	90
6	218	205	90
6	599	204	90
6	566	204	90
6	469	204	90
6	453	204	90
6	182	204	90
6	177	204	90
6	83	204	90
6	42	204	90
6	1065	203	90
6	632	203	90
6	628	203	90
6	467	203	90
6	332	203	90
6	326	203	90
6	229	203	90
6	130	203	90
6	107	203	90
6	50	203	90
6	961	202	90

6	633	202	90
6	511	202	90
6	456	202	90
6	27	202	90
6	502	201	90
6	215	201	90
6	144	201	90
6	115	201	90
6	87	201	90
6	60	201	90
6	529	200	90
6	233	200	90
6	120	200	90
6	917	199	90
6	451	199	90
6	331	199	90
6	271	199	90
6	258	199	90
6	221	199	90
6	1172	198	90
6	70	198	90
6	59	198	90
6	33	198	90
6	279	197	90
6	212	197	90
6	112	197	90
6	69	197	90
6	66	197	90
6	242	196	90
6	8	196	90
6	988	195	90
6	612	195	90
6	416	195	90
6	130	195	90
6	435	194	90
6	49	194	90
6	856	193	90
6	261	193	90
6	235	193	90
6	170	193	90
6	54	193	90
6	631	192	90
6	287	192	90
6	599	191	90
6	421	191	90
6	29	191	90
6	407	190	90
6	17	189	90
6	244	188	90
6	48	188	90
6	349	187	90
6	1010	186	90
6	391	183	90
6	628	182	90
6	17	180	90
6	79	178	90
6	22	141	90
6	256	57	90
6	1665	56	90
6	75	46	90
6	243	42	90
6	450	38	90
6	70	27	90
6	524	24	90
6	160	16	90

Table B3. Google Earth Pro lineament analysis data. Six main orientations were observed and are denoted by the numbers 1-6 in the table.

Silica cemented breccia locations

Silica cemented breccias were located in the field. Locations were recorded using the North American Datum of 1927 (NAD27) to be able to use available paper maps in the field. Locations were recorded in Universal Transverse Mercator Zone 12. These locations are presented in the following Table B4. Abbreviations in the table: UMB = unmineralized breccia; MB = mineralized breccia; GS = general station; FS = fracture station; dd = dip direction.

Station	Datum	UTM Easting	UTM Northing	**Notes**
UMB	NAD27	702214	4996426	Sandra mine area
UMB	NAD27	702447	4996035	UMB S. of Sandra mine area
MB	NAD27	723975	4984961	Leo Incline area
GS15	NAD27	702263	4996229	UMB 100m so. Sandra mine area
FS106	NAD27	702263	4996198	GS16 UMB 100m 2nd so. Sandra mine area
GS19	NAD27	702337	4996106	UMB so. Sandra mine area
GS21	NAD27	702454	4996034	UMB 1st so. Sandra mine area 279/60
GS23	NAD27	702541	4996007	UMB next so. Sandra mine area
GS24	NAD27	702460	4995986	UMB (slightly min.) next so. Sandra mine area
GS25	NAD27	702434	4995886	next collapse breccia dd: 195/8
GS32	NAD27	702042	4996577	UMB north of Sandra mine area dd: 195/12
GS33	NAD27	702149	4996609	UMB east of GS32 dd: 195/12

GS34	NAD27	702176	4996609	4 small UMB "dikes" east of GS32 (dd: 195/13)
GS35	NAD27	702212	4996632	UMB as above
GS37	NAD27	702243	4996647	UMB dd: 205/8 & 265/60 overturned
GS40	NAD27	702298	4996821	UMB dd: 220/12
FS097	NAD27	700975	4998656	MB
FS098	NAD27	701050	4998472	slightly MB
P004	NAD27	701034	4990411	slightly MB south of FS098 (brown calcite speleothem near here)
P005	NAD27	701017	4998400	Prospect with high cps
UMB	NAD27	700859	4998816	UMB
FS099	NAD27	700881	4998643	
UMB	NAD27	700881	4998661	UMB
MB OGM	NAD27	701892	4997182	OGM area MB
FS106	NAD27	702263	4996198	UMB 2nd south of Sandra mine
FS107	NAD27	702339	4996095	UMB south of Sandra mine
FS108	NAD27	702449	4996036	UMB south of Sandra mine
MB35	NAD27	702492	4995661	FS ~ 20 meters to the south
FS111	NAD27	702528	4995636	
FS112	NAD27	702511	4995490	Same as MB37
FS113	NAD27	702492	4995389	Same as UMB38
MB01	NAD27	702050	4996850	Mm dd: 200/18
MB02	NAD27	701896	4996976	Mineralized near bottom of breccia along bedding plane
FS115	NAD27	701867	4997045	same as OGM-MB02 so. Of OGM
UMB	NAD27	701910	4997090	UMB ~ 8 m wide & 2 m long
FS116	NAD27	701093	4997174	MB w/UMB at Old Glory Mine adit
FS118	NAD27	701944	4993897	Dandy Mine adit
FS119	NAD27	702668	4994752	Lisbon Mine adit

FS126	NAD27	709173	4993733	UMB in Mm East Pryor mountain area
MB	NAD27	709129	4993712	mineralized breccia NE side of road
FS132	NAD27	702426	4994849	MB51
UMB 52	NAD27	702432	4994833	~15 m south and down the dipslope from MB51
FS133	NAD27	702443	4994822	UMB53
UMB54	NAD27	702428	4994802	UMB54
FS134	NAD27	702412	4994812	UMB55
UMB56	NAD27	702404	4994810	~ 5 m west of UMB 55
UMB57	NAD27	702403	4994819	
FS135	NAD27	702389	4994829	UMB58
FS136	NAD27	702493	4995389	UMB38
UMB39	NAD27	702657	4994713	
UMB59	NAD27	702305	4994842	
UMB61	NAD27	702648	4994780	
UMB62	NAD27	702627	4994710	
FS137	NAD27	702585	4994726	same as MB63
UMB64	NAD27	702649	4994652	
UMB65	NAD27	702657	4994653	
UMB65b	NAD27	702671	4993954	frac. 232/80 330/42 3-4 m wide 4-6 m long
PPL1	NAD27	702675	4994462	prospect pit with high cps no htd here possibly removed
PPL2	NAD27	702699	4994441	prospect pit with cave floor? Deposits
PERC1	NAD27	702732	4994383	UV filling cave material vugs pix. Barite, relict sulfides
PERC2	NAD27	702696	4994308	LS breccia contact 050/75
FS138	NAD27	696532	5003639	
FS140	NAD27	701743	4991712	UMB70
FS141	NAD27	701932	4991483	UMB71
FS142	NAD27	702004	4991439	Swmp_B

Table B4. Silica cemented breccia locations Big Pryor Mountain.

Fracture analysis data

A field based fracture analysis was conducted on mineralized and unmineralized silica cemented breccia to determine if there might be a preferred orientation in fractures for mineralization. The fracture data used in Chapter 4 of this dissertation are presented in Table B5. Abbreviations used in the table include: dd = dip direction; cps = counts per second readings for hand held radiation counter (average unmineralized background readings for the limestone is approximately 10-15 cps.); m = meters; cm = centimeters; min. = mineralized; unmin. = unmineralized; Mm = Mississippian Madison Group; UMB = unmineralized breccia; MB = mineralized breccia; fracture types associated with the anticline fold a-c = perpendicular to bedding; b-c = parallel to the hinge of the fold; and a-c = oblique to the hinge and the bedding of the fold. Most fractures were mode I extension fractures. Mode II = sliding perpendicular to the fracture tip (edge) and mode III = sliding parallel to the fracture tip (edge) if a fracture differed from mode I it was noted in the Notes section. The green highlighted fracture stations indicate mineralization. Those stations with slickenlines recorded are highlighted in orange in the notes section. Blue highlighted fracture stations indicate a mine adit and red highlighted fracture station labels indicate unmineralized breccia. Length of fractures and spacing was measured in meters (m).

Station	#	Dip Dir.	Strike	Dip	length m	Notes
FS097	1	245	155	80	3.0	700975E 4998656N
	2	235	145	81	3.0	Prospect 2E on S wall to prospect
	3	42	312	80	2.0	Madison Limestone bedding
	4	228	138	83	1.8	dd 329 dip 30
	5	30	300	47	2.4	
	6	39	309	53	3.8	
	7	210	120	85	1.2	
	8	46	316	80	1.3	
	9	75	345	20	2.0	
	10	50	320	54	1.4	
FS102	1	23	293	42	5.0	702208E 4996307N 2293m
1st section	2	145	55	10	2.5	Sandra Mine area
N side of	3	285	195	20	1.3	mineralized breccia (segments)
E -facing wall	4	85	355	30	2.0	Mm selection method
	5	150	60	24	1.8	bedding dd 075 dip 14
	6	90	0	24	2.5	
	7	85	355	30	3.0	
	8	200	110	76	2.0	
	9	235	145	60	2.0	
	10	220	130	44	0.8	
	11	348	200	32	2.0	
	12	210	120	42	2.5	
	13	212	122	50	1.5	
	14	230	140	66	2.8	
	15	210	120	70	3.0	
	16	210	120	70	2.0	
	17	210	120	70	2.0	
	18	210	120	70	2.0	
	19	210	120	70	2.0	
	20	210	120	70	2.0	
	21	210	120	70	2.0	
	22	35	305	27	2.0	
	23	23	293	42	2.0	

	24	33	303	38	2.0	
	25	356	266	40	2.0	Second set
	26	30	300	30	2.0	fractures under segment 1 & 2
	27	8	278	66	1.8	of breccia vein
	28	360	270	32	1.7	
	29	215	125	20	2.0	
	30	225	135	74	0.7	
	31	230	140	80	3.0	
	32	235	145	84	4.0	
	33	80	350	66	4.0	
	34	70	340	52	4.0	
	35	95	5	46	4.0	
	36	190	100	76	2.5	
	37	240	150	68	5.0	
	38	45	315	60	1.5	
	39	45	315	60	1.1	
	40	45	315	60	1.1	
	41	45	315	60	1.1	
	42	45	315	60	1.1	
	43	45	315	60	1.1	
	44	120	30	56	0.7	Under segment 4 of breccia
	45	120	30	42	1.5	
	46	138	48	30	1.5	
	47	125	35	30	3.0	
	48	75	345	82	3.0	
	49	305	215	75	1.5	S. side of E. facing wall 102A
	50	305	215	75	1.5	
	51	220	130	68	6.0	
	52	235	145	70	3.0	
	53	225	135	70	6.0	
	54	228	138	54	6.0	
	55	218	128	68	2.0	
	56	232	142	68	2.0	
	57	215	125	60	6.0	
	58	132	42	80	4.0	

	59	145	55	70	4.0	
	60	145	55	70	4.0	
	61	145	55	70	4.0	
	62	145	55	70	4.0	
	63	150	60	18	4.0	
	64	290	200	82	4.0	
	65	290	200	82	4.0	
	66	290	200	82	4.0	
	67	290	200	82	4.0	
	68	225	135	56	3.0	
	69	225	135	56	3.0	
	70	5	275	84	2.0	
	71	48	318	56	6.0	
	72	50	320	56	6.0	
	73	36	306	56	4.0	
	74	32	302	74	6.0	
	75	20	290	38	4.0	
	76	44	314	30	2.5	
	77	50	320	44	2.0	
	78	60	330	36	6.0	
	79	129	39	86	3.0	
	80	129	39	86	3.0	
	81	129	39	86	3.0	
	82	220	130	44	1.5	
	83	234	144	80	2.5	
	84	50	320	8	2.0	
	85	107	17	70	4.0	top of outcrop
	86	118	28	75	2.0	top of outcrop
	87	117	27	84	2.0	top of outcrop
	88	117	27	80	4.0	top of outcrop
	89	117	27	80	4.0	top of outcrop
	90	117	27	80	4.0	top of outcrop
	91	117	27	80	4.0	top of outcrop
	92	117	27	80	4.0	top of outcrop
	93	130	40	78	4.0	top of outcrop
	94	134	44	80	1.6	top of outcrop
	95	130	40	70	5.0	top of outcrop
	96	126	36	78	5.0	top of outcrop

	97	312	222	66	4.0	top of outcrop
	98	228	138	76	6.0	top of outcrop
	99	246	156	80	3.0	top of outcrop
	##	314	224	60	2.0	top of outcrop
	##	288	198	40	4.0	top of outcrop
	##	290	200	60	4.0	top of outcrop
FS109	1	90	0	38	2.0	selection method; dd 290 dip 4
Same as MB015	2	90	0	60	1.0	4995918N 702481E 2270m
in 2011-13 field	3	90	0	60	1.0	
book	4	90	0	60	1.0	
	5	90	0	60	1.0	
	6	90	0	60	1.0	
	7	90	0	60	1.0	
	8	90	0	60	1.0	
	9	110	20	48	0.5	
	10	244	154	80	1.0	
	11	310	220	84	2.0	
	12	72	342	82	1.0	
	13	348	258	45	1.0	
	14	28	298	80	1.0	
	15	28	298	80	12.0	
	16	52	322	82	1.0	400 cps
	17	110	20	80	0.5	
	18	150	60	30	0.5	
	19	346	256	40	2.0	
	20	240	150	60	1.0	
	21	240	150	60	1.0	
FS112	1	200	110	60	4.0	dd 330 dip 10; So. of FS111
	2	346	256	60	3.0	4995490N 702511E 2205m
	3	4	274	70	3.0	
	4	356	266	80	3.0	
	5	126	36	84	3.0	
	6	350	260	50	2.0	
	7	350	260	50	2.0	
	8	218	128	80	1.0	

	9	218	128	80	1.0	
	10	52	322	76	1.0	
	11	336	246	60	5.0	
	12	65	335	88	3.0	
	13	352	262	60	4.0	
	14	352	262	60	3.0	
	15	240	150	80	3.0	
	16	20	290	80	4.0	
	17	20	290	24	2.0	
	18	62	332	40	3.0	
FS114	1	310	220	60	3.0	UMB that Min. in a few places
	2	2	272	88	2.0	4996975N 701894E 2371m
	3	50	-40	80	2.0	Selection method
	4	350	260	80	3.0	near OGM
	5	330	240	70	2.0	
	6	90	0	70	2.0	
	7	20	290	40	3.0	
	8	90	0	70	2.0	
	9	300	210	40	4.0	
	10	300	210	40	4.0	
	11	300	210	40	4.0	*slickenlines rake 86; dd 50 dip 10
	12	300	210	40	4.0	E side up; elev. Radiation
	13	18	288	70	4.0	
	14	100	10	40	2.0	
	15	300	210	70	4.0	
	16	354	264	80	2.0	
	17	170	80	70	2.0	
	18	270	180	40	3.0	
	19	310	220	35	2.0	
	20	140	50	80	2.0	
	21	165	75	85	1.5	
	22	300	210	40	4.0	
	23	350	260	50	3.0	
	24	300	210	50	3.0	
FS115	1	52	322	60	3.0	4997045N 701867E

						2383m
	2	65	335	50	3.0	no visible bedding
	3	32	302	85	2.0	min. breccia surrounded
	4	10	280	85	4.0	by unmin. Breccia
	5	90	0	60	5.0	strike 310 dip 70 (breccia)
	6	310	220	40	2.0	#6 - #7 conjugate
	7	110	20	60	2.0	
	8	148	58	65	1.0	
	9	148	58	65	1.0	
	10	148	58	65	1.0	
	11	148	58	65	1.0	
	12	24	294	80	1.0	fold axis 176
	13	260	170	70	4.0	plunge direction 14 plunge 10
	14	80	350	80	2.0	
	15	270	180	70	2.0	
	16	75	345	70	4.0	
	17	110	20	50	8.0	
	18	4	274	60	8.0	fold axis 210 plunge drxn 6
	19	4	274	60	8.0	
	20	4	274	60	8.0	
	21	4	274	60	8.0	
	22	4	274	60	8.0	
FS116	1	320	230	70	4.0	4997174N 701093E 2391m
	2	55	325	80	4.0	dd 216 dip 16; selection method
	3	25	295	70	4.0	Min. breccia w/some unmin.
	4	105	15	75	6.0	One of sev. adits @ Old Glory Mine
	5	142	52	86	2.0	
	6	142	52	86	2.0	Slickenslines rake 85, 83;
	7	165	75	70	3.0	N side up
	8	54	324	55	2.0	
	9	54	324	55	2.0	
	10	36	306	80	2.0	

	11	36	306	80	2.0	
	12	310	220	80	4.0	
	13	60	330	15	0.5	
	14	200	110	60	2.0	
	15	152	62	60	3.0	
	16	170	80	55	3.0	
	17	150	60	80	4.0	
	18	250	160	70	2.0	
	19	112	22	60	3.0	
	20	275	185	80	15.0	
FS118	1	50	320	30	2.0	Dandy Mine adit dd 36 dip 8
	2	358	268	50	2.0	4993897N 701944E 1882m
	3	346	256	36	3.0	Frac 1 slickenlines strike 306 rake
	4	348	258	40	3.0	75; NE down
	5	358	268	54	2.0	Frac 2 slickenlines strike 346
	6	354	264	50	3.0	rake 54; NE down
	7	60	330	40	2.0	Slickenlines Strike 156
	8	60	330	40	3.0	rake 77 U min
	9	40	310	45	1.0	#8 Slickenlines Strike 156
	10	60	330	85	2.0	rake 77 U min.
	11	60	330	85	2.0	
	12	346	256	45	2.0	
	13	20	290	84	1.0	
	14	15	285	70	1.0	
	15	15	285	70	1.0	
	16	136	46	80	1.5	
	17	136	46	80	1.5	
	18	296	206	85	2.0	
	19	296	206	85	2.0	
	20	296	206	85	2.0	
	21	296	206	85	2.0	
FS119	1	102	12	84	2.0	Lisbon Mine Adit; dd 176 dip 16
	2	108	18	86	1.5	4994752N 702668E

						2086m
	3	288	198	82	2.0	no anomalous radiation readings
	4	296	206	68	2.0	Mm selection Method
	5	296	206	68	2.0	
	6	80	350	78	2.0	
	7	232	142	86	2.5	
	8	236	146	82	2.0	
	9	100	10	80	2.0	
	10	90	0	82	2.0	
	11	246	156	78	2.0	
	12	220	130	80	2.0	
	13	228	138	84	1.5	
	14	228	138	84	1.5	
	15	228	138	84	1.5	
	16	6	276	20	1.5	
	17	350	260	45	2.0	
	18	338	248	70	2.0	
	19	104	14	60	3.0	
	20	55	325	45	2.0	
	21	55	325	45	2.0	
	22	55	325	45	2.0	
	23	250	160	80	3.0	
	24	45	315	26	2.0	
	25	18	288	20	2.0	
	26	190	100	45	1.5	
	27	148	58	82	2.0	
	28	40	310	70	2.0	
	29	310	220	78	1.0	
	30	310	220	78	1.0	
	31	310	220	78	1.0	
	32	118	28	70	2.0	
	33	45	315	20	1.0	
	34	26	296	76	2.0	
	35	30	300	20	1.0	
	36	34	304	70	1.5	
	37	44	314	18	2.0	
	38	328	238	70	2.0	

	39	328	238	70	2.0	
	40	328	238	70	2.0	
	41	328	238	70	2.0	
	42	45	315	76	2.0	
FS123	1	344	254	60	4.0	4994948N 702700E 2110m
	2	86	356	64	1.0	Mm selection method
	3	158	68	85	1.5	mineralized breccia prob 2 UMB
	4	90	0	80	1.0	cut by fractures min.
	5	9	279	78	2.5	
	6	9	279	78	2.5	
	7	232	142	75	1.0	
	8	72	342	76	1.5	
	9	72	342	76	1.5	
	10	72	342	76	1.5	
	11	312	222	78	2.0	
	12	116	26	80	3.0	
	13	116	26	80	3.0	
	14	116	26	80	3.0	
	15	56	326	60	1.9	
	16	40	310	70	2.0	
	17	100	10	75	4.0	
	18	60	330	70	3.0	
	19	124	34	85	1.0	
	20	248	158	32	4.0	
	21	248	158	32	4.0	
	22	248	158	32	4.0	
	23	30	300	80	4.0	
	24	30	300	80	4.0	
	25	30	300	80	4.0	
	26	306	216	83	2.0	
	27	306	216	83	2.0	
	28	306	216	83	2.0	
	29	306	216	83	2.0	
	30	306	216	83	2.0	
	31	306	216	83	2.0	
	32	148	58	50	1.0	

	33	148	58	50	1.0	
	34	148	58	50	1.0	
	35	148	58	50	1.0	
	36	148	58	50	1.0	
	37	178	88	28	2.0	
	38	178	88	28	2.0	
	39	178	88	28	2.0	
	40	24	294	82	2.0	
	41	24	294	82	2.0	
	42	24	294	82	2.0	
	43	182	92	74	2.0	
	44	182	92	74	1.0	barite in vugs
	45	182	92	74	1.0	
	46	182	92	74	1.0	
FS131	1	82	352	55	3.0	along rd. below Dandy
	2	82	352	55	3.0	mine; 4993076N 702561E 1747m
	3	82	352	55	3.0	most fractures are filled with
	4	44	314	76	2.0	caliche two with barite #15 & 22
	5	260	170	54	1.0	#1 U/V and caliche
	6	252	162	72	2.0	
	7	280	550	77	1.0	
	8	58	328	82	3.0	
	9	64	334	84	2.0	
	10	82	352	58	2.0	slightly min. (50 cps)
	11	18	288	80	2.0	
	12	246	156	70	2.0	
	13	72	342	16	1.0	
	14	214	124	60	2.0	plus 2
	15	214	124	60	2.0	Barite & caliche vein fill
	16	214	124	60	2.0	
	17	34	304	80	2.0	plus 2
	18	34	304	80	2.0	
	19	34	304	80	2.0	
	20	56	326	48	2.5	plus 1
	21	56	326	48	2.5	

	22	316	226	76	4.0	Barite & caliche vein fill
	23	54	324	52	2.5	plus2
	24	54	324	52	2.5	
	25	54	324	52	2.5	
	26	145	55	28	4.0	plus1
	27	145	55	28	4.0	
	28	140	50	26	2.0	
	29	224	134	70	0.5	plus1
	30	224	134	70	0.5	
	31	246	156	30	1.0	plus1
	32	246	156	30	1.0	
	33	252	162	32	0.5	
FS132 (MB51)	1	326	236	58	4.0	4994849N 702426E 2087m
>1500 cps	2	326	236	58	4.0	near Lisbon mine
	3	326	236	58	4.0	Silicified Mm selection method
	4	250	160	82	2.0	strike 255 dip 30 breccia
	5	250	160	82	2.0	bedding dd 188;48
	6	160	70	78	2.0	
	7	160	70	78	2.0	
	8	160	70	78	2.0	
	9	160	70	78	2.0	
	10	14	284	82	2.0	
	11	14	284	82	2.0	
	12	14	284	82	2.0	
	13	14	284	82	2.0	
	14	14	284	82	2.0	
	15	14	284	82	2.0	
	16	14	284	82	2.0	
	17	14	284	82	2.0	
	18	14	284	82	2.0	
	19	290	200	68	3.0	
	20	290	200	68	3.0	
	21	290	200	68	3.0	
	22	290	200	68	3.0	
	23	290	200	68	3.0	
	24	140	50	80	2.5	

	25	140	50	80	2.5	
	26	140	50	80	2.5	
	27	140	50	80	2.5	
	28	140	50	80	2.5	
	29	140	50	80	2.5	#29 & 30 conjugate
	30	48	318	74	1.5	probably overprinted by 2nd
	31	48	318	74	1.5	set many healed fractures
	32	48	318	74	1.5	
	33	48	318	74	1.5	
	34	280	190	70	1.5	
	35	280	190	70	1.5	
	36	280	190	70	1.5	
	37	280	190	70	1.5	
	38	24	294	73	0.8	#38 slickenlines rake 40
	39	24	294	73	0.8	can't tell up/down
	40	24	294	73	0.8	
	41	64	334	80	1.5	
	42	100	10	80	2.0	
	43	285	195	60	2.0	
	44	285	195	60	2.0	
	45	285	195	60	2.0	
	46	47	317	85	2.0	Conjugate pair sort of
	47	132	42	70	2.0	#46 mineralized most here
	48	132	42	70	2.0	
	49	188	98	48	1.0	
FS137 = MB63	1	120	30	50	1.0	10 cm spacing *min. small breccia
	2	120	30	50	1.0	to w. on strike with this fracture
	3	120	30	50	1.0	10 cm spacing
	4	120	30	50	1.0	10 cm spacing
	5	145	55	64	1.5	28 cm spacing
	6	145	55	64	1.5	28 cm spacing
	7	145	55	64	1.5	28 cm spacing
	8	145	55	64	1.5	28 cm spacing
	9	145	55	64	1.5	28 cm spacing

	10	145	55	64	1.5	28 cm spacing
	11	145	55	64	1.5	28 cm spacing
	12	65	335	70	6.0	10-15 cm spacing
	13	65	335	70	6.0	10-15 cm spacing
	14	65	335	70	6.0	10-15 cm spacing
	15	65	335	70	6.0	10-15 cm spacing
	16	70	340	78	3.0	10 cm spacing
	17	70	340	78	3.0	10 cm spacing
	18	80	350	80	5.0	20 cm spacing
	19	80	350	80	5.0	20 cm spacing
	20	80	350	80	5.0	20 cm spacing
	21	80	350	80	5.0	20 cm spacing
	22	330	240	88	2.0	25 cm spacing
	23	330	240	88	2.0	25 cm spacing
	24	330	240	88	2.0	25 cm spacing
	25	120	30	70	2.0	30 cm spacing
	26	120	30	70	2.0	30 cm spacing
	27	120	30	70	2.0	30 cm spacing
	28	120	30	70	2.0	30 cm spacing
	29	120	30	70	2.0	30 cm spacing
	30	250	160	60	1.5	10-25 cm spacing
	31	250	160	60	1.5	10-25 cm spacing
	32	250	160	60	1.5	10-25 cm spacing
	33	250	160	60	1.5	10-25 cm spacing
	34	250	160	60	1.5	10-25 cm spacing
	35	96	6	85	1.5	next 8 healed; most are cross cut
	36	96	6	85	1.5	by 26-34 and 44-49
	37	96	6	85	1.5	
	38	96	6	85	1.5	
	39	96	6	85	1.5	
	40	96	6	85	1.5	
	41	96	6	85	1.5	
	42	96	6	85	1.5	
	43	96	6	85	1.5	
	44	142	52	48	2.0	35 cm spacing
	45	142	52	48	2.0	35 cm spacing
	46	142	52	48	2.0	35 cm spacing

	47	142	52	48	2.0	35 cm spacing
	48	142	52	48	2.0	35 cm spacing
	49	70	340	78	2.0	*looks like the same set as
	50	270	180	80	2.0	35-43 (mode III dextral)
	51	270	180	80	2.0	10 cm spacing
	52	270	180	80	2.0	10 cm spacing
	53	270	180	80	2.0	10 cm spacing
	54	90	0	80	2.0	#54 & 55 have 35 cm spacing
	55	90	0	80	2.0	& Mode III dextral 13cm offset
	56	124	34	70	2.0	10 cm spacing
	57	124	34	70	2.0	10 cm spacing
	58	124	34	70	2.0	10 cm spacing
	59	124	34	70	2.0	10 cm spacing
	60	124	34	70	2.0	10 cm spacing
FS142 MB	1	138	48	72	2.0	Swamp Frog Adit
	2	139	49	72	2.0	dd: 48 dip 12
	3	32	302	85	1.0	#3 & 4 20 cm spacing; 0-3 mm
	4	146	56	60	2.0	aperture barite vein fill
	5	146	56	60	2.0	
	6	100	10	48	2.0	20 cm spacing
	7	100	10	48	2.0	barite and caliche
	8	100	10	48	2.0	vf 0-1 cm aperture
	9	100	10	48	2.0	
	10	100	10	48	2.0	
	11	290	200	24	0.5	
	12	165	75	24	1.0	
	13	130	40	44	1.0	10 cm spacing
	14	130	40	44	1.0	10 cm spacing
	15	130	40	44	1.0	10 cm spacing
	16	130	40	44	1.0	10 cm spacing
	17	130	40	44	1.0	10 cm spacing
	18	130	40	44	1.0	10 cm spacing
	19	60	330	46	3.0	30 cm spacing
	20	60	330	46	3.0	30 cm spacing
FS106	1	96	6	70	2.6	selection method; dd

						268 dip 16
	2	124	34	84	3.0	4996198N 702263E 2296m
	3	122	32	80	3.0	
	4	322	232	60	2.0	
	5	136	46	68	1.0	
	6	136	46	68	1.0	
	7	136	46	68	1.0	
	8	136	46	68	1.0	
	9	136	46	68	1.0	
	10	26	296	45	1.0	
	11	166	76	68	3.0	
	12	166	76	68	3.0	
	13	166	76	68	3.0	
	14	166	76	68	3.0	
	15	182	92	68	1.5	
	16	352	262	76	4.0	
	17	142	52	80	2.0	
	18	142	52	80	2.0	
	19	142	52	80	2.0	
	20	132	42	60	1.5	
	21	8	278	60	3.0	
	22	140	50	76	1.0	
	23	140	50	76	1.0	
	24	84	354	72	2.5	b-c
	25	84	354	72	2.5	b-c
	26	84	354	72	2.5	b-c
	27	258	168	70	3.0	b-c
	28	70	340	68	3.0	b-c
	29	108	18	60	2.5	b-c
	30	148	58	80	4.0	a-c
	31	148	58	80	4.0	a-c
	32	148	58	80	4.0	a-c
	33	144	54	76	2.0	a-c
	34	144	54	76	2.0	a-c
	35	144	54	76	2.0	a-c
	36	144	54	76	2.0	a-c
	37	144	54	76	2.0	a-c

	38	144	54	76	2.0	a-c
	39	144	54	76	2.0	a-c
	40	110	20	80	3.0	a-c
	41	110	20	80	3.0	a-c
	42	110	20	80	3.0	a-c
	43	154	64	76	2.0	
	44	143	53	60	2.0	slickenlines dd 148 dip 60
	45	114	24	84	3.0	rake 88,90,85, 88, 86 N side up
	46	114	24	84	3.0	
	47	114	24	84	3.0	
	48	114	24	84	3.0	
	49	210	120	76	4.0	
	50	173	83	68	2.0	
	51	163	73	62	2.0	
	52	352	262	70	1.5	
	53	352	262	70	1.5	
	54	352	262	70	1.5	
	55	352	262	70	1.5	
	56	166	76	80	1.5	
	57	158	68	80	1.5	
	58	158	68	80	1.5	
	59	158	68	80	1.5	
	60	116	26	70	3.0	conjugate with next
	61	22	292	66	1.0	
	62	138	48	70	2.0	
	63	28	298	78	3.0	Bleached Mm
	64	28	298	78	3.0	
	65	28	298	78	3.0	
	66	215	125	64	1.0	
	67	132	42	74	4.0	
	68	132	42	74	4.0	
	69	132	42	74	4.0	
	70	132	42	88	2.5	
	71	53	323	70	2.5	
	72	106	16	60	3.0	
	73	172	82	72	4.0	

	74	172	82	72	4.0	
	75	172	82	72	4.0	
	76	172	82	72	4.0	
	77	106	16	76	3.0	
	78	106	16	76	3.0	
	79	106	16	76	3.0	conjugate with next
	80	182	92	64	3.0	conjugate with next
	81	316	226	64	3.0	
	82	12	282	70	4.0	
	83	270	180	70	10.0	
	84	274	184	80	8.0	
FS107	1	92	2	88	1.0	Amsden dd 240 dip 14
	2	132	42	86	1.0	4996095N 702339E 2282m
	3	300	210	72	2.0	selection method
	4	120	30	70	2.0	breccia trend 65
	5	132	42	86	3.0	
	6	270	180	75	3.0	a-c
	7	270	180	75	3.0	a-c
	8	270	180	75	3.0	a-c
	9	270	180	75	3.0	a-c
	10	286	196	70	3.0	
	11	286	196	34	3.0	
	12	318	228	46	2.0	
	13	270	180	72	2.0	slickenlines strike 342 dip 78
	14	232	142	80	3.0	rake 10, 12 W side N E side S
	15	340	250	76	2.0	right lateral
	16	148	58	80	3.0	
	17	330	240	70	3.0	
	18	280	190	55	3.0	
	19	338	248	88	3.0	
	20	174	84	85	2.0	
	21	186	96	80	2.0	
	22	344	254	74	2.0	
	23	282	192	74	3.0	
	24	306	216	70	3.0	

FS108	1	324	234	74	2.0	4996036N 702449E 2287m
	2	324	234	74	1.0	So. of Sandra mine
	3	324	234	74	2.0	bedding dd 214 dip 12 selection method
	4	324	234	74	2.0	
	5	114	24	70	2.0	
	6	142	52	80	2.0	
	7	142	52	80	2.0	
	8	142	52	80	2.0	
	9	142	52	80	2.0	
	10	142	52	80	2.0	
	11	142	52	80	2.0	
	12	142	52	80	2.0	
	13	142	52	80	2.0	
	14	142	52	80	2.0	
	15	142	52	80	2.0	
	16	142	52	80	2.0	
	17	162	72	74	2.0	
	18	145	55	82	2.0	
	19	320	230	80	2.0	
	20	4	274	80	2.0	breccia
	21	35	305	60	3.0	
	22	126	36	70	2.0	
	23	126	36	70	2.0	
	24	126	36	70	2.0	
	25	18	288	70	2.0	
	26	90	0	80	2.0	
	27	90	0	80	2.0	
	28	90	0	80	2.0	
	29	144	54	40	3.0	
	30	55	325	62	2.0	
	31	270	180	70	2.0	
	32	90	0	70	2.0	
	33	276	186	80	2.0	
	34	180	90	60	1.5	
	35	128	38	60	2.0	
	36	128	38	60	2.0	

	37	128	38	60	2.0	
	38	128	38	60	2.0	
	39	242	152	76	2.0	
	40	118	28	80	4.0	
	41	118	28	80	4.0	
	42	118	28	80	4.0	
	43	4	274	70	2.0	
FS111	1	170	80	75	1.8	40995636N 702528E 2245m
	2	120	30	55	3.0	Min. breccia ~ 20 m N with several
	3	76	346	55	2.0	unmin. Breccias nearby
	4	90	0	50	2.0	selection method
	5	320	230	80	1.8	
	6	335	245	70	1.6	
	7	75	345	40	2.0	
	8	310	220	85	1.0	
	9	310	220	85	1.0	
	10	310	220	85	1.0	
	11	310	220	85	1.0	
	12	60	330	80	1.4	
	13	8	278	72	1.4	
	14	295	205	70	1.0	
	15	60	330	88	1.0	
	16	84	354	50	1.0	
	17	65	335	60	1.0	
	18	206	116	68	0.7	
	19	90	0	80	0.5	
	20	138	48	78	2.2	
	21	142	52	78	1.4	
	22	134	44	85	2.0	
	23	342	252	60	0.4	
	24	245	155	76	0.9	
FS113	1	90	0	57	4.0	4995389N 702492E 2183m
	2	55	325	55	1.5	dd 336 dip 6; bleached ls.
	3	10	280	50	2.0	
	4	30	300	70	3.0	

	5	358	268	70	4.0	
	6	310	220	60	2.0	
	7	290	200	45	1.0	conjugate with 8
	8	340	250	70	2.0	
	9	296	206	84	2.0	
	10	38	308	72	3.0	
	11	20	290	45	3.0	
	12	50	320	35	33.0	
	13	290	200	45	3.0	
	14	60	330	60	3.0	
	15	60	330	48	3.0	
	16	56	326	50	2.0	
	17	354	264	56	4.0	
	18	80	350	70	2.0	
	19	20	290	65	4.0	conjugate with 20
	20	70	340	74	1.0	
	21	70	340	80	1.0	
	22	136	46	65	1.0	
	23	340	250	75	1.0	
	24	176	86	80	3.0	
	25	40	310	66	3.0	
	26	44	314	80	2.0	conjugate with next
	27	160	70	80	1.0	
	28	160	70	80	3.0	
FS133 = UMB53	1	340	250	52	1.0	702443E 4994822N 2080m
	2	340	250	52	1.0	10 m to east of UMB52
	3	340	250	52	1.0	very small UMB 2x2 m
	4	340	250	52	1.0	Mm selection method
	5	340	250	52	1.0	
	6	49	319	60	1.0	
	7	49	319	60	1.0	
	8	49	319	60	1.0	
	9	49	319	60	1.0	
	10	49	319	60	1.0	
UMB 52	1	310	220	80	3.0	fractures trend dd 310 dip 80
	2	310	220	80	3.0	15 m so. and down the

						dip slope
	3	310	220	80	3.0	from MB51
UMB54	1	324	234	82	1.0	silicified 4x6 m
	2	324	234	82	1.0	dd 002 dip 20; pg. 19
	3	324	234	82	1.0	702428E 4994802N 2076.5m
	4	324	234	82	1.0	
	5	324	234	82	1.0	
	6	236	146	70	1.0	
	7	236	146	70	1.0	
	8	236	146	70	1.0	
	9	236	146	70	1.0	
	10	236	146	70	1.0	
	11	236	146	70	1.0	
	12	236	146	70	1.0	
FS134	1	48	318	60	3.0	4994812N 702412E 2075 m
	2	48	318	60	3.0	6 fractures below 5 are closed
	3	48	318	60	3.0	and 2 are reopened
	4	48	318	60	3.0	spacing ~ 60 cm
	5	48	318	60	3.0	
	6	48	318	60	3.0	
	7	48	318	60	3.0	
	8	140	50	60	2.0	
	9	140	50	60	2.0	
	10	140	50	60	2.0	
	11	47	317	75	1.0	
	12	47	317	75	1.0	
	13	47	317	75	1.0	
	14	47	317	75	1.0	
	15	47	317	75	1.0	
	16	320	230	80	4.0	
	17	320	230	80	4.0	
	18	320	230	80	4.0	
	19	320	230	80	4.0	
	20	144	54	75	1.0	Conjugate with 21
	21	104	14	48	1.0	

	22	104	14	48	1.0	
	23	104	14	48	1.0	
	24	154	64	85	0.5	
	25	154	64	85	0.5	
	26	154	64	85	0.5	
	27	154	64	85	0.5	
	28	212	122	84	1.0	
	29	212	122	84	1.0	Conjugate with 30
	30	346	256	56	0.5	
	32	40	310	72	2.0	
	33	40	310	72	2.0	
	34	224	134	60	1.0	
	35	224	134	60	1.0	
	36	224	134	60	1.0	
UMB57	1	47	317	60	1.0	silicified 2x3 3 m west of 56
	2	47	317	60	1.0	702403E 4994819N 2076.5m
	3	47	317	60	1.0	
	4	176	86	80	1.0	
	5	176	86	80	1.0	
	6	348	258	62	1.0	
	7	348	258	62	1.0	
	8	348	258	62	1.0	
	9	348	258	62	1.0	
	10	295	205	40	1.0	
	11	295	205	40	1.0	
	12	295	205	40	1.0	
	13	295	205	40	1.0	
FS135=UMB58	1	270	180	84	4.0	Silicified breccia Pennsylvanian
	2	270	180	84	4.0	selection method
	3	270	180	84	4.0	0702389E 4994829N 2076.6m
	4	270	180	84	4.0	25-30 cm spacing (1-4)
	5	270	180	84	4.0	
	6	72	342	70	1.5	
	7	68	338	84	3.0	mode III left lateral 4 cm offset

	8	156	66	80	2.0	plus 2; 40 cm spacing
	9	156	66	80	2.0	
	10	156	66	80	2.0	
	11	204	114	80	1.5	plus 3; 50 cm spacing
	12	204	114	80	1.5	
	13	204	114	80	1.5	
	14	204	114	80	1.5	
	15	45	315	84	1.0	plus 1;25 cm spacing
	16	45	315	84	1.0	
	17	38	308	18	0.5	
	18	310	220	88	1.0	plus 2; 30-35 cm spacing with barite on some parts of
	19	310	220	88	2.0	fracture plane and in vugs
	20	310	220	88	2.0	
	21	72	342	80	2.0	plus 9; 12 cm spacing
	22	72	342	80	1.0	
	23	72	342	80	2.0	
	24	72	342	80	1.0	
	25	72	342	80	2.0	
	26	72	342	80	1.0	
	27	72	342	80	2.0	
	28	72	342	80	1.0	
	29	72	342	80	2.0	
	30	72	342	80	2.0	
	31	100	10	85	1.5	plus 3;27 cm spacing
	32	100	10	85	1.5	
	33	100	10	85	1.5	
	34	100	10	85	1.5	
	35	326	236	70	1.5	plus 3; 25cm spacing
	36	326	236	70	1.5	
	37	326	236	70	1.5	
	38	326	236	70	1.5	
	39	270	180	82	2.0	plus 2; 40 cm spacing
	40	270	180	82	2.0	
	41	270	180	82	2.0	
	42	242	152	55	3.0	plus 3; 30 cm spacing

	43	242	152	55	3.0	
	44	242	152	55	3.0	
	45	242	152	55	3.0	
FS136=UMB38	1	74	344	50	4.0	
	2	90	0	60	4.0	plus 2; 60 cm spacing
	3	90	0	60	4.0	
	4	90	0	60	4.0	
	5	26	296	80	2.0	plus 5; 55-60 cm spacing
	6	26	296	80	2.0	
	7	26	296	80	2.0	
	8	26	296	80	2.0	
	9	26	296	80	2.0	
	10	26	296	80	2.0	
	11	322	232	76	3.0	plus 1; 40 cm spacing
	12	322	232	76	3.0	
	13	43	313	68	1.5	plus 2; 50 cm spacing
	14	43	313	68	1.5	
	15	43	313	68	1.5	
	16	74	344	16	4.0	plus 1; 70 cm spacing
	17	74	344	16	4.0	
	18	22	292	40	2.0	
	19	309	219	76	4.0	plus 2; 10 cm spacing; in breccia only
	20	309	219	76	4.0	
	21	309	219	76	4.0	
	22	49	319	30	3.0	plus 4; 30 cm spacing; in breccia only
	23	49	319	30	3.0	
	24	49	319	30	3.0	
	25	49	319	30	3.0	
	26	49	319	30	3.0	
	27	90	0	80	4.0	plus 2; 25 cm spacing; in breccia only
	28	90	0	80	4.0	
	29	90	0	80	4.0	
	30	46	316	65	2.0	plus 2; 35 cm spacing; in breccia only

	31	46	316	65	2.0	
	32	46	316	65	2.0	
	33	58	328	44	4.0	plus 4; 30 cm spacing; in breccia only
	34	58	328	44	4.0	
	35	58	328	44	4.0	
	36	58	328	44	4.0	
	37	58	328	44	4.0	
	38	6	276	74	2.0	plus 6; 10 cm spacing; in breccia only
	39	6	276	74	2.0	
	40	6	276	74	2.0	
	41	6	276	74	2.0	
	42	6	276	74	2.0	
	43	6	276	74	2.0	
	44	6	276	74	2.0	
	45	110	20	70	2.0	plus 3; 10 cm spacing; in breccia only
	46	110	20	70	2.0	
	47	110	20	70	2.0	
	48	110	20	70	2.0	
	49	56	326	75	2.0	plus 1; 10 cm spacing; in breccia only
	50	56	326	75	2.0	
	51	70	340	44	3.0	plus 5; 25-28 cm spacing; in Mm Ls
	52	70	340	44	3.0	
	53	70	340	44	3.0	
	54	70	340	44	4.0	
	55	70	340	44	4.0	
	56	70	340	44	4.0	conjugate with 57
	57	142	52	72	1.0	next2; 20 cm spacing
	58	142	52	72	1.0	
	59	142	52	72	1.0	
	60	78	348	52	0.5	conjugate with 61; in Mm LS
	61	360	270	78	0.5	

	62	320	230	70	1.0	next 7; in breccia only; 20 cm spacing
	63	320	230	70	1.0	
	64	320	230	70	1.0	
	65	320	230	70	1.0	
	66	320	230	70	0.5	
	67	320	230	70	0.5	
	68	320	230	70	0.5	
	69	320	230	70	0.5	
	70	340	250	80	1.0	next 3; 20 cm spacing; in breccia only
	71	340	250	80	1.0	
	72	340	250	80	1.0	
	73	340	250	80	1.0	
FS140 = UMB70	1	198	108	66	3.0	Near Swamp Frog Mine
	2	154	64	60	2.0	
	3	212	122	68	3.0	
	4	243	153	84	1.0	Next two,12 cm spacing
	5	243	153	84	1.0	
	6	158	68	60	2.0	
	7	166	76	40	2.0	4 cm spacing
	8	166	76	40	2.0	4 cm spacing
	9	166	76	40	2.0	4 cm spacing
	10	166	76	40	2.0	4 cm spacing
	11	330	240	60	2.0	
	12	164	74	42	1.0	next 8; 4 cm spacing
	13	164	74	42	1.0	
	14	164	74	42	1.0	
	15	164	74	42	1.0	
	16	164	74	42	1.0	
	17	164	74	42	1.0	
	18	164	74	42	1.0	
	19	164	74	42	1.0	
	20	164	74	42	1.0	
	21	122	32	88	1.0	next 2; 20 cm spacing
	22	122	32	88	1.0	
	23	122	32	88	1.0	

FS141=UMB71	1	22	292	70	2.0	bedding dd: 272 dip: 24
	2	22	292	70	2.0	beds at this site 50 mm spacing
	3	22	292	70	2.0	& 2-5 mm thick
	4	22	292	70	2.0	
	5	22	292	70	2.0	
	6	22	292	70	2.0	
	7	22	292	70	2.0	
	8	22	292	70	2.0	
	9	22	292	70	2.0	
	10	95	5	66	2.0	set is conjugate to 13-15
	11	95	5	66	2.0	30 cm spacing
	12	95	5	66	2.0	30 cm spacing
	13	160	70	80	1.0	30 cm spacing
	14	160	70	80	1.0	30 cm spacing
	15	160	70	80	1.0	30 cm spacing
	16	140	50	76	1.0	Plus 7; 20 cm spacing
	17	140	50	76	1.0	
	18	140	50	76	1.0	
	19	140	50	76	1.0	
	20	140	50	76	1.0	
	21	140	50	76	1.0	
	22	140	50	76	1.0	
	23	140	50	76	1.0	
	24	14	284	76	2.0	Plus 2; 20 cm spacing
	25	14	284	76	2.0	
	26	14	284	76	2.0	
	27	20	290	74	2.0	Plus 3; 14 cm spacing
	28	20	290	74	2.0	
	29	20	290	74	2.0	
	30	20	290	74	2.0	
	31	245	155	75	4.0	Plus 1; 50 cm spacing
	32	245	155	75	4.0	
	33	115	25	78	2.0	Plus 1; 50 cm spacing
	34	115	25	78	2.0	
	35	340	250	80	1.0	crosscuts #41 15 cm spacing
	36	340	250	80	1.0	Plus 5; 15 cm spacing

	37	340	250	80	1.0	
	38	340	250	80	1.0	
	39	340	250	80	1.0	
	40	340	250	80	1.0	
	41	78	348	74	2.0	Plus 6; 9 cm spacing
	42	78	348	74	2.0	
	43	78	348	74	2.0	
	44	78	348	74	2.0	
	45	78	348	74	2.0	
	46	78	348	74	2.0	
	47	78	348	74	2.0	
	48	66	336	66	1.5	Linked to 49
	49	72	342	60	2.0	Plus 4; 35 cm spacing
	50	72	342	60	2.0	
	51	72	342	60	2.0	
	52	72	342	60	2.0	
	53	72	342	60	2.0	

Table B5. Fracture analysis data collected on Red Pryor Mountain. Green filled fracture stations indicate mineralized breccia and red filled fracture stations indicate unmineralized breccia.

APPENDIX C

SUPPORTING INFORMATION FOR CHAPTER 5

PGM and Au Analysis

Five samples were analyzed for PGM and Au by Fire Assay with ICP finish by American Analytical Services (AAS), Osburn, Idaho. The samples included two UV mineralized breccia, two barites, and a fluorite. Table C1 shows these results.

Element		Sandra713B UV Mineral	DandyF Fluorite	FS142 Barite	FS131 UV-mineral	OGMB Barite
Pt	ppm	<0.020	<0.020	na	<0.020	na
Pd	ppm	<0.020	<0.020	na	<0.020	na
Rh	ppm	<0.020	<0.020	na	<0.020	na
Au	ppm	0.031	0.067	<0.005	0.055	2.35

Table C1. PGM and Au Results AAS laboratory.

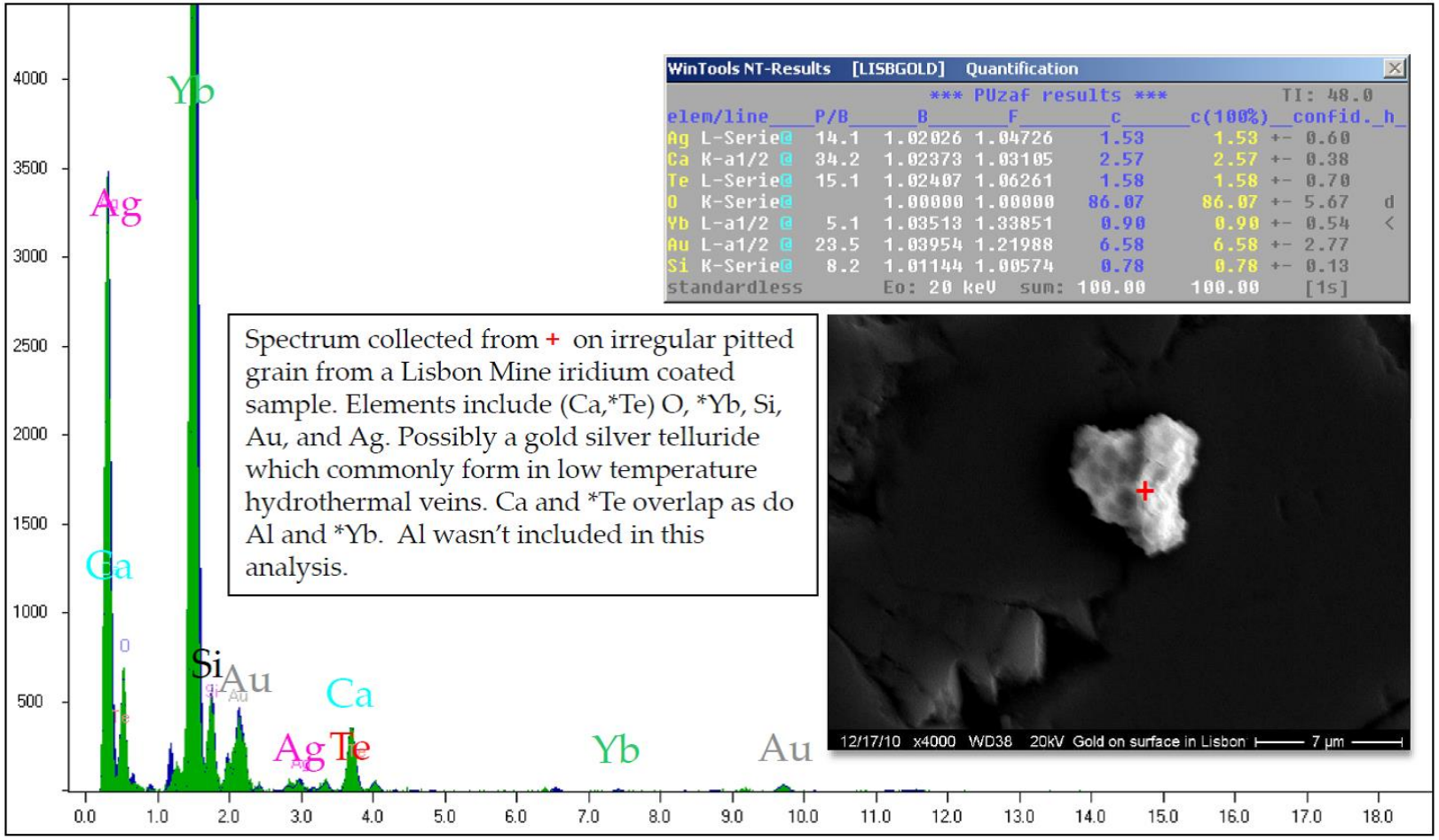


Figure C1. EDS spectrum of Au mineral from Lisbon mine sample.

Trace Element Analyses

The Nevada branch of Australian Laboratory Services (ALS) Global analyzed samples for REE and trace elements. A total of 41 samples were analyzed: 18 U V mineralized breccia, 6 limestone and dolomite host rock, 5 calcite, 1 bentonite, 1 barite, 5 fluorite, and 4 quartz were analyzed for REE by by Lithium Borate Fusion and ICP-MS (Fused bead, acid digestion and ICP-MS) in a 30 element package (ME-MS81).

Three samples containing bitumen were analyzed for REE by Aqua Regia and ICP-AES/ICP-MS (ME-MS41r) a 51-element package. Twenty-two samples were analyzed for base metals by a four acid digestion and ICP-MS (ME-4ACD81) to test for Pb and 17 samples were analyzed for trace element Hg by Aqua Regia and ICP-MS (Hg-MS42). Additionally 17 mineralized samples were analyzed by by XRF (V, U-XRF10) for ore grade % U and 3 for ore grade %V as these samples were above the maximum detection level using ME-MS81.

Trace element data is presented in Table C2 which is split into four pages with the first two pages showing the trace elements Ag-Nb and the next two pages showing the trace elements Ni-Zr. The mineralized breccia samples are numbered 1-18 and host rock, gangue minerals and unmineralized breccia samples are numbered 19-41. REE data is presented in Table B3, also split into two pages with the mineralized samples on the first page and the remaining samples on the following page

Trace metals analyzed by ALS laboratory results are shown in Table C3 with elements listed across the top of the table and samples to the side. The table is split into four pages. The first 18 samples are the mineralized breccia samples. The next 23 samples are the host rock, gangue minerals and unmineralized breccia samples. Values are in ppm. Not analyzed is abbreviated na.

No.	Sample	Ag	As	Ba	Cd	Co	Cr	Cs	Cu	Fe	Ga	Hf	Hg	Li	Mo	Nb
1	FS131A UV br	1.3	262	1230	1.7	<1	<10	0.63	<1	na	3.4	<0.2	2.84	<10	53	0.6
2	LMLisbon UV br	<0.5	89	42.6	0.9	9	<10	0.37	94	na	28.2	<0.2	0.197	<10	25	<0.2
3	Swamp Frog UV br	1.3	556	1320	<0.5	1	20	1.65	7	na	7.5	0.6	0.396	20	791	1.4
4	SBRX01 UV br	<0.5	49	5460	<0.5	8	100	1.64	4	na	9.5	<0.2	0.333	30	11	<0.2
5	LMLeo02 UV br	<0.5	726	255	3.8	70	20	0.77	109	na	43.1	0.7	0.179	10	137	1.2
6	MarieMine001 UV br	<0.5	87	533	2.6	<1	60	1.9	<1	na	7.7	3.1	1.715	10	319	3.2
7	Perc01 UV br	<0.5	329	5170	<0.5	<1	10	1.2	6	na	8.7	<0.2	1.21	10	52	<0.2
8	OGM04 UV br	<0.5	1295	2310	0.5	7	40	0.84	12	na	10.6	0.6	0.354	10	152	1.4
9	P005 UV br	<0.5	1080	1305	<0.5	9	50	1.24	2	na	15.4	2.3	1.255	10	386	6.6
10	Sandra713B UV br	<0.5	99	6550	0.5	6	240	1.63	14	na	42.1	<0.2	1.485	40	29	0.2
11	D2001 UV br	<0.5	87	79.5	3.2	<1	<10	0.36	<1	na	6	<0.2	6.32	<10	9	2.2
12	DandyMSPF UV br	<0.5	30	39.6	0.5	<1	10	0.24	<1	na	2.2	<0.2	3.4	<10	4	0.6
13	DandyMBr UV br	<0.5	130	61.3	1.7	5	10	0.78	<1	na	10.4	0.2	12.8	10	28	0.7
14	OGM UV blk UV br	0.5	46	1530	<0.5	12	10	0.78	1	na	2	0.3	na	<10	21	0.4
15	DandyMSP UV br	<0.5	94	2470	<0.5	37	10	5.42	5	na	4.6	0.5	na	10	20	1.4
16	EP001 UV br	<0.5	50	27.6	0.9	7	10	0.46	2	na	1.7	0.4	na	<10	2	0.6
17	LMLeoIncline UV br	<0.5	116	183	2.1	22	10	0.21	90	na	11.8	0.3	na	<10	98	0.7
18	LMLisbonBX UV br	<0.5	212	140	0.6	22	10	0.66	17	na	9.3	0.4	na	<10	93	0.5

Table C2. Mineralized breccia sample trace element data for the elements Ag-Nb, values are ppm.

Table C2 continued samples 19-41.

No.	Sample	Ag	As	Ba	Cd	Co	Cr	Cs	Cu	Fe	Ga	Hf	Hg	Li	Mo	Nb
19	LMLisbonSB breccia	na	na	4330	na	na	10	0.14	na	na	0.7	<0.2	na	na	na	<0.2
20	EP001DB breccia	na	na	29.2	na	na	20	0.36	na	na	1.2	0.2	na	na	na	<0.2
21	SWMP_H limestone	na	na	9.7	na	na	10	0.11	na	na	0.6	<0.2	na	na	na	<0.2
22	Sandra002 limestone	na	na	23.2	na	na	10	0.05	na	na	0.8	<0.2	na	na	na	<0.2
23	UMB018 breccia	na	na	6.5	na	na	10	0.02	na	na	1	<0.2	na	na	na	<0.2
24	FS139 calcite	na	na	16.5	na	na	10	0.05	na	na	0.5	0.2	na	na	na	<0.2
25	BPM_BC calcite	na	na	46.9	na	na	<10	0.02	na	na	0.3	<0.2	na	na	na	<0.2
26	BCS calcite	<0.5	<5	24	<0.5	9	<10	0.03	3	na	0.3	<0.2	0.034	<10	2	<0.2
27	LeoGC calcite	na	na	24.2	na	na	<10	0.02	na	na	1	<0.2	na	na	na	<0.2
28	Dandy Mine fluorite	<0.5	22	29.7	<0.5	3	10	0.17	<1	na	1.1	<0.2	0.618	<10	8	<0.2
29	MarieF fluorite	<0.5	64	72	0.5	8	20	0.37	<1	na	2.4	0.2	1.05	10	10	0.2
30	EPryorF fluorite	na	na	729	na	na	40	0.51	na	na	2.1	0.3	na	na	na	0.4
31	DandyF fluorite	na	na	331	na	na	30	0.5	na	na	2	0.3	na	na	na	0.3
32	SandraF fluorite	na	na	9.7	na	na	10	0.15	na	na	1	<0.2	na	na	na	1.4
33	SWMP_B barite	na	na	>10000	na	na	20	0.47	na	na	2.1	0.4	na	na	na	0.8
34	Lisbon001-dolomite br	<0.5	<5	200	<0.5	3	20	1.65	1	na	3.7	1	0.02	10	2	2.5
35	LisbonQP quartz	<0.5	<5	87.5	<0.5	18	<10	0.05	1	na	1	<0.2	0.095	<10	1	<0.2
36	GS32 quartz	na	na	264	na	na	10	0.04	na	na	1.2	<0.2	na	na	na	<0.2
37	TS-53 quartz	na	na	562	na	na	<10	0.14	na	na	1.1	0.2	na	na	na	<0.2
38	Bentonite	<0.5	6	597	<0.5	3	<10	0.86	2	na	24	7.8	<0.005	20	1	21.4
39	Mm Bitumen	0.05	0.2	10	0.05	9.9	1	0.06	3	300	<0.05	<0.02	0.01	0.5	1.63	<0.05
40	Mm Bitumen Breccia	0.01	<0.1	20	0.1	0.9	<1	<0.05	1.2	500	<0.05	<0.02	<0.01	0.1	0.12	<0.05
41	Goose Egg bitumen	0.01	1	630	0.08	2.4	1	0.06	2.8	800	0.21	<0.02	0.01	2.2	0.46	0.05

Table C2. Host rock, gangue minerals and unmineralized breccia sample trace element data for elements Ag-Nb, values are ppm.

Table C2 continued for elements Ni - Zr.

No.	Sample	Ni	Pb	Rb	Sc	Se	Sn	Sr	Ta	Th	Tl	U	V	W	Zn	Zr
1	FS131A UV br	<1	<2	1.5	4	na	<1	257	<0.1	0.66	180	86800	18900	94	16	4
2	LMLisbon UV br	421	146	5.9	1	na	4	261	<0.1	0.09	30	31100	8520	11	1300	2
3	Swamp Frog UV br	11	<2	13	3	na	1	192.5	0.1	1.3	340	6100	4160	81	44	23
4	SBRX01 UV br	38	7	4.4	8	na	<1	182.5	<0.1	0.16	10	2600	1950	71	136	2
5	LMLeo02 UV br	517	57	5.5	2	na	7	401	0.1	1.27	230	16000	10300	11	2230	29
6	MarieMine001 UV br	15	<2	18.1	6	na	1	62.5	0.2	6.57	30	2100	6740	40	57	128
7	Perc01 UV br	19	51	3	12	na	<1	227	<0.1	0.24	170	20700	6700	30	95	4
8	OGM04 UV br	2	13	4.8	9	na	1	1355	0.1	1.12	100	10600	4410	105	26	22
9	P005 UV br	80	18	9.7	9	na	2	980	0.4	6.12	340	9000	6010	19	165	91
10	Sandra713B UV br	167	44	14.8	39	na	1	188.5	<0.1	0.55	20	21400	8730	24	804	4
11	D2001 UV br	2	35	2	1	na	1	132.5	<0.1	0.15	50	17700	6310	16	849	2
12	DandyMSPF UV br	21	8	2.7	2	na	<1	128	<0.1	0.25	10	3000	3320	12	76	5
13	DandyMBr UV br	102	55	6.4	4	na	<1	147.5	<0.1	0.5	20	28100	10500	26	1110	10
14	OGM UV blk UV br	<1	2	6.4	1	na	<1	110	0.1	0.36	50	4900	1240	107	7	12
15	DandyMSP UV br	<1	35	31.5	5	na	6	513	0.3	0.94	490	8600	2220	382	9	20
16	EP001 UV br	63	11	6.7	2	na	<1	84.7	<0.1	0.63	10	907	25	6	143	18
17	LMLeoIncline UV br	191	28	2.4	1	na	10	168.5	<0.1	0.73	20	>1000	4330	13	970	16
18	LMLisbonBX UV br	122	4	5.5	1	na	10	151.5	<0.1	0.55	10	1300	1850	12	569	15

Table C2 Mineralized breccia sample trace element data for the elements Ni-Zr.

Table C2 continued for samples 21-41.

No.	Sample	Ni	Pb	Rb	Sc	Se	Sn	Sr	Ta	Th	Tl	U	V	W	Zn	Zr
19	LMLisbonSB breccia	na	na	2.3	na	na	<1	191	0.1	0.19	na	32.7	164	13	na	4
20	EP001DB breccia	na	na	4.5	na	na	<1	105	0.1	0.35	na	407	28	28	na	7
21	SWMP_H limestone	na	na	1.5	na	na	<1	108	<0.1	0.15	na	3.07	7	10	na	5
22	Sandra002 limestone	na	na	0.5	na	na	<1	158.5	<0.1	0.1	na	0.52	6	4	na	4
23	UMB018 breccia	na	na	0.2	na	na	<1	63.5	<0.1	<0.05	na	3.02	12	23	na	<2
24	FS139 calcite	na	na	0.9	na	na	<1	97.8	<0.1	0.15	na	25.1	123	10	na	11
25	BPM_BC calcite	na	na	<0.2	na	na	<1	43.2	<0.1	<0.05	na	14.8	<5	4	na	<2
26	BCS calcite	4	2	0.2	<1	na	<1	590	0.1	<0.05	<10	43.3	20	47	15	<2
27	LeoGC calcite	na	na	0.5	na	na	<1	174.5	<0.1	0.09	na	159	268	9	na	2
28	Dandy Mine fluorite	3	3	1.7	3	na	1	26.1	<0.1	0.66	<10	518	439	14	41	5
29	MarieF fluorite	31	3	3.8	3	na	1	33.7	0.1	0.7	<10	842	871	25	65	7
30	EPryorF fluorite	na	na	8.2	na	na	<1	132	0.1	1.14	na	87.7	51	23	na	13
31	DandyF fluorite	na	na	7.7	na	na	<1	44.1	0.1	0.65	na	105	542	18	na	11
32	SandraF fluorite	na	na	2	na	na	<1	52.4	<0.1	0.67	na	53.4	655	1	na	4
33	SWMP_B barite	na	na	5.6	na	na	1	8260	0.1	1.15	na	15.2	195	11	na	14
34	Lisbon001-dolomite br	6	2	25.9	2	na	<1	116.5	0.2	2.09	<10	6.75	25	11	17	42
35	LisbonQP quartz	<1	<2	1.2	<1	na	<1	14.2	0.2	0.09	<10	1.34	<5	199	<2	3
36	GS32 quartz	na	na	0.5	na	na	<1	12.2	0.1	0.06	na	27.7	17	209	na	6
37	TS-53 quartz	na	na	1.4	na	na	<1	33.7	0.2	0.21	na	25.3	26	279	na	12
38	Bentonite	2	32	20.1	2	na	7	381	2.3	32.1	<10	56.7	22	6	64	245
39	Mm Bitumen	14.1	0.9	0.4	0.1	3.2	3.2	76.4	<0.01	<0.2	0.02	6.8	73	8.63	5	<0.5
40	Mm Bitumen Breccia	1.5	0.5	0.1	0.1	0.5	0.5	156	<0.01	<0.2	<0.02	4.04	7	2.38	2	<0.5
41	Goose Egg bitumen	3.2	1.5	0.8	0.1	0.5	0.5	2720	<0.01	<0.2	0.03	11.6	8	20.8	9	0.5

Table C2 Host rock, gangue minerals, and unmineralized breccia sample trace element data for the elements Ni-Zr..

REE plus Y ALS laboratory results are shown in Table C3 with elements listed across the top of the table and samples to the side. The first 18 samples are mineralized breccia samples. The next 23 samples are the host rock, gangue minerals and unmineralized breccia samples.

No.	Sample Number	La	Ce	Pr	Nd	Sm	Eu	Gd	Tb	Dy	Ho	Er	Tm	Yb	Lu	Y
1	FS131A UV br	0.9	5.9	1	6.6	3.54	1.06	4.76	1.21	7.92	1.45	4.26	0.53	3.46	0.42	33.1
2	LM LisbonUV Br	9.5	13.9	1.86	7.9	1.66	0.4	2.08	0.3	1.85	0.39	1.13	0.12	0.76	0.12	17
3	Swamp Frog UV Br	4.5	21.2	2.03	9	2.09	0.41	1.28	0.16	0.72	0.13	0.32	0.05	0.36	0.03	2.8
4	SBRX01 UV Br	6.7	24.7	5.57	32.5	12.25	3.51	19.1	3.07	18.55	3.92	10.65	1.32	7.21	1.02	172
5	LM Leo02 UV Br	10.1	18.6	2.37	9.6	2.05	0.53	2.32	0.37	2.03	0.43	1.29	0.16	1.02	0.14	15.6
6	MarieMine001 UV Br	9.7	32.4	4.96	26.9	6.97	1.2	3.54	0.38	1.68	0.33	1.05	0.14	0.93	0.12	7.6
7	PERC01 UV Br	10.7	52.7	4.29	19	3.87	0.81	3.46	0.48	2.53	0.46	1.06	0.13	0.9	0.11	17.4
8	OGM04 UV Br	13.7	44.5	8.2	40.9	8.88	1.69	5.76	0.95	5.7	0.96	2.56	0.4	3.17	0.32	21.3
9	P005 UV Br	22.3	54.3	8.21	35.2	7.19	1.76	8.33	1.33	8.28	1.76	4.94	0.61	4.11	0.57	65
10	Sandra713B UV Br	44.8	222	44.1	245	76.5	20.6	103	15.4	87.7	17.85	46.9	5.55	33.3	4.45	840
11	D2001 UV Br	1.5	3.9	0.49	2.4	0.75	0.17	0.84	0.14	0.9	0.19	0.41	0.07	0.34	0.03	10.4
12	DandyMineSP UV Br	2.1	5.3	0.95	4.8	1.46	0.43	2.39	0.36	2.06	0.49	1.3	0.12	0.74	0.09	19.8
13	DandyMineBr UV Br	4.8	15	2.44	13.3	4.7	1.38	7.52	1.33	8.12	1.74	4.51	0.61	3.41	0.47	70.6
14	OGM UV blk UV Br	1.6	3.8	0.38	1.6	0.55	0.1	0.27	0.05	0.3	0.05	0.08	0.02	0.17	0.01	1
15	DandyMineSP UV Br	13.7	40.6	8.46	43.8	8.45	1.6	4.7	0.98	5.91	0.77	1.94	0.31	2.53	0.17	12.3
16	EP001 UV Br	2.8	5.7	0.74	3.5	0.8	0.17	1.06	0.16	1.09	0.26	0.7	0.11	0.6	0.09	8.5
17	LM LeoIncline UV Br	5.2	10.4	1.31	5.4	0.98	0.3	1.35	0.21	1.16	0.27	0.57	0.1	0.47	0.07	8.9
18	LM LisbonBX UV Br	3.4	6.1	0.82	3.5	0.51	0.14	0.6	0.08	0.51	0.11	0.36	0.04	0.24	0.03	4.3

Table C3. REE plus Y data for mineralized breccia samples.

Table C3 continued.

No.	Sample Number	La	Ce	Pr	Nd	Sm	Eu	Gd	Tb	Dy	Ho	Er	Tm	Yb	Lu	Y
19	LMLisbonSB breccia	0.9	1.4	0.18	0.7	0.14		0.13	0.02	0.12	0.02	0.05	0.01	0.05	0.01	0.5
20	EP001DB breccia	1.3	2.7	0.39	1.7	0.39	0.09	0.5	0.06	0.38	0.08	0.26	0.03	0.23	0.03	3.2
21	SWMP_H limestone	1.1	1.4	0.21	0.9	0.12		0.15	0.02	0.12	0.03	0.1	0.01	0.11	0.02	1.3
22	Sandra002 limestone	1.1	1.4	0.22	1	0.16		0.18	0.03	0.18	0.05	0.15	0.02	0.12	0.03	2.4
23	UMB018 breccia	2.3	4	0.65	2.7	0.57	0.14	0.67	0.09	0.58	0.12	0.39	0.05	0.24	0.05	4.9
24	FS139 calcite	2.50	9.10	0.96	4.10	0.79	0.20	0.89	0.12	0.62	0.14	0.37	0.04	0.33	0.05	3.60
25	FS139	2.30	4.20	0.41	2.00	0.44	0.07	0.53	0.09	0.47	0.13	0.43	0.04	0.37	0.06	4.30
26	BPM_BC calcite				0.10										0.01	
27	BCS calcite			0.03	0.10											
28	LeoGC calcite	0.60	0.80	0.08	0.30	0.04		0.05	0.01				0.01		0.01	
29	Dandy Mine fluorite	2.70	6.40	1.11	5.80	1.78	0.50	2.85	0.49	2.63	0.57	1.52	0.20	1.21	0.17	35.90
30	MarieF fluorite	3.00	9.50	1.81	11.20	3.84	0.96	5.06	0.72	3.57	0.70	1.89	0.23	1.45	0.19	35.20
31	EPryorF fluorite	4.90	9.60	1.41	6.90	1.76	0.49	3.09	0.47	2.69	0.60	1.50	0.20	1.24	0.16	35.10
32	DandyF fluorite	2.00	4.00	0.50	2.50	0.64	0.19	1.01	0.19	1.04	0.21	0.57	0.07	0.41	0.07	11.80
33	SandraF fluorite	2.00	4.30	0.66	3.30	0.85	0.18	0.98	0.15	0.90	0.17	0.45	0.06	0.34	0.06	8.80
34	SWMP_B barite	5.60	4.30	0.66	3.80	3.43		0.89	0.09	0.38	0.09	0.16	0.04	0.52	0.16	3.00
35	Lisbon001-dolomite br	6.70	12.70	1.44	6.10	1.05	0.22	1.04	0.16	0.88	0.21	0.58	0.07	0.56	0.09	5.10
36	LisbonQP quartz		0.70	0.10	0.40	0.11		0.16	0.02	0.08	0.02	0.06	0.01	0.04	0.02	0.50
37	GS32 quartz		0.60	0.08	0.40	0.07		0.16	0.01	0.08	0.02	0.05		0.03	0.01	0.80
38	TS-53 quartz	0.60	1.30	0.16	0.60	0.09		0.21	0.04	0.27	0.07	0.22	0.04	0.22	0.03	2.20
39	Bentonite	2.00	4.20	0.51	2.10	0.33	0.07	0.42	0.05	0.32	0.07	0.21	0.02	0.21	0.03	2.10
40	Mm Bitumen	51.10	96.20	10.20	35.60	6.19	0.70	4.50	0.64	3.61	0.69	1.96	0.26	1.92	0.28	16.30
41	Mm Bitumen Breccia	0.50	1.28	0.16	0.80	0.18	0.04	0.20	0.03	0.16	0.03	0.08	0.01	0.05	0.01	1.07
42	Goose Egg bitumen	1.80	3.70	0.44	2.00	0.42	0.09	0.54	0.08	0.42	0.08	0.22	0.03	0.15	0.02	2.88
43	Goose Egg bitumen	0.7	1.34	0.6	0.15	0.1		0.09	0.01	0.07	0.02	0.04	0.01	0.03		0.49

Table C3 Continued. REE plus Y data for host rock, gangue minerals and unmineralized breccia samples.

The following Figures C2-C10, referred to in section 4.1 of the Chapter 5, are for samples analyzed using the SEM.

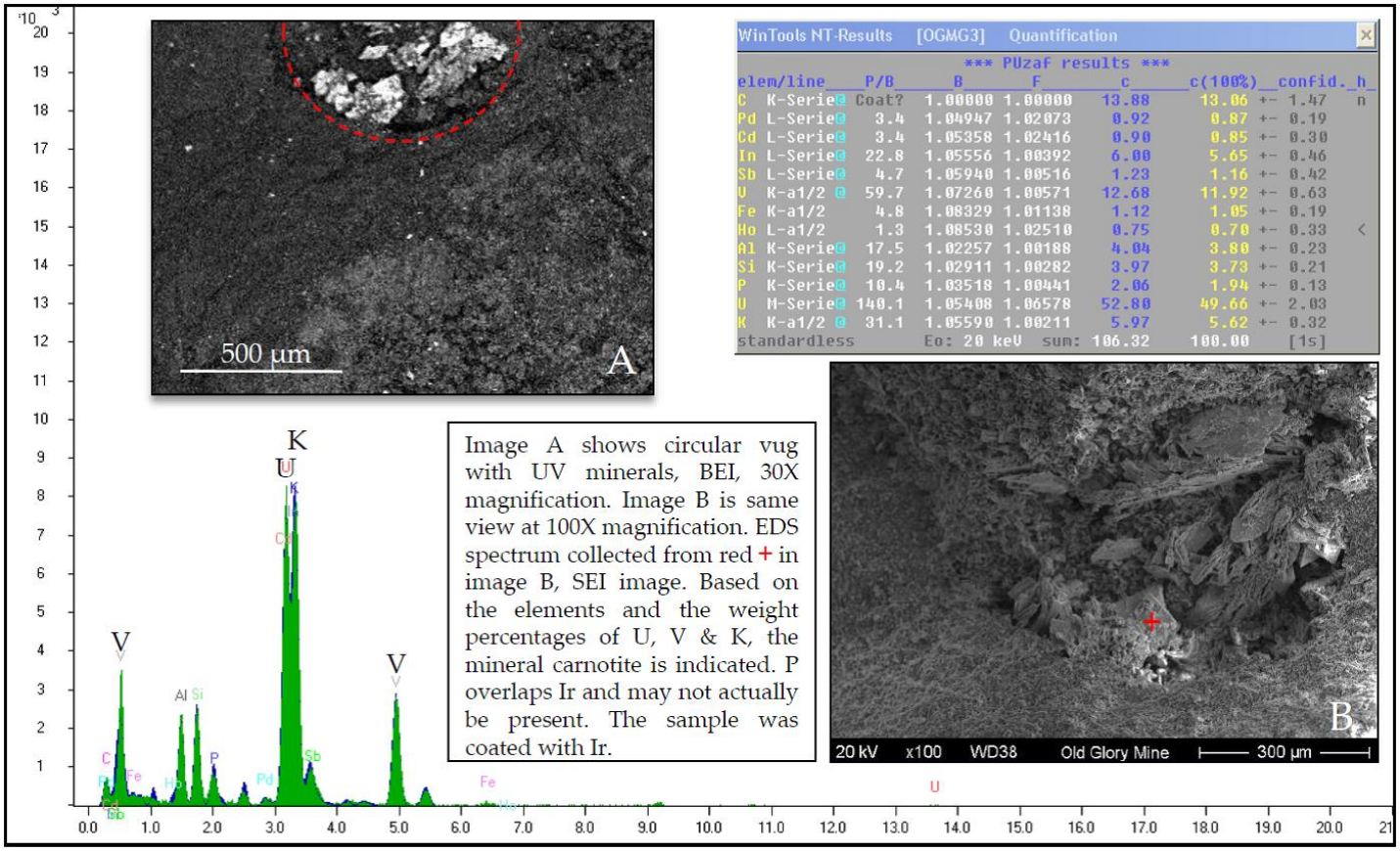


Figure C2. Old Glory mine silicified breccia sample with U-V minerals in a vug, Image A in figure above. EDS spectrum from + in Figure B, a higher magnification of Image A. Carnotite, a K-uranyl vanadate, is indicated based on the elements detected, though the weight percentages of U, V and K are higher and O is lower than stoichiometrically values should be for the mineral. P and Ir overlap and P may not actually be part of the sample, which was coated with Ir. Sb is actually a secondary U peak.

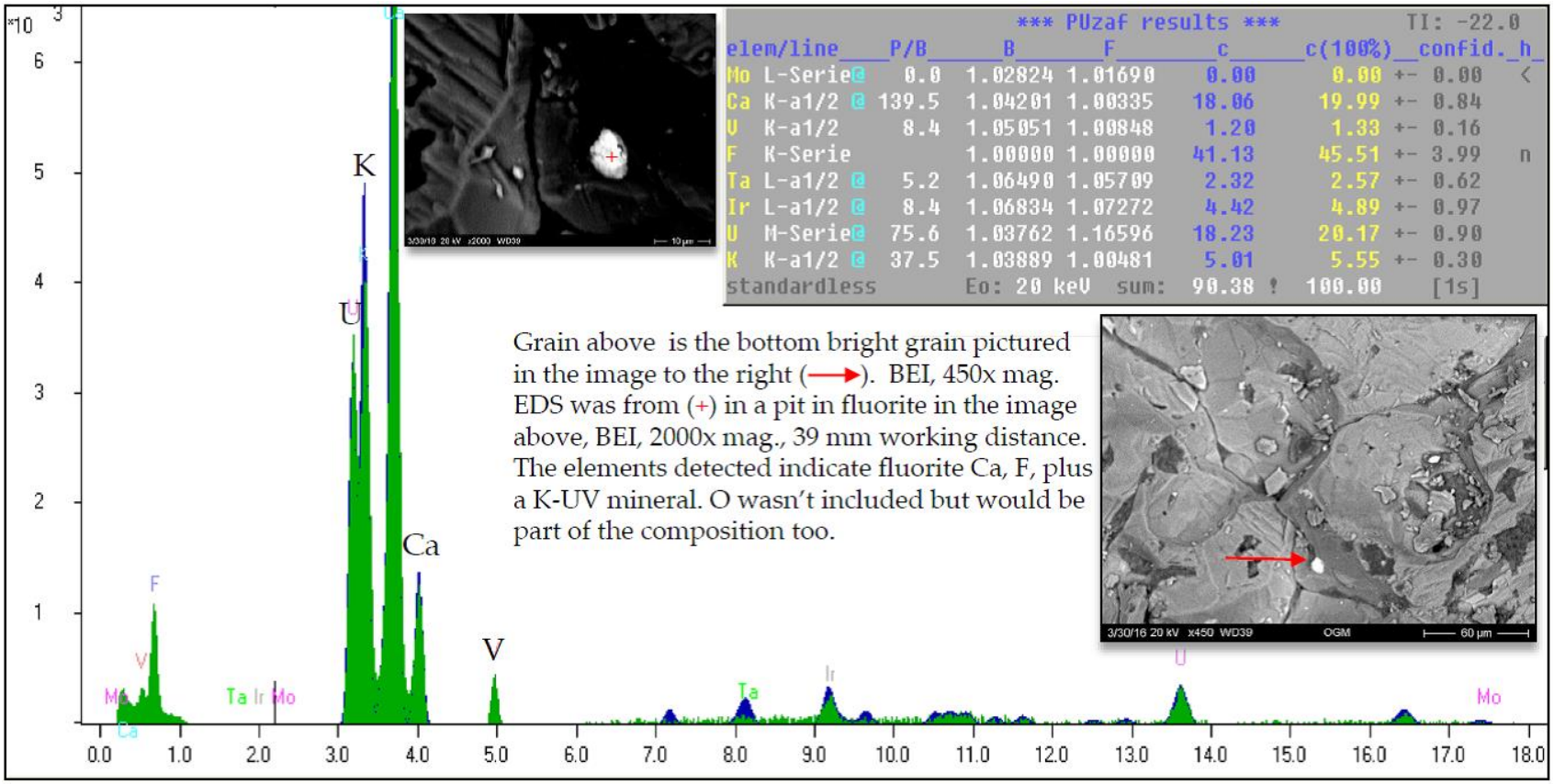


Figure C3. EDS spectrum for Old Glory mine fluorite sample with small grains of a K U-V mineral. Spectrum taken from the bright grain in the top BEI image, 2000X magnification. Same grain is pictured in the image on the right at the bottom center, BEI, 450X magnification, 39 mm working distance. The large Ca and F peaks are from the beam penetrating the K U-Vmineral and picking up the fluorite matrix. The mineral is probably carnotite. The weight percentage of U and K are low for carnotite, but this may be due to the addition of Ca and F in the overall measurement of elements detected.

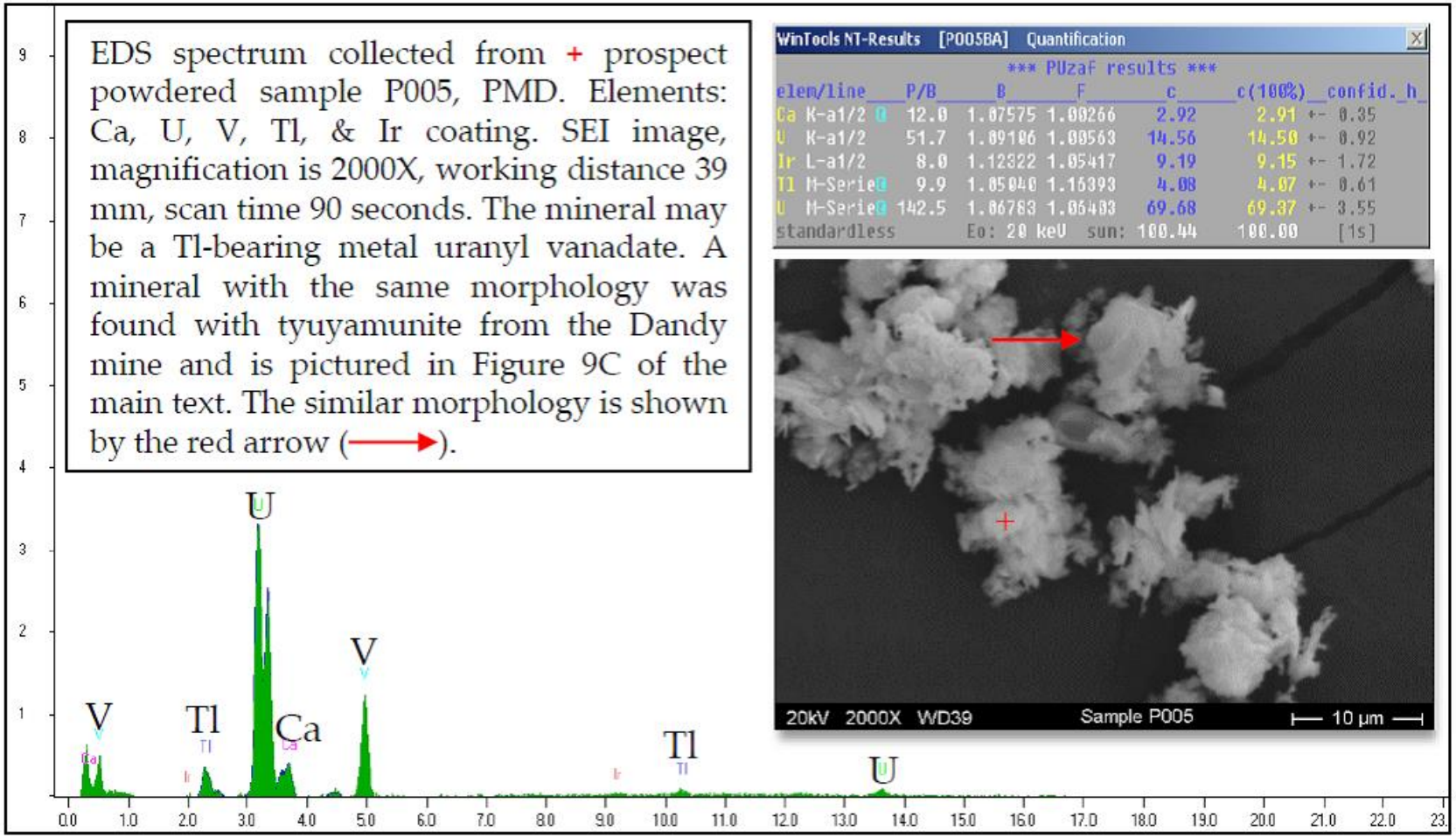


Figure C4. EDS spectrum for Tl-bearing uranyl vanadate from sample P005 collected from a U prospect in the PMD. The weight percent of the elements are similar to metal-uranyl vanadates; the mineral may be a Tl-bearing variety. A mineral with the same morphology was found with tyuyamunite in a sample from the Dandy mine (Figure 9 main document). This sample had 340 ppm Tl (Table C2). Tl and Pb have similar atomic and covalent radii: Tl (1.70 Å and 1.47Å) and Pb (1.75 Å and 146 +/- 5 Å). O was not included in the analysis, which would change the weight percentages of the mineral.

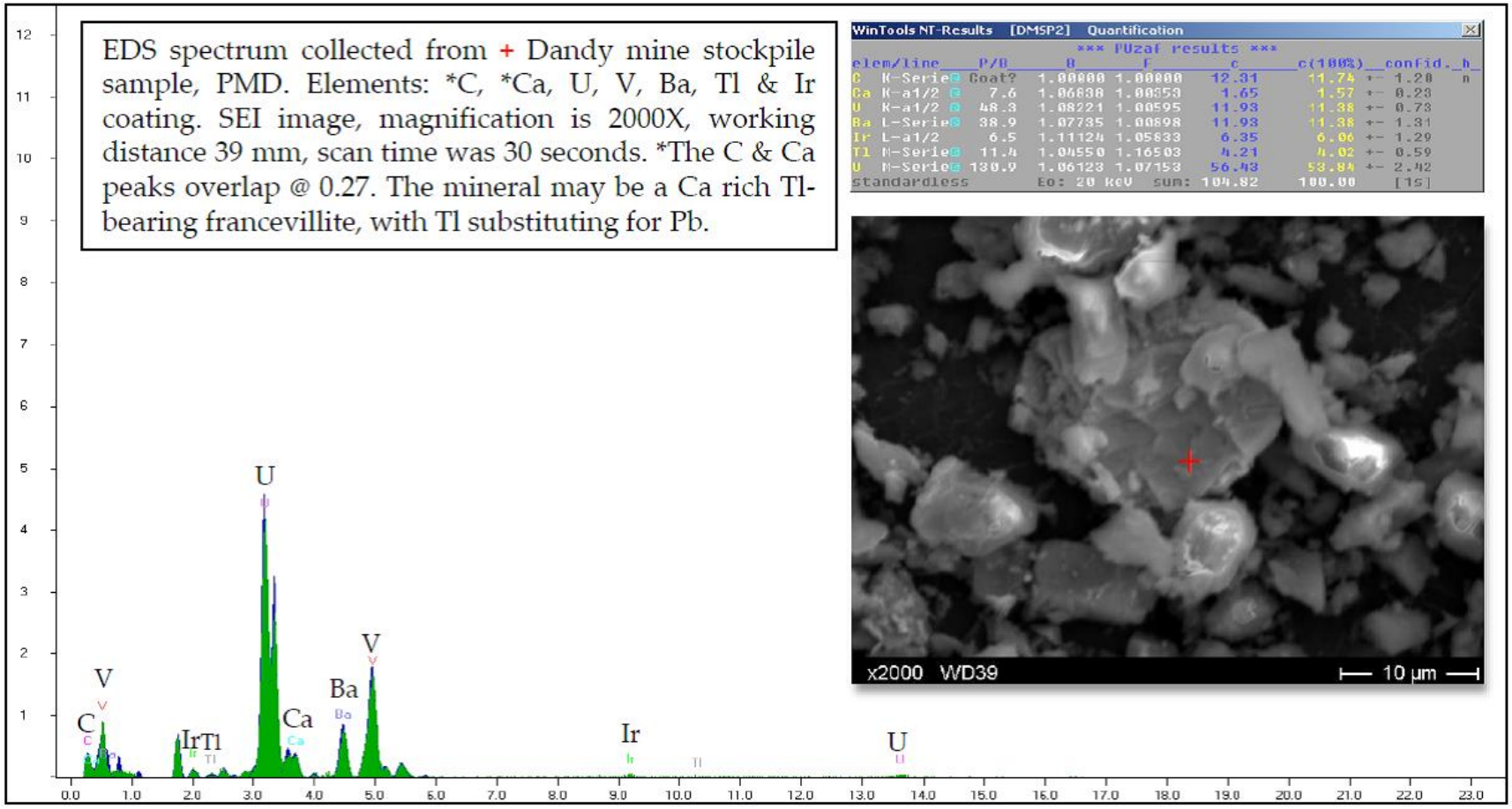


Figure C5. EDS spectrum for Tl-bearing uranyl vanadate from a sample collected from a stockpile area near the Dandy mine in the PMD. The weight percent of the elements are similar to francevillite. The sample may be a Tl-francevillite with Tl substituting for Pb.

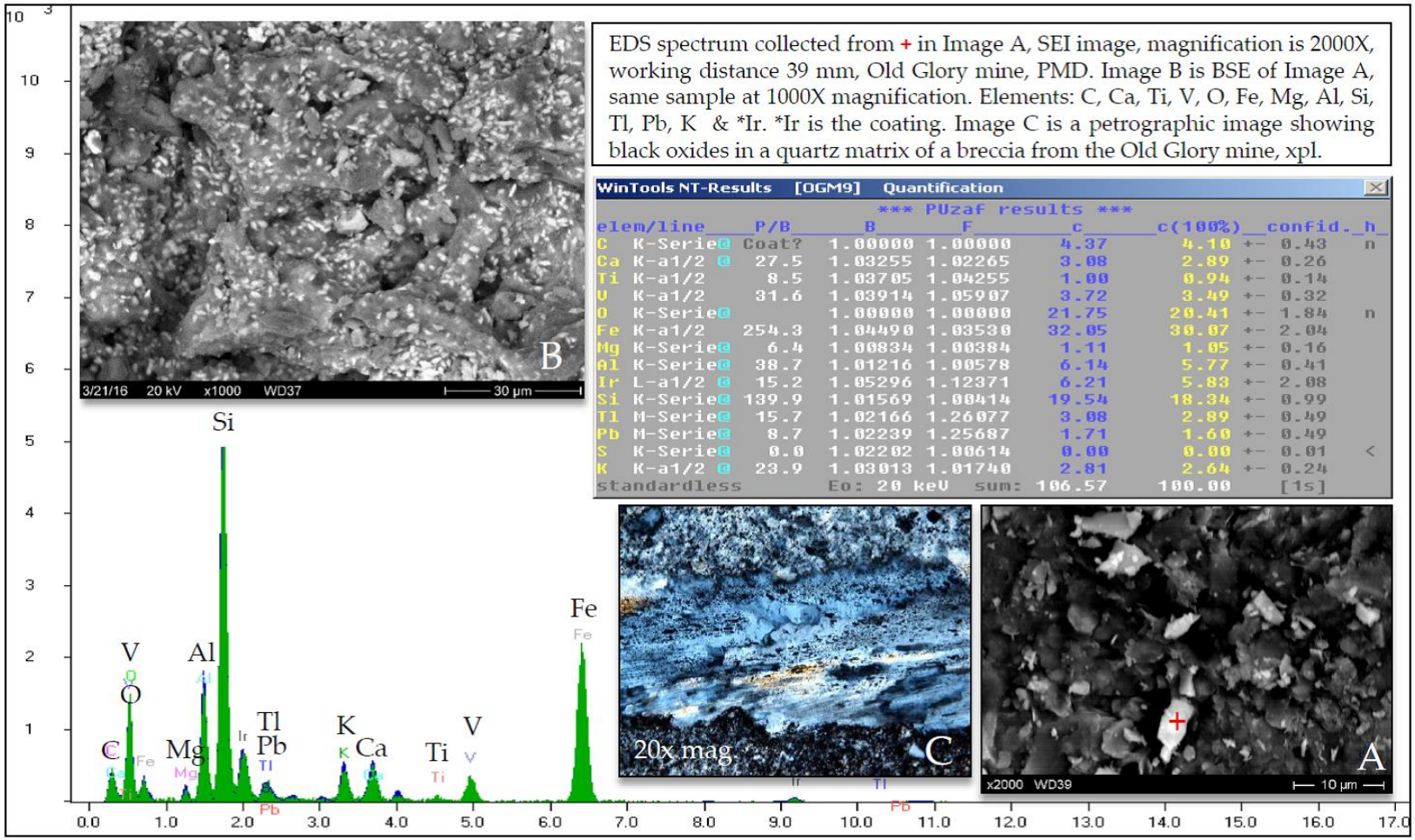


Figure C6. Fe-V oxides with Tl, Pb and Ti from the Old Glory mine, PMD. The large Si peak is likely picked up by the Si matrix. Fe has the largest weight percent in the oxides of this sample. The Fe-V oxides show up well in image B, BEI, 1000x magnification. EDS collection site + is shown in image A, SEI 2000x magnification. Petrographic image C shows inclusions of dark oxides in a quartz matrix and vein from the Old Glory mine, PMD, xpl, 20x magnification.

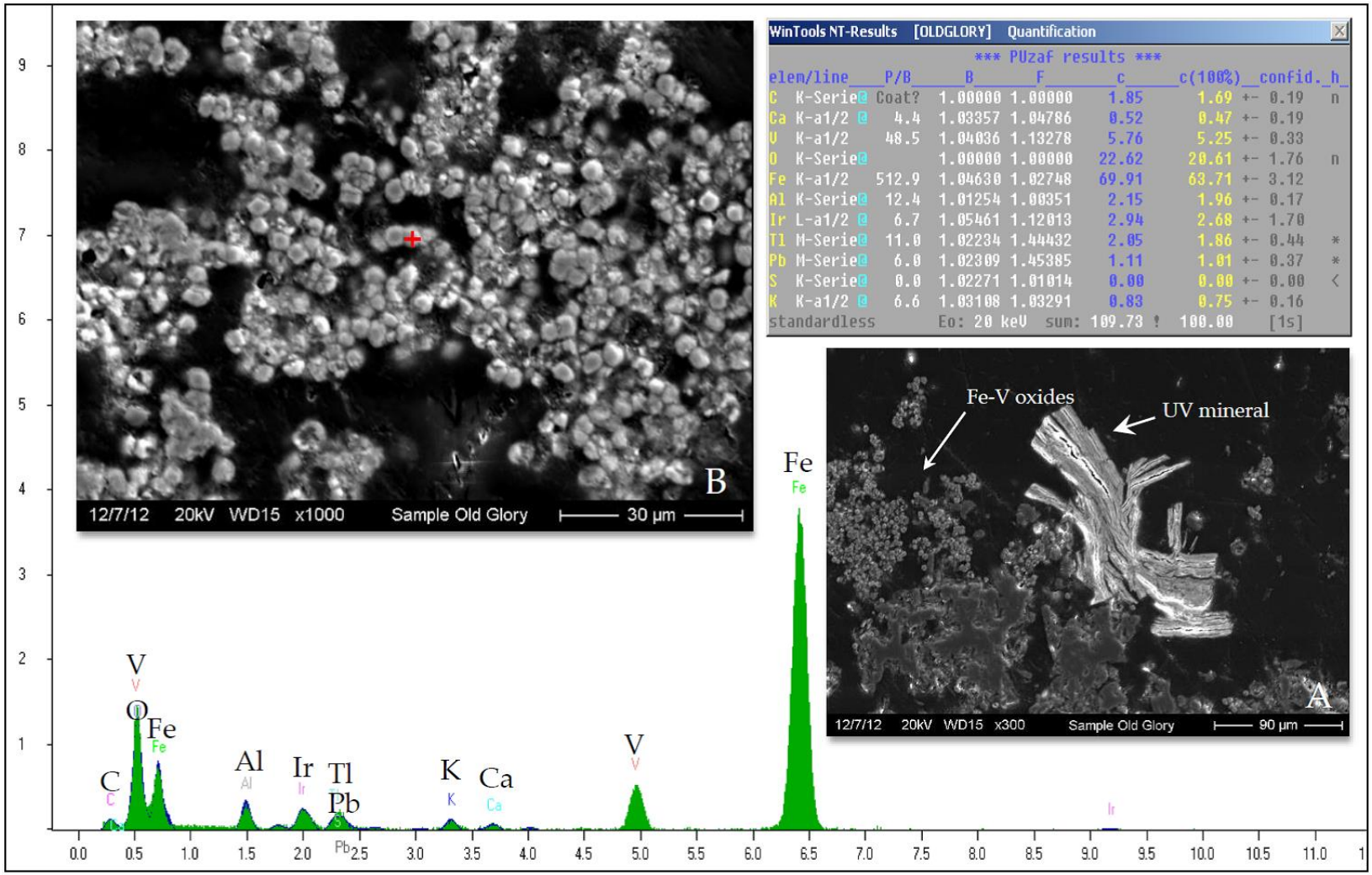


Figure C7. EDS spectrum for FeV oxides from the Old Glory mine, PMD. The elements Fe, V, *(Tl,Pb), K, Ca and O. *Tl and Pb overlap. These oxides have a lighter colored rim indicating element(s) with larger Z. The rims of the oxides may have the Tl and or Pb.

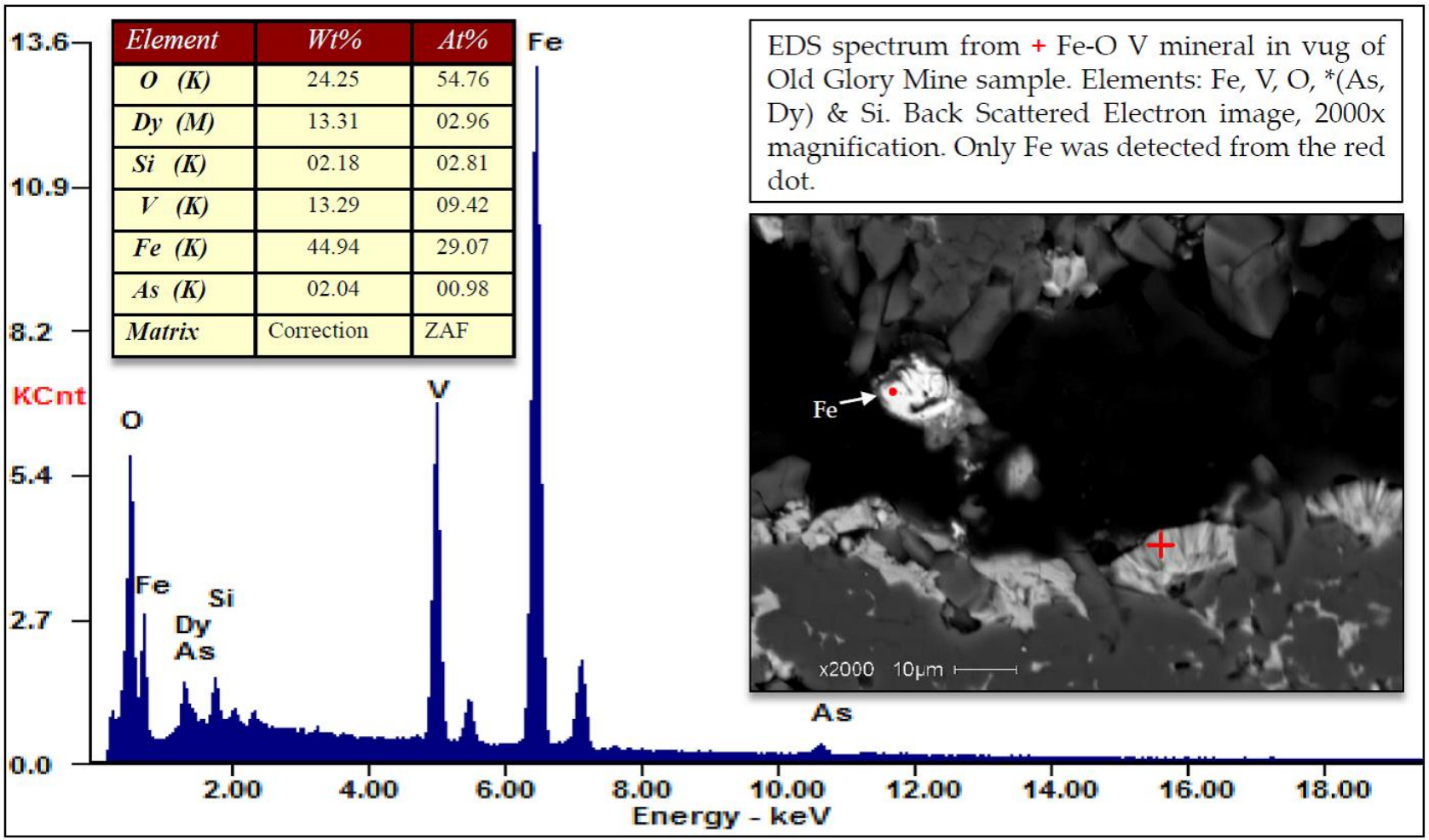


Figure C8. EDS spectrum from + in image below. Elements detected were Fe, V, *As, *Dy, Si and O. Sample is a polished thin-section from a silicified breccia, Old Glory mine, PMD. *As and Dy are the same peak but detected at different energy (keV). Only Fe was detected from the red dot. This may be an artifact of the polishing? Or possible native iron. This work was performed at the Montana Tech University, by Gary Weiss.

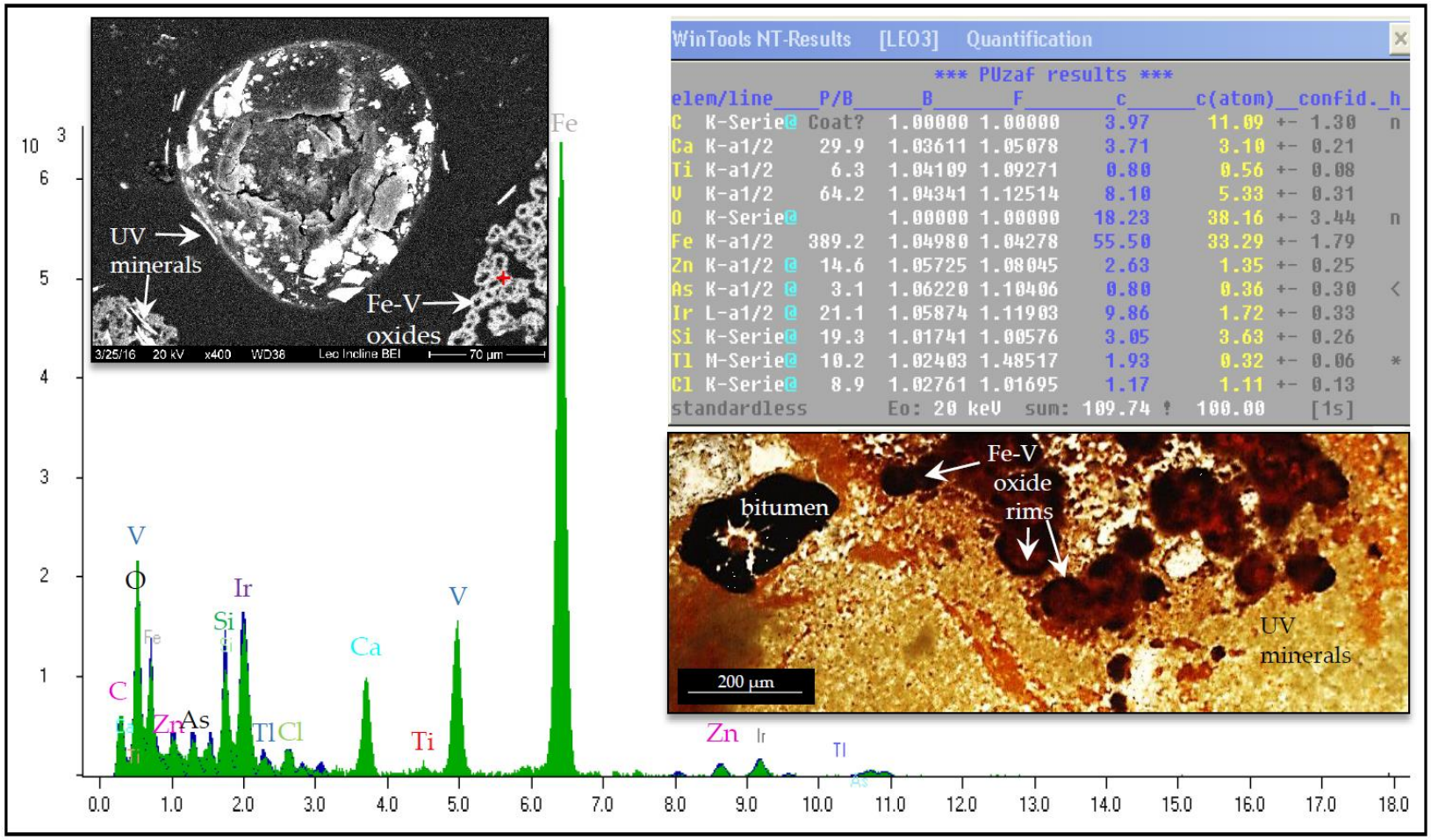


Figure C9. EDS spectrum from + in the BSE image below. Elements detected were C, Ca, Fe, V, Ti, Zn, As, Tl, Si, *Cl and O. The sample was coated with Ir. Cl is likely from the epoxy for mounting the sample. Sample is a polished thin-section from a limestone breccia, Leo Incline area, LMD. The UV minerals occur in close association with Fe-oxides and or hydroxides and bitumen. The black area in the image is an inclusion of bitumen. The red orange Fe-oxides, some with darker Fe-V rims show up well in plain polarized light as do the yellow to yellow green UV minerals.

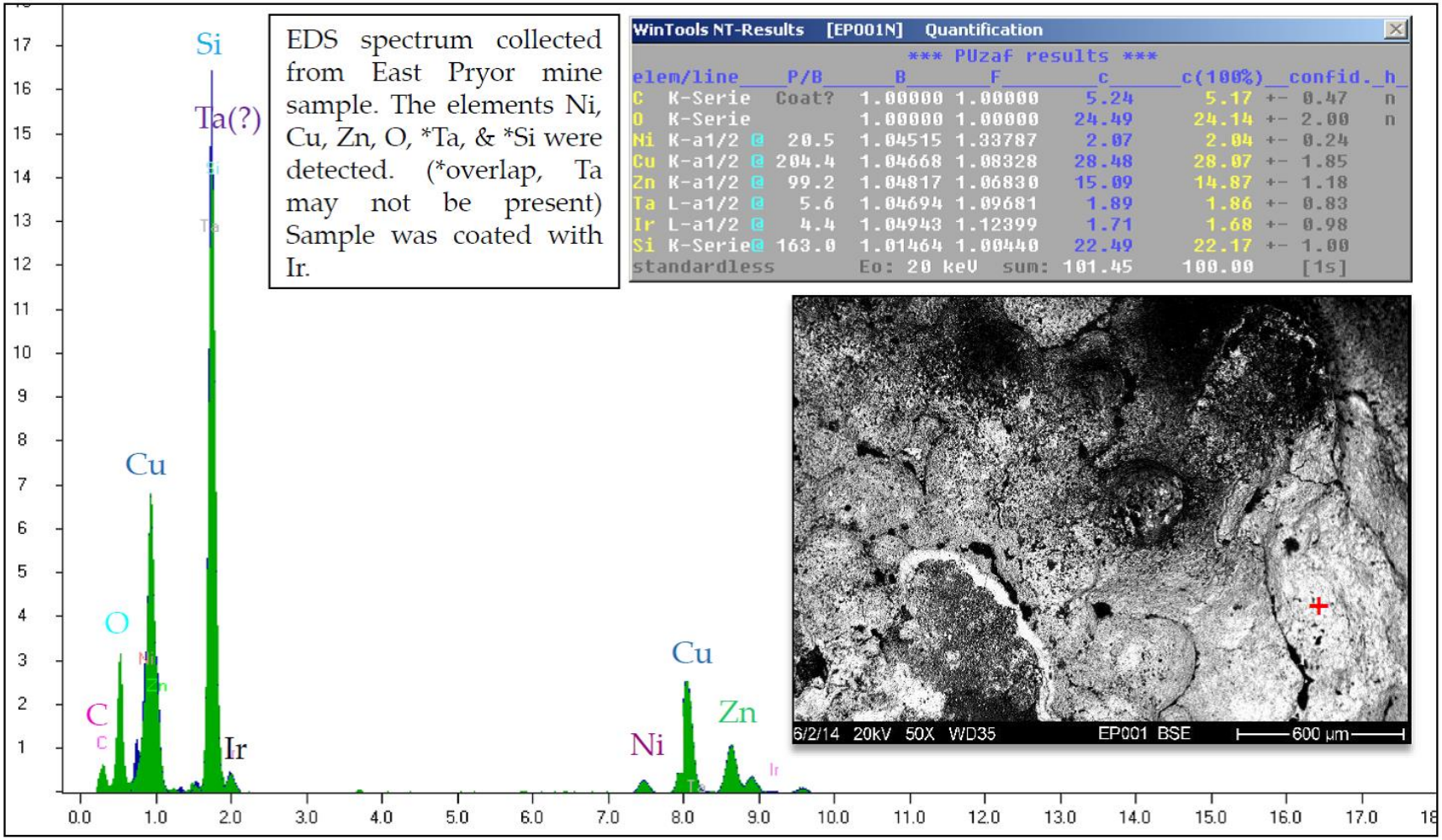


Figure C10. EDS spectrum from the red plus symbol + in the BSE image for unidentified mineral from the East Pryor mine, PMD, that did not have U. The elements Zn, Ni, Cu, *(Si,Ta) and O were detected. Si and Ta overlap though Ta may not actually be present. This mineral likely formed from the metals derived from hydrothermal fluids associated with Permian Phosphoria Formation sourced oil.